Characterisation of a novel calcium sensor in *Arabidopsis thaliana*

Bo Xu

M.Biotech

A dissertation submitted for the degree of
Doctor of Philosophy
School of Agriculture, Food and Wine
Faculty of Sciences
The University of Adelaide

THE UNIVERSITY
of ADELAIDE

2013

Declaration

This work contains no material which has been accepted for the award of any other degree or diploma in any university or other tertiary institution to Bo Xu and, to the best of my knowledge and belief, contains no material previously published or written by another person, except where due reference has been made in the text.

I give consent to this copy of my thesis when deposited in the University Library, being made available for loan and photocopying, subject to the provisions of the Copyright Act 1968.

I also give permission for the digital version of my thesis to be made available on the web, via the University's digital research repository, the Library catalogue, the Australasian Digital Theses Program (ADTP) and also through web search engines, unless permission has been granted by the University to restrict access for a period of time.

……………………………….   ………………………………

            Bo Xu   Date

Acknowledgements

Table of Contents

List of Figures

List of Tables

List of abbreviations

Abbreviation	Full term
3′	Three prime, of nucleic acid sequence
5'	Five prime, of nucleic acid sequence
~	Approximately
#	Number
%	Percent
±	Plus and minus
×	Times
β	Beta
°C	Degree Celsius
μg	Microgram(s)
μM	Micromolar
μL	Microliter(s)
AGRF	Australian Genome Research Facility
Ala	Alanine
Asn	Asparagine
ATTED-II	*Arabidopsis thaliana* trans-factor and cis-element prediction database
BLAST	Basic Local Alignment Search Tool
bp	Base pairs, of nucleic acid
BSA	Bovine serum albumin
C-terminal	Carboxyl terminal
C-terminus	Carboxyl terminus
$Ca(NO_3)_2$	Calcium nitrate
$CaCl_2$	Calcium chloride
cAMP	Adenosine 3′,5′-cyclic monophosphate
Cd^{2+}	Cadmium ion
cDNA	Complementary deoxyribonucleic acid
cGMP	Guanosine 3′,5′-cyclic monophosphate
Cl^-	Chloride ion
cm	Centimetre(s)
$CuSO_4$	Cupric sulfate

Cys	Cysteine
d	Day(s)
Da	Dalton
DNA	Deoxyribonucleic acid
EDTA	Ethylenediaminetetraacetic acid
EGAT	Ethylene glycol-bis(2-aminoethylether) -N,N,N′,N′-tetraacetic acid
FW	Fresh weight
g	Gram(s)
GFP	Green fluorescent protein
Glu	Glutamic acid
Gly	Glycine
GSH	L-Glutathione
GSSG	L-Glutathione oxidized
H_3BO_3	Boric acid
His	Polyhistidine tag
hr	Hour(s)
K^+	Potassium ion
kb	Kilo base pairs, of nucleic acid
kcal	Kilocalorie
KCl	Potassium chloride
kDa	Kilo dalton
KH_2PO_4	Monopotassium phosphate
KNO_3	Potassium nitrate
KOH	Potassium hydroxide
M	Molar
MAMP	Microbe-associated molecular patterns
MES	2- (N-Morpholino) ethanesulfonic acid, 4-morpholineethanesulfonic acid
mg	Milligram(s)
Mg^{2+}	Magnesium ion
$MgSO_4$	Magnesium sulfate
min	Minute(s)
mL	Millilitre(s)
mm	Millimetre(s)
mM	Millimolar

Mn^{2+}	Manganese ion
$MnCl_2$	Manganese chloride
mol	Mole
mRNA	Messenger RNA
N-terminal	Amine terminal
N-terminus	Amine terminus
Na^+	Sodium ion
Na_2HPO_4	Sodium phosphate dibasic
Na_2MoO_3	Sodium molybdate
NaCl	Sodium chloride
NaFe(III)EDTA	Sodium iron EDTA
NH_4NO_3	Ammonium nitrate
No.	Number
NO_3^-	Nitrate ion
ng	Nanogram(s)
nm	Nanometre(s)
nM	Nanomolar
RNA	Ribonucleic acid
PAGE	Polyacrylamide gel electrophoresis
PBS	Phosphate buffered saline
PEG 4000	Polyethylene glycol 4000
PO_4^{3-}	Phosphate ion
pv.	Pathovars
SD	Standard deviation
SE	Standard error
sec	Second(s)
Ser	Serine
SDS	Sodium dodecyl sulfate
T-DNA	Transfer deoxyribonucleic acid
Tm	Melting temperature, of primers
Tris-HCl	Tris(hydroxymethyl)aminomethane hydrochloride
Triton X-100	Toctylphenoxypolyethoxyethanol
v/v	Volume per volume
w/v	Weight per volume

YFP	YFP fluorescent protein
Zn^{2+}	Zinc ion
ZnSO$_4$	Zinc sulfate

Abstract

In dicotyledonous plants calcium is predominantly stored in the vacuoles of leaf mesophyll cells, a process in which the *Arabidopsis thaliana* tonoplast-localised Ca^{2+}/H^+ antiporter 1 (AtCAX1) was previously identified as having an essential role. Simultaneous loss-of-function of *AtCAX1,* and its close homolog *AtCAX3*, or an overexpression of a constitutively active form (*sCAX1*) can cause a number of physiological perturbations. The transcriptional profiles concurrent with these perturbations were examined in a set of Arabidopsis *cax* mutants (*cax1*, *cax3*, *cax1/cax3* and *cax1/sCAX1,* and parental wildtype Col-0) as means to uncover novel Ca^{2+}-signalling elements. A core set of misexpressed genes was examined, in a preliminary screen using putative loss-of-function Arabidopsis mutants, but no calcium-related phenotypes were identified. Instead, the most highly misexpressed gene in *cax1* and *cax1/cax3* lines was selected for further functional characterisation. Calmodulin-like 41 (*CML41*) was negatively correlated with *CAX1* expression so it was hypothesised that it might behave as a transcriptional regulator of *CAX1* or as a Ca^{2+} signalling element downstream of CAX1 function.

During cloning it was discovered that *CML41* was likely transcribed into two transcripts – a full-length *CML41* (*CML41FL*), which is annotated in the NCBI database, and a novel shorter-splicing transcript named *CML41* Short (*CML41S*). The proteins encoded by *CML41FL* and *CML41S* were predicted to have 4 and 3 putative EF-hand calcium binding domains respectively, and both were demonstrated to have calcium-binding capacity *in vitro*, indicating that CML41FL and CML41S may act as Ca^{2+} sensors *in planta*. Both proteins have the same targeting signal peptide and share a similar subcellular localisation pattern being predominantly localised in the cytoplasm of young developing leaves, and roots under standard growth conditions, but are translocated to plasmodesmata (PD) in mature and old vegetative leaves. Furthermore, a TEOSINTE BRANCHED 1, cycloidea and proliferating cell factor (TCP) transcription factor 14 (TCP14) was demonstrated to interact with both CML41FL and CML41S, but the function of these interactions remains obscure.

Misexpression (35S CMV driven amiRNA knockdown or overexpression) of either *CML41FL* or *CML41S* had no effect on *CAX1* transcript abundance, so it is more likely that CML41 acts as a downstream Ca^{2+} signal element rather than in controlling *CAX1* expression. *In silico* analysis of gene expression indicates that *CML41* is highly up-regulated during biotic stress, senescence, in response to changes in photoperiod and calcium treatments, so the phenotypes of *CML41* misexpressing plants were examined under these and related conditions.

Both *CML41FL* and *CML41S* expression was induced in leaves infiltrated with flg22 – an elicitor of *P. syringae* inducing pathogen-associated molecular pattern (PAMP)-triggered immunity (PTI) signalling in plants. Knocking-down *CML41FL* expression significantly reduced the callose

14

deposition at PD in leaves in response to flg22, whereas in normal conditions a constitutive overexpression of *CML41FL* failed to increased callose deposition. Together this implies that CML41FL (and/or CML41S) may function as a Ca^{2+} sensor downstream of the flg22-triggered immune response to modulate callose accumulation, and its activation may require an elevation of cytosolic Ca^{2+}. The overexpression of *CML41S* and silencing of *CML41FL* both accelerated chlorophyll breakdown and senescence of individual leaves induced by dark, although their expression was not altered during the conditions imposed here. High calcium supplementation (50 mM) inhibited primary root growth of wild-type and *CML41* overexpression lines whereas it was not affected in *CML41*-knocked-down amiRNA lines. At 12.5 mM calcium, as compared to 0.3 mM, primary root growth of wild-type and *CML41*-knocked-down amiRNA plants was stimulated but this was not observed in *CML41FL-* or *CML41S*-overexpression plants. In plants expressing *CML41-GFP* translational fusions, both CML41FL and CML41S were translocated from the cytoplasm to the PD at the root tip under high calcium conditions. These results suggest that a root-growth responses to high external calcium might involve the translocation of CML41 from the cytoplasm to the PD.

Here, I demonstrate that a previously uncharacterised member of the CML family is likely to have key roles in biotic stress responses, in regulation of dark-induced leaf senescence and regulation of root sensitivity to environmental calcium levels. A number of experimental avenues are opened up by this work, especially in respect to the relative contributions of CML41FL and CML41S to the above phenotypes.

Chapter 1: General introduction and literature review

1.1 Introduction

Calcium is unique amongst plant and animal essential macronutrients as it has key structural and signalling roles in both kingdoms (Berridge et al., 2003; White and Broadley, 2003; Cosgrove, 2005; Weaver and Heaney, 2006; Hirschi, 2009). In plants, calcium's status as the major signalling intermediate is well established and has been much reviewed (see for examples of the more recent reviews McAinsh and Pittman, 2009; Dodd et al., 2010; Reddy et al., 2011). The subtlety of how calcium imparts its structural roles in plants and how these are regulated is less well understood. However, it is clear that calcium is required for membrane stability and as an agent for cross-linking demethylesterified pectins within the cell wall to ensure an adequate level of rigidity whilst maintaining sufficient fluidity for growth (White and Broadley, 2003). Excess ionic calcium (Ca^{2+}) in plant tissue is rarely a physiological problem in plants as they are ordinarily able to store or compartmentalise it in various tissues prior to it causing a problem with Ca^{2+} signalling (in the form of phosphate, oxalate or tartrate crystals, or as the divalent inorganic cation Ca^{2+} in organelles or bound to Ca^{2+} binding proteins) (Pittman and Hirschi, 2003; Hirschi, 2004 and 2009; Dodd et al., 2010). However, calcium deficiency in plants can lead to cracks and splits in fruit (e.g. tomato, apple and cherry) as a result of structural instabilities in calcium-deficient cell walls or cell membranes, and for the same reason induces necrosis in young calcium-deficient tissues and leaves (Bullock, 1952; Dickinson and McCollum, 1964; Shear, 1975; Simon, 1978; White and Broadley, 2003). This can lead to high wastage in the horticultural and agricultural industries and reduced profits (Dayod et al., 2010). Likewise, low daily calcium intake for humans, which is common, can ultimately result in diseases such as osteoporosis, and in extreme cases rickets. These are conditions of low bone density stemming from bone demineralisation or insufficient initial calcium deposition (Walker, 1972; Legius et al., 1989; Bhatia, 2008) that can ultimately lead to high medical costs (Dayod et al., 2010). Milk or dairy foods are a major source of calcium to diets but may be avoided in some populations due to lactose intolerance or ethical reasons. Grains, fruits and vegetables are poor sources of bioavailable calcium so when eaten as staple crops can lead to such deficiencies without calcium supplementation in diets, but these crops have the potential to act as major calcium sources through calcium biofortification straetgies (Willett, 1994; Weaver et al., 1999; Guéguen and Pointillart, 2000; Weaver and Heaney, 2006; Hirschi, 2009). As a result, it has been speculated that biofortifying plants to have an increased bioavailable calcium could be performed to reduce plant spoilage and to provide a suitable alternative to dairy products for humans (Weaver et al., 1999; White and Broadley, 2005; Hirschi, 2008 and 2009; White and Broadley, 2009).

In terms of genetic manipulation, calcium biofortification strategies have concentrated predominantly on altering the expression of a particular family of Ca^{2+}-transporter genes and these studies have had very interesting results (reviewed in Dayod et al., 2010). In most cases, these have been successful. In most cases the calcium content of plant tissues increased but in some cases there were side-effects with disruptions to plant physiology or growth (Hirschi 1999; Park et al., 2004; Kim et al., 2005; Park et al., 2005a and 2005b; Park et al., 2009; Han et al., 2009; Kim, 2012; Wu et al., 2012). These phenotypes have highlighted how important it is for plants to maintain tight control of Ca^{2+} homeostasis, as well as highlighting the difficulty in separating and studying aspects of calcium nutrition from its structural, storage and signalling roles in plants without perturbing plant growth. On the other hand, these studies provide an opportunity for further examination of the networks that control calcium homeostasis and Ca^{2+} signalling by examining how genetic manipulation of Ca^{2+} transporter expression can cause these aberrant plant phenotypes. Such studies are likely to result in not only a better understanding of the upstream regulators of Ca^{2+} transport or the downstream targets of signals derived from these major Ca^{2+} transporters, but also may open up new avenues for calcium biofortification strategies in plants that have minimal impacts on other physiological processes (Conn and Gilliham, 2010; Dayod et al., 2010). The following chapter reviews aspects of Ca^{2+} transport, storage and signalling in plants, identifies knowledge gaps pertinent to calcium -storage, especially its relationship to Ca^{2+} signalling and identifies an experimental approach to study the signalling associated with the major Ca^{2+} transporter(s) that control calcium accumulation in plants.

1.2 Calcium transport and storage in plants

1.2.1 Ca²⁺ delivery in plants

Calcium in the soil is predominantly available to plants as a divalent cation (Ca^{2+}). This enters the root apoplasm along with the mass flow of water and follows apoplastic (extracellular) or symplasmic (intracellular) pathways into the xylem (Figure 1.1) (Barber, 1995). Calcium ions are drawn toward the xylem in the transpiration stream, and unrestricted delivery of Ca^{2+} into the xylem can occur in apical areas of the root (White, 1998 and 2001). However the casparian band, surrounding the root endodermis, can limit the apoplastic passage of solutes across the endodermis into the xylem. Therefore, translocation of Ca^{2+} to the xylem must use a symplasmic pathway when an impermeable casparian band is present (Clarkson, 1993; White, 2001). In this case, apoplastic Ca^{2+} is loaded into the cytoplasm of cells prior to the endodermis on the cortical side through Ca^{2+}-permeable channels (White, 2001). Subsequently, Ca^{2+}-transporters (e.g. Ca^{2+}-ATPases) actively move Ca^{2+} out across the plasma membrane of the endodermal cells facing the stele, or from cells that

are symplastically connected with these in the stelar interior. White (2001) proposes that calcium might also traverse the symplasm in calcium-chelates so to maintain low-level cytosolic $[Ca^{2+}]$ ($[Ca^{2+}]_{cyt}$). The pathway for Ca^{2+} loading into xylem depends on the absence or presence of the casparian band (Figure 1.1A) (Clarkson, 1993; White, 2001). The apoplastic or symplasmic pathways have distinct characteristics. The Ca^{2+} apoplastic pathway is dependent on the transpiration rate and is relatively non-selective for divalent cations (White, 2001). In contrast, the symplasmic pathway is more selective and controls Ca^{2+} transport into the xylem depending on the demand of calcium in the shoot (Clarkson, 1993; White, 1998 and 2001; White and Broadley, 2003). In plants, these two pathways together are usually sufficient to meet the calcium requirement of shoots whilst not perturbing the low resting $[Ca^{2+}]_{cyt}$ of root cells (White, 2001; White and Broadley, 2003). The proportion of apoplastic and symplasmic pathways contributing to the calcium delivery into xylem is unclear in most plants but appears to be dependent on species (Cholewa and Peterson, 2004; Hayter and Peterson, 2004; Baxter et al., 2009; Conn and Gilliham, 2010).

In *Arabidopsis thaliana*, long-distance Ca^{2+} delivery in xylem is believed to primarily follow apoplastic pathways (Conn and Gilliham, 2010). Enhanced suberisation of root observed in the Arabidopsis knockout line *esb1* displayed reduced daytime transpiration and approximately a 50% reduction in shoot calcium, resulting from the increased suberin barrier restricting water and solute movement through root apoplasm (Baxter et al., 2009). Once the Ca^{2+} enters into xylem, it follows the xylem-transpiration stream into shoot and Ca^{2+} is distributed in the leaf apoplastically driven by transpiration, whereby Ca^{2+} delivery is linked to water flow (Figure 1.1B) (reviewed in Gilliham et al., 2011b, see Appendix 1).
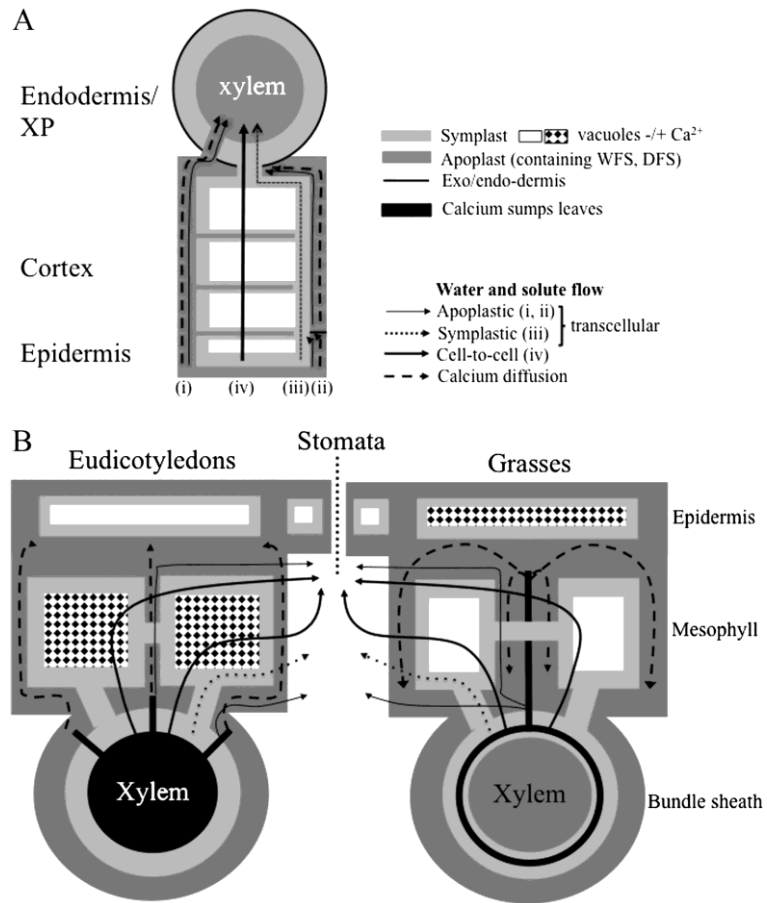
Figure 1.1 Diagrammatic summary of Ca^{2+} storage and water flow in roots (A) and leaves (B).
Distinct calcium distribution in the leaves between eudicots and grasses (monocots) as indicated in **B**:
Ca^{2+} is transport via xylem to shoot and is distributed following apoplastic sumps located at the
intercellular space of the inside bundle sheath parenchyma cells in monocots or at site around bundle
sheath cells in eudicots; this apoplastic Ca^{2+} diffusion in the apoplast is correlated with symplasmic
water flow that can be regulated by aquaporins, proposed by Gilliham et al (2011b). Images adapted
from Gilliham et al (2011b).

1.2.2 Cell-specific calcium storage in plants

Solutes in plants can be retrieved and recycled through the plant by the phloem (Patrick,
1997). But, due to the immobility of Ca^{2+} in the phloem, it is not generally redistributed once reaching
the leaf, so that the majority of calcium in plant is essentially stored in leaf tissue (Figure 1.2) (White
and Broadley, 2003; Storey and Leigh, 2004; Conn and Gilliham, 2010). Such a Ca^{2+} load cannot
simply be stored in the leaf apoplasm (although cation exchange sites on pectic residues within the
cell wall do bind with Ca^{2+} but these are often saturated). Apoplastic Ca^{2+} ([Ca^{2+}]$_{apo}$) above ~0.75 mM

induces stomatal closure and perturbs plant transpiration, excessive $[Ca^{2+}]_{apo}$ is also correlated with increased cell-wall thickness, thus the majority of leaf calcium is accumulated within the leaf cells (Jarvis, et al., 1984; Smith, 1991; de Silva et al., 1996; Hirschi, 2004; Cosgrove, 2005).

Leaf cellular calcium storage displays a cell-specific pattern dependent on plant species. In general, it has been observed that calcium is specifically accumulated in cereal epidermal cells or eudicot mesophyll cells (e.g. when fed 2 mM Ca^{2+} in the growth media the calcium content of the epidermis/mesophyll in: 1) barley, an example of the poales, is 27.5 ± 0.5 mM / 4.0 ± 0.8 mM, or 2) Arabidopsis, as an example eudicot, it is 10.1 ± 8.2 mM / 68 ± 14 mM) (Figure 1.1 and 1.2) (Conn and Gilliham, 2010). The majority of calcium within leaves and within different cell-types is stored in the vacuole, as the $[Ca^{2+}]_{cyt}$ is generally maintained around ~100 nM when at "resting" levels (as discussed in Section 1.4), with other intracellular organelles, such as the endoplasmic reticulum (ER) also contributing to calcium storage and acting as a buffer for $[Ca^{2+}]_{cyt}$ (Marschner, 1995; Sanders et al., 2002; Åkesson et al., 2005; McAinsh and Pittman, 2009).
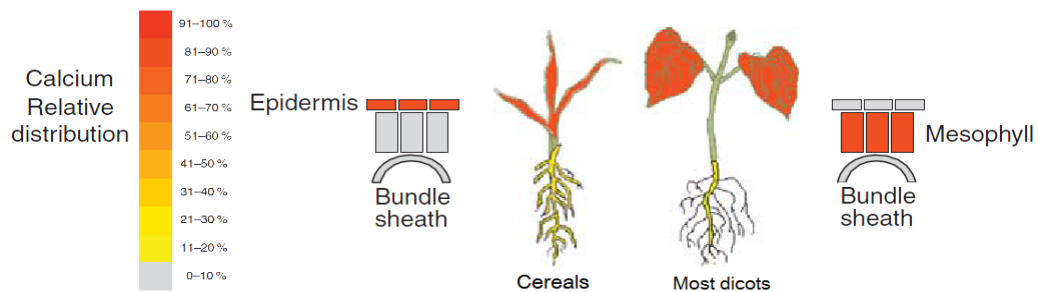
Figure 1.2 A summary of calcium **distribution in cereals and most dicots.** Calcium relative accumulation in shoots and roots of monocots (cereals on the left) and dicot (on the right). Relative calcium distribution is also represented in leaf cross-section with different cell types. Adapted from Conn and Gilliham (2010).

A mechanism that underpins distinct cell-specific calcium accumulation storage differences between the poales and other plants was proposed by Karley et al (2000), who stated that these distributions are a result of differences in the architecture of the venation of leaves. In the poales, vein extensions emerge and extend from the main veins to connect the xylem Ca^{2+} sump directly to the epidermis, so delivering Ca^{2+} first to the epidermis. Whereas in other plants the mesophyll is in closer vicinity to the xylem Ca^{2+} sump than the epidermis so it is likely to come into contact with apoplastic flows of Ca^{2+} prior to the epidermis, as shown in Figure 1.1. However, this cannot explain why calcium is not accumulated within bundle sheath cells as discussed by Conn and Gilliham (2010). As

such, differential calcium compartmentation is also believed to be correlated with the expression of certain Ca^{2+} transporters in particular cell types (Conn and Gilliham 2010).

1.3 Ca²⁺ transporters in plants

In the past two decades, a number of Ca^{2+} permeable-channels or transporters have been discovered and characterised that are present either on the plasma membrane or the vacuolar membrane in Arabidopsis as summarised in Table 1.1, including P-type Ca^{2+}-ATPases (ACA), Annexins (ANN), Ca^{2+}/H^{+} exchangers (CAX), Cyclic nucleotide-gated channels (CNGC), Glutamate Receptor-like channels (GLR), Mechanosensitive cation-permeable channel (MCA) and Two-pore channel (TPC) families. Although, many of these channels are not specific for Ca^{2+}, rather they are Ca^{2+} permeable, and in some cases there is not yet definitive proof that they act as Ca^{2+}-channels *in planta*, misexpression of many of them induces Ca^{2+}-related phenotypes. A more complete list of Ca^{2+} channels/transporters in plants and their proposed roles can be found listed in Table 1.1. The role of those involved with cell-specific calcium storage in leaves will be discussed in more detail in the remainder of this review.

Table 1.1 Summary of plasma/vacuolar membrane Ca^{2+} transporters/channels in Arabidopsis

Gene families	Gene locus	Membrane localisation*	Physiological roles	References
Ca^{2+}- ATPase (ACA)				
ACA1	At1g27770	P	n/d	Huang et al., 1993
ACA2	At4g37640	ER	n/d	Harper et al., 1998; Hong et al., 1999;
ACA4	At2g41560	TM	Wounding response; induction of SA-mediated PCD	Geisler et al., 2000; Gfeller et al., 2011; Boursiac et al., 2010
ACA7	At1g08080	PM	Pollen development	Bock et al., 2006; Lucca and León, 2012
ACA8	At5g57110	PM	Regulation of MAMP response; inflorescence height and root length; ABA increases expression	Bonza et al., 2000; Maathuis et al., 2003; Cerana et al., 2006; George et al., 2008; Frey et al., 2012
ACA9	At3g21180	PM	Pollen development and fertilization; ABA increases expression	Schiøtt et al., 2004; Bock et al., 2006; Cerana et al., 2006
ACA10	At4g29900	PM	Inflorescence architecture and vegetative development; regulation of MAMP response	Bock et al., 2006; George et al., 2008; Frey et al., 2012
ACA11	At3g57330	TM	Induction of SA-mediated PCD	Lee et al., 2007; Boursiac et al.,2010
ACA12	At3g63380	n/d	n/d	
ACA13	At3g22910	n/d	n/d	
Annexins (ANN)				
ANN1	At1g35720	PM	Drought tolerance; increase in ROS accumulation; channel conductance sensitive to external pH	Gorecka et al., 2007; Konopka-Postupolska et al., 2009; Clark et al., 2010, Laohavisit et al., 2012
Ca^{2+}/H^{+} Exchangers (CAX)				
CAX1	At2g38170	TM	Interaction with CAX3; control of cell-specific calcium storage, ion homeostasis, element distribution and abundance in seeds, gas exchange, apoplastic Ca^{2+} and pH, auxin and ABA response; regulation of cold-acclimation response	Hirschi et al., 1996; Hirschi, 1999; Catalá et al., 2003; Cheng et al., 2003 and 2005; Pittman et al., 2005; Zhao et al., 2009; Conn et al., 2011; Cho et al.,2012; Punshon et al., 2012
CAX2	At3g13320	TM	Transport Ca^{2+}, Zn^{2+}, Cd^{2+} and Mn^{2+}; heavy metal detoxification (e.g. Cd^{2+} and Mn^{2+})	Hirschi et al., 2000; Schaaf et al., 2002; Pittman et al., 2004; Korenkov et al., 2007; Edmond et al., 2009; Korenkov et al., 2009

Continued

CAX3	At3g51860	TM	Interaction with CAX1; compensation of loss of *CAX1*; reduction of plasma membrane H^+-ATPase activity in *cax3*; involved in salt tolerance of seedlings, regulation of calcium, K and Zn elemental distribution and abundance in seeds, regulates auxin response and apoplastic pH	Cheng et al., 2005; Zhao et al., 2008 and 2009; Conn et al., 2011; Cho et al.,2012; Punshon et al., 2012; Hocking et al., unpublished.
CAX4	At5g01490	TM	Transport to Ca^{2+} and Cd^{2+}; heavy metal tolerance (Cd^{2+} and Mn^{2+}) and regulation of auxin response	Cheng et al., 2002; Korenkov et al., 2007; Korenkov et al., 2009; Mei et al., 2009
CAX5	At1g55730	TM	Permeable to Ca^{2+} and Mn^{2+}	Edmond et al., 2009
CAX6	At1g55720	n/d	n/d	
Cyclic nucleotide-gated channels (CNGC)				
CNGC1	At5g53130	PM	Ca^{2+} and K^+ channel; K^+ transport activated by cAMP; involved in plant Ca^{2+} uptake in roots	Köhler et al., 1999; Köhler and Neuhaus, 2000; Ali et al., 2006; Ma et al.,2006; Kanter et al., 2010
CNGC2	At5g15410	PM	Regulation of plant innate immunity through interaction with CaM to control downstream NO production, endogenous SA level; activation of Ca^{2+} transport by cAMP, permeable to K^+; regulation of early senescence and shoot calcium level	Köhler et al., 1999; Köhler and Neuhaus, 2000; Clough et al., 2000; Köhler et al., 2001; Leng et al., 2002; Ali et al., 2007; Genger et al., 2008; Ma et al., 2008 and 2010
CNGC3	At2g46430	PM	Na^+ and K^+ channel; involved in seed germination	Gobert et al., 2006
CNGC4	At5g54250	PM	Ca^{2+} transport activated by cAMP and cGMP; regulation of endogenous SA level; suppression of PCD in response to pathogen; permeable to K^+	Balagué et al., 2003; Jurkowski et al., 2004
CNGC5	At5g57940	PM	n/d	Christopher et al., 2007
CNGC6	At2g23980	PM	Activation of Ca^{2+}-signalling influx by cAMP; in response to heat shock	Gao et al., 2012
CNGC7	At1g15990	PM	Function at the initiation of pollen tip growth	Tunc-Ozdemir et al., 2013a
CNGC8	At1g19780	n/d	Function at the initiation of pollen tip growth	Tunc-Ozdemir et al., 2013a
CNGC9	At4g30560	n/d	n/d	
CNGC10	At1g01340	PM	Transport Ca^{2+} and Mg^{2+}; regulation K^+ and Na^+ uptake, salt tolerance	Christopher et al., 2007, Guo et al., 2008 and 2010
CNGC11	At2g46440	PM	Positive regulation of resistance to pathogen; Ca^{2+} and K^+ channel; function synergistically with CNGC12 in senescence; induction of pathogen resistance response and cell death by chimeric CNGC11/12 in Ca^{2+} dependent manner as well as requirement of NDR1 and EDS1/PAD4-dependent pathways	Yoshioka et al., 2006; Urquhart et al., 2007; Baxter et al., 2008; Chin et al., 2010; Urquhart et al., 2011

Continued

CNGC12	At2g46450	PM	Positive regulation of resistance to pathogen; Ca^{2+} and K^+ channel; function synergistically with CNGC11 in senescence; induction of pathogen resistance response and cell death by chimeric CNGC11/12 in Ca^{2+} dependent manner as well as requirement of NDR1 and EDS1/PAD4-dependent pathways; complementation of chimeric CNGC11/12 phenotype	Yoshioka et al., 2006; Urquhart et al., 2007; Baxter et al., 2008; Chin et al., 2010; Urquhart et al., 2011
CNGC13	At4g01010	n/d	n/d	
CNGC14	At2g24610	n/d	n/d	
CNGC15	At2g28260	n/d	n/d	
CNGC16	At3g48010	n/d	Involved in pollen reproductive development in heat stress response	Tunc-Ozdemir et al., 2013b
CNGC17	At4g30360	n/d	n/d	
CNGC18	At5g14870	PM	Regulation of calcium signalling in pollen tube growth	Frietsch et al., 2007
CNGC19	At3g17690	TM	Expressed in root; up-regulated in shoot by salt	Kugler et al., 2009; Yuen and Chrisopher, 2013
CNGC20	At3g17700	TM	Expressed in shoot; up-regulated in shoot by salt	Kugler et al., 2009; Yuen and Chrisopher, 2013
Glutamate Receptor-like channel (GLR)				
GLR1.1	At3g04110	PM	Transport Na^+, K^+ and Ca^{2+}	Tapken and Hollmann et al., 2008
GLR1.2	At5g48400	PM	Control of Ca^{2+} signal oscillations in apical pollen tube and pollen morphogenesis activated by D-serine	Michard et al., 2011
GLR1.3	At5g48410	n/d	n/d	
GLR1.4	At3g07520	PM	Function as a ligand-gated, nonselective, Ca^{2+}-permeable cation channel in membrane depolarization in leaves induced by Met; Met-induced current inhibited by Arg, Gln, Lys, Val, Ile, His, Cys, Ala and Ser.	Tapken and Hollmann et al., 2008; Tapken et al., 2013
GLR2.1	At5g27100	n/d	n/d	
GLR2.2	At2g24720	n/d	n/d	
GLR2.3	At2g24710	n/d	n/d	
GLR2.4	At4g31710	n/d	n/d	
GLR2.5	At5g11210	n/d	n/d	
GLR2.6	At5g11180	n/d	n/d	
GLR2.7	At2g29120	n/d	n/d	
GLR2.8	At2g29110	n/d	n/d	

Continued

GLR2.9	At2g29100	n/d	n/d	
GLR3.1	At2g17260	n/d	Specifically expressed in guard cell; no impact on Ca^{2+}-induced Ca^{2+} oscillation; an effect on long-term Ca^{2+}-induced stomatal closure	Cho et al., 2009
GLR3.2	At4g35290	n/d	Highly expressed in vascular tissue and rapid dividing tissues; regulate lateral root development; regulation of plant ion sensitivity to Na^+ and K^+, related to Ca^{2+} homeostasis, regulation of long-distance signalling in wound-stimulated distal production of JA	Kim et al., 2001; Turano et al., 2002; Mousavi et al., 2013; Vincill et al., 2013
GLR3.3	At1gG42540	n/d	Mediate Ca^{2+} signalling oscillation; Ca^{2+} transport activated by Glu, Asn, Ala,Cys, Gly, Ser and glutathione (GSH & GSSG), but suppressed by increasing extracellular pH; desensitization phenomenon but different from GLR3.4, regulation of long-distance signalling in wound-stimulated distal production of JA	Qi et al., 2006; Stephens et al., 2008; Mousavi et al., 2013
GLR3.4	At1g05200	PM & P	Ca^{2+} signalling oscillation in response to touch, osmotic stress cold and ABA; regulate lateral root development; Ca^{2+} transport activated by many amino acids; desensitization phenomenon but different from GLR3.3	Meyerhoff et al., 2005; Stephens et al., 2008; Teardo et al., 2011; Vincill et al.,2012 and 2013
GLR3.5	At2g32390	n/d	n/d	
GLR3.6	At3g51480	n/d	Regulation of long-distance signalling in wound-stimulated distal production of JA	Mousavi et al., 2013
GLR3.7	At2g32400	PM	Regulation of growth rate of pollen tube	Michard et al., 2011
Mechanosensitive Cation-permeable Channel (MCA)				
MCA1	At4g35920	PM	Mediate Ca^{2+} influx/signalling by mechanical stimuli, regulation of root mechanotransduction; highly expressed in guard cells and root vascular tissue, possible involvement in symplasmic Ca^{2+} transport and/or Ca^{2+} signal in endodermal and vascular cells as well as stomatal dynamics; its expression negatively correlated with total calcium accumulation in plant; *mca1/mac2* sensitive to Mg^{2+} that is suppressed by additional Ca^{2+} supplementation	Nakagawa et al., 2007; Yamanaka et al., 2010; Conn et al., 2012; Furuichi et al., 2012
MCA2	At2g17780	PM	Mediate Ca^{2+} influx/signalling by mechanical stimuli; possible involvement in symplasmic Ca^{2+} transport and/or Ca^{2+} signal in endodermal and vascular cells; *mca1/mac2* sensitive to Mg^{2+} that is suppressed by additional Ca^{2+} supplementation	Yamanaka et al., 2010

25

Continued

Two-Pore Channel (TPC)				
TPC1	At4g03560	TM	Sense luminal Ca^{2+} concentration and mediate Ca^{2+} signalling of downstream activation of S-type anion channel in stomata; regulation of calcium accumulation in epidermis; post-transcriptionally regulated by wounding	Furuichi et al., 2001; Peiter et al., 2005; Islam et al., 2010; Rienmüller et al., 2010; Gfeller et al., 2011; Dadacz-Narloch et al., 2011; Gilliham et al., 2011a; Kuśnierczyk et al., 2011

[*]Membrane localisation: P = plastids, ER = endoplasmic reticulum; PM = plasma membrane; TM = tonoplast membrane.

PCD = programmed cell death; JA = jasmonates; Met = methionine; Arg = arginine; Gln = glutamine; Lys = lysine; Val = valine; Ile = isoleucine; His = histidine; Cys = cysteine; Ala = alanine; Ser = serine; n/d = no data.

1.3.1 The role of plasma membrane Ca²⁺ channels in calcium storage

Plasma membrane Ca^{2+}-permeable channels such as those encoded by *MCA*, *ANN1*, *CNGC* and *GLR* members listed in Table 1.1 mediate Ca^{2+} influx across the plasma membrane. They are also proposed to regulate cytosolic Ca^{2+}-signalling during different biological processes, and some of these transporters have been reported to be associated with calcium nutrient uptake and storage in plants (Table 1.1, references therein). Those calcium uptake- or storage-related genes include *GLR3*.2, which is predominantly expressed in the vascular tissue of roots and its overexpression induces a calcium deficiency phenotype of plants without altering the total calcium content of shoots (Kim et al., 2001). The overexpression of *MCA1* has been found to enhance calcium accumulation in the roots but simultaneously induces a calcium -sensitive phenotype that is associated with the induction of leaf lesions and a growth reduction in high calcium conditions – this is similar with the phenotype of the loss-of-function *cax1/cax3* mutant lines (as discussed later) (Nakagawa et al., 2007; Conn et al., 2011 and 2012). The role of MCA1, proposed by Nakagawa et al (2007), is that it mediates root Ca^{2+} uptake, however later analysis by Conn et al (2012) that compares the transcriptional abundance of ion transporters with elemental accumulation in plants reveals that the total calcium content of Arabidopsis is negatively correlated with *MCA1* expression arguing against such a role (Conn et al., 2012). The detection of *MCA1* transcripts in guard cells suggests a putative role of MCA1 in modulation of leaf transpiration and stomatal closure that also is associated with calcium storage in plants (Conn et al., 2012; Gilliham et al., 2011b). *CNGC1* is expressed in the roots and encodes a plasma membrane Ca^{2+} channel that mediates Ca^{2+}-uptake into the roots. The disruption of *CNGC1* decreases the total calcium amount in the shoots (by 6-22%) and is proposed to reduce root Ca^{2+}-uptake (Ali et al., 2006; Ma et al., 2006). *CNGC2*, another member of the *CNGC* family encodes a plasma membrane Ca^{2+} channel, whose transport is activated by cAMP and was also found to be permeable to K^+ (Leng et al., 2002; Ali et al., 2007). The *cngc2* loss-of-function mutant line accumulates less calcium in the leaves and displays a Ca^{2+} hypersensitive phenotype, suggesting that CNGC2 probably mediates Ca^{2+}-uptake into leaf cells from the apoplasm (Chan et al., 2008; Conn and Gilliham, 2010; Ma et al., 2010). Apoplastic Ca^{2+} enters into the cytoplasm by crossing the plasma membrane passively down its electrochemical gradient, assisted by Ca^{2+}-permeable channels on the plasma membrane; however, no obvious evidence suggests there is a direct correlation between Ca^{2+} channels such as CNGC1 and CNGC2 with the cell-specific accumulation pattern of calcium in Arabidopsis leaves (White and Broadley, 2003; Conn and Gilliham, 2010). Moreover, there is no evidence that links known plasma membrane Ca^{2+} transporters/channels with cell-type specific calcium storage in as described in model of Figure 1.2.

1.3.2 The role of vacuolar membrane Ca^{2+} transporters in calcium storage

The majority of cellular Ca^{2+} uptake from the apoplasm is actively carried against an electrochemical gradient and stored in the vacuole by tonoplast-localised Ca^{2+} transporters. Therefore, vacuolar Ca^{2+}-transporters are likely to play a major role in the regulation of cell-type calcium accumulation in plants (Pottosin and Schönknecht, 2007; McAinsh and Pittman, 2009; Conn and Gilliham, 2010). Among these gene families listed in Table 1.1, *CAXs*, *ACA4*, *ACA11* and *TPC1* are reported to encode proteins that are targeted to the vacuolar membrane (Geisler et al., 2000; Peiter et al., 2005; Shigaki and Hirschi, 2006; Lee et al., 2007). CAX2 and CAX4-6 appear to be related to cation homeostasis for metals such as Zn^{2+}, Cd^{2+} and Mn^{2+}, or are related to hormone responses rather than calcium accumulation in plants (Table 1.1, reference therein). The other two CAX members – CAX1 and CAX3 (from *Arabidopsis thaliana*) mediate Ca^{2+} uptake into vacuoles when expressed in *Saccharomyces cerevisiae* (Hirschi, 1996; Carter et al., 2004; Manohar et al., 2011). The simultaneous loss-of-function of Arabidopsis *CAX1* and *CAX3* results in a significant reduction in mesophyll calcium by up to 35% in the *cax1/cax3* double mutant line (Conn et al., 2011). Additionally, *CAX1* is preferential expressed in the mesophyll, while *CAX3* is usually expressed in the roots but shows a mesophyll-preferential expression pattern in leaves in *cax1* plants and is thought to physiologically compensate for the absence of *CAX1* (Conn et al., 2011; Conn et al., unpublished results). Thereby, CAX1 contributes to the mesophyll-specific calcium compartmentation in leaves, whereas CAX3 usually does not ordinarily function in mesophyll calcium storage unless it is compensating for CAX1 in the loss-of-function *cax1* line (Conn et al., unpublished results). *ACA4* and *ACA11*, similar to *CAX1* are also expressed preferentially in the mesophyll and have been demonstrated to encode Ca^{2+} transporters on the vacuolar membrane but they function in Ca^{2+}-signalling that regulates a salicylic acid (SA)-dependent program cell death (PCD) (Boursiac et al., 2010). The *aca4*/*aca11* double mutant line accelerates the plant defence response to *Pseudomonas syringae* (*P. syringae*), induces leaf lesions and impairs plant growth, which can be restored by additional anion supplements (e.g. Cl^-, PO_4^{3-} and NO_3^-) (Geisler et al., 2000; Lee et al., 2007; Boursiac et al., 2010; Conn et al., 2011). Compared to the wild type plant, calcium accumulation is not impaired in any of the *aca4* or *aca11* single mutant lines, or the *aca4*/*aca11* double mutant line, suggesting that ACA4 and ACA11 are likely to play little or no role in calcium storage in plants (Conn et al., 2011). Instead, the unique slow vacuolar (SV) Ca^{2+} channel gene, *TPC1* exhibits an epidermal and bundle sheath preferential expression pattern within leaves (Gilliham et al., 2011a). The knock-out *tpc1* mutant line has a significantly increased calcium accumulation in the epidermis

but not an altered mesophyll calcium compartmentation (Gilliham et al., 2011a). This phenotype is speculated to be attributed to a Ca^{2+} release from the epidermis by TPC1 on the tonoplast, the majority of calcium is still stored in mesophyll and so an insignificant change in total leaf calcium content was observed in the *tpc1* line, in this case the role of TPC1 is proposed to be the release calcium from the vacuoles and the reduction of calcium accumulation in the epidermis (Gilliham et al., 2011a). Notably, TPC1 possesses two EF-hand Ca^{2+}-binding domains that directly sense the luminal Ca^{2+} concentration and regulates the SV channels gating (Dadacz-Narloch et al., 2011; Hedrich and Marten, 2011; Schulze et al., 2011). Likewise, excessive calcium accumulated in the vacuoles of epidermis can be sensed and moved out by TPC1 to constantly maintain a low epidermal calcium level in Arabidopsis perhaps even in extreme circumstances such as in the *cax1*/*cax3* line where calcium accumulation is not altered in the epidermis and still tends to be preferentially in the mesophyll whilst withstanding a reduction in the capacity of the mesophyll to store calciumCa (Dadacz-Narloch et al., 2011; Gilliham et al., 2011a; Schulze et al., 2011; Conn et al., unpublished results). The disruption of *CAX1*, *CAX3* and *TPC1* may disorder this cell-type specific calcium accumulation in Arabidopsis. Comparison of all mesophyll-specific vacuolar Ca^{2+} transporters, *CAX1* expression is unique in that it is the one positively correlated with relative leaf calcium concentration across 15 Arabidopsis ecotypes (Conn et al., 2011). Together, it is believed that the mesophyll-specific calcium compartmentation in leaves is achieved via vacuolar Ca^{2+} uptake in mesophyll by CAX1 and vacuolar Ca^{2+} release in epidermis and bundle sheath conferred by TPC1; CAX1 is the major Ca^{2+} transporter controlling calcium accumulation in Arabidopsis (Conn et al., 2011; Gilliham et al., 2011a; Conn et al., unpublished results).

In terms of the nature of cell-type calcium accumulation in plants, several mechanisms have been proposed of how Ca^{2+} is stored in particular cell-types and the consequences of disruption of this have described (Conn and Gilliham, 2010; Conn et al., 2011). One of the possible reasons is that the majority of calcium and the large proportion of phosphate (Pi) within plants is stored in the vacuoles of leaves but CaPi is an insoluble compound, thereby this elements have to be stored in different cell types within leaves in order to retain high amounts of soluble/nutrient calcium and Pi in plants. For instance, in eudicots about ~90% of total calcium is accumulated in the mesophyll with less that 10% in the epidermis, whereas for Pi about 0~10% is stored in the mesophyll whereas 51~60% is found within the epidermis (Conn and Gilliham, 2010). Nevertheless, no studies have directly tested the specific reason for why calcium is stored in the mesophyll of eudicots or the epidermis of monocots rather than in the other cell-types (e.g. bundle sheath) (Conn and Gilliham, 2010).

1.4 Cross talk between calcium accumulation and Ca²⁺ signalling in plants

1.4.1 Correlation with CAX1 and calcium biofortification

As the critical transporter in calcium accumulation in plants, CAX1 is a low affinity and high capacity Ca^{2+} transport protein (K_m= 10–15 μM), that exchanges Ca^{2+} with protons (Hirschi et al., 1996). It contains an N-terminus autoinhibitory region within the first 36 amino acids (aa) of the open reading frame (ORF); full-length *CAX1* expressed in the calcium-hypersensitive yeast strain K667 fails to suppress the calcium-sensitive phenotype unlike a truncated short-CAX1 (*sCAX1*) with the N-terminus autoinhibitory region removed (Shigaki et al., 2001; Pittman et al., 2002a and 2002b). The yeast two-hybrid (Y2H) system was employed to decipher the key amino-acid residues (residue 56-62) within CAX1 that interacts with the N-terminal autoinhibitory region and inhibits CAX1 activity (Shigaki et al., 2001; Pittman et al., 2002b). In Arabidopsis, several proteins have been demonstrated *in vitro* to bind the autoinhibitory region of CAX1 for the activation of its Ca^{2+}/H^+ antiport capacity, such as SOS2, CXIP1 and CXIP4 (Cheng and Hirschi, 2003; Cheng et al., 2004a and 2004b). Hirschi and co-workers have introduced the *sCAX1* into a number of plant species, and the constitutive expression of *sCAX1* enhances calcium accumulation in tomato, potato, lettuce, carrot, tobacco and rice (from ~15% up to ~300%) (Hirschi, 1999; Park et al., 2004; Kim et al., 2005; Park et al., 2005b; Park et al., 2009; de Freitas et al., 2011; Kim, 2012). Amongst these, *sCAX1* overexpression doubled calcium accumulation in carrots and feeding trials increased the amount of calcium assimilated in rat by 40% compared to rats fed control carrots (Morris et al., 2008). In spite of this, the constitutive overexpression of de-regulated *CAX1* can also cause calcium-deficiency-related phenotypes in transgenic plants such as reduced biomass, necrotic necrosis of tobacco leaf tip and blossom end rot (BER) of tomato fruit (Hirschi, 1999; de Freitas et al., 2011). Leaf tips and fruit are lowly-transpiring organs, and as calcium distribution primarily follows apoplastic flow in these tissues, Ca^{2+} supply is minimal (Gilliham et al., 2011b). As tonoplast Ca^{2+} uptake tends to affect Ca^{2+} flux across the plasma membrane into the cytoplasm, overexpression of *sCAX1* lowers $[Ca^{2+}]_{apo}$ in transgenic tomato, and presumably in transgenic tobacco, as it suffers similar calcium deficient phenotypes (Hirschi, 1999; MacRobbie, 2006a and 2006b; Conn and Gilliham, 2010; Dayod et al., 2010; de Freitas et al., 2011; Gilliham et al., 2011b). These calcium-deficiency phenotypes in *sCAX1*-overexpressing plants are proposed to be the consequence of lower $[Ca^{2+}]_{apo}$ which then leads to insufficient calcium delivery into low-transpiring organs (e.g. leaf tip and fruit) (Dayod et al., 2010; Gilliham et al., 2011b). Therefore, the simple overexpression of *sCAX1* is not likely to be an optimal strategy for calcium biofortification in plants as it disturbs normal growth, although the supply of additional calcium to the

growth medium seems to rescue the calcium-deficiency phenotype of transgenic tobacco (Hirschi, 1999; Dayod et al., 2010; Gilliham et al., 2011b).

As discussed above, calcium accumulation in plants displays a cell-specific pattern. This pattern is still evident even if the two major vacuolar Ca^{2+} transporter genes responsible for calcium accumulation in vacuoles (*CAX1* and *CAX3*) are both disrupted (Conn et al., unpublished results). Dayod et al (2010) propose that the manipulation of Ca^{2+} transporter gene expression and activity in a cell-specific manner is likely to be a more advantageous approach to improve calcium biofortification in plant vegetative tissue as it is likely to have minimal side-effects on other physiological processes. Notably, the loss-of-function *cax1* mutant plant is reported to accumulate 22% higher calcium in seeds compared to wildtype plants, whereas *sCAX1* overexpression plants accumulates less calcium in seeds; the reason for this is not yet clear (Phushon et al., 2012). But this study potentially provides an example for improvement of calcium biofortification in grains of cereals.

1.4.2 Perturbed calcium storage associated with impaired intracellular Ca^{2+}-signalling

Ca^{2+} serves as a versatile signalling molecule, which transmits its message through transient Ca^{2+}-oscillations in the cytoplasm facilitated by Ca^{2+} transporters/channels (McAinsh and Pittman, 2009; Dodd et al., 2010). Not surprisingly, the misexpression of Ca^{2+} transporters or channels related to calcium storage can impair intracellular signalling, as those Ca^{2+} transporters also function in Ca^{2+} signalling. For instance, GLR3.2 regulates lateral root development via generation of Ca^{2+} signalling in the phloem; the knock-out *glr3.2* line produces greater lateral root primordia and impairs the wound-stimulated Ca^{2+} signalling into distal production of jasmonates (JA) from unwound leaves (Mousavi et al., 2013; Vincill et al., 2013). MCA1 has been found to mediate mechanical stimulated Ca^{2+}-uptake/signalling, loss-of-function *mca1* mutant plant abolishes the ability of primary roots to penetrate the harder agar (1.6 %), suggesting that MCA1 may be play a role in sensing the hardness of agar or soil (Nakagawa et al., 2007). CNGC1 is reported to mediate the Ca^{2+} signalling in production of root nitric oxide (NO), and the *cngc1* mutant line produces less NO in roots during gravistimulation (Ma et al., 2006). Similarly, CNGC2 mediates Ca^{2+} influx activated by cAMP across the plasma membrane and cytosolic Ca^{2+}-signalling required for the generation of NO in a calmodulin (CaM)-dependent manner to stimulate hypersensitive response (HR) to *P. syringae* in leaves (Clough et al., 2000; Ali et al., 2007; Ma et al., 2010). The *cngc2* mutant line also displays leaf early senescence due to endogenous NO production being abolished (Ma et al., 2010). TPC1 as a SV Ca^{2+} channel regulates stomatal closure via priming the S-type anion channel on the plasma membrane in response to high external Ca^{2+} but not to abscisic acid (ABA) and methyl jasmonate (MeJA) (Peiter et

al., 2005; Islam et al., 2010; Rienmüller et al., 2010). *TPC1* is regulated by wounding at a posttranscriptional level in JA dependent manner, meanwhile the *fou2* line with the point mutant D454N displays overproduction of JA (Bonaventure et al., 2007; Ranf et al., 2008; Beyhl et al., 2009; Gfeller et al., 2011). The loss-of-function *cax1/cax3* mutant line has a significant reduction of calcium compartmentation in the mesophyll as discussed in Section 1.3.2 but also has a number of physiological processes that are altered (Cheng et al., 2005; Conn et al., 2011; Cho et al., 2012; Conn et al., unpublished results). Physiological alterations in *cax1/cax3* include modified cell wall thickness, reduced stomatal aperture, transpiration and growth rates and increased shoot Pi accumulation. These all involve impaired intracellular Ca^{2+} signalling and are proposed to be correlated with the increased $[Ca^{2+}]_{apo}$, which is a direct consequence of the reduction of mesophyll calcium compartmentation in the *cax1/cax3* line (Cheng et al., 2005; Kudla et al., 2010; Conn et al., 2011; Liu et al., 2011; Conn et al., unpublished results). As a consequence, the reduced capacity for mesophyll calcium accumulation is correlated with impaired intracellular signalling that results in physiological alterations in the *cax1/cax3* line. Also, an increase in apoplastic pH and an insensitive response to external 3-Indoleacetic acid (IAA) observed in *cax1/cax3* line were also found in the *cax1* and *cax3* single mutant lines. This is attributed to the disruption of *CAX1* and/or *CAX3*, which reduces plasma membrane H^+-ATPase activity, increasing apoplastic pH, down-regulating plasma membrane auxin transporter AUX1 and reducing auxin permeability into cells (Cho et al., 2012). This stomatal insensitivity to IAA in *cax1*, *cax3* and *cax1/cax3* indicates that the loss of CAX1 and/or CAX3, rather than an alteration in calcium storage is reason for this phenotype (Cho et al., 2012; Conn et al., unpublished results). Moreover, the biofortification for calcium via the overexpression of *sCAX1* in tomato fruit, which lowers both $[Ca^{2+}]_{cyt}$ and $[Ca^{2+}]_{apo}$, presumably affects the cellular Ca^{2+} signalling network (de Freitas et al., 2011). More than 500 genes are misexpressed in tomato plants that overexpress *sCAX1*. These include 11 Ca^{2+}-binding proteins, 23 signalling-related proteins and 49 cell-wall proteins (22 up- and 27 down-regulated, including 5 Expansin proteins, 3 Xyloglucan endotransglucosylase hydrolases (XTH), 3 pectin-related proteins, 3 Glycosyl hydrolases and 7 glucanases). Resulting phenotypes include increased membrane leakage and BER symptoms in tomato fruit, and these are considered to be the impact of enhanced calcium storage on Ca^{2+}-signalling related proteins. In particular, the role of perturbed $[Ca^{2+}]_{apo}$ is thought to be significant as it results in significant cell wall modification (de Freitas et al., 2011). Two pathogen-related proteins of tomatoes – *PR* P2 precursor and *PR* leaf protein 4-like gene that are homologs of *PR4* and *PR1* from *Arabidopsis thaliana* (based on protein BLAST in National Centre for Biotechnology Information (NCBI) database) are up-regulated by ~8- and ~23-fold respectively by *sCAX1* overexpression. Similarly four *PR* genes are induced in *cax1/cax3* plants including *PR1* by 17-fold and *PR5* by 11-

fold (Conn et al., 2011; de Freitas et al., 2011). This *PR* gene up-regulation in calcium-biofortified s*CAX1* tomatoes and calcium-defected *cax1/cax3* lines suggests that calcium perturbation in plants by gain of *sCAX1* or loss of *CAX1* and *CAX3* is likely linked to defects in proper pathogen response of plants. This could be reasonably hypothesised to be from certain perturbed pathogen-responsive Ca^{2+}-signalling elements and the result of a altered cell wall sturcture by high $[Ca^{2+}]_{apo}$. All this evidence suggests that the perturbed calcium homeostasis via misexpression of Ca^{2+} transporters/channels is likely to be associated with the impaired cellular Ca^{2+} signalling. This impaired cellular Ca^{2+} signalling is linked to the disruption of Ca^{2+}-signalling regulators at either the transcriptional or translational level, which could further induce cellular and physiological alterations in plants.

1.4.3 Biofortification for calcium with a minimal impact on intracellular Ca^{2+} signalling

In Arabidopsis, the role of the Ca^{2+} transporter CAX1 in calcium compartmentation is relatively well understood (Hirschi, 1999; Cheng et al., 2003; Conn et al., 2011; Conn et al., unpublished results). Due to its cell-preferential expression pattern in the leaf mesophyll, a strategy for increasing calcium content of leaves without perturbing leaf function was proposed by Dayod et al (2010). This involved the manipulation of Ca^{2+} transporter gene expression and Ca^{2+} transporter activity in the cell types in which these transporters are ordinarily expressed. This relies on the capacity of the mesophyll cells to deal with the extra calcium load whilst not accumulating additional calcium in cells that ordinarily have low calcium content (and may not be capable of dealing with such a high calcium load). Interestingly, another approach has been shown to be successful, performed by Wu et al (2012), where they co-expresses Arabidopsis *sCAX1* with a ER-localised Ca^{2+}-binding Calreticulin *CRT1*, from maize, in tobacco and tomato. This results in an increase in calcium accumulation in tobacco and tomato fruit together with an alleviation of the calcium deficiency phenotype in tobacco and of BER symptom in tomato fruit (Wu et al., 2012). This maize CRT1 has been reported to be a Ca^{2+}-binding protein and function as a stress-inducible regulator to positively facilitate plant adaptation to various abiotic and biotic stresses. Overexpression of *CRT1* is suggested to alleviate the adverse physiological alterations in plants overexpressing *sCAX1* due to sustained increases in $[Ca^{2+}]_{cyt}$ during Ca^{2+} signalling (Jia et al., 2009; Wu et al., 2012).

1.5 Thesis outline/hypotheses generation

The intention of the above review was to outline knowledge gaps that span the nexus between calcium transport, storage and signalling in plants. The reasons for this was to identify lines of experimentation that would assist in better understanding the underlying mechanisms that result in the

detrimental phenotypes associated with perturbed calcium storage. Knowledge of these would be valuable for attempting to avoid deficiency or toxicity symptoms when manipulating calcium levels in plants. Such studies should also lead to the elucidation of novel and physiologically relevant Ca^{2+}-signalling elements in a variety of pathways, so adding to the knowledge base for Ca^{2+} signalling in plants.

To summarise, the identified key facts and associated knowledge gaps are:

A) Specific Ca^{2+} transporters have specific roles in plant physiology, although gaining full comprehension of the roles of each transporter is difficult due to the interrelatedness, and multiseriate roles, of Ca^{2+}-signalling in plants.

B) In plants with loss-of-function of *CAX1* and *CAX3* there are many physiological perturbations caused by a limited ability to store calcium in the mesophyll and excess calcium in the apoplast transcriptional basis of these physiological perturbations has only been partially examined previously, and has concentrated on Ca^{2+}-transporters and cell wall related genes, but not on Ca^{2+}-signalling elements nor on biotic stress adaptation.

C) CAX1 has been identified as the major Ca^{2+} transporter modulating calcium storage in plants. Discovering the transcription regulator of *CAX1* and/or the Ca^{2+} signalling elements downstream of CAX1 will lead to a better understanding of the factors that control and rely upon cell-type calcium accumulation.

D) The manipulation of *CAX1* expression in plants, such as the overexpression of *sCAX1* in tomatoes or its loss-of-function together with *CAX3* in Arabidopsis, likely initiates pathogen responses in plants as evidenced by a stimulation of pathogen-related proteins. The signalling components correlated with this defect may be altered in these plants as well.

These knowledge gaps have led to the generation of these specific hypotheses:

i. The transcriptional regulators of *CAX1* and/or the signalling elements regulated by CAX1 are misexpressed in plants that have *CAX1*-misexpressed.

ii. Functional characterisation of genes misexpressed in *cax1* and/or *cax1/cax3* mutant lines will lead to the discovery of novel Ca^{2+}- signalling elements, or processes mediated by CAX1.

iii. Such studies will lead to a better understanding of the need for cell-specific calcium storage in plants.

Accordingly, to test these hypotheses, the aims of the following study were to:

1) To screen for and select an uncharacterised CAX1-related Ca^{2+}-signalling component,

2) To localise the corresponding gene and protein,

3) To misexpress the corresponding gene *in planta*,

4) To investigate its physiological role *in planta*.

To achieve these goals, this thesis is outlined as followed:

Chapter 1 is a preliminary literature review to identify knowledge gaps related to the connections between Ca^{2+}-transport, storage and signalling in plants.

Chapter 2 describes a screen conducted to identify a novel CAX1-related signalling component using loss-of-function *cax* mutant lines; the cloning of *CML41* and its initial *in silico* characterisation.

Chapter 3 investigates the Ca^{2+}-binding capacity of CML41 using an electrophoresis mobility assay.

Chapter 4 investigates the role of CML41 using misexpression

Chapter 5 identifies the subcellular localisation of CML41 and its interaction with a transcription factor *in planta* via bimolecular fluroescence assays.

Chapter 6 summarises the major characteristics of CML41 and discusses remaining questions and future experimental directions.

Attached appendices are publications that I have contributed towards whilst performing the work associated with this thesis:

1) The above review concerning aspects of Ca^{2+} transport has been published, in parts, as in Gilliham et al., 2011b, see Appendix 1.

2) An optimization of hydroponic growth method to develop a rapid screen for selection of transformants has been published, in Conn et al., 2013, see Appendix 2.

3) A part of my work continuing my Master project in characterisation of a Na^+ transporter gene from ancestral wheat – *Triticum monococcum* using heterologous expression systems including *Saccharomyces cerevisiae*, *Xenopus laevis* oocytes and *Arabidopsis* mesophyll protoplasts, has been published as a joint first author in Munns et al., 2012, see Appendix 3.

Chapter 2: Candidate gene screening, cloning and *in silico* analysis of novel regulatory genes associated with CAX1

2.1 Introduction

In plants, calcium is predominantly accumulated in the vacuoles of mesophyll cells (in eudicots) or those of epidermal cells (in cereal monocots). Long distance and intercellular Ca^{2+} transport is linked to apoplastic water flow (reviewed in Section 1.2.2, references therein). CAX1 has been identified as the major Ca^{2+} transporter for the regulation of mesophyll cell-specific calcium storage in Arabidopsis (Hirschi, 1999; Conn et al., 2011). The overexpression of *sCAX1* increases the amount of bioavailable calcium in a number of species (reviewed in Section 1.4.1, references therein). However, *sCAX1* overexpression also induces ion hypersensitivity to Mg^{2+}, K^+ and Na^+ and causes a calcium deficiency phenotype in tobacco, while reducing its root biomass. In tomato, sCAX1 overexpression can give rise to blossom end rot of tomato fruit and alters tomato root architecture, if insufficient Ca^{2+} is supplied to the plant (reviewed in Section 1.4.2, references therein). All of these are likely to be linked to the alterations in apoplastic Ca^{2+} and pH, and the perturbed responses to hormones caused by the overexpression of *CAX1* (Cheng et al., 2003; Conn et al., 2011; Cho et al., 2012).

At the same time, these studies nicely highlight clear complexities in the roles of particular Ca^{2+} transporters and associated signalling elements, and the utility of plants misexpressing Ca^{2+} transporters in order to perturb calcium concentration in various compartments to probe both their physiological roles and the signalling networks that depend on these transporters (Conn et al., 2011). Several CAX1 transport activators having already been discovered and characterised, including CXIP1, CXIP4 and SOS2 (Cheng and Hirschi, 2003; Cheng et al., 2004a and 2004b) but it is not known whether this is an exhaustive list of regulatory factors involved in controlling CAX1 expression and activity. Furthermore, the genomic consequences behind the altered phenotypes of plants misexpressing *CAX1* are less well understood, in particular this includes the targets downstream of CAX1 mediated Ca^{2+} signalling. Understanding the basis and need for the mesophyll cell-specific calcium storage mechanism in dicots, and the downstream signalling targets of CAX1 in Arabidopsis may provide knowledge required to improve biofortification strategies for calcium in plants, and minimise disturbance of other physiological processes (reviewed in Section 1.4.3, references therein), whilst increasing our knowledge of Ca^{2+} signalling networks in plants.

The *cax1/cax3* double mutant line exhibits a significant reduction in calcium accumulation in the mesophyll, meanwhile the expression of a range of other *CAXs* and *ACAs* are up-regulated seemingly in order to compensate the absence of *CAX1* and *CAX3* (Conn et al., 2011; Conn et al.,

unpublished results). Similarly, it appears likely that *CAX1* regulators or CAX1 downstream targets may also be significantly misexpressed in Arabidopsis with the loss of *CAX1* and/or *CAX3* expression, these include genes that encode Ca^{2+} signalling proteins directly downstream of perturbations in Ca^{2+} homeostasis caused by loss of CAX1 and/or CAX3. Therefore, these plants provide a perfect resource for probing Ca^{2+} signalling processes. The aim of this chapter is to screen for the candidate genes that are involved in the regulation of, or regulated by, *CAX1* in Arabidopsis by identifying genes that are correlated with *CAX1* expression in a variety of conditions. This will be investigated using global transcriptional profiling of a range of T-DNA insertional mutants for *cax1*, *cax3*, *cax1*/*cax3*, *cax1/sCAX1* and of Col-0 using *in silico* analysis.

2.2 Material and Methods

2.2.1 Analysis of *cax1*, *cax3*, *cax1/cax3* and *cax1/sCAX1* microarray

Microarrays were performed on *Arabidopsis thaliana* ecotype Columbia-0 wild type (Col-0), (Col-0 background) *cax1*, *cax3*, *cax1/cax3*, and *cax1/sCAX1* T-DNA insertion mutant lines by Kendal Hirschi's group (Conn et al., 2011; Hirschi et al., unpublished data). Briefly, the plant materials of Col-0 and these *cax* mutant lines were grown in half-strength Murashige and Skoog medium (½ MS medium) for 10 d in long-day conditions (16 hr light/8 hr dark, 22 ºC) and transferred into the soil for another 3 weeks; the whole plant was harvested for RNA extraction, as described in Conn et al (2011). The global transcriptional profile was measured on total RNA performed at Baylor College of Medicine Microarray Core Facility using the GeneChip Arabidopsis ATH1 genome array (Affymetrix) and normalised based on Robust Multichip Average method by Dr. Ute Baumann, ACPFG, as described in Irizarry et al (2003) and Conn et al (2011). I took the normalised expression data and searched for genes that were differentially expressed between each genotype, concentrating on genes encoding transcription factors, calcium signalling related proteins or protein kinases. These genes when identified were analysed using Genesis 1.7.6 following Sturn et al (2002). Genes that were commonly misexpressed in multiple genotypes where shortlisted and their relative expression between treatments was also used to calculate the correlation with *CAX1* expression, as plotted by Graphpad Prism v6. Additionally, ATTED-II version 6.1 database was used to search the co-expression network of those shortlisted candidates (http://atted.jp/top_search.shtml) (Obayashi et al., 2009 and 2010).

2.2.2 Plant material and growth condition

The plant materials used in all experiments of this dissertation were Col-0 or Col-0 background plants. Plants were grown in a hydroponic system as described in Conn et al (2013) (see Appendix 2). Briefly, each individual Arabidopsis seed was sown in a small hole made in the lid of a 1.5 mL black tube and supported on a 0.7% agar plug that contained germination solution (0.75 mM $CaCl_2$, 1 mM KCl, 0.25 mM $Ca(NO_3)_2$, 1 mM $MgSO_4$, 0.2 mM KH_2PO_4, 50 µM NaFe(III)EDTA, 50 µM H_3BO_3, 5 µM $MnCl_2$, 10 µM $ZnSO_4$, 0.5 µM $CuSO_4$, 0.1 µM Na_2MoO_3, pH = 5.6 by KOH). All seeds were stratified at 4°C in the dark for 2 d and germinated in short day conditions (9 hr light/15 hr dark, 22 ºC) for 1 week, after which they were transferred to Basal Nutrient Solution (BNS, 2 mM NH_4NO_3, 3 mM KNO_3, 0.1 mM $CaCl_2$, 2 mM KCl, 2 mM $Ca(NO_3)_2$, 2 mM $MgSO_4$, 0.6 mM KH_2PO_4, 1.5 mM NaCl, 50 µM NaFe(III)EDTA, 50 µM H_3BO_3, 5 µM $MnCl_2$, 10 µM $ZnSO_4$, 0.5 µM $CuSO_4$, 0.1 µM Na_2MoO_3, pH = 5.6 by KOH). Arabidopsis were then grown in BNS, which was replaced weekly unless otherwise specified.

2.2.3 RNA extraction and Calmodulin-like protein 41 (*CML41*) cloning

The shoot tissue of 6 week-old Arabidopsis plants were harvested and frozen in liquid nitrogen, from which total RNA was extracted using TRIzol (Invitrogen), this was then DNase-treated using the Turbo DNA-free kit (Ambion). Reverse transcription was performed to synthesize cDNA from RNA using SuperScript® III Reverse Transcriptase (Invitrogen). Using cDNA as template, the coding sequence (CDS) of *CML41* (618 bp) was amplified by Polymerase Chain Reaction (PCR) reaction using Phusion™ Hot Start High-Fidelity DNA polymerase (FINNZYMES) with the primers CML41_CDS_F and CML41_CDS_R as listed in Table 2.1 and following the manufacturers' instructions. Additionally, a PCR to amplify *CML41* CDS without the stop codon (*CML41*-stop) was performed by Bradleigh Hocking using the same conditions but with different primer sets (as listed in Table 2.1). Both PCR amplification products were ligated into the Gateway® entry vector pCR8/GW/TOPO (Invitrogen) by TOPO TA cloning after an A-tailing reaction following the manufacturers' instructions. Meanwhile, I identified a smaller PCR product about 500 bp in size, which was always obtained and this, which was designated as *CML41-Short* (*CML41S*); whereas *CML41* (618 bp) was designated as *CML41-Full-Length* (*CML41FL*). Such *CML41S* PCR products then were ligated into Gateway® entry vector pENTR™/D-TOPO (Invitrogen) by Directional TOPO cloning following the manufacturers' instructions. All TOPO cloning reactions were transformed into TOP10 Chemically Competent *E. coli* cells (Invitrogen) using heat-shock at 42 ºC for 30 sec. The sequence of *CML41FL*, *CML41FL*-stop, *CML41S* and *CML41S*-stop was confirmed in the entry

vectors via sequencing with the primer M13_Forward (5'-GTAAAACGACGGCCAGT-3')
(performed by AGRF) before further subcloning.

Table 2.1 Primers used to clone *CML41* coding sequence from Arabidopsis cDNA. Primer
sequence underlined refers to directional cloning sequence used for directional TOPO cloning.

Product name	Primers	Sequence (5'-3')	Tm* (°C)	Product size
CML41FL	CML41_CDS_F	ATGGCAACTCAAAAAGAGAAACCT	61	618 bp
	CML41_CDS_R	CTAAACCGTCATCATTTGACGAAAC	62	
CML41S	CML41_CDS_F_CACC	CACCATGGCAACTCAAAAAGAGAAACCT	69	505 bp
	CML41_CDS_R	CTAAACCGTCATCATTTGACGAAAC	62	
CML41FL-stop	CML41_CDS_F	ATGGCAACTCAAAAAGAGAAACCT	61	615 bp
	CML41_CDS_R-stop	AACCGTCATCATTTGACGAAACTC	62	
CML41S-stop	CML41_CDS_F_CACC	CACCATGGCAACTCAAAAAGAGAAACCT	69	502 bp
	CML41_CDS_R-stop	AACCGTCATCATTTGACGAAACTC	62	

*Primer Tm as calculated by NetPrimer (http://www.premierbiosoft.com/netprimer/index.html)

2.2.4 *In silico* analysis of CML41 and its split variant

To analyse the difference between *CML41FL* and *CML41S*, their nucleotide sequence and
translated protein sequence were aligned using Geneious Pro v5.6 (Biomatters). The translated protein
sequence of CML41FL and CML41S was examined using InterProScan v4.8
(http://www.ebi.ac.uk/interpro/). TargetP (http://www.cbs.dtu.dk/services/TargetP/) was employed to
predict the protein localisation and, with the assistance from Dr. David Chiasson, to identify putative
cleavage sites for signal peptides. The gene locus of *CML41* – At3g50770 was used in the
Genevestigator (www.genevestigator.com) database to analyse expression of *CML41* in Arabidopsis
and to search for potential gene regulatory networks in which CML41 maybe involved (Grennan,
2006; Hruz et al., 2008).

2.3 Results

2.3.1 Screening for candidate genes using microarray analysis of cax mutants

The microarrays performed by K. Hirschi's group (Baylor College of Medicine, USA) on *cax1*, *cax3*, *cax1/cax3*, *cax1/sCAX1*, and wild-type Col-0 as control, were used to generate a list of candidate genes that are: likely to regulate *CAX1* expression or *CAX1* activity; involved in co-ordinating Ca^{2+} distribution in Arabidopsis; or, involved in signalling downstream of perturbations in Ca^{2+} caused by disruption of *CAX1* and/or *CAX3* expression.

Compared to the gene expression profile in the microarray of wild-type Col-0, the transcript level of about 1000 genes was significantly increased or decreased by ≥1-fold (log2) in the mutant lines *cax1*, *cax3*, *cax1/cax3* or *cax1/sCAX1* ($P < 0.05$) (Appendix 4). Amongst these, there were a total of: 78 genes encoding transcription factors; 19 CaMs/CMLs and CaM-binding proteins; 66 protein kinases; 4 cation proton exchangers (including *CAX1* and *CAX3*), and 6 calcium ATPases (Figure 2.1A). In the single mutant lines, only 12 genes were significantly misexpressed in the *cax1* line above a threshold of 1-fold (log2) (*CAX1*, *CAX3*, *CML41*, *bHLH137*, *ADR1*, *CML35*, *ANAC016*, At1g63750, *KIC*, *ACA10* and *SFAR3*, $P < 0.05$). Only 5 genes were misexpressed in the *cax3* line (*CAX3*, *TET8*, *PUP18*, At2g22880 and At1g19380, $P < 0.05$) and 5 genes in *cax1/sCAX1* (*CAX1*, *CAX3*, *CML41*, *bHLH137* and *δVPE*, $P < 0.05$) (Figure 2.1B).

A

-3.0 1:1 3.0

	cax1	cax3	cax1/cax3	cax1/scCAX1

Gene ID	Description
At2g38170	"CAX1, calcium exchanger"
At3g51860	"CAX3, cation exchanger"
At5g13330	AP2 domain-containing transcription factor family protein
At2g44940	"AP2 domain-containing transcription factor TINY, putative"
At3g50260	"AP2 domain-containing transcription factor, putative"
At1g01250	"AP2 domain-containing transcription factor, putative"
At1g64380	"AP2 domain-containing transcription factor, putative"
At3g61630	"AP2 domain-containing transcription factor, putative"
At1g77640	"AP2 domain-containing transcription factor, putative"
At5g50915	"bHLH137, basic helix-loop-helix (bHLH) family protein"
At2g18300	"bHLH064, basic helix-loop-helix (bHLH) family protein"
At3g47640	"bHLH047, basic helix-loop-helix (bHLH) family protein"
At5g67110	"bHLH073, basic helix-loop-helix (bHLH) family protein"
At1g51140	"bHLH122, basic helix-loop-helix (bHLH) family protein"
At3g61950	"bHLH067, basic helix-loop-helix (bHLH) family protein"
At3g07340	"bHLH062, basic helix-loop-helix (bHLH) family protein"
At5g48560	"bHLH078, basic helix-loop-helix (bHLH) family protein"
At2g42280	"bHLH130, basic helix-loop-helix (bHLH) family protein"
At4g00050	"bHLH006, basic helix-loop-helix (bHLH) family protein"
At4g34590	"bZIP11, bZIP transcription factor family protein"
At3g02310	developmental protein SEPALLATA2/floral homeotic protein (AGL4) (SEP2)
At1g13260	DNA-binding protein RAV1 (RAV1)
At2g36080	"DNA-binding protein, putative, RAV Transcription Factor Family"
At3g55560	"AGF2, DNA-binding protein-related"
At5g25190	"AtERF3, ethylene-responsive element-binding protein, putative"
At1g72360	"AtERF73, ethylene-responsive element-binding protein, putative"
At1g67970	"heat shock factor protein, putative (HSF5) / (HSTF5)"
At4g18880	heat shock transcription factor 21 (HSF21)
At3g61890	homeobox-leucine zipper protein 12 (HB-12) / HD-ZIP transcription factor 12
At2g46680	homeobox-leucine zipper protein 7 (HB-7) / HD-ZIP transcription factor 7
At1g62990	homeodomain transcription factor (KNAT7)
At5g49330	"MYB111, myb family transcription factor"
At5g67300	"MYB44, myb family transcription factor"
At4g37180	myb family transcription factor
At2g38090	myb family transcription factor
At1g74650	"MYB31, myb family transcription factor (cY13)"
At1g63910	"MYB103, myb family transcription factor "
At2g47190	"MYB2, myb family transcription factor "
At3g27810	"MYB21, myb family transcription factor "
At4g34990	"MYB32, myb family transcription factor "
At4g38620	"MYB4, myb family transcription factor"
At5g26660	"MYB86, myb family transcription factor"
At5g12870	"MYB46, myb family transcription factor "
At1g18710	"MYB47, myb family transcription factor"
At1g18570	"MYB51, myb family transcription factor "
At4g01680	"MYB55, myb family transcription factor "
At1g09540	"MYB61, myb family transcription factor"
At4g22680	"MYB85, myb family transcription factor"
At1g01010	"ANAC001, no apical meristem (NAM) family protein"
At1g02220	"ANAC003, no apical meristem (NAM) family protein"
At1g34180	"ANAC016, no apical meristem (NAM) family protein"
At1g52890	"ANAC019, no apical meristem (NAM) family protein"
At2g17040	"ANAC022, no apical meristem (NAM) family protein"
At3g04070	"ANAC047, no apical meristem (NAM) family protein"
At5g18270	"ANAC087, no apical meristem (NAM) family protein"
At5g13180	"ANAC083, no apical meristem (NAM) family protein"
At1g69490	"ANAC029, no apical meristem (NAM) family protein"
At2g46770	"ANAC043, no apical meristem (NAM) family protein"
At1g32770	"ANAC012, no apical meristem (NAM) family protein"
At4g28500	"ANAC073, no apical meristem (NAM) family protein"

Continued

cax1	cax3	cax1/cax3	cax1/sCAX1	

At1g28470 — "ANAC010, no apical meristem (NAM) family protein"
At1g27360 — "SPL11, squamosa promoter-binding protein-like 11"
At2g42200 — "SPL9, squamosa promoter-binding protein-like 9"
At3g02150 — "TCP17, TCP family transcription factor, putative"
At3g06160 — AP2/B3-like transcriptional factor family protein
At4g31800 — "WRKY18, WRKY family transcription factor"
At2g30250 — "WRKY25, WRKY family transcription factor"
At5g07100 — "WRKY26, WRKY family transcription factor"
At2g38470 — "WRKY33, WRKY family transcription factor"
At5g22570 — "WRKY38, WRKY family transcription factor"
At3g01970 — "WRKY45, WRKY family transcription factor"
At4g01720 — "WRKY47, WRKY family transcription factor"
At5g49520 — "WRKY48, WRKY family transcription factor"
At4g23810 — "WRKY53, WRKY family transcription factor"
At1g62300 — "WRKY6, WRKY family transcription factor"
At2g25000 — "WRKY60, WRKY family transcription factor"
At5g13080 — "WRKY75, WRKY family transcription factor"
At5g46350 — "WRKY8, WRKY family transcription factor"
At2g44745 — "WRKY12, WRKY family transcription factor"
At5g25830 — zinc finger (GATA type) family protein
At3g15050 — "IQD10, calmodulin-binding family protein"
At3g59690 — "IQD13, calmodulin-binding family protein"
At4g00820 — "IQD17, calmodulin-binding protein-related"
At4g33050 — "IQM1, calmodulin-binding family protein"
At1g73805 — "ICS1, calmodulin-binding protein"
At1g73805 — calmodulin-binding protein
At5g26920 — "CBP60g, calmodulin-binding protein"
At4g31000 — calmodulin-binding protein
At2g26190 — calmodulin-binding family protein
At3g51920 — "CML9/CAM9, calmodulin-9"
At2g41100 — "CML12/TCH3, touch-responsive protein/calmodulin-related protein 3"
At2g41410 — "CML35, calmodulin, putative"
At1g76650 — "CML38, calcium-binding EF hand family protein"
At3g01830 — "CML40, calmodulin-related protein, putative"
At3g50770 — "CML41, calmodulin-related protein, putative"
At1g21550 — "CML44, calcium-binding protein, putative"
At5g39670 — "CML45, calcium-binding EF hand family protein"
At3g47480 — "CML47, calcium-binding EF hand family protein"
At2g46600 — "calcium-binding protein, putative"
At5g57630 — "CIPK21, CBL-interacting protein kinase 21, putative"
At5g10930 — "CIPK5, CBL-interacting protein kinase 5"
At1g01140 — "CIPK9, CBL-interacting protein kinase 9 "
At5g18470 — curculin-like (mannose-binding) lectin family protein
At2g30500 — "NET4B, kinase interacting family protein"
At1g67520 — lectin protein kinase family protein
At5g60280 — "LecRK-I.8, lectin protein kinase family protein"
At1g53070 — legume lectin family protein
At2g13790 — "BAK7/SERK4, leucine-rich repeat family protein / protein kinase family protein"
At1g34420 — leucine-rich repeat family protein / protein kinase family protein
At5g25930 — leucine-rich repeat family protein / protein kinase family protein
At4g08850 — leucine-rich repeat family protein / protein kinase family protein
At1g51790 — "leucine-rich repeat protein kinase, putative"
At1g51860 — "leucine-rich repeat protein kinase, putative"
At1g51800 — "leucine-rich repeat protein kinase, putative"
At1g51890 — "leucine-rich repeat protein kinase, putative"
At1g79620 — "leucine-rich repeat transmembrane protein kinase, putative"
At4g18640 — "leucine-rich repeat transmembrane protein kinase, putative"
At3g03770 — "leucine-rich repeat transmembrane protein kinase, putative"
At4g22730 — "leucine-rich repeat transmembrane protein kinase, putative"
At1g74360 — "leucine-rich repeat transmembrane protein kinase, putative"

Continued

				Gene ID	Description
cax1	cax3	cax1/cax3	cax1/sCAX1		
				At5g45800	"leucine-rich repeat transmembrane protein kinase, putative"
				At2g31880	"leucine-rich repeat transmembrane protein kinase, putative"
				At1g35710	"leucine-rich repeat transmembrane protein kinase, putative"
				At2g19190	"senescence-responsive receptor-like serine/threonine kinase, putative (SIRK)"
				At4g08470	"MAPKKK11/MEKK3, mitogen-activated protein kinase, putative"
				At1g01560	"MPK11, mitogen-activated protein kinase, putative / MAPK, putative "
				At5g43910	pfkB-type carbohydrate kinase family protein
				At1g14370	"APK2a, protein kinase "
				At2g40120	protein kinase family protein
				At1g09440	protein kinase family protein
				At1g24030	protein kinase family protein
				At1g56720	protein kinase family protein
				At5g39420	protein kinase family protein
				At2g18890	protein kinase family protein
				At5g11410	protein kinase family protein
				At5g58350	protein kinase family protein
				At4g23300	protein kinase family protein
				At5g58940	protein kinase family protein
				At1g70520	protein kinase family protein
				At2g32800	protein kinase family protein
				At4g23190	protein kinase family protein
				At1g70530	protein kinase family protein
				At4g25390	protein kinase family protein
				At2g31010	protein kinase family protein
				At4g23240	protein kinase family protein
				At4g04490	protein kinase family protein
				At5g25440	protein kinase family protein
				At4g23220	protein kinase family protein
				At4g11890	protein kinase family protein
				At4g23150	protein kinase family protein
				At4g04500	protein kinase family protein
				At2g45910	"PUB33, protein kinase family protein / U-box domain-containing protein"
				At5g65530	"protein kinase, putative"
				At5g02290	"protein kinase, putative"
				At5g47070	"protein kinase, putative"
				At2g39660	"protein kinase, putative"
				At3g46280	protein kinase-related
				At3g22060	receptor protein kinase-related
				At4g23140	"CRK6, receptor-like protein kinase 5 (RLK5)"
				At4g23310	"CRK23, receptor-like protein kinase, putative"
				At3g45860	"CRK4, receptor-like protein kinase, putative"
				At5g38210	serine/threonine protein kinase family protein
				At1g66880	serine/threonine protein kinase family protein
				At5g38240	"serine/threonine protein kinase, putative"
				At1g21240	"WAK3, wall-associated kinase, putative"
				At5g04220	"NTMC2T1.3, C2 domain-containing protein (sytC)"
				At1g64170	"CHX16, cation/hydrogen exchanger, putative"
				At4g23700	"CHX17, cation/hydrogen exchanger, putative "
				At1g27770	"ACA1, calcium-transporting ATPase 1, plasma membrane-type "
				At3g57330	"ACA11, calcium-transporting ATPase, plasma membrane-type, putative "
				At5g57110	"ACA8, calcium-transporting ATPase 8, plasma membrane-type"
				At4g29900	"ACA10, calcium-transporting ATPase, plasma membrane-type, putative"
				At3g22910	"ACA13, calcium-transporting ATPase, plasma membrane-type, putative "
				At3g63380	"ACA12, calcium-transporting ATPase, plasma membrane-type, putative "

B

			Locus	Description
cax1	cax3	cax1/sCAX1	At2g38170	"CAX1, calcium exchanger"
			At3g51860	"CAX3, cation exchanger"
			At3g50770	"CML41, Calmodulin-like protein"
			At1g33560	"ADR1, disease resistance protein (CC-NBS-LRR class), putative"
			At5g50915	"bHLH137, basic helix-loop-helix transcription factor"
			At2g41410	"CML35, Calmodulin-like protein"
			At1g34180	"ANAC016, no apical meristem (NAM) family protein"
			At1g63750	Disease resistance protein
			At2g46600	"KIC, calcium-binding protein, putative"
			At4g29900	"ACA10, P-type calcium ATPase"
			At2g42990	"SFAR3, GDSL-type seed fatty acid reducer"
			At2g22880	VQ motif-containing protein
			At2g23810	"TET8, TETRASPANIN family protein"
			At1g19380	expressed protein
			At1g57990	"PUP18, purine permease-related"
			At3g20210	"δVPE, vacuolar processing enzyme, putative "

Figure 2.1 Summary of misexpressed genes in *cax* mutants shortlisted from microarray analysis. A, summary of misexpressed genes encoding transcription factors, calcium signalling related proteins or protein kinases in between any of the listed genotypes (*cax1*, *cax3*, *cax1/cax3* and *cax1/sCAX1*). **B**, summary of misexpressed genes in *cax1*, *cax3* or *cax1/sCAX1*. Green indicates down-regulated transcription; red indicates up-regulated transcription.

Four genes misexpressed not only in the double mutant line but also in either of the single mutant lines or the complemented line (*cax1/sCAX1*) were further shortlisted in Table 2.2. Another five genes misexpressed in double mutants, encoding either transcription factors, CaMs/CMLs or kinases, and highly expressed in leaves tissues as indicated in the Arabidopsis eFP Browser database (http://bar.utoronto.ca/efp/cgi-bin/efpWeb.cgi) (Winter et al., 2007) were also shortlisted in Table 2.2. Mutation of these putative regulators of *CAX1* or CAX1-regulated targets (in Table 2.2) may result in a similar phenotype to *cax1* or *cax1/cax3* mutant lines in some aspects, and/or have a calcium-responsive/sensitive growth phenotype. For instance, as described in Cheng et al (2003 and 2005) and Conn et al (2011) *cax1* displays better growth than wild-type Col-0 with 1.5 mM $MnCl_2$ and 25 mM $MgCl_2$ supplementation, and *cax1/cax3* better tolerates Ca^{2+}-starvation conditions than wild-type Col-0. Therefore, a rapid screen was performed on T-DNA insertion lines of the corresponding genes listed in Table 2.2 using a hydroponic growth test alongside either Col-0 or *cax1* and *cax1/cax3* lines under various ionic treatments (Appendix 5). These lines were first identified as homozygous with the

primers listed in Appendix 6 (ordered from T-DNA Express database, http://signal.salk.edu/cgi-bin/tdnaexpress). However, none of these homozygous T-DNA insertion lines, including *ANAC047* – SALK_066615, *bHLH064* – SALK_090958C, *bHLH122* – SALK_049022C, *CML44* – SALK_107191C and *LRR-RLK* – SALK_061769C displayed any distinct phenotype from Col-0 or a similar growth to either *cax1* or *cax1/cax3* under Mn^{2+}, Mg^{2+} or Ca^{2+}-depletion treatments (Appendix 5). Nor did any T-DNA insertion line (of *CML35* – SALK_041710C, *ANAC016* – SALK_001597, *bHLH137* – SALK_141414) exhibit a clear Ca^{2+}-sensitive phenotype relative to wild-type Col-0 when grown in low (300 μM), normal (2 mM) or high (25 mM) Ca^{2+} conditions (Appendix 5). Interestingly one of the candidates, calmodulin-like gene 41 (*CML41*, At3g50770), had no T-DNA insertion line available in T-DNA Express database. As such, it was not possible to test whether the T-DNA insertion in the candidate *CML41* would result in an expected calcium-related phenotype. This may mean that the insertion in this gene is lethal or it is a chance event as it is a relative small gene (at 823 bp of mRNA). Therefore, other approaches were considered to further narrow down the number of candidates in Table 2.2.

Table 2.2 A further shortlisted candidates screened from Figure 2.1. '–' refers to insignificant change of corresponding gene expression in the indicated mutant line. All SALK lines have been identified as homozygous T-DNA insertion plant using primers listed in Appendix 6 following the method as described at url: http://signal.salk.edu/tdnaprimers.2.html.

Gene	Locus	T-DNA lines	Protein family	Mutant lines relative to Col-0, log (2) ratio, ($P < 0.05$)			
				cax1	*cax3*	*cax1/cax3*	*cax1/sCAX1*
ANAC016	At1g34180	SALK_001597	Transcription factor	0.91	-	2.30	-
ANAC047	At3g04070	SALK_066615		-	-	2.41	-
bHLH064	At2g18300	SALK_090958C		-	-	1.18	-
bHLH122	At1g51140	SALK_049022C		-	-	-0.91	-
bHLH137	At5g50915	SALK_141414		2.01	-	1.09	1.67
CML35	At2g41410	SALK_041710C	CaMs/CMLs	0.88	-	1.06	-
CML41	At3g50770	not available		3.20	-	3.85	2.79
CML44	At1g21550	SALK_107191C		-	-	1.52	-
LRR-RLK	At4g08850	SALK_061769C	Kinase	-	-	1.31	-

2.3.2 Strong and negative correlation of *CML41* with *CAX1* expression

In the shortlisted candidates, only *bHLH137* and calmodulin-like gene 41 (*CML41*, At3g50770) were consistently up-regulated when *CAX1* was absent in *cax1*, *cax1/sCAX1* and

cax1/*cax3* lines (Table 2.2). Comparative to *bHLH137*, the *CML41* transcription was better correlated with *CAX1* expression, albeit negatively (Figure 2.2).

ATTED-II is a database of functional and regulatory networks of genes based on public microarray datasets and provides a guide for studying regulatory relationships, since genes that function in related biological pathways often display correlated expression pattern (Eisen et al., 1998; Obayashi et al., 2009 and 2010). *CML41* in this ATTED-II database appears to have very strong co-expression with a few genes, including *CAX3* with a mutual rank of the Pearson's correlation coefficient (MR) of about 7.1 (Figure 2.3). As none of the available T-DNA insertion lines listed in Table 2.2 showed any significant calcium-related phenotypes these were not analysed further as part of this study. Instead, *CML41* which showed the strongest negative correlation with *CAX1* expression in the analysed *cax* mutant lines was considered as the best candidate for examination as a *CAX1* regulator or as a CAX1-regulated target.
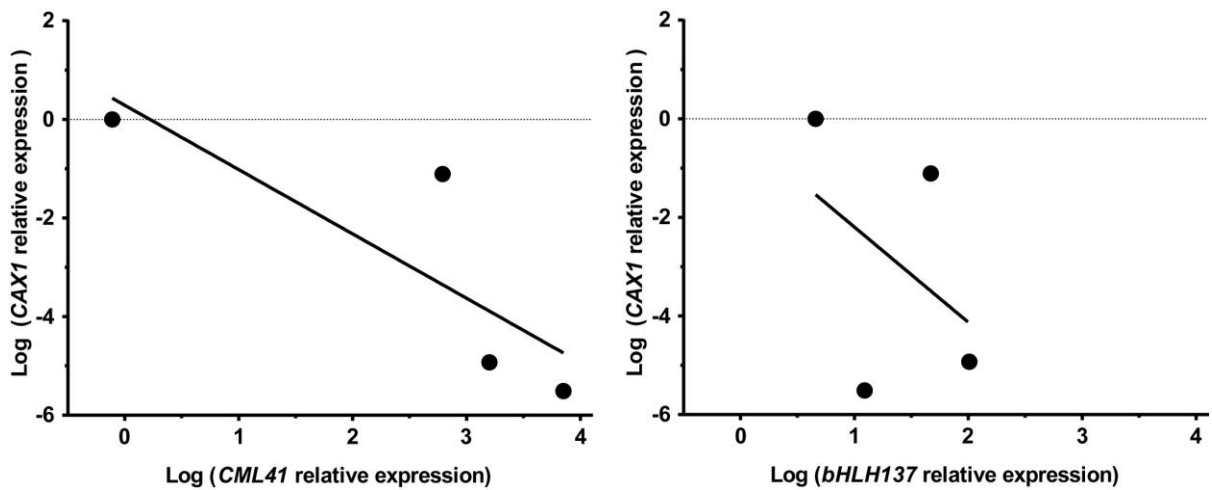
Figure 2.2 Correlation of *CML41* and *bHLH137* relative transcript level to *CAX1* relative expression in *cax1*, *cax3*, *cax1*/*cax3* and *cax1*/*sCAX1* lines.

At5g23660 MTN3

At5g13320 PBS3

At2g14610 PR1

At4g38460 GGR

At3g47480 calcium-binding..

At1g33960 AIG1

At5g58570

At5g41410 BEL1

At5g66890 CC-NBS-LRR

At3g50770 CML41

At5g44570

At2g29350 SAG13

At1g32960 SBT3.3

At3g51860 CAX3

At2g43570 CHI

At5g39090 transferase

At2g43510 ATTI1

At1g22930 T-complex 11

At5g38900 oxidoreductase

At3g51130

At2g42890 AML2

MR*	Cor*	Locus	Function
2.6	0.68	At2g29350	SAG13
4.6	0.64	At1g33960	AIG1 (AVRRPT2-INDUCED GENE 1)
4.7	0.6	At5g58570	unknown protein
7.1	0.62	At3g51860	CAX3 (CATION EXCHANGER 3)

Figure 2.3 Co-expression map of *CML41* in ATTED-II co-expression network database. MR indicates the mutual rank of the Pearson's correlation coefficient, MR < 50 is a strong coexpression; Cor indicates the correlation coefficient, ● and ○ indicate genes in the same color sharing similar Kyoto Encyclopedia of Genes and Genomes pathway. Explanation adapted from Obayashi et al (2010).

2.3.3 Calmodulin-like protein 41 (CML41) cloning

Initially, the PCR reaction to amplify the *CML41* cloning coding sequence was performed on the cDNA from the 5-6 week-old Col-0 shoot with 2 mM calcium supplementation (a normal level of calcium supply used in our laboratory). This PCR not only amplified an expected-size product of 618 bp for the *CML41* cDNA, but also another smaller-size and faint product around ~500 bp despite the manipulation of different PCR conditions (data not shown). Due to very low abundance of this ~500 bp product (named *CML41 Short* or *CML41S*), it was difficult to amplify *CML41S* from Col-0 grown at this normal level of calcium supplementation (Figure 2.4). The PCR amplification of this *CML41S* was attempted using various cDNA templates (Figure 2.4). In most cases, *CML41FL* appeared to be

the major PCR product in Col-0, *cax1* and *cax1*/*cax3* with a 2 mM calcium supply and from Col-0 and *cax1* treated with high calcium (12 mM) treatment (Figure 2.4). Notably, the *CML41S* PCR product were purified and cloned from high-calcium treated *cax1*/*cax3* plants and wildtype Col-0 mesophyll protoplasts. Such a result suggests that the transcription of *CML41FL* versus *CML41S* might be regulated in *cax1/cax3* lines in response to normal/high calcium treatment or in Col-0 leaf cells in response to cell-wall removal. This implicates that *CML41S* is likely to be a true splice variant of *CML41FL* and the two different proteins made bmay have distinct roles in the plant (Figure 2.4).
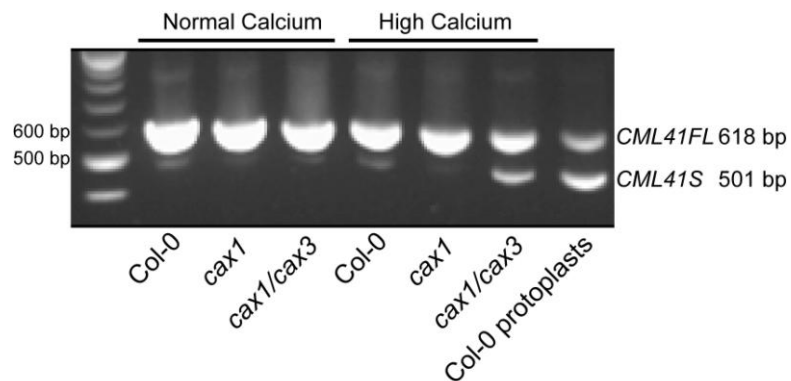
Figure 2.4 PCR amplification of *CML41* on various Arabidopsis cDNA templates. cDNA samples were synthesized from RNA of shoot tissue of 5-6 week-old wild-type Col-0, *cax1* and *cax1*/*cax3* grown hydroponically in short-day conditions (9 hr light/15 hr dark, 22 ℃) in 2 mM calcium supply or with an additional 12 mM high calcium treatment for 24 hr before harvest; cDNA of Col-0 protoplasts was reverse transcribed from RNA of 5-6 week-old Arabidopsis mesophyll protoplasts (method for protoplasts isolation refers to Section 5.2.2).

2.3.4 The alignment of *CML41* and its splicing variant

The 618 bp PCR fragments were cloned into pCR8/GW/TOPO, however the ~500 bp PCR fragments were rather difficult to clone in the right orientation into pCR8/GW/TOPO, so directional cloning was utilized to clone this ~500 bp PCR fragment into the pENTR/D/TOPO vector (Appendix 7 and 8). The sequence of both PCR fragments were determined by sequencing and compared by nucleotide alignment, suggesting that this shorter 501 bp fragment (*CML41S*) was a splice variant of *CML41FL* (Figure 2.5 and Appendix 9). The sequence alignment indicated that *CML41S* lacked 117 bp nucleotides of *CML41FL* positioned at 232 to 348 bp (Appendix 9).

Figure 2.5 Sequence alignments between *CML41FL* and its splicing variant. The coding sequence of *CML41FL* and *CML41S* was aligned by Geneious Alignment using Geneious Pro v5.6.5, the sequence in the box indicates the spliced region of *CML41FL* relative to *CML41S*; for the full nucleotide sequence of *CML41FL* and *S* in FASTA format refer to Appendix 9.

2.3.5 *in silico* analysis of *CML41*

InterProScan is a web-based database (http://www.ebi.ac.uk/interpro/) that provides a versatile tool to search for protein families, domains and functional sites within a protein sequence, including EF-hand domains (Day et al., 2002; Hunter et al., 2009 and 2012). As a Ca^{2+}-signalling transducer, CML family proteins possess various numbers of EF-hand Ca^{2+}-binding domains (from 2 up to 6), each of which consists of a helix-loop-helix secondary structure capable of binding Ca^{2+} (Day et al., 2002; McCormack and Braam, 2003, McCormack et al., 2005; Gifford et al., 2007). The translated amino-acid sequence of *CML41FL* and *CML41S* (Appendix 9) was entered into the InterProScan database to diagnose their calcium signature domains (Figure 2.6). Comparatively, CML41FL was predicted to contain 4 Ca^{2+}-binding EF-hand domains (EF-h1 to EF-h4), instead CML41S was predicted to have 3 EF-hand domains (New EF-h, EF-h3 and EF-h4). CML41S was spliced with the loss of 39 amino-acid residues (78 to 116) of CML41FL, which was positioned at the region between the EF-h1 and EF-h2 domains of CML41FL with the partial fragments of EF-h1 and EF-h2 likely to form a new EF-h domain in CML41S, as predicted by InterProScan.
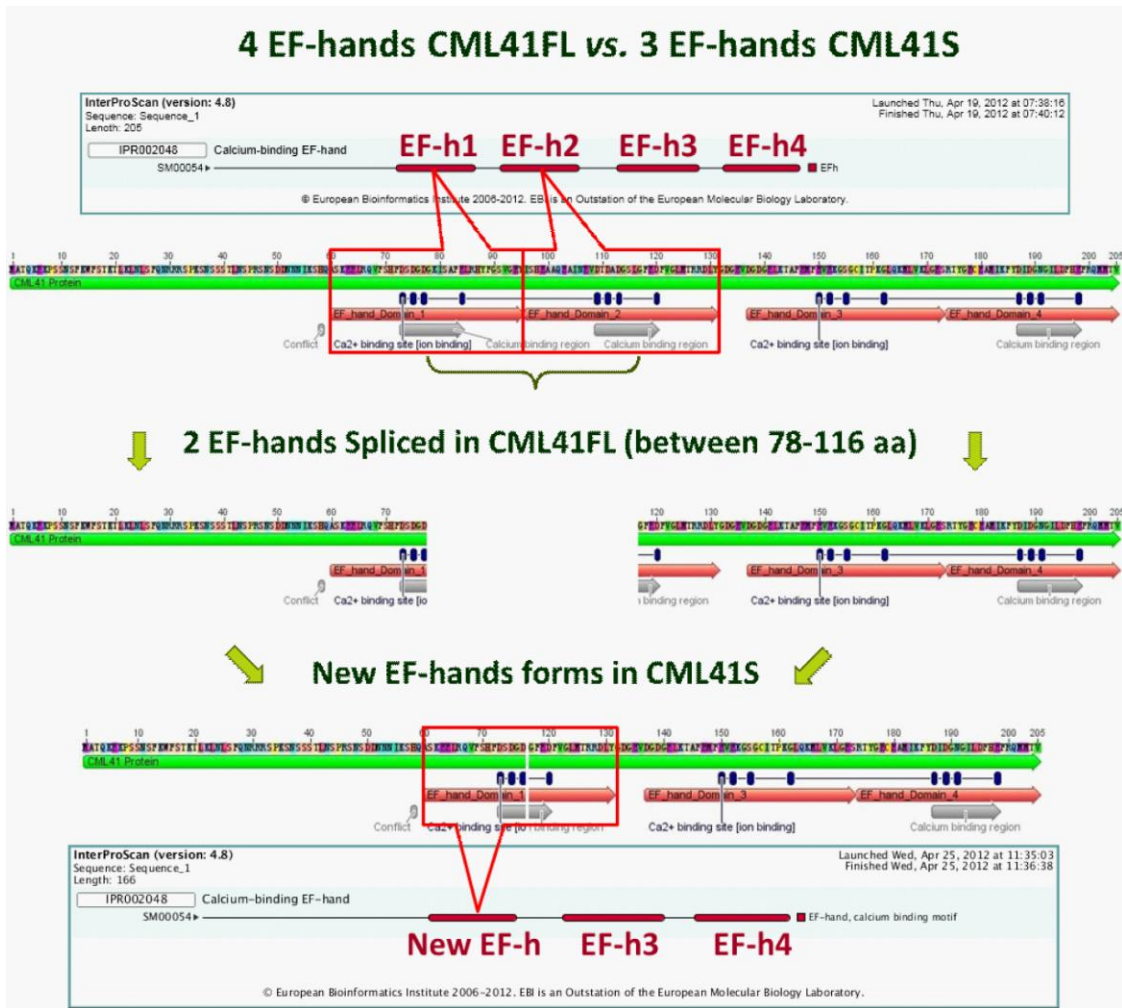
Figure 2.6 Integrated diagram of InterProScan output result and protein sequence alignment between CML41FL and CML41S. The red region of InterProScan result indicates the putative EF-hand Ca^{2+}-binding domains of the proteins. There is a 39 amino-acid gap between CML41FL (205 aa) and the CML41S (166 aa) alignment; for the full amino-acid sequence of CML41FL and S in FASTA format refer to Appendix 9.

TargetP 1.1 Server is an *in silico* analysis tool for the prediction of eukaryotic protein subcellular location including plant proteins (Emanuelsson et al., 2007). The output result of CML41FL and CML41S by TargetP indicated that both of proteins were predicted to contain chloroplast transit peptides (cTP) with a score of 0.97 (out of 1). This prediction got the highest reliability coefficient (RC) rank (score 1), a score proposed to be a reliable prediction by Emanuelsson et al (2007). As a result, the TargetP predicted subcellular localisation (Loc) of CML41FL and CML41S was in the chloroplasts. The putative cleavage site for the putative transit

peptide of CML41FL and CML41S was predicted to be at amino acid 46 on the N-terminus of the proteins. Experimental interrogation of this prediction is carried out in Chapter 5, as prediction programs are notoriously prone to error.


```
### targetp v1.1 prediction results ##############################
Number of query sequences:  2
Cleavage site predictions included.
Using PLANT networks.

Name                      Len    cTP    mTP     SP  other  Loc  RC  TPlen
----------------------------------------------------------------------
CML41FL                   205  0.970  0.070  0.010  0.044   C    1     46
CML41S                    166  0.971  0.073  0.009  0.041   C    1     46
----------------------------------------------------------------------
cutoff                         0.000  0.000  0.000  0.000
```
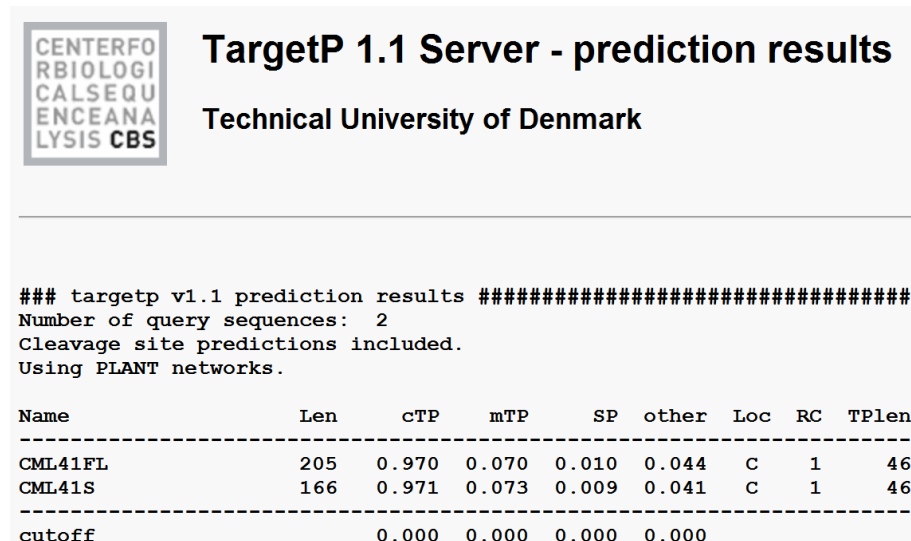
Figure 2.7 Subcellular localisation predictions of CML41FL and CML41S by TargetP v1.1. Len = protein sequence length; cTP = chloroplast transit peptide; mTP = mitochondria targeting peptide; SP = secretory signal peptide; other = no sorting signal; Loc = a predicted localisation (C = chloroplast; M = mitochondrial; S = signal peptide; - = other localisation; * = don't know); RC = reliability coefficient (score from 1 to 5 means from very reliable prediction to no false positives detected), RC = 1 indicates very reliable prediction; TPlen = the predicted length of signal amino-acid residues. Output explanation adapted from Emanuelsson et al (2007).

The web-based program Genevestigator collects in excess of 20,000 microarrays from a number of model organisms, including human, mouse, rat, Arabidopsis and barley to provide a meta-analysis database for gene expression and regulatory networks (Grennan, 2006; Hruz et al., 2008). *CML41* (At3g50770) in this database was identified as being misexpressed in 290 arrays out of 2213 studies, in 261 of which *CML41* expression was significantly regulated by ≥ 2-fold (log (2) = 1) (*P < 0.05*). *CML41* expression was down-regulated by 69 perturbations and up-regulated in the other 192 (Figure 2.8 and Appendix 10). Interestingly, when 261 arrays were divided into 11 different groups of perturbations, *CML41* expression was consistently up-regulated by biotic stresses or in response to pathogen elicitors, whereas the transcriptional response showed a less consistent pattern in the rest of groups (e.g. chemical, hormones, light, abiotic stresses) (Figure 2.8 and Appendix 10). The co-expression network outlined for *CML41* in the Genevestigator database was similar to that of the

ATTED-II co-expression network database (data not shown), probably due to the co-expression network constructed by either Genevestigator or ATTED-II being based on the analysis of the same subset of published microarrays in Arabidopsis (Grennan, 2006; Hruz et al., 2008; Obayashi et al., 2009 and 2010). From both databases, the preidction can be made that CML41 responds or has a role in response to a biotic stress.

Dataset: 290 perturbations (sample selection: AT-SAMPLES-1)
1 gene (gene selection: AT-GENES-1)

● AT3G50770

261 of 2213 perturbations fulfilled the filter criteria

Filter values for ● AT3G50770

Arabidopsis thaliana (261)

	Log(2)-ratio	Fold-Change	p-value
			0.05
▼ Biotic			
B. cinerea / non-infected rosette leaf samples	3.04	14.01	0.006
B. graminis (ataf1-1) / non-infected rosette leaf samples	2.01	4.04	<0.001
B. graminis (Col-0) / non-infected rosette leaf samples	1.38	2.55	0.005
B. tabaci type B / non-infected rosette tissue samples	3.57	11.86	<0.001
CaLCuV / non-infected rosette leaf samples	3.02	8.09	0.001
E. cichoracearum (pmr4-1) / non-infected pmr4-1 samples	1.67	3.11	0.002
G. cichoracearum study 2 (18h) / non-infected whole rosette samples (Col-0)	1.26	2.53	0.004
G. cichoracearum study 2 (36h) / non-infected whole rosette samples (Col-0)	1.77	3.47	<0.001
G. cichoracearum study 2 (96h) / non-infected whole rosette samples (Col-0)	1.14	2.26	0.001
G. cichoracearum study 3 (18h) / non-infected whole rosette samples (edr1)	1.70	3.13	0.004
G. cichoracearum study 3 (36h) / non-infected whole rosette samples (edr1)	2.46	5.50	0.001
G. cichoracearum study 3 (96h) / non-infected whole rosette samples (edr1)	1.39	2.55	0.014
G. orontii study 6 (Col-0) / untreated rosette leaf samples (Col-0)	1.95	4.61	0.008
G. orontii study 6 (Col-0) / untreated rosette leaf samples (Col-0)	1.89	4.42	0.009
G. orontii study 6 (eds16-1) / untreated rosette leaf samples (eds16-1)	1.47	2.84	<0.001
G. orontii study 6 (eds16-1) / untreated rosette leaf samples (eds16-1)	1.24	2.41	<0.001
H. arabidopsidis (4dpi + 6dpi) / mock treated cotyledon samples	1.96	4.01	0.039
H. arabidopsidis study 4 (rpp4) / untreated seedling samples (rpp4)	2.60	5.91	0.016
H. arabidopsidis study 5 (rpp4) / untreated seedling samples (rpp4)	3.80	13.54	0.008
P. infestans (12h) / mock treated leaf samples (12h)	4.17	18.29	<0.001
P. infestans (6h) / mock treated leaf samples (6h)	4.68	25.50	<0.001
P. syringae pv. maculicola (Col-0) / mock treated leaf samples (Col-0)	4.56	22.35	<0.001
P. syringae pv. phaseolicola (24h) / mock inoculated leaf samples (24h)	1.07	2.10	<0.001
P. syringae pv. phaseolicola (6h) / mock inoculated leaf samples (6h)	0.98	2.03	0.025
P. syringae pv. syringae (OE7a-1) / non-infected leaf samples (OE7a-1)	3.30	9.83	0.003
P. syringae pv. syringae study 2 (Col-0) / P. syringae pv. syringae (Col-0)	1.42	2.68	0.004
P. syringae pv. syringae study 2 (OE7a-1) / non-infected leaf samples (OE7a-1)	3.36	10.22	0.002
P. syringae pv. tomato study 11 (penta) / untreated leaf disc samples (penta)	1.16	2.15	0.026
P. syringae pv. tomato study 12 (atgsnor1-1) / untreated leaf tissue samples (at...	3.68	13.60	0.018
P. syringae pv. tomato study 12 (Col-0) / untreated leaf tissue samples (Col-0)	3.59	11.83	0.005
P. syringae pv. tomato study 12 (sid2) / untreated leaf tissue samples (sid2)	4.60	23.97	0.003
P. syringae pv. tomato study 15 (DC3000) / P. syringae pv. tomato study 13 (DC...	1.10	2.18	0.006
P. syringae pv. tomato study 2 (DC3000 avrRpm1) / P. syringae pv. tomato study...	1.02	2.00	0.006
P. syringae pv. tomato study 3 (DC3000 avrRpm1) / mock inoculated leaf sampl...	2.12	4.44	<0.001
P. syringae pv. tomato study 3 (DC3000 hrcC-) / mock inoculated leaf samples (...	1.71	3.35	0.002
P. syringae pv. tomato study 3 (DC3000) / mock inoculated leaf samples (24h)	2.51	5.75	<0.001
P. syringae pv. tomato study 5 (Col-0) / non-infected leaf samples (Col-0)	3.13	7.11	0.018
P. syringae pv. tomato study 5 (gh3.5-1D) / non-infected leaf samples (gh3.5-1D)	3.47	11.14	<0.001
P. syringae pv. tomato study 8 (DC3000) / mock inoculated leaf samples	3.41	10.26	0.008
R. solani (AG8) / mock inoculated whole plant samples	1.90	4.25	0.026
TuMV (zone 0) / leaf sap treated leaf samples	2.05	4.76	0.023
▼ Elicitor			
EF-Tu (elf18) study 3 (Col-0) / mock treated seedling samples (Col-0)	0.96	2.01	0.031
EF-Tu (elf18) study 3 (ein2-1) / mock treated seedling samples (ein2-1)	1.46	2.89	0.023
EF-Tu (elf18) study 4 (Col-0) / mock treated seedling samples (Col-0)	2.03	4.09	<0.001
EF-Tu (elf18) study 4 (ein2-1) / mock treated seedling samples (ein2-1)	1.23	2.37	0.010
FLG22 study 11 (2h) / FLG22 study 11 (0h)	-1.07	-2.06	0.006
FLG22 study 5 (35S:miR393) / untreated leaf disc samples (35S:miR393)	1.87	3.70	0.044
Pep2 (bak1-3) / mock treated seedling samples (bak1-3)	2.03	3.71	0.016
Pep2 (Col-0) / mock treated seedling samples (Col-0)	1.75	3.44	0.003
Pep2 (ein2-1) / mock treated seedling samples (ein2-1)	1.61	3.05	0.003
Pep2 study 2 (bak1-3) / mock treated seedling samples (bak1-3)	3.72	11.84	0.001
Pep2 study 2 (Col-0) / mock treated seedling samples (Col-0)	3.31	10.11	<0.001

Figure 2.8 *CML41* **gene expression in the groups of biotic and elicitor perturbations within 261 gene microarray studies in Arabidopsis created by Genevestigator.** The value within log (2) ratio scales pointed by red dots indicates regulated ratio of *CML41* expression by corresponding treatments

or stresses, log (2) ratio > 0 refers to up-regulation and log (2) ratio < 0 refers to down-regulation. A full list of *CML41* regulation by these 261 perturbations is shown in Appendix 10.

2.4 Discussion

2.4.1 *CML41* is identified as candidate gene correlated with *CAX1* expression

The comparison of the global gene transcriptional profile of *cax1*, *cax3*, *cax1/sCAX1* and *cax1/cax3* with wild-type Col-0 was employed to screen for candidate genes involved either in the regulation of *CAX1* or by CAX1. More than 1,000 genes were observed to be misexpressed in the *cax1/cax3* line, which could possibly be attributed to the reduction in mesophyll-specific vacuolar calcium storage, an increase in leaf apoplastic free Ca^{2+} and perturbations in cytosolic Ca^{2+} signalling all seen in *cax1/cax3* (Conn et al., 2011, Conn et al., unpublished results; Hirschi et al., unpublished results). As a signalling molecule, excessive Ca^{2+} accumulated in the extracellular space can perturb both extracellular and intracellular signalling networks and lead to the significant alteration of plant size and physiological processes, such as apoplastic pH, hormone response, gas exchange and cell wall integrity (Conn and Gilliham 2010; Conn et al., 2011; Gilliham et al., 2011a; Cho et al., 2012). Therefore, a large number of misexpressed genes between Col-0 and the *cax1/cax3* mutant would not be unexpected as the plant has an altered physiological state; misexpressed genes may possibly include genes involved in regulation of cell-specific calcium storage or signalling elements regulated by CAX1 (Conn et al., 2011; Gilliham et al., 2011a). Mesophyll cell-specific calcium compartmentation is proposed to be accomplished through the regulation of the major Ca^{2+} transporter CAX1 at either the ranscriptional or post-translational level (Hirschi, 1996 and 1999; Cheng et al., 2003; Dayod et al., 2010; Conn and Gilliham, 2010; Conn et al., 2011; Gilliham et al., 2011a). As a result, genes encoding transcription factors, Ca^{2+} signalling-related proteins, protein kinases or Ca^{2+} transporters were pooled out from these ~1000 misexpressed genes in the *cax1/cax3* line (Figure 2.1) in an attempt to identify these factors.

No obvious reduction was observed in the cell-specific calcium accumulation in mesophyll of *cax1* or *cax3* lines, and only a few genes were misexpressed in *cax1* and *cax3* (Figure 2.1B) (Conn et al., unpublished results; Hirschi et al., unpublished). Similarly, few genes in *cax1/sCAX1* were expressed differently relative to wild-type Col-0. It is noted that *CAX3* transcription is significantly up-regulated in the *cax1* mutant line, which likely compensates for the loss of *CAX1* to maintain the cell-specific calcium compartmentation in the leaf (Figure 2.1) (Cheng et al., 2003 and 2005; Conn et al., 2011; Conn et al., unpublished results). *CAX1* expression did not change in the *cax3* mutant line

(Figure 2.1). However, *CAX3* expression was up-regulated in *cax1/sCAX1* even though the loss of *CAX1* had been complemented via overexpressing in the *cax1* mutant line a constitutively active truncated version of *CAX1* (*sCAX1*) that has its N-terminal regulatory-region removed (Figure 2.1 and 2.2) (Conn et al., unpublished results). This may mean that there are regulators of *CAX1* and *CAX3* transcription or activity still misexpressed in the *cax1/sCAX1* line. The transcriptional profiles of the single knockout lines are of interest because the transcription of *CAX1* and *CAX3* are changed but they do not have such an obviously perturbed phenotype as does *cax1/cax3*.

Nine candidates were shortlisted from Figure 2.1 into Table 2.2, eight of which had available T-DNA insertion lines in T-DNA Express database, except *CML41*. However, none of these T-DNA insertion lines displayed any obvious calcium-related phenotype (Appendix 6). Amongst these 9 shortlisted genes, *CML41* (the only one not to have a T-DNA insertion line available) was highly and negatively correlated with *CAX1* expression in the examined microarrays (Figure 2.2). Meanwhile, the ATTED-II co-expression database suggestzed that *CML41* was co-expressed with *CAX3* in Arabidopsis (Figure 2.3). As *CAX3* and *CAX1* displays a separate expression pattern in Arabidopsis, in the roots and the shoots respectively, coexpression of *CML41* and *CAX3* implies that *CML41* might be similar to *CAX3* in that it also has an opposite expression pattern to *CAX1 in planta*. Together, *CML41* was considered as an important candidate gene that is likely involved in the regulation of *CAX1* or *CAX3*, or in response to *CAX1* down-regulation; it may even contribute to cell-specific calcium compartmentation in Arabidopsis. Caution must be exercised when interpreting gene expression data as it does not necessarily reflect protein abundance or activity changes. To examine whether this is the case for this gene misexpression studies were carried out that also measured protein abundance via fluorescent tags (Chapter 4). Alternative approaches could have also been performed on the mutant plants including western blot analyses with specific antibodies designed to CML41 (see Chapter 6 for further discussion of the limitations of relying upon gene expression data to form hypotheses).

2.4.2 *CML41* splicing variant identified

As a strong candidate, *CML41* was cloned. A splicing variant, *CML41S* was identified discovered by PCR amplification and appeared to have higher transcriptional abundance relative to *CML41FL* in cDNA samples from the shoot tissue of high calcium-treated *cax1/cax3* line and Col-0 mesophyll protoplasts (Figure 2.4). Although this requires futher validation (as later discussed in Chapter 6). *CML41S* is 117 bp shorter than *CML41FL*, which gives rise to CML41S, a protein containing 39 amino-acids less than CML41FL (Figure 2.5 and 2.7). Four putative EF-hand Ca^{2+}-

binding domains were predicted in CML41FL, consistent with Day et al (2002) and McCormack and Braam (2003); however CML41S was predicted to only have 3 putative EF-hand domains (Figure 2.6). This was because the 39 amino-acid gap was positioned between two putative EF hands on the N-terminus of CML41FL. Accordingly, this split the putative EF-h1 and EF-h2 of CML41FL but likely formed a new putative EF-hand domain (New EF-h) of CML41S (Figure 2.6). Different EF-hand motifs with Ca^{2+}-binding sites have a different Ca^{2+}-binding affinity in order to recognize specific spatial and temporal cytosolic Ca^{2+} signals (from 100 nM to 10 μM) and induce a conformational change of proteins (e.g. calmodulin) (Berridge et al., 2000 and 2003; Bhattacharya et al., 2004; Gifford et al., 2007; McAinsh and Pittman, 2009; Dodd et al., 2010). For instance, CML42 has been reported to possess distinct Ca^{2+}-binding kinetics of its three EF-hand domains from 7 nM up to 350 nM (Dobney et al., 2009). In this case, putative EF-h1 and EF-h2 of CML41FL versus putative New EF-h of CML41S may have different Ca^{2+}-binding characteristics, the major role of putative New EF-h in CML41S may serve to stabilise the protein structure rather than bind Ca^{2+} or even CML41S lacks Ca^{2+} binding capacity, similar with the case of Calcineurin B-Like 10 proteins (CBL10s) from Arabidopsis (Babini et al., 2005; Quan et al., 2007; Monihan, 2011). In fact, this *CBL10* has also been reported to be transcribed into dual transcripts that encode a full-length CBL10 protein and another 46-aa shorter one, named CBL10 LONG A (CBL10LA) (Quan et al., 2007; Monihan, 2011). Similar with CML41FL and CML41S, CBL10 acquires 4 EF-h domains versus 3 EF-h of CBL10LA that comparatively lacks the last EF-h of CBL10 (Monihan, 2011). These different EF-h properties between CBL10 variants result in CBL10 acquiring Ca^{2+}-binding capacity, whereas CBL10LA not (Monihan, 2011). Moreover, the loss-of-function *cbl10* mutant line displays a salt-sensitive phenotype that can be rescued via a re-complementation by overexpressing *CBL10* instead of *CBL10LA*, the overexpression of *CBL10LA* alone notably results in a salt-sensitive phenotype in wild-type plants (Monihan, 2011). The further characterisation of *CBL10* and *CBL10LA* reveals that the role of CBL10LA is to inactivate the Salt Over Sensitive (SOS) pathway under non-stressed conditions (Monihan, 2011). However under salt stress, the down regulation of *CBL10LA* is proposed by Monihan (2011) to be essential to elicit the CBL10-activatied SOS pathway that excludes toxic Na^+ from the cytoplasm. As such, CML41FL and CML41S may decode separate Ca^{2+} signals to regulate different cellular processes, or they may have different Ca^{2+} sensing capacities but function together in the same signalling/cellular pathway in Arabidopsis.

2.4.3 The predicted role of CML41 by *in silico* analysis

The calmodulin-like (CML) protein family of *Arabidopsis thaliana* consists of 50 members and likely involves diverse functions and/or interacting targets at different developmental stages, organs and physiological processes including the plants response to various environmental stimuli at various organelles. However, only a few of them have been well characterised, as shown in Figure 2.9 summarised by Bender and Snedden (2013, references therein). On one hand, these 50 CML members harbour high variability in protein sequence and have been divided into nine sub groups based on their sequence similarity, dissimilar groups of CMLs are engaged in different physiological processes in plant, such CML23 and CML24 (of sub group 8) in the regulation of flowering response to photoperiod, CML19 (of sub group 5) is critical for DNA repair following UV damage and CML42 and CML43 (of sub group 7) in modulation of plant immunity (Figure 2.9 and 2.10) (reviewed in McCormack and Braam, 2003; McCormack et al., 2005; Bender and Snedden, 2013, and references therein). On the other hand, CML members, even though they may share high amino-acid similarity or are divided into the same sub group could still function in distinct signalling pathways. For instance, the protein sequence of CML42 and CML43 share 79.6 % similarity but CML43 behaves as a Ca^{2+}-signalling regulator in the immune response of plants to bacterial pathogens whereas CML42 in is involved in the plant defence against insect attack and in the regulation of trichome development (as discussed more in Section 6.2) (McCormack and Braam, 2003; Chiasson et al., 2005; McCormack et al., 2005; Dobney et al., 2009; Vadassery et al., 2012). As a consequence, to identify the signalling pathway in which a particular CML is involved is a challenge.

Very limited published data exists concerning the role of *CML41* and no close homologs of CML41 are found in the phylogenetic tree of the CML family in Arabidopsis (protein sequence similarities: 36.2% to CML37, 44.1% to CML38, 39.6% to CML39 and 36.3% to CML40) (Figure 2.10) (McCormack and Braam, 2003). My preliminary study employed Genevestigator to search for the potential role of CML41 in certain physiological processes or stresses. The 261 perturbations where *CML41* was significantly misexpressed suggested that CML41 may be involved in plant adaptation to diverse stresses, particularly biotic stresses (Figure 2.8 and Appendix 10). Consistently, the ATTED-II database indicated that *CML41* is co-expressed with *PR1* and senescence-associated gene 13 (*SAG13*) (Figure 2.3). In addition, the regulation of *CML41* by pathogens is was further explored by Denoux et al (2008) and Bricchi et al (2012) and showed that *CML41* expression peaked after a 12 hour treatment by flagellin 22 (flg22, the elicitor of *P. syringae*) by up to > 30-fold, and by about 6 fold after 16 hr of *P. syringae* infection (when the plasma membrane potential of cell starts depolarization upon the infection) (Denoux et al., 2008; Bricchi et al., 2012). The subcellular localisation of CML41 predicted by TargetP is putatively in chloroplasts but this requires further

validation as prediction programs only provide a guide. Therefore, such a result will require further experimental validation (Figure 2.7) (Emanuelsson et al., 2007) (see Chapter 5). However, these *in silico* analyses have offered some guidance as to the experiments that could be carried out to further characterise *CML41* both *in vitro* and *in planta*. For instance, it might have a function in the regulation of plant adaptation to biotic stress, and maybe therefore have a somewhat similar role to CML9, CML42 and CML43 in plants (Chiasson et al., 2005; Leba et al., 2012a and 2012b; Vadassery et al., 2012).
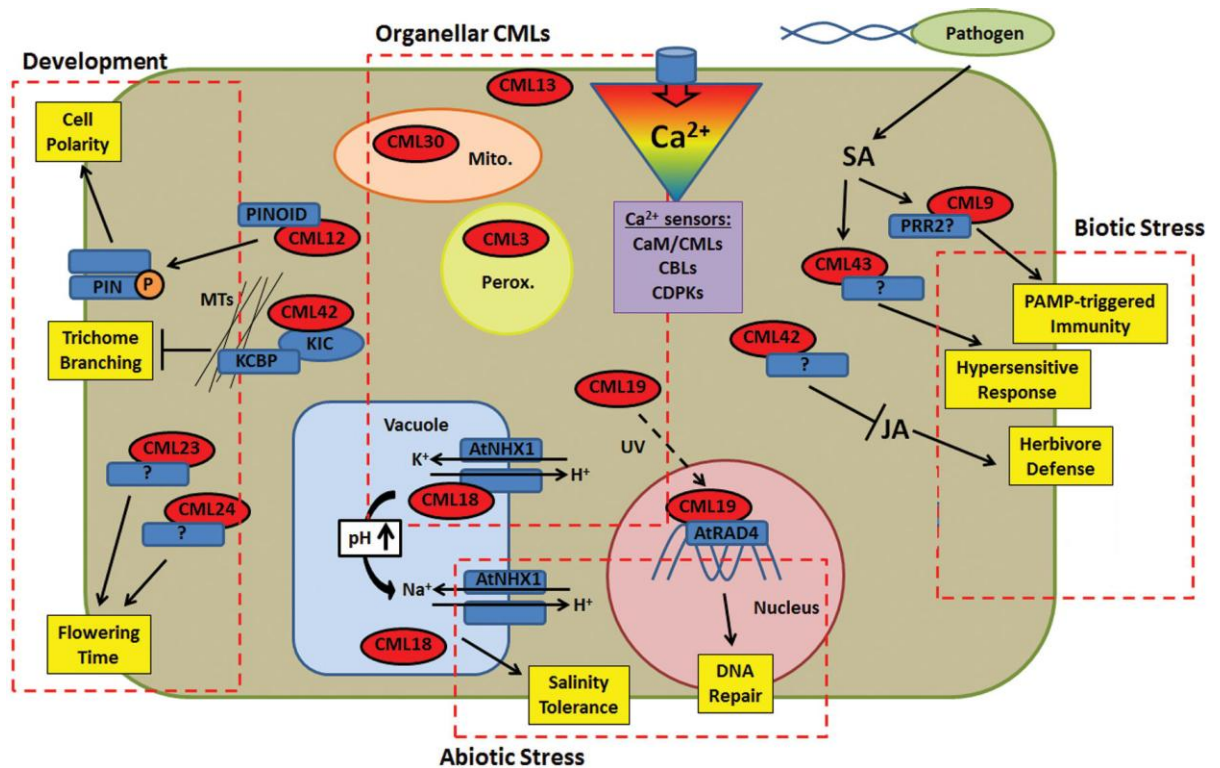
Figure 2.9 Summary of CMLs functions in different plant physiological processes. Each cellular process in which CMLs are involved is indicated in yellow box. The downstream interaction targets of CMLs are indicated in blue boxes (question mark refers to unknown targets) and 'P' in orange circle refers to protein phosphorylation. The solid and blunted arrows respectively refer to positive and negative regulation; break-line arrow refers to the translocation of CML19 from the cytoplasm into the nucleus in response to UV. JA = jasmonates, SA = salicylic acid, Perox = peroxisome, Mito = mitochondria, MTs = microtubes, UV = ultraviolet light. Adapted from Bender and Snedden (2013).
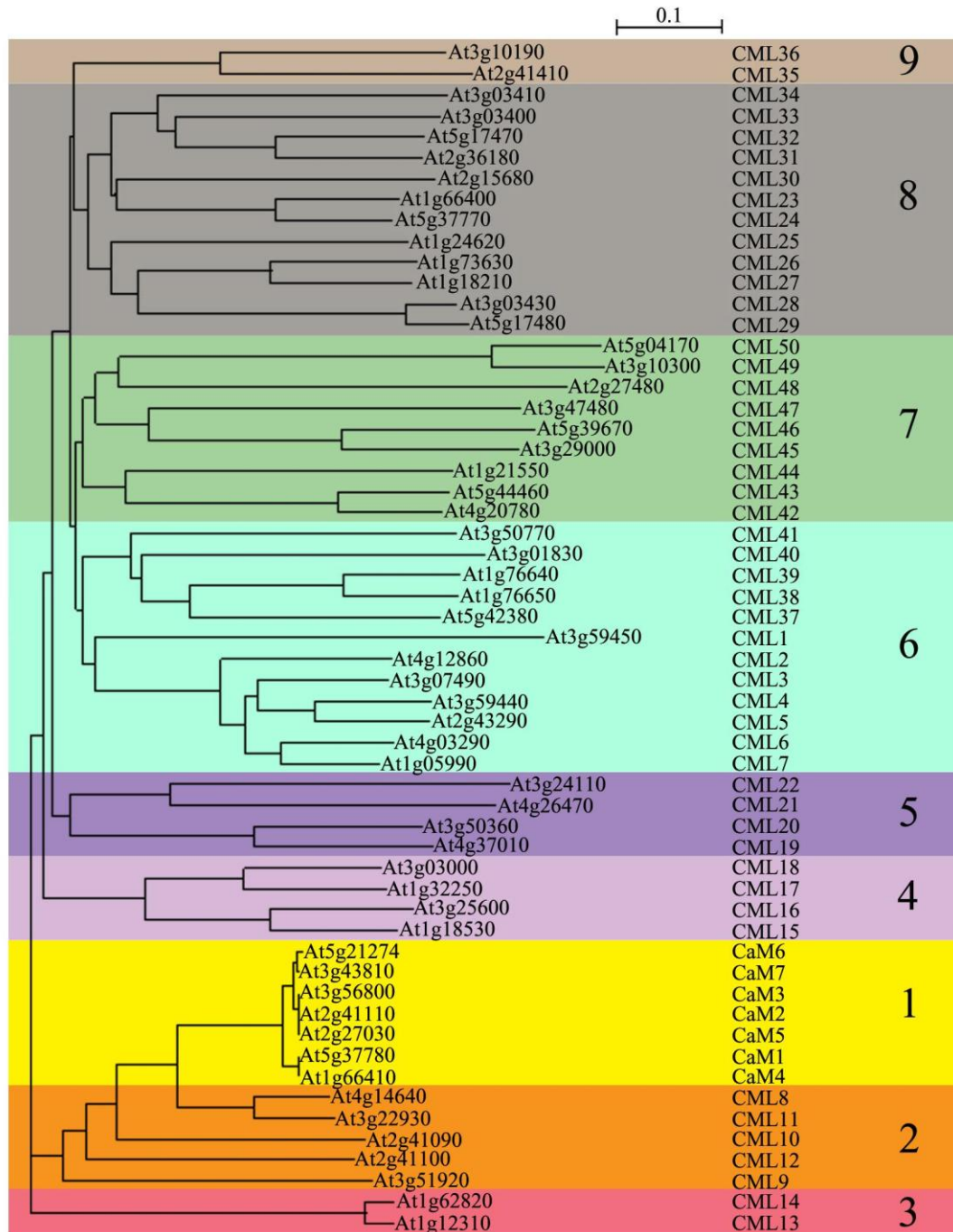
Figure 2.10 Phylogenic tree of CaMs and CMLs (CaMs/CMLs) in Arabidopsis based on amino-acid sequence similarities. CaMs/CMLs are divided into nine groups; '0.1' indicates the distance of the percent sequence divergence. Adapted from McCormack et al (2005).

Chapter 3: Gel shift Ca²⁺ binding assay

3.1 Introduction

Cellular Ca^{2+} signals are a key messenger in the response and adaptation to environmental stimuli, and during different developmental processes (Sanders et al., 2002; White and Broadley, 2003; Dodd et al., 2010; Kudla et al., 2010). The stimuli-triggered change in cellular Ca^{2+} is named the "Ca^{2+}-signature", and is decoded by diverse families of Ca^{2+}-sensors that are believed to encode some specificity to the downstream responses. Most Ca^{2+}-sensors have EF-hand domains, for instance Calmodulins (CaMs), Calmodulin-like proteins (CMLs), Calcineurin B-Like proteins (CBLs), Calcium-Dependent-Protein Kinases (CDPKs/CPKs) and CDPK-related kinases (CRKs) (Day et al., 2002; Sanders et al., 2002; Hrabak et al., 2003; Kolukisaoglu et al., 2004; McCormack et al., 2005; Dodd et al., 2010; Kudla et al., 2010). The EF-hand motif is, with some exceptions, a conserved structure (Nelson and Chazin, 1998; Day et al., 2002). A typical EF-hand domain is compromised of a 29 amino acid helix-loop-helix structure consisting of a loop (residues 10-21) flanked by a E α-helix (residues 1-10) and a F α-helix (residues 19-29) on either side, which in combination confers Ca^{2+} sensors with Ca^{2+}-binding capacity (Figure 3.1A) (Kretsinger and Nockolds, 1973; Nakayama et al., 2000). In a canonical EF-loop, there are 6 residues in positions 1(X), 3(Y), 5(Z), 7(-Y), 9(-X) and 12(-Z) supplying oxygen ligands to a Ca^{2+} ion (Figure 3.1B) (Kretsinger and Nockolds, 1973; Strynadka and James, 1989; Gifford et al., 2007). However, not all EF-hands share the same or canonical binding loop composition, although they still may bind Ca^{2+}, such as CBL2 from Arabidopsis whose EF-hand 4 binds Ca^{2+} via its main-chain carbonyl groups instead of canonical ligands (Nagae et al., 2003; Gifford et al., 2007). Additionally, not all EF-hands actually can bind Ca^{2+}; nor do all Ca^{2+}-binding proteins have an EF-hand motif (Day et al., 2002; Gifford et al., 2007).
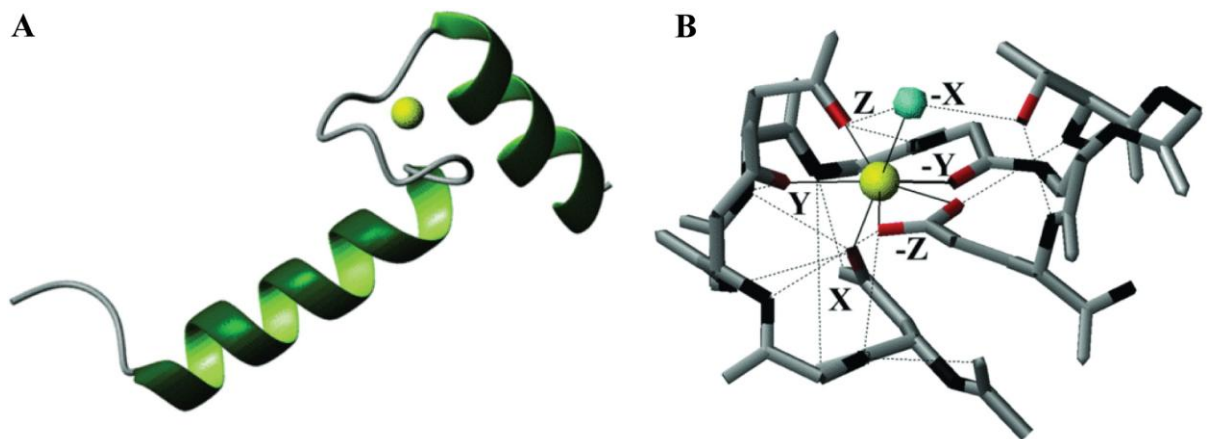
Figure 3.1 Structure of typical EF-hand Ca^{2+}-binding motif. A; a single EF-hand from the N-terminal domain of CaM. **B**; Ca^{2+}-coordination by oxygen ligands in a canonical EF-loop, continuous lines indicate the pentagonal bipyramidal coordination of Ca^{2+} ion, broken lines indicate the hydrogen bonding, black sticks indicate NH groups on the backbone, red sticks indicates the oxygen atoms on the side chain, blue ball indicates the coordinated water. Yellow ball indicates the Ca^{2+} ion in both **A** and **B**. Adapted from Gifford et al (2007).

Approximately 250 proteins have been identified with various numbers of EF-hand motifs, however only a fraction of these have had their Ca^{2+}-binding properties examined (Day et al., 2002; Reddy et al., 2011). Several approaches are available to detect the Ca^{2+}-binding characteristics of a protein, including CD spectroscopy and electrophoresis separation (Garrigos et al., 1991; Dobney et al., 2009). Both of these methods may involve protein expression and purification. In this chapter, *CML41FL* and *S*, which both putatively contain EF hands (4 and 3 respectively), were heterologous expressed in *E. coli* and the electrophoresis migration technique was employed to determine the Ca^{2+}-binding ability of recombinant CML41FL and S. This was performed on both full-length versions of these two proteins and truncated versions with putative signal peptides removed to test whether this would affect protein Ca^{2+} ability. This approach is a pre-requisite to determining whether CML41FL and S have a role in Ca^{2+} signal transduction.

3.2 Material and Methods

3.2.1 Gene cloning and plasmid construction

A preliminary experiment involving the expression of *CML41FL* and *S* in *E. coli* using pDEST17 and pDEST14 expression vectors for protein purification was performed by Dr. David Chiasson (Figure. 3.4A and Appendix 7). However, both proteins appeared to form insoluble bodies within *E. coli*, and therefore were unsuitable for purification (data not shown). Subsequently, I performed PCR amplification to mutate *CML41FL* and *CML41S* (*CML41FL* and *S*) to truncate their 5' end (of 138 bp nucleotides encoding a putative targeting peptide) and introduce an ATG start codon with the primers listed in Table 3.1, using Phusion™ Hot Start High-Fidelity DNA polymerase (FINNZYMES) following the manufacturers' instructions. PCR amplification products were correspondingly designated *CML41FL*Δ1-46 and *CML41S*Δ1-46 and ligated by Directional TOPO cloning into Gateway® entry vector pENTR™/D-TOPO (Invitrogen) (listed in Appendix 7) following the manufacturers' instructions. The TOPO reactions were then transformed into TOP10 Chemically

Competent *E. coli* cells (Invitrogen). Both *CML41FL*Δ1-46 and *CML41S*Δ1-46 were then recombined into expression vectors pDEST14, pDEST17, pDEST565 and pDEST566 using Gateway® LR Clonase® II Enzyme Mix (Invitrogen) (Figure 3.4, Appendix 7 and 8). The same experiment was performed to recombine *CML41FL* and *S* into expression vectors pDEST565 and pDEST566. All LR reactions were subsequently transformed into Subcloning Efficiency™ DH5α™ *E. coli* Competent Cells (Invitrogen).

Table 3.1 Primers used to clone *CML41FL*Δ1-46 and *S*Δ1-46 transcripts with signal-peptide sequence truncated. Primer sequence underlined refers to the directional-cloning sequence used for directional TOPO cloning.

Product name	Primers	Sequence (5'-3')	Tm* (°C)	Product size
CML41FL Δ1-46	CML41_TNT_F_CACC	<u>CACC</u>ATGAGCAACAGTGATGACAACAAC	68.7	487 bp
	CML41_CDS_R	CTAAACCGTCATCATTTGACGAAAC	62	
*CML41S*Δ1 -46	CML41_TNT_F_CACC	<u>CACC</u>ATGAGCAACAGTGATGACAACAAC	68.7	370 bp
	CML41_CDS_R	CTAAACCGTCATCATTTGACGAAAC	62	
CML41FL Δ1-46-stop	CML41_TNT_F_CACC	<u>CACC</u>ATGAGCAACAGTGATGACAACAAC	68.7	484 bp
	CML41_CDS_R-stop	AACCGTCATCATTTGACGAAACTC	62	
*CML41S*Δ1 -46-stop	CML41_TNT_F_CACC	<u>CACC</u>ATGAGCAACAGTGATGACAACAAC	68.7	367 bp
	CML41_CDS_R-stop	AACCGTCATCATTTGACGAAACTC	62	

*Primer Tm as calculated by NetPrimer (http://www.premierbiosoft.com/netprimer/index.html)

3.2.2 Mutagenesis PCR

Mutagenesis PCR amplification was also performed to mutate the expression plasmid pDEST566 containing-*CML41FL* and *S* and a maltose binding proteins (MBP) to assist with solubility of the purified protein *in vitro* (Kapust and Waugh, 1999). This was performed to insert a Tobacco Etch Virus (TEV) protease site sequence inbetween the MBP sequence and the attR1 site with the primers – pDEST566_TEV_StyI_F3/pDEST566_R3 (listed in Table 3.2), using Phusion™ Hot Start High-Fidelity DNA polymerase (FINNZYMES) (Figure 3.2 and 3.7A). The TEV protease sequence, using the mutagenesis primer, had a silent mutation added to which made a *Sty*I restriction site. The mutagenesised PCR products were purified from the agarose gel using the GenElute™ Gel Extraction Kit (Sigma-Aldrich). The purified products were phosphorylated by T4 Polynucleotide Kinase (New England Biolabs) to add Pi to the 5' and 3' end of the products at 37 ºC for 30 min,

which were subsequently self-ligated by T4 DNA Ligase (New England Biolabs) at 4 ºC overnight. The ligase reactions were transformed into TOP10 Chemically Competent *E. coli* cells (Invitrogen). The mutated expression plasmids – pDEST566-TEV-StyI-*CML41FL* and pDEST566-TEV-StyI-*CML41S* were confirmed by restriction enzyme *Sty*I and sequenced.

Table 3.2 Primers used in the mutagenesis of pDEST566 -*CML41FL* and -*CML41S* expression plasmids.

Product name	Primers	Sequence (5'-3')	Tm* (°C)	Product size
pDEST566-TEV-StyI-*CML41FL*	pDEST566_TEV_StyI_F3	GAGAACCTGTACTTCCAAGGTTACAA AAAAGCAGGCTCCGAA	81.2	7444
pDEST566-TEV-StyI-*CML41S*	pDEST566_R3	CAAACTTGTGATATCAGATCCCG	59	7338

* Primer Tm as calculated by NetPrimer (http://www.premierbiosoft.com/netprimer/index.html)
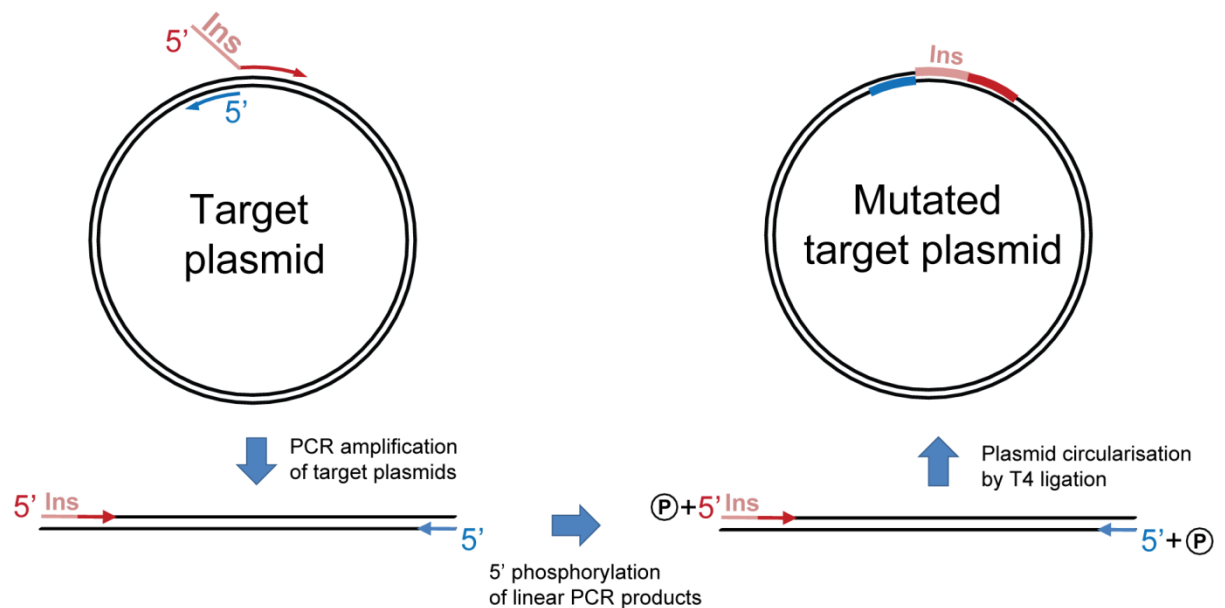
Figure 3.2 Mutagenesis PCR process to insert TEV-StyI into pDEST566-*CML41FL* and *S* plasmids. Ins = insertion site, method modified from the manual of Phusion Site-Directed Mutagenesis Kit (Thermo Scientific)

3.2.3 Protein expression

All the expression plasmids (constructed in Section 3.2.2 and 3.2.3) were extracted using an ISOLATE Plasmid Mini Kit (Bioline) and confirmed by sequencing. About 1 ng of each expression construct was re-transformed into T7 Expression $lysY/I^q$ Competent *E. coli* cells (New England Biolabs) for protein expression. The T7 expression *E. coli* colonies harbouring expression constructs were cultured overnight at 37ºC in 10 mL Luria Broth medium (LB) with 0.5% (w/v) glucose and 100 µg/mL ampicillin. Overnight cell culture was diluted 1:100 into 200 mL fresh LB with 0.5% (w/v) glucose and 100 µg/mL ampicillin and cultured at 37ºC on the next day. After 90 min, isopropyl-β-ᴅ-thiogalactopyranoside (IPTG) (Promega) was added into cell culture at 0.5 mM to induce protein expression for another 120 min. Finally, 50 mL of the cell culture was aliquoted into a 50 mL falcon tube and centrifuged at 5500 rpm at 4ºC for 10 min to collect *E. coli* cells, and the pellet was frozen in liquid nitrogen and stored in -80ºC till use.

3.2.4 Protein extraction

The isoelectric point (PI) of CML41FL, CML41S, CML41FLΔ1-46 and CML41SΔ1-46 was calculated by Protein Isoelectric Point Calculator (http://www.endmemo.com/bio/proie.php, ENDMEMO) ($PI_{CML41FL}$ = 4.88, PI_{CML41S} = 5.76, $PI_{CML41FLΔ1-46}$ = 4.20 and $PI_{CML41SΔ1-46}$ = 4.26), based on which each *E. coli* cell pellet was resuspended in 5 mL ice-cold optimized Resuspension Buffer (50 mM Na phosphate, 300 mM NaCl, 10 mM Imidazole pH= 7.0) in the presence of SIGMAFAST™ EDTA-Free Protease Inhibitor Cocktail (Sigma-Aldrich). The cells were homogenized using a sonicator (Brason Sonic Power), at power 5, with repeated cooling until all cells were lysed. Soluble and insoluble proteins were separated by centrifugation at 13,300 rpm for 10 min at 4°C. Supernatant was then transferred into a new 2 mL microcentrifuge tube that contained all soluble proteins, while the pellet the contained the insoluble fraction was resuspended in 2×SDS PAGE gel loading buffer (0.01% (w/v) bromophenol blue, 2.5% (w/v) SDS, 25% (v/v) glycerol, 125 mM Tri-HCl pH = 6.8). Soluble proteins were also mixed with an equal volume of 2×SDS PAGE gel loading buffer for gel separation. The soluble or insoluble protein samples were mixed with loading buffer and heated at 90°C for 5 min, centrifuged at 13,300 rpm for 3 min at 4ºC and transferred to ice. An equal amount of protein was loaded and checked on a 15 % SDS-PAGE gel after which it was stained in Coomassie Stain Buffer (50% (v/v) ethanol, 10% (v/v) acetic acid and 0.05% (v/v) Brilliant Blue R-250) for 1.5 hr and then washed in Destain Buffer (50% (v/v) ethanol, 10% (v/v) acetic acid) overnight with gentle shaking.

3.2.5 Protein purification

Once the proteins were confirmed soluble on the 15% SDS-PAGE gel, the expressed His-tagged proteins in *E. coli* were purified using a TALON® Metal Affinity Resin (Clontech) following the manufacturer's instructions. Briefly, TALON resin was washed twice in ten volumes of Wash Buffer (50 mM Na phosphate, 300 mM NaCl, 10 mM Imidazole, pH = 7.0) and centrifuged at $700 \times g$ for 2 min at 4°C. Then 5 mL of the soluble protein was mixed with 1 mL TALON resin and gently shaken at 4°C for 20 min to allow the His-tagged protein to bind to the resin. This was then centrifuged at $700 \times g$ for 2 min at 4°C, then the supernatant containing the unbound soluble proteins was removed whilst the resin contained His-tagged proteins was washed twice in 15 mL Wash Buffer and centrifuged at $700 \times g$ for 2 min at 4°C. The resin was resuspended in one resin volume of Wash Buffer and transferred into 2 mL Poly-Prep® Chromatography Columns (Bio-Rad). The supernatant was removed after the resin settled out of suspension. The resin was washed again with five volumes of Wash Buffer, after that His-tagged protein was eluted from resin with 5 mL Elution Buffer (50 mM Na phosphate, 300 mM NaCl, 200 mM Imidazole, pH = 7.0) and collected in 500 µL fractions by gravity flow. The protein fractions were checked on a 15% SDS-PAGE gel to determine the amount of purified protein in each fraction. Purified His-tagged proteins were desalted using 5 mL Zeba™ Spin Desalting Columns (Thermo Scientific) and collected in 2.5 mL 50 mM Na phosphate buffer (pH = 7.0) by centrifugation at $1000 \times g$ for 2 min at 4°C, as described in the manufacturers' guide. The eluted solution contained the desalted His-tagged proteins ready for the electrophoresis mobility shift assay.

3.2.6 Protein digestion

The purified and desalted recombinant protein from *E. coli* expressing pDEST566-TEV-StyI-*CML41FL* and *S* were treated by AcTEV™ protease (Invitrogen) at 4 ℃ overnight. Then the recombinant CML41FL and CML41S with His-MBP tag removed were used for the electrophoresis mobility shift assay.

3.2.7 Electrophoresis mobility shift assay

The electrophoresis mobility shift assay was optimized from the methods as described in Garrigos et al (1991), Chiasson et al (2005) and Xu et al (2011). 1 mM $CaCl_2$ was added to purified recombinant proteins that were incubated at room temperature for 5 min to allow for Ca^{2+} binding to proteins. Meanwhile, 10 mM EGTA was added to recombinant proteins as a control in the mobility shift assay. Protein samples with either $CaCl_2$ or EGTA were mixed with equal volume of 2×SDS

PAGE gel loading buffer, heated at 95°C for 2 min and centrifuged at 13,300 rpm for 90 sec before gel separation. The protein samples were mixed with 1 mM CaCl$_2$ then separated in an SDS PAGE gel containing 1 mM CaCl$_2$, whilst the protein samples mixed with 10 mM EGTA were separated in another SDS PAGE gel containing 10 mM EGTA. The gels were stained and destained following the protocols described in Section 3.2.4. The mobility of proteins was determined by comparison with the Precision Plus Protein™ Standards (Bio Rad).

3.3 Results

3.3.1 Truncation of chloroplastic transit-peptide of CML41FL and CML41S

A mutagenesis PCR amplification truncated the first 138 bp nucleotides (46 aa) of *CML41FL* and *S* and removed their putative targeting signal, and the resulting proteins were named *CML41FL*Δ1-46 and *CML41S*Δ1-46. Removal of the putative signal peptide from CML41FL and CML41S altered their predicted membrane targeting (Figure 2.7 and 3.3). Previously CML41FL and CML41S had been predicted to be putatively targeted at chloroplast, however CML41FLΔ1-46 and CML41S Δ1-46 were preficted to be targeted to other unknown organelles by InterProScan (Figure 2.7 and 3.3) With each, the predicted score for chloroplast localisation was significantly reduced to 0.208 and 0.122 in cTP, but increased up to 0.873 and 0.862 for other (organelle localisation), respectively (Figure 2.7 and 3.3). Such a result suggests that the absence of this putative signal peptide may impair the proper subcellular targeting of CML41FLΔ1-46 and CML41SΔ1-46 (and this was confirmed by further investigation (see Chapter 5).


```
### targetp v1.1 prediction results ###############################
Number of query sequences:  2
Cleavage site predictions included.
Using PLANT networks.

Name                   Len    cTP    mTP     SP   other  Loc  RC  TPlen
----------------------------------------------------------------------
CML41FL_Trancuated     160   0.208  0.078  0.073  0.873   _    2    -
CML41S_Trancuated      121   0.122  0.105  0.148  0.862   _    2    -
----------------------------------------------------------------------
cutoff                       0.000  0.000  0.000  0.000
```

Figure 3.3 Prediction of CML41FL and SΔ1-46 subcellular localisation by TargetP v1.1.
CML41FL_Truncated = CML41FLΔ1-46; CML41S_Truncated = CML41SΔ1-46; Len = protein sequence length; cTP = chloroplast transit peptide; mTP = mitochondria targeting peptide; SP = secretory signal peptide; other = no sorting signal; Loc = a predicted localisation (C = chloroplast; M = mitochondrial; S = signal peptide; - = other localisation; * = don't know); RC = 2 indicates the prediction ranked as reliable (score from 1 to 5 means from very reliable prediction to no false positives detected); TPlen = the predicted length of signal amino-acid residues. Output explanation adapted from Emanuelsson et al (2007).

3.2.2 Soluble CML41FL, CML41S, CML41FLΔ1-46 and CML41SΔ1-46 were successfully tagged by His-MBP

CML41FL, *CML41S*, *CML41FL*Δ1-46 and *CML41S*Δ1-46 were recombinant into serial expression vectors as indicated in Figure 3.4 (details see Appendix 7 and 8). Only when fused to MBP, were soluble CML41FL, CML41S, CML41FLΔ1-46 and CML41SΔ1-46 proteins of the expected size made in *E. coli* (Figure 3.4B). As all expressed recombinant protein possessed a polyhistidine tag (His-), this enabled its chelation and immobilization by a metal ion, i.e. Ni^{2+} or Co^{2+}, and so it could be separated and purified from other soluble proteins (Hochuli et al., 1988; Bornhorst and Flake, 2000). To this end, immobilized metal ion affinity chromatography was employed to purify the recombinant CML41FL and CML41S, and CML41FLΔ1-46 and CML41SΔ1-46, from the total *E. coli* soluble proteins using a TALON cobalt resin. Eight protein fractions were collected for each construct, four of which (protein fractions on F2-F5 lane) contained a major protein band of the appropriate size on SDS-PAGE gel. The purified protein was then desalted to remove the imidazole before performing the electrophoresis mobility shift assay (Figure 3.5).
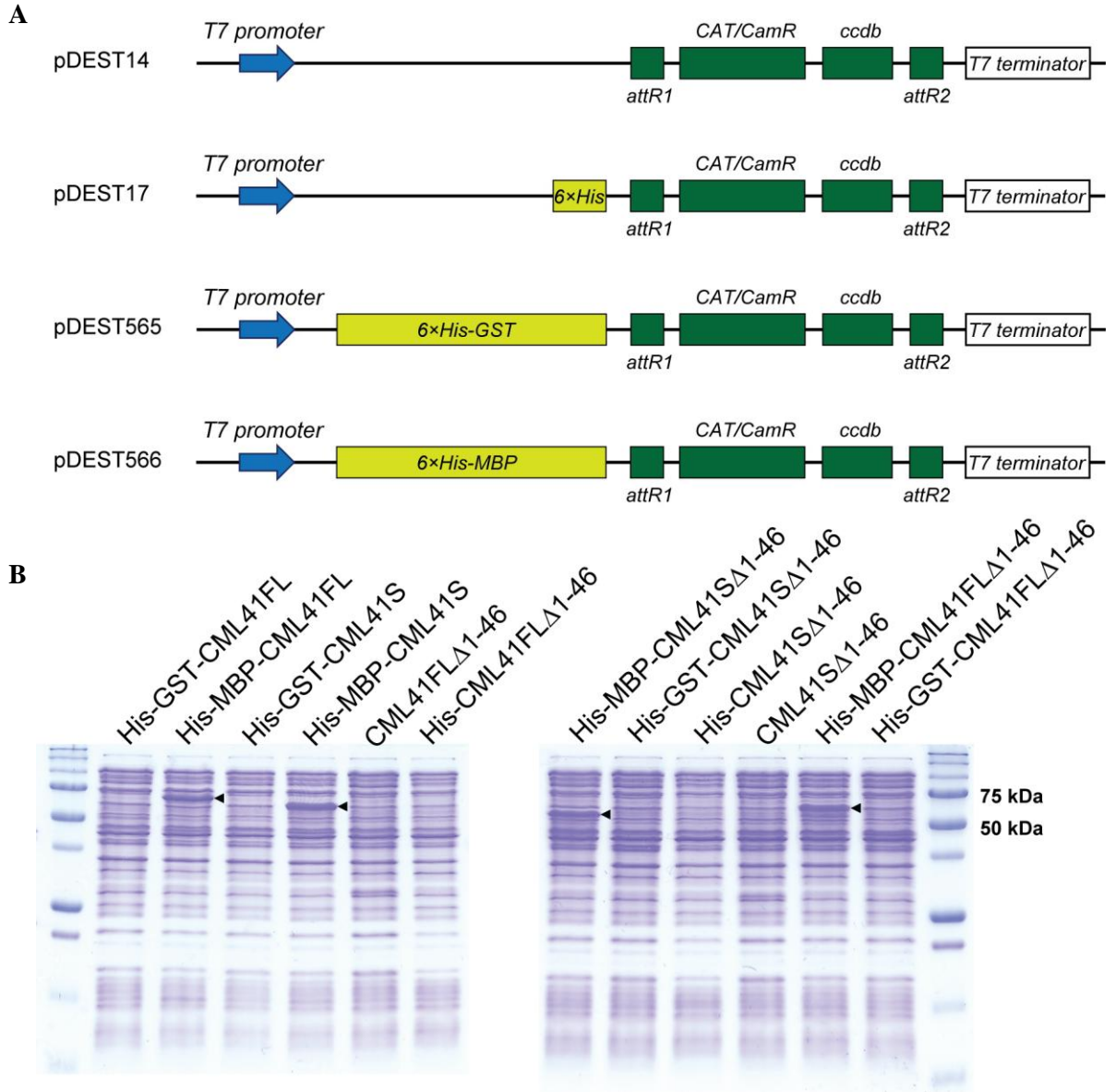
Figure 3.4 Expression vectors used for protein expression and soluble proteins of *E. coli* strain T7 Expression *lysY/I^q* expressing CML41FL, CML41S, CML41FLΔ1-46 and CML41SΔ1-46 constructs. A, diagram of Gateway enabled *E. coli* expression vectors, 6×His = polyhistidine tag, 6×His-GST = His-tagged glutathione *S*-transferase, 6×His-MBP = His tagged maltose binding protein. **B**, '►' indicates a soluble recombinant protein band of the expected protein size for each construct calculated by Geneious Pro v5.6.5: (~52 kDa of) His-GST-CML41FL; (~67 kDa of) His-MBP-CML41FL; (~48 kDa of) His-GST-CML41S; (~62 kDa of) His-MBP-CML41S; (~18 kDa of) CML41FLΔ1-46; (~21 kDa of) His-CML41FLΔ1-46; (~61 kDa of) His-MBP-CML41FLΔ1-46; (~47 kDa of) His-GST-CML41FLΔ1-46; (~14 kDa of) CML41SΔ1-46; (~17 kDa of) His-CML41SΔ1-46; (~57 kDa of) His-MBP-CML41SΔ1-46; (~47 kDa of) His-GST-CML41SΔ1-46.
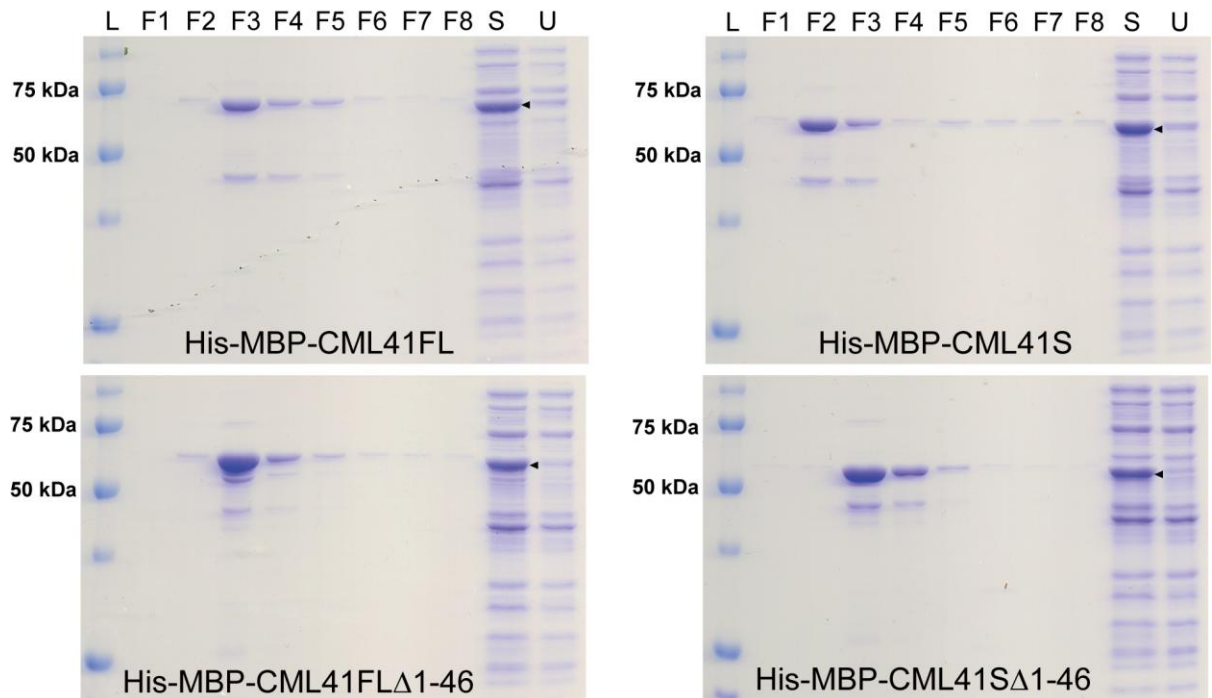
Figure 3.5 Purified recombinant proteins on SDS-PAGE gel. L = protein ladder, Precision Plus Protein™ Standards (Bio Rad); F1-8 = collected protein fractions No.1 to 8; S = soluble proteins extracted from *E. coli*; U = unbound proteins collected from the chromatography column flow through; '►' points to the recombinant proteins to be purified from soluble proteins extracted from *E. coli*.

3.2.3 His-MBP tagged CML41FL, CML41S, CML41FLΔ1-46 and CML41SΔ1-46 migrate faster in presence of Ca²⁺

An electrophoresis mobility shift assay has been widely applied for the determination of Ca^{2+}-binding in proteins including Calmodulin/Calmodulin-like proteins (Garrigos et al., 1991, Maune et al., 1992; Sistrunk et al., 1994; Chiasson et al., 2005; Delk et al., 2005; Vanderbeld and Snedden, 2007; Park et al., 2010; Xu et al., 2011; Chigri et al., 2012). This assay was also employed to test if either CML41FL or CML41S can bind Ca^{2+}. The purified recombinant proteins were pre-treated either 10 mM $CaCl_2$ or 10 mM EGTA (a Ca^{2+} chelator) (Chiasson et al., 2005; Xu et al., 2011). The use of 10 mM $CaCl_2$ precipitated the protein (data not shown); therefore, the amount of $CaCl_2$ used in the pre-treatment was reduced to 1 mM (Chigri et al., 2012). The pre-treated proteins were migrated on a SDS-PAGE gel in the presence of either 1 mM $CaCl_2$ or 10 mM EGTA. As shown in Figure 3.6,

the recombinant His-MBP tagged proteins migrated faster in the presence of Ca^{2+} compared to when it was in the presence of EGTA. This faster migration can be attributed to the Ca^{2+} induced-conformational change of the recombinant protein and a consequent change in the migration rate (Garrigos et al., 1991; Maune et al., 1992; Finn et al., 1995). As it has been determined that Ca^{2+} cannot induce a conformational change in maltose binding proteins (Ozawa and Muramatsu, 1993), the faster migration of this protein was probably due to a conformational change in CML41FL, CML41S, CML41FLΔ1-46 and CML41SΔ1-46 elicited by Ca^{2+}.
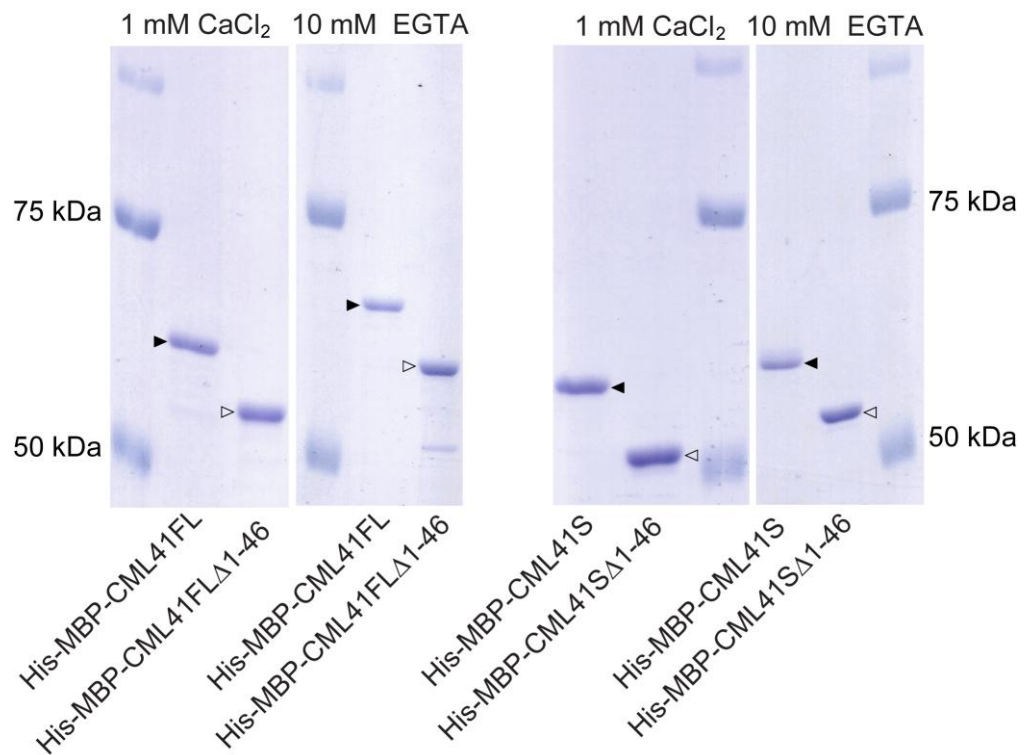
Figure 3.6 Gel shift Ca^{2+} binding assay. His-MBP-CML41FL and His-MBP-CML41S and His-MBP-CML41FLΔ1-46 and His-MBP-CML41SΔ1-46 protein migration on 8% SDS-PAGE gel in the presence of 1 mM $CaCl_2$ or 10 mM EGTA; '▶' points to CML41FL and CML41S as indicated; '▷' points to CML41FLΔ1-46 and CML41SΔ1-46 as indicated.

3.2.4 CML41FL and S migration is faster in the presence of Ca^{2+}

The His-MBP tag of >40 kDa is much larger than CML41FL and S of ~20 kDa. The migration of CML41FL and S tagged with His-MBP is supposed to be slower than the untagged protein, and the proportion of potential conformational change in the fused protein by Ca^{2+} is also

69

reduced, making the impact of Ca^{2+} on the migration of the protein more difficult to detect when CML41 is fused to MBP. Removal of His-MBP tag would remove its influence on the assay and allow a greater proportional change in the rate of CML41FL and S migration with Ca^{2+} compared to CML41FL and S with EGTA, than when fused to the MBP. To remove the MBP, mutagenesis PCR amplification was performed to modify the expression plasmids. Following the method as described by Nallamsetty and Waugh (2007), a TEV protease-site sequence was inserted into pDEST566-CML41FL and S plasmids to generate pDEST566-TEV-StyI-CML41FL and S plasmids, so that *E. coli* expressing these mutated plasmids enabled the production of His-MBP-TEV-CML41FL and S protein with a cleavable TEV protease site between His-MBP and CML41FL and S (Figure. 3.7A). In actual fact, a few 'spacer' residues were also inserted inbetween the TEV site and CML41FL and S in order to enhance the cleavage efficiency of the TEV protease (Nallamsetty and Waugh, 2007). After the recombinant His-MBP-TEV-CML41FL and S were purified from *E. coli*, the application of TEV protease recognised and cleaved the TEV protease site separating His-MBP and CML41FL and S (Figure. 3.7B and Figure 3.8A). Due to the similar size of cleaved CML41FL with the TEV protease, it was hard to separate these protein bands from each other (Figure 3.8A and B). As TEV protease cannot bind phenyl-sepharose, which is commonly used to purify Ca^{2+}-bound proteins (e.g. CaM), this suggests that TEV protease doesn't have Ca^{2+}-binding characteristics and can be used as control (Gopalakrishna and Anderson, 1982; Sarhan et al., 2012). It was clearly seen that both the CML41FL and CML41S proteins (with removal of His-MBP) migrated faster in the presence of Ca^{2+} compared to in the presence of EGTA (Figure 3.8B).

A

pDEST566-TEV-StyI-*CML41FL / S*

B

His-MBP-TEV-CML41FL   His-MBP-TEV-CML41S
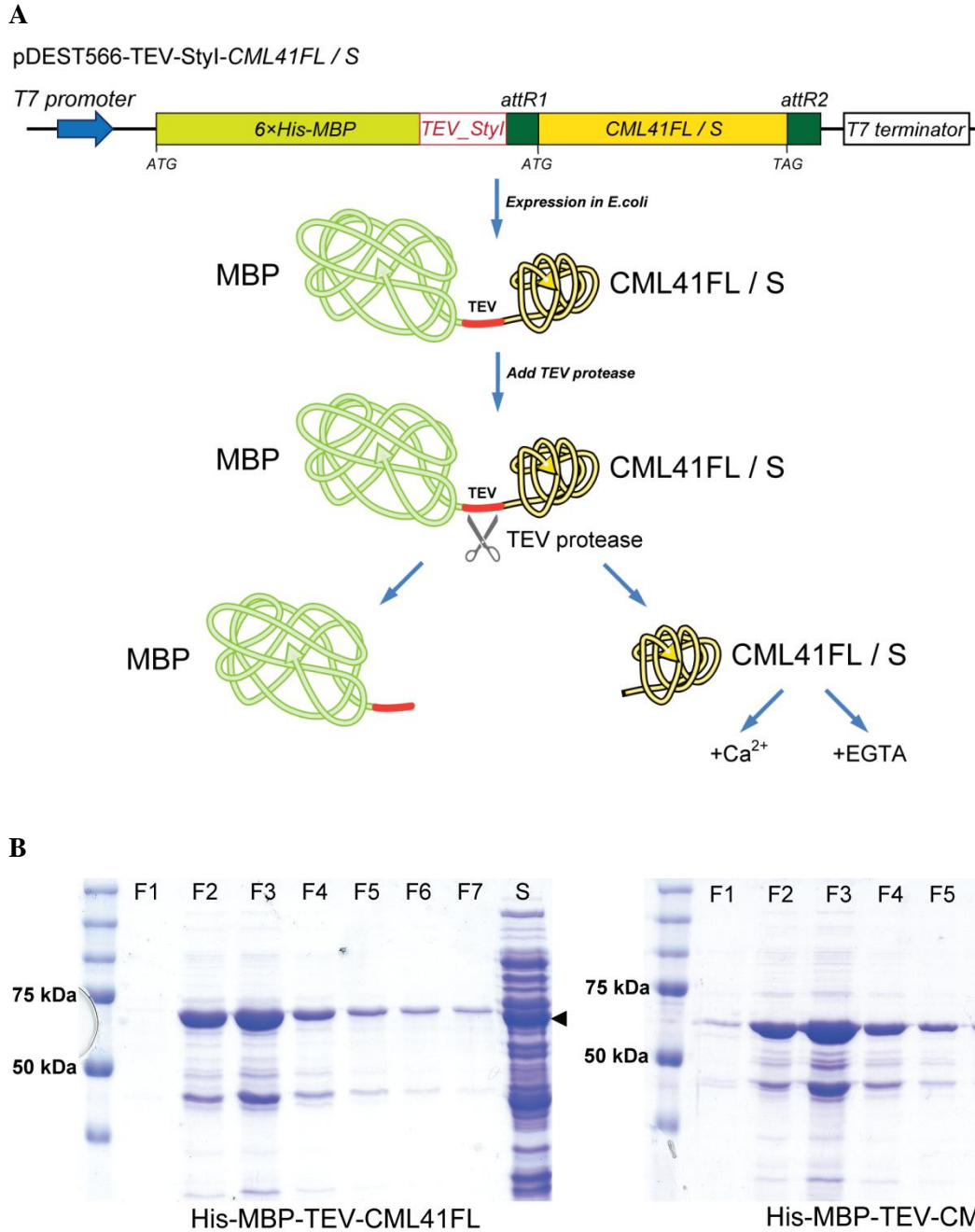
Figure 3.7 His-MBP-TEV fusion protein purification and digestion. A, the diagram of mutated pDEST566-TEV-StyI-*CML41FL* and *S* plasmid and process of His-MBP tag removal before the gel shift Ca^{2+}-binding assay. **B**, recombinant protein purification from the *E. coli* expressing mutated pDEST566 plasmid; L = protein ladder, Precision Plus Protein™ Standards (Bio Rad); F1-7 = collected protein fractions No.1 to 7; S = soluble proteins extracted from *E. coli*; '►' points to the expected recombinant proteins.
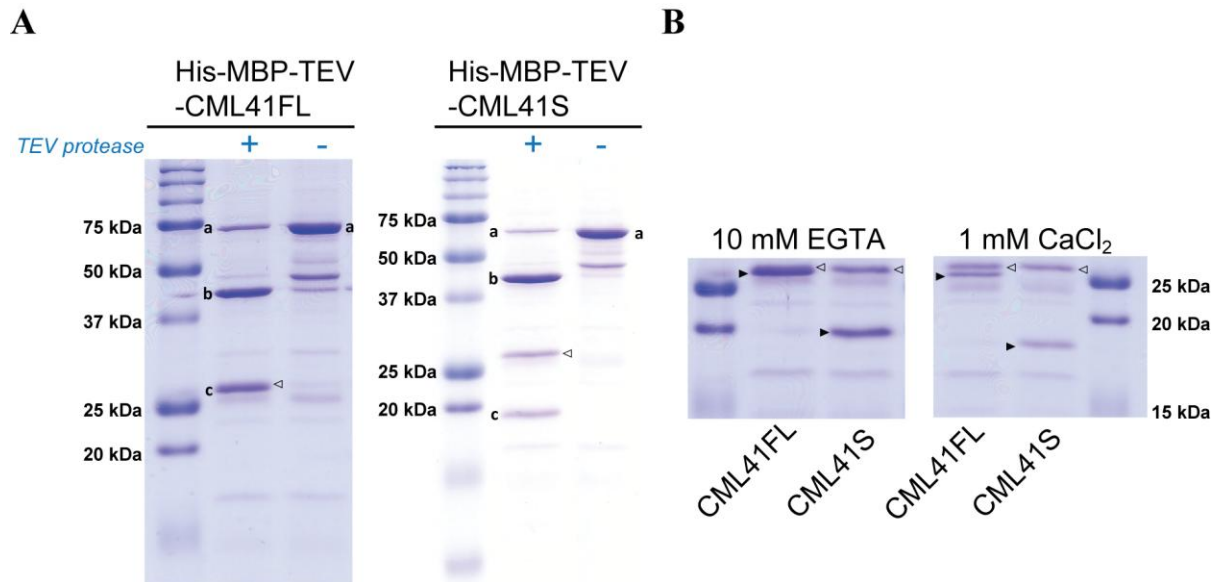
Figure 3.8 Cleavage of recombinant proteins and gel shift assay. A, His-MBP-TEV-CML41FL and S on 15% SDS-PAGE with or without TEV protease pre-treatment; '+' indicates TEV protease pre-treatment; '-' indicates no TEV protease pre-treatment; 'a' points to undigested His-MBP-TEV-CML41FL and S as indicated; 'b' points to His-MBP-TEV; 'c' points to CML41FL and S after TEV cleavage as indicated; '▷ ' points to the TEV protease. **B**, Electrophoresis migration with 1 mM Ca^{2+} or 10 mM EGTA on 15% SDS-PAGE; '►' points to CML41FL and S as indicated; '▷ ' points to the TEV protease. The expected size of each protein in **A** and **B** is: ~67 kDa of His-MBP-TEV-CML41FL, ~63 kDa of His-MBP-TEV-CML41S, ~43 kDa of His-MBP-TEV), > 23 kDa of CML41FL after cleavage by TEV, > 19 kDa of CML41S after cleavage by TEV, ~27 kDa of TEV.

3.4 Discussion

3.4.1 MBP facilitated the purification of soluble recombinant CML41FL and CML41S from *E. coli*

The *in silico* analysis in Section 2.3.5 predicted that both CML41FL and CML41S have putative chloroplastic transit-peptide sequences that might direct them to chloroplasts. Previous studies have reported that the truncation of the putative chloroplastic transit-peptide facilitates Arabidopsis chloroplastic protein, encoded by At5g39790, to be soluble in *E. coli* (Lohmeier-Vogel et al., 2008). Based on this information, we presumed that truncation of the putative (chloroplastic)

signal peptide from CML41FL and S might enhance the solubility of both proteins in *E. coli*. However, this approach failed, most likely owing to the frequently observed improper folding of heterologous proteins in *E. coli* (Figure 3.3 and 3.4B) (Baneyx and Mujacic, 2004). Generally, native proteins of *E. coli* are relative small, have simple-domains and efficiently fold in the correct conformation, whereas the large and multi-domain heterologous proteins often require folding helpers, such as chaperones (Baneyx and Mujacic, 2004). Fusion to affinity tags, such as Glutathione *S*-transferase (GST) and MBP have been proposed to improve the solubility of heterologous proteins in *E. coli* (Kapust and Waugh, 1999; Esposito and Chatterjee, 2006; Tolia and Joshua-Tor, 2006). In the case of CML41FL and S, MBP but not GST enhanced the solubility of the recombinant proteins in *E. coli* (Figure. 3.4B). MBP has been widely reported to function as a chaperone-like protein, particularly in the form of N-terminal fusion to prevent insoluble aggregations of recombinant proteins and improve eukaryotic protein solubility in *E. coli*, whereas GST is a poorer solubility enhancer than MBP (Kapust and Waugh, 1999; Sachdev and Chirgwin, 1999; Routzahn and Waugh, 2002; Terpe, 2003; Waugh, 2005; Esposito and Chatterjee, 2006). The application of an N-terminal MBP fusion made CML41FL and S soluble and capable of being purified from *E. coli* (Figure 3.5 and 3.7).

3.4.2 CML41FL and CML41S bind Ca^{2+}

CML41FL and CML41S exhibited a faster migration rate on a SDS-PAGE gel in the presence of Ca^{2+} compared to when Ca^{2+} was absent (i.e. in the presence of EGTA); this occurred either with His-MBP fused to the protein or after its cleavage (Figure 3.6 and 3.8). This shift is commonly considered as an indication of a Ca^{2+}-induced conformational change in the target protein indicative of Ca^{2+} binding (Gifford et al., 2007). This observation was similar to the properties of other CML family proteins – CML3, CML8, CML12 (TCH3), CML24 (TCH2), CML37-39 and CML42-43; all of these CMLs are believed to have Ca^{2+}-binding ability and be Ca^{2+} signal transducers (Sistrunk et al., 1994; Chiasson et al., 2005; Delk et al., 2005; Vanderbeld and Snedden, 2007; Park et al., 2010; Chigri et al., 2012). Accordingly, CML41FL and CML41S are likely to bind Ca^{2+} ions and act as Ca^{2+} sensors, with the conformational change being a consequence of Ca^{2+} chelation within the loop formed from helix-loop-helix EF-hand motifs within CML41FL and S. To confirm Ca^{2+} binding alternative assays could be used such as a phenyl-sepharose column to purify the recombinant CML41FL and S (Gopalakrishna and Anderson, 1982; Gifford et al., 2007).

Following the binding of Ca^{2+}, the new protein conformation is usually associated with the exposure of hydrophobic regions that have negative charges on the CaM/CML protein, which creates interaction sites that are required for extensive protein interactions with other proteins (LaPorte et al., 1980; Strynadka and James, 1989; Snedden and Fromm, 1998; Gifford et al., 2007). Using an Arabidopsis protein microarray, more than 170 targets were observed to interact with CaM1, CaM6, CaM7 and CML9-12 (Popescu et al., 2007), which suggests that CML41FL and S, as Ca^{2+} signal transducer, may also have extensive targets.

Chapter 4: Characterisation of *CML41 in planta*

4.1 Introduction

CaMs/CMLs are reported to sense diverse Ca^{2+} signals during various cellular processes, including biotic and abiotic environmental stimuli responses; a number of these Ca^{2+} 'sensors' are required to translate a Ca^{2+}-signature through to a specific transcriptional response (reviewed in Kim et al., 2009a; Kudla et al., 2010; Reddy et al., 2011). In some instances, CaMs/CMLs enable the transduction of a Ca^{2+}-signal by directly binding to DNA to regulate gene expression, such CAM7 (Kushwaha et al., 2008). Alternatively, they can regulate gene expression via an interaction with intermediary proteins (e.g. transcription factors (TFs) TF-binding protein) or by modulation of TFs phosphorylation status (Figure 4.1) (Kushwaha et al., 2008; Kim et al., 2009a; Reddy et al., 2011). For instance, the transcription factor DWF1, which is essential for brassinosteroid (BR) biosynthesis in plants, requires for its activation a prior binding to calmodulin (Du and Poovaiah, 2005). In Chapter 2 and 3, *CML41* was observed to be negatively correlated with *CAX1* expression and I have observed that both CML41FL and S have a capacity to bind Ca^{2+}. Furthermore, *CAX1* expression is reported to be Ca^{2+}-dependent, increasing in expression if treated with high concentrations of Ca^{2+} in the growth media (Hirschi, 1999). Thus, it is possible that *CML41FL* and *S* may play a role in controlling expression of *CAX1* in a manner outlined for other Ca^{2+}/CaM-sensors listed in Figure 4.1, or it is possible that *CML41* expression is induced when *CAX1* expression is perturbed. In this chapter, *CML41FL* and *S* were misexpressed in plants to test these hypothesis, and to see if *CML41* misexpression altered the expression of other genes. To this end, I developed a qRT-PCR assay aimed at discriminating the *CML41FL* and *CML41S* transcripts. Additionally, the expression pattern of *CML41* was also examined via examining native *CML41* promoter chimerias with the β-glucuronidase gene (*GUS*) *in planta*.
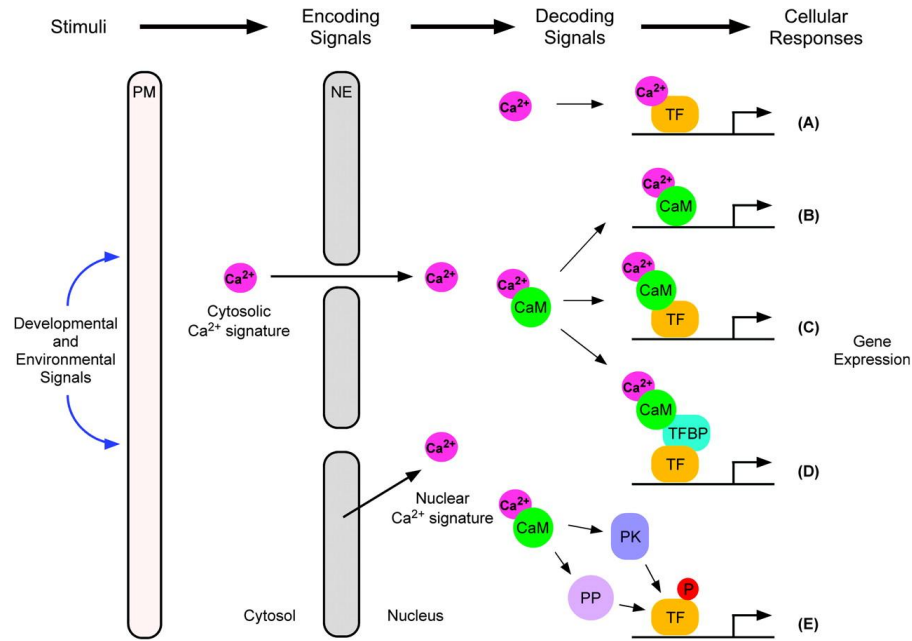
Figure 4.1 Mechanisms of Ca^{2+}-mediated regulation of gene expression in plants. A, Ca^{2+}-mediated gene expression via regulation by of a Ca^{2+}-bound transcription factor. **B-E**, Ca^{2+}/CaM-mediated transcriptional regulation: **B**, Ca^{2+}-mediated CaMs function as a TF; **C**, Ca^{2+}-mediated CaMs interact with TFs to regulate gene expression; **D**, Ca^{2+}-mediated CaMs interact with TF-binding proteins to regulate gene expression; **E**, Ca^{2+}-mediated CaMs regulate gene expression via phosphorylation or dephosphorylation of TFs. Adapted from Kim et al (2009a).

4.2 Material and Methods

4.2.1 Artificial micro RNA design and cloning

Artificial micro RNA (amiRNA) were designed against the *CML41* mRNA sequence by Bradleigh Hocking using Web Micro RNA Designer (WMD3, http://wmd3.weigelworld.org/cgi-bin/webapp.cgi) and following the guide of Schwab et al (2006). Two *CML41*-amiRNA sequences were selected from the output result of WMD3 designer, the BLAST result indicated that both of selected amiRNA were specifically targeted to *CML41* mRNA towards the 3' region, as indicated in Figure 4.2. Two amiRNA sequences were subsequently input into WMD3 Oligo to generate amiRNA cloning primers (Table 4.1). Following the amiRNA cloning guide (http://wmd3.weigelworld.org/downloads/Cloning_of_artificial_microRNAs.pdf) three separate PCR reactions amplified the partial fragments of *CML41*-amiRNA#1 (*CML41-amiRNA#1_f1*, *f2* and *f3*). These were then purified and mixed together as a template for a PCR that amplified the full-length

CML41-amiRNA#1 with the primers of amiRNA_A/B listed in Table 4.1. *CML41*-amiRNA#2 was amplified following the same protocol but with different primer sets listed in Table 4.1 by Brad Hocking. Both *CML41*-amiRNA#1 and *CML41*-amiRNA#2 were separately ligated into the pCR8/GW/TOPO entry vector and transformed into TOP10 Chemically Competent *E. coli* cells (Invitrogen) following the manufacturers' guide (Appendix 7 and 8). The sequence of *CML41*-amiRNA#1 and *CML41*-amiRNA#2 was confirmed in the entry vectors by restriction digest with *EcoR*V and sequencing with primers M13_ Forward (see Section 2.2.3) and M13_Reverse (5'-CAGGAAACAGCTATGAC-3') (performed by AGRF).

Table 4.1 Primers used to clone *CML41-amiRNA#1* and *CML41-amiRNA#2* into the pRS300 vector as a template. Upper cases in CML41_amiRNA cloning primers indicate sequence to be mutated when PCR amplification on pRS300 vector as template, lower cases in the CML41_amiRNA primer indicate sequence to bind to pRS300 vector as template and prime the PCR amplification.

Product name	Primers	Sequence (5'-3')	Tm* (°C)	Product size
CML41-amiRNA#1_f1	amiRNA_A	CTGCAAGGCGATTAAGTTGGGTAAC	65.6	273 bp
	CML41_amiRNA#1_IV	gaAATATAGAAGGGTAATTATGGctacatatatattccta	66.5	
CML41-amiRNA#1_f2	CML41_amiRNA#1_III	agCCATAATTACCCTTCTATATTtcacaggtcgtgatatg	74.8	176 bp
	CML41_amiRNA#1_II	agCCGTAATTACCCTACTATATAtcaaagagaatcaatga	71.1	
CML41-amiRNA#1_f3	CML41_amiRNA#1_I	gaTATATAGTAGGGTAATTACGGctctcttttgtattcca	70.9	300 bp
	amiRNA_B	GCGGATAACAATTTCACACAGGAAACAG	68.3	
CML41-amiRNA#1	amiRNA_A	CTGCAAGGCGATTAAGTTGGGTAAC	65.6	699 bp
	amiRNA_B	GCGGATAACAATTTCACACAGGAAACAG	68.3	
CML41-amiRNA#2_f1	amiRNA_A	CTGCAAGGCGATTAAGTTGGGTAAC	65.6	273 bp
	CML41_amiRNA#2_IV	gaAAAACCGACATCATTTGATCActacatatatattccta	71	
CML41-amiRNA#2_f2	CML41_amiRNA#2_III	agTGATCAAATGATGTCGGTTTTtcacaggtcgtgatatg	79.2	176 bp
	CML41_amiRNA#2_II	agTGGTCAAATGATGACGGTTTAtcaaagagaatcaatga	77.1	
CML41-amiRNA#2_f3	CML41_amiRNA#2_I	gaTAAACCGTCATCATTTGACCActctcttttgtattcca	76.7	300 bp
	amiRNA_B	GCGGATAACAATTTCACACAGGAAACAG	68.3	
CML41-amiRNA#2	amiRNA_A	CTGCAAGGCGATTAAGTTGGGTAAC	65.6	699 bp
	amiRNA_B	GCGGATAACAATTTCACACAGGAAACAG	68.3	

* Primer Tm as calculated by NetPrimer (http://www.premierbiosoft.com/netprimer/index.html)

CML41-amiRNA#1 (5'-TATATAGTAGGGTAATTACGG-3')

```
AT3G50770.1 | Symbols: | calmodulin-related protein, putative | chr3:18884939-18885761 FORWARD
Target region: ACGTAATTACCCTACTATATG

Hybridization energy: -36.64kcal/mol (94.95 %)

Target gene 5'->3' /668-688        ACGTAATTACCCTACTATATG
amiRNA (rev. complement)           CCGTAATTACCCTACTATATA
                                   *****************
0                                                    668            823
```

CML41-amiRNA#2 (5'-TAAACCGTCATCATTTGACCA-3')

```
AT3G50770.1 | Symbols: | calmodulin-related protein, putative | chr3:18884939-18885761 FORWARD
Target region: TCGTCAAATGATGACGGTTTA

Hybridization energy: -36.25kcal/mol (88.76 %)

Target gene 5'->3' /626-646        TCGTCAAATGATGACGGTTTA
amiRNA (rev. complement)           TGGTCAAATGATGACGGTTTA
                                   * *****************
0                                                    626            823
```

Figure 4.2 *CML41*-amiRNA sequences designed by WMD3 Designer and targeting site on *CML41 mRNA* sequence. Designed sequences of *CML41*-amiRNA#1 and *CML41*-amiRNA#2 as shown in bracket, the output of amiRNA targets blasted using WMD3 target search (http://wmd3.weigelworld.org/cgi-bin/webapp.cgi?page=TargetSearch;project=stdwmd)

4.2.2 *CML41* promoter cloning and plasmid construction

The *CML41* promoter sequence was examined using the Arabidopsis transcription factor database (http://arabidopsis.med.ohio-state.edu/AtTFDB/). A 2 kb sequence upstream from the *CML41* ATG start codon was amplified by PCR with the primers listed in Table 4.2 using Phusion™ Hot Start High-Fidelity DNA polymerase (FINNZYMES) following the manufacturers' instructions. The putative *CML41* promoter region (*proCML41*) included a 5' untranslated region (5'-UTR). The PCR amplification products were cloned into a pCR8/GW/TOPO entry vector and transformed into TOP10 Chemically Competent *E. coli* cells (Invitrogen) (listed in Appendix 7 and 8). The sequence of *proCML41* was confirmed in the entry vector by sequencing with primers M13_ Forward (see

Section 2.2.3), proCML41_F1_seq (5'-GTTTGTATTTGTTTTTGGTGAGTAC-3'), proCML41_F2_seq (5'-GAGGAAGCTGCGATGAAAT-3') and proCML41_F3_seq (5'-TGTATGCACTTAAGACATCTCCAT-3') (performed by AGRF). Using the Gateway® LR Clonase® II Enzyme Mix (Invitrogen) *proCML41* within the entry vector was subsequently recombined into the binary vector pMDC162, which contained the *GUS* gene (Curtis and Grossniklaus, 2003), and was designated pMDC162-*pro*CML41 (Appendix 7 and 8). Meanwhile, the same technique was performed to recombine *CML41FL*, *CML41S*, *CML41*-amiRNA#1 and *CML41*-amiRNA#2 from the entry vectors into the binary vector pMDC32, which contained a 2×35S promoter for overexpression in plants. *CML41FL* and *CML41S*-stop were recombined into the binary vector pMDC83, which contained the *GFP* gene in an orientation appropriate to create a C-terminal-fusion as used in Chapter 5 for protein subcellular localisation (listed in Appendix 7 and 8) (Curtis and Grossniklaus, 2003).

Table 4.2 Primers used to clone *CML41* promoter region from Arabidopsis genomic DNA by PCR

Product name	Primers	Sequence (5'-3')	Tm* (°C)	Product size
proCML41	proCML41_2kb_F1	TAACGCGCAAGGAAACGC	60.5	2000 bp
	proCML41_2kb_R1	ATCATTGAGTTTATATGCTGTAGTGTGTT	60	

*Primer Tm as calculated by NetPrimer (http://www.premierbiosoft.com/netprimer/index.html)

4.2.4 Plant material and growth

Arabidopsis ecotype Col-0 was used as plant material for stable gene expression with the above constructs. Seeds were sterilized in 30% bleach for 5-10 min with gentle agitation, followed by 5 washes in sterile water and drying in a laminar flow cabinet on sterile filter paper (Whatman). About 20-30 sterile seeds were sown on a pot of sterile coco-peat soil with a clear plastic cover to maintain high humidity. The pots with seeds were placed in the dark for 2 d at 4 °C for stratification before being transferred and grown in long day conditions (16 hr light/8 hr dark, 23 ºC) with watering every 3 or 4 d with light level at 80 µmol m^{-2} s^{-1}. The plastic cover was removed after 2-3 weeks and plants were grown for another 3-4 weeks. Then the flowering Arabidopsis seedlings were ready for transformation.

4.2.5 *A. tumefaciens*-mediated transformation

The binary vectors carrying genes of interest were transformed into *Agrobacterium tumefaciens* strain AGL1 using the freeze-thaw method as described in Höfgen and Willmitzer (1988). Briefly, 1 µg plasmid DNA was mixed with *A. tumefaciens* competent cells (50 µL) and incubated on the ice for 5 min, followed by freezing in liquid nitrogen for 5 min and thawing at 37 ℃ for another 5 min using a heating block. 1 mL of LB was added to the competent cells and cultured in suspension at 30 ℃ for 2 hr before being plated on LB agar medium with Rifampicin (25 µg/mL) and Kanamycin (50 µg/mL) and incubated at 30 ℃ for 2 d. The transformed *A. tumefaciens* colonies harbouring the genes of interest in binary vectors were confirmed by colony PCR with gene specific primers that had been used in initial gene cloning as corresponding tables above. Arabidopsis plants were transformed using the flora-dip method, mediated by *A. tumefaciens* following the protocols described by Zhang et al (2006). The confirmed colonies were grown in LB liquid medium with the above antibiotics at 30 ℃ for 2 d, 1 mL of which was inoculated into another fresh 500 mL LB liquid medium with the same antibiotics and cultured at 30 ℃ for another 16 hr. The *A. tumefaciens* cells were collected by centrifugation at $4000 \times$ g for 10 min at room temperature and resuspended in equal volumes of 5% (w/v) sucrose solution with 0.025 % (v/v) Silwet L-77. The flowers of Arabidopsis plants were immersed into the *A. tumefaciens* cell suspension for 45 sec, wrapped with clear polyethylene film and placed in the dark with high humidity. Two pots containing 10–20 Arabidopsis seedlings per pot were dipped for each construct. The covering film was removed after 24 hr and the plants were transferred to long day conditions with normal watering for another 4 weeks to allow seed maturation.

4.2.6 Genomic DNA extraction

Genomic DNA (gDNA) was extracted from 5-6 week-old Arabidopsis. 1-2 rosette leaves were harvested in 1.5 mL microcentrifuge tubes and frozen in liquid nitrogen. Afterwards, leaf tissue was ground into powder in the microcentrifuge tube using a micropestle and mixed thoroughly with 600 µL DNA extraction buffer (100 mM Tris-HCl, 100 mM NaCl, 10 mM EDTA, 1% (w/v) sarkosyl and 2% (w/v) polyvinylpyrrolidone, pH = 8.5) plus 600 µL phenol/chloroform/isoamyl alcohol (25:24:1, pH = 8.0) by vortexing. Homogenized tissue was centrifuged at maximum speed for 10 min in a desktop microcentrifuge. The upper-phase supernatant (500 µL) was transferred into a new 1.5 mL microcentrifuge tube and mixed thoroughly with 50 µL 3 M Na acetate (pH = 4.8) and 600 µL isopropanol, followed by 30 min incubation at room temperature. gDNA was precipitated by centrifugation at maximum speed for 10 min, washed in 70% ethanol and resuspended in 50 µL sterile H_2O with RNase (40 mg/mL).

4.2.7 Selection of primary transformed Arabidopsis plants

Primary selection of transformants was performed using an optimized version of the method described by Harrison et al (2006). Briefly, seeds harvested from floral-dipped Arabidopsis plants were sterilized as described above. Sterile seeds were germinated on a petri dish with ½ MS medium plus 0.8% (w/v) phytogel and 25 µg/mL hygromycin-B, placed in the dark for 2 d at 4 ℃. Then seeds were transferred to the light at 23 ℃ for 6 h, then wrapped with aluminium foil and placed back in the growth chamber for another 2 d. The foil was removed and the seeds were placed in the light for 24 hr. The seedlings of Arabidopsis transformants were discriminated by the length of cotyledons under hygromycin selection. The seedlings that had hypocotyls longer than 0.7 cm were deemed to be likely positive transformants, and were transferred to a new ½ MS medium plus 0.8% (w/v) phytogel and grown in short day conditions for 3–4 weeks before being transferred into soil. Arabidopsis putative transformants were confirmed by a PCR on their gDNA which was designed to amplify the insert fragment specific to the binary vectors used to transform the plants as indicated, with the primers listed in Table 4.3. Seeds were collected from these confirmed primary Arabidopsis transformants (T_1) and classified as the second-transgenic generation (T_2), and were used for further analysis.

Table 4.3 Primers used to screen T$_1$ *Arabidopsis* transformants using PCR on genomic DNA as templates.

Template gDNA name	Primers	Sequence (5'-3')	Tm* (°C)	Product size
CML41FL-OEX-2	pMDC32_35S_F	TCTAGAGGATCCCCGGGTA	56.7	
CML41FL-OEX-12	CML41_FL_qPCR_R1	GTCAGTGTCAACTTCGTTTATCG	57	425 bp
pMDC32-*CML41FL*				
CML41S-OEX-3	CML41S_specific_F4	AGCGACGGCGACGGGT	62.6	
CML41S-OEX-4				440 bp
CML41S-OEX-6	nos_Terminator_R1	CGGCAACAGGATTCAATCTTAAG	61	
pMDC32-*CML41S*				
CML41-amiRNA#1-1	35S_F	GATGTGATATCTCCACTGACGTAA	56.4	
CML41-amiRNA#1-2				
CML41-amiRNA#1-8	CML41-amiRNA#1_R	AGCCGTAATTACCCTACTATATATC	54	622 bp
pMDC32-*CML41*-amiRNA#1				
CML41-amiRNA#2-1	35S_F	GATGTGATATCTCCACTGACGTAA	56.4	
CML41-amiRNA#2-4				
CML41-amiRNA#2-8				620 bp
pMDC32-*CML41*-amiRNA#2	CML41_amiRNA#2_R	TGGTCAAATGATGACGGTTTA	56.3	
CML41FL-OEX-2	CML41_CDS_F	ATGGCAACTCAAAAAGAGAAACCT	61	
CML41FL-OEX-12				
CML41FL-Null				
pMDC32-*CML41FL*				
CML41-amiRNA#1-1				
CML41-amiRNA#1-2				
CML41-amiRNA#1-8				
pMDC32-*CML41*-amiRNA#1				618 bp
CML41-amiRNA#2-1				
CML41-amiRNA#2-4				
CML41-amiRNA#2-8	CML41_CDS_R	CTAAACCGTCATCATTTGACGAAAC	62	
pMDC32-*CML41*-amiRNA#2				
CML41-amiRNA#2-Null				
WT Col-0				
CML41S-OEX-3	CML41_CDS_F	ATGGCAACTCAAAAAGAGAAACCT	61	
CML41S-OEX-4				618 bp + 501 bp
CML41S-OEX-6	CML41_CDS_R	CTAAACCGTCATCATTTGACGAAAC	62	
pMDC32-*CML41S*				

* Primer Tm as calculated by NetPrimer (http://www.premierbiosoft.com/netprimer/index.html)

4.2.8 Quantitative RT-PCR of gene expression analysis in Arabidopsis transformants

To determine the up- and/or down-regulation of *CML41FL* and *S* expression in Arabidopsis transformants, quantitative Real-Time PCR (qRT-PCR) was performed to quantify their relative transcript level in plants. RNA was extracted from 5-6 week-old T_2 Arabidopsis grown hydroponically in short day conditions, 2 µg of which was used to synthesise cDNA following the methods outlined in Section 2.2.3. The primers for qRT-PCR were designed using Primer 3 (http://frodo.wi.mit.edu/primer3/), and the products were confirmed by sequencing (see Table 4.4). qRT-PCR was performed on the cDNA samples using fluorescence output from the IQ™ SYBR$^®$ Green Supermix and iCycler real-time PCR system (Bio Rad) and the following conditions: 95 °C for 2 min 30 sec, 40 cycles of 95 °C for 30 sec, 55 °C for 30 sec and 72 °C 20 sec plus melt curve analysis from 55 °C to 95 °C for 10 sec at 0.5 °C increments. qRT-PCR result analysis followed the method as described in Schmittgen and Livak (2008) using $2^{-\Delta C_T}$ to calculate gene expression level relative to *GAPDH-A* (At3g26650) as an internal control.

Table 4.4 Primers used to qRT-PCR analysis in this chapter.

Gene name	Primers	Sequence (5'-3')	Tm* (°C)	Product size
ARR5	ARR5_qPCR_F1	CAGCTAAAACGCGCAAAG	55.7	134 bp
	ARR5_qPCR_R1	GCAAAAGAAGCCGTAATGTC	55.4	
BR6ox2	BR6ox2_qPCR_F1	TGGAGGTGGAGTTAGGCTT	54.4	156 bp
	BR6ox2_qPCR_R1	AGATGGTATCCTTTTGGTGC	54.2	
CAX1	CAX1_qPCR_F1	ACTGGTCCTCTTGCTTTGCT	56.5	201 bp
	CAX1_qPCR_R1	CTCCATTGTCTCTCGCTTTG	55.7	
CAX3	CAX3_qPCR_F1	ACTGGTTCTATTGTTATGCTATGTCA	57.7	258 bp
	CAX3_qPCR_R1	CAAGCTCCCTCCCTCATTC	56.7	
CML41FL/S	CML41_qPCR_F1	GAGGACTTTGTTGGATTGATG	54.5	191 bp
	CML41_qPCR_R1	ATGGCTTCACACTCTCCGTA	55.3	
CML41FL	CML41_FL_qPCR_F1	AGCGACGGCGACGGTAAG	61.8	114 bp
	CML41_FL_qPCR_R1	GTCAGTGTCAACTTCGTTTATCG	57	
CML41S	CML41_Short_qPCR_F1	ACGGCGACGGGTTTGA	58	141 bp
	CML41_Short_qPCR_R3	TTGGTGTTATGCAGCCTGATC	58.5	
IAA1	IAA1_qPCR_F1	TCCGAGAGAGAAGGCTACAA	55	169 bp
	IAA1_qPCR_R1	AGACAATGGATCATAAGGCAGT	55.7	
ICS1	ICS1_qPCR_F2	TCCAGCAGAAGAAGCAAGG	56.1	172 bp
	ICS1_qPCR_R2	TATCCCTGTCCCCGCATAG	58.2	

NOA1	NOA1_qPCR_F2	GAACCAATCCGCAAAACAC	56	189 bp
	NOA1_qPCR_R2	GGGTCTTACTTCTTCTTCCTTATC	55.4	
PR1	PR1_qPCR_F2	GCTCTTGTAGGTGCTCTTGTTCT	57.7	163 bp
	PR1_qPCR_R2	TGCCTCTTAGTTGTTCTGCGT	57.8	
SCL3	SCL3_qPCR_F1	TACGCAGCATTGTTTGATTG	55.6	143 bp
	SCL3_qPCR_R1	TTCTCGTGTCTTTCTCTTCTCTC	55.1	
ACA8	ACA8_qPCR_F1	TCGTAAACCAGATGAGAAGAACA	57	172 bp
	ACA8_qPCR_R1	ACCGATGCCAACACAGATAAG	57.6	
ACA10	ACA10_qPCR_F1	TCGTCTGTATCGGAATCGG	56.4	186 bp
	ACA10_qPCR_R1	CAAGTACCACTAAAAGCCACCT	56	

*Primer Tm as calculated by NetPrimer (http://www.premierbiosoft.com/netprimer/index.html)

4.2.9 Homozygote screening of Arabidopsis transformants

The T_2 Arabidopsis seedlings that were confirmed with expected up- or down-regulated transcript level of *CML41FL* or *CML41S* by qRT-PCR were transferred from the hydroponic system into soil for seed collection. At least 2 lines for each construct were selected from T_2 Arabidopsis plants to create a third-transgenic generation (T_3). Germination of about 120 T_3 seeds of each line on ½ MS phytogel medium with 25 µg/mL hygromycin-B followed the selection method of transformants in Section 4.2.5. Lines were considered as homozygous lines, as long as > 95% of the seedlings germinated on selective media as described in the method of Harrison et al (2006). Seeds of homozygous lines were stored at 4 ºC for further assays.

4.2.10 GUS histochemical analysis

A GUS histochemical assay was performed using the methods described in Jefferson (1987). Transgenic *proCML41*::*GUS* plants were immersed in a staining buffer (50 mM Na phosphate pH = 7.0, 10 mM EDTA, 2 mM potassium ferrocyanide, 2 mM potassium ferricyanide, 0.1% (v/v) Triton X-100, 0.1% (w/v) X-Gluc (5-bromo-4-chloro-3-indolyl β-ᴅ-glucuronide)) in a 6-well plate and vacuum infiltrated for 15 min in the dark, followed by a 3 hr incubation at 37 ºC in the dark. The stained plants were destained in 70% ethanol. *GUS*-stained plants were imaged using NIKON SMZ800 Stereo Fluorescence microscope (NIKON).

4.2.11 Embedding and sectioning of GUS stained seedlings

GUS stained seedlings were embedded using the Technovit 7100 hydroxyethyl-methacrylate kit (Heraeus Kulzer). Fresh 3 hr GUS-stained Arabidopsis seedlings were immediately transferred into 150 mM Na phosphate buffer (pH = 7) and kept at 4 °C overnight in a 6-well plate (Iwaki). These seedlings were subsequently washed three-time using ultrapure H_2O, cut into 3 mm pieces using a razor blade and fixed in 100 mM Na phosphate buffer with 5% glutaraldehyde (pH = 7.4) in a 2 mL microcentrifuge tube at 4 °C overnight. Then, fixed tissue was washed in 1×PBS buffer (137 mM NaCl, 2.7 mM KCl, 10 mM Na_2HPO_4, 1.8 mM KH_2PO_4, pH = 7.4) for 10 min and transferred into 1×PBS with 1% (w/v) agarose in a 6-well plate (Iwaki). The solid agarose was cut into small blocks containing the fixed tissue, dehydrated in 50% ethanol for 30 min and then taken through a dehydration series containing 70%, 90% and 100% ethanol for 30 min for each change. The dehydrated agarose blocks were gradually infiltrated via a change of 100% ethanol with infiltration solution I (ethanol : Technovit 7100 liquid plus 1% (w/v) Technovit harderner I, 3:1) for 2 h, with infiltration solution II (ethanol : Technovit 7100 liquid plus 1% (w/v) Technovit harderner I, 1:1) for 2 hr and with infiltration solution III (ethanol : Technovit 7100 liquid plus 1% (w/v) Technovit harderner I, 1:3) for another 2 h. After that, these agarose blocks were stored in Technovit 7100 liquid plus 1% Technovit harderner I overnight at 4 °C. These infiltrated agarose blocks were polymerised in Technovit polymerisation solution (6.25 % (v/v) Technovit hardener II in Technovit 7100 liquid plus 1% (w/v) Technovit harderner I) for 1 d. The polymerised tissue was sectioned in 10 μm thickness using Leica RM2265 rotary microtome (Leica). The sectioned tissues were imaged using LEICA ASLMD Laser dissection microscope (Leica)

4.2.12 Growth assays of transgenic Arabidopsis

A rapid growth-test assay for Arabidopsis transgenic lines at T_2 generation underwent a rapid screening of transformants via germination on ½ MS agar medium plus 25 μg/mL hygromycin-B for 2-3 d as described in Section 4.2.7, then the transformants were selected and transferred to BNS agar medium without antibiotics, and grown together with same-age wild-type Col-0 seedlings that were germinated in the same condition but without hygromycin-B selection in short-day conditions (9 hr light/15 hr dark, at 22 ºC). In the growth assay on T_3 homozygous Arabidopsis transgenic lines as well as wild-type Col-0, seeds were germinated and grown in ½ MS agar medium with or without different $CaCl_2$ supplementation for a week in long-day conditions (16 hr light/8 hr dark, 22 ºC), after 2 d stratification at 4 °C in the dark. The details of flg22 treatment, salt stress and root growth assay methods are referred in the respective figure legends.

4.2.13 Dark-induced chlorophyll measurement

Dark treatment was optimized from Weaver and Amasino (2001) and Keech et al (2007). Two rosette leaves were given a dark treatment by wrapping the leaf with aluminium foil to keep it from the light before harvesting as shown in Figure 4.3. The fresh weight of 0 d, 2 d, and 4 d dark-treated rosette leaves was measured before transferring into a 2 mL microcentrifuge tube and freezing immediately in liquid nitrogen. Chlorophyll measurement followed the protocol described by Warren (2008). Basically, the leaf tissue was freeze-dried overnight and ground into a fine powder in the microcentrifuge tube. Chlorophyll was extracted from the tissue powder in 1 mL methanol by vortexing for 2 min and centrifuging at maximum speed for 2 min. Supernatant containing chlorophyll was transferred into a fresh 2 mL microcentrifuge tube. The tissue pellet was re-extracted in another 1 mL methanol, followed by vortexing and centrifuging again for 2 min at each step. The second supernatant containing the additional chlorophyll extracts was mixed with the first supernatant in 2 mL microcentrifuge tube. The chlorophyll extract (200 µL for each sample performed in triplicate) was transferred into a clear 96-well plate (Greiner bio-one). The absorbance (A) of each sample in the 96-well plate was measured at 655 nm and 665 nm using FLUOstar Optima multi-mode microplate reader (BMG LABTECH). The calculation of chlorophyll concentration followed equation published by Ritchie (2006):

$$\text{Chlorophyll } a \text{ } (\mu g/mL) = -8.0962 \text{ } A_{652, \text{ } 1 \text{ cm}} + 16.5169 \text{ } A_{665, \text{ } 1 \text{ cm}}$$
$$\text{Chlorophyll } b \text{ } (\mu g/mL) = 27.4405 \text{ } A_{652, \text{ } 1 \text{ cm}} - 12.1688 \text{ } A_{665, \text{ } 1 \text{ cm}}$$

$$\text{Chlorophyll content } (\mu g/mg) = 2 \times (\text{Chlorophyll } a + \text{Chlorophyll } b) \text{ / fresh weight (mg)}$$

Figure 4.3 Experimental system of dark-induced senescence using aluminium foil. Arabidopsis plants were grown in BNS in short-day conditions for 5-6 weeks before dark-treatment; two mature leaves from No.10-15 were selected and wrapped in aluminium foil.

4.2.14 Callose measurement

Callose measurement was optimized from Currier and Strugger (1956), Galletti et al (2008), Choi et al (2010) and Daudi et al (2012). Arabidopsis plants that were 5-6 week-old and grown in short-days were used for callose deposition assays. Either 2 μM flg22 or ultrapure H_2O was infiltrated into an individual rosette leaf. Three leaves per plant and six plants per line per treatment were used as replicates for the assay. After 20-24 hr, the infiltrated leaves were sampled, cleared and dehydrated in 100% ethanol for more than 8 hr in a 12-well plate (Iwaki) with the ethanol changed twice and gently shaken at room temperature. The clear leaves were fixed in fixation buffer I (acetic : ethanol, 1:3) for 1 h, and followed by exchanging it with 50% (v/v) ethanol for 15 min and 30% (v/v) ethanol for 15 min. The fixed leaves were washed in 150 mM Na phosphate buffer (pH = 8.0) for 1 hr before aniline staining in staining buffer (150 mM Na phosphate, 0.05% (w/v) aniline blue, pH = 8.0) for another 1 hr in the dark at 37ºC. The stained leaves were mounted in 50% (v/v) glycerol and imaged with an Axiophot Pol Photomicroscope excitation from a mercury light source and captured with a UV filter (LP = 470 nm) (Carl Zeiss). Callose deposited in leaves was measured by ImageJ, using particle analysis (http://rsbweb.nih.gov/ij/).

4.2.15 Statistical analysis

Graphing and statistical analysis of all data was performed in GraphPad Prism v6.

4.3 Results

4.3.1 Expression pattern of *proCML41*::*GUS* in Arabidopsis

GUS fused to a native promoter provides a versatile tool for the investigation of gene expression patterns in higher plants (e.g. Arabidopsis) (Jefferson et al., 1987). To elucidate the *CML41* expression pattern *in planta*, 2 kb of the putative *CML41* promoter was fused to the *GUS* gene and expressed in Arabidopsis. GUS histochemical staining revealed a strong GUS activity mainly in the root vascular tissue of 5 day-old Arabidopsis seedlings and in the cotyledons of 10 day-old seedlings, whereas no GUS activity was observed at all in a negative control (Figure 4.4a-f, n). In 17 day-old seedlings, GUS activity was still predominantly observed in the root and cotyledon but also at the leaf margin (Figure 4.4g and h). The sepals, stamens and apex and base of siliques were the tissues with strongest GUS activity at the flowering stage of *proCML41*::*GUS* plants (Figure 4.4i-m). As discussed in Section 2.4.3, up-regulated *CML41* expression was reported in a few microarrays in response to flg22. Here I also investigate GUS activity under control *proCML41* in response to flg22. After, flg22 treatment there was a significant systemic increase in the GUS activity of rosette leaves at 4-hr after infiltration, whereas H_2O-treated rosette leaves induced a barely perceptible difference in GUS activity when compared to non-treated leaves, however there was a localised increase in GUS activity induced by both flg22 and H_2O injection at the wound/infiltration site as indicated by arrows (Figure 4.5). Notably, GUS activity was very much different in the seedlings when grown in long-day conditions and short-day conditions (Figure 4.4-4.6). Twenty-four day-old seedling grown in long-day conditions started bolting, and the GUS activity clearly was observed in leaves and likely increased along with leaf age; this GUS activity was firstly seen in the petiole of the young leaf, then gradually increased in the petiole and appeared in veins of mature leaves and the whole tissue of old leaves (Figure 4.6 a, c-e). Additionally, GUS activity was also observed in young cauline leaves and sepals but not in stems when bolting (Figure 4.6b). This age-dependent *CML41* expression in the seedling in long-day conditions was initially considered as an indication that CML41 was involved in response to leaf age or even senescence.

Individual-leaf senescence can be induced by dark-treatment and is associated with a spectacular phenomenon on this leaf – the breakdown of chlorophyll (Weaver and Amasino, 2001; Hörtensteiner, 2006; Keech et al., 2007). As such, 2-week dark was imposed on individual rosette leaf of 6 week-old *proCML41*::*GUS* plants grown in short-day conditions. GUS histochemical assay again

was utilized to stain the leaves with or without this dark treatment to reveal the possibility of senescence-induced *CML41* expression. Obviously, this 2-week dark treatment imposed a significant senescence on leaves with a clear breakdown of chlorophyll, compared to leaves without dark treatment (Figure 4.6f, g). GUS activity was observed highly in the main vein of 8 week-old rosette leaves and somewhat on the other part of those leaves; whereas there was barely GUS activity on the chlorophyll-degraded site of 8 week-old rosette leaves with 2-week dark treatment (Figure 4.6f-i).
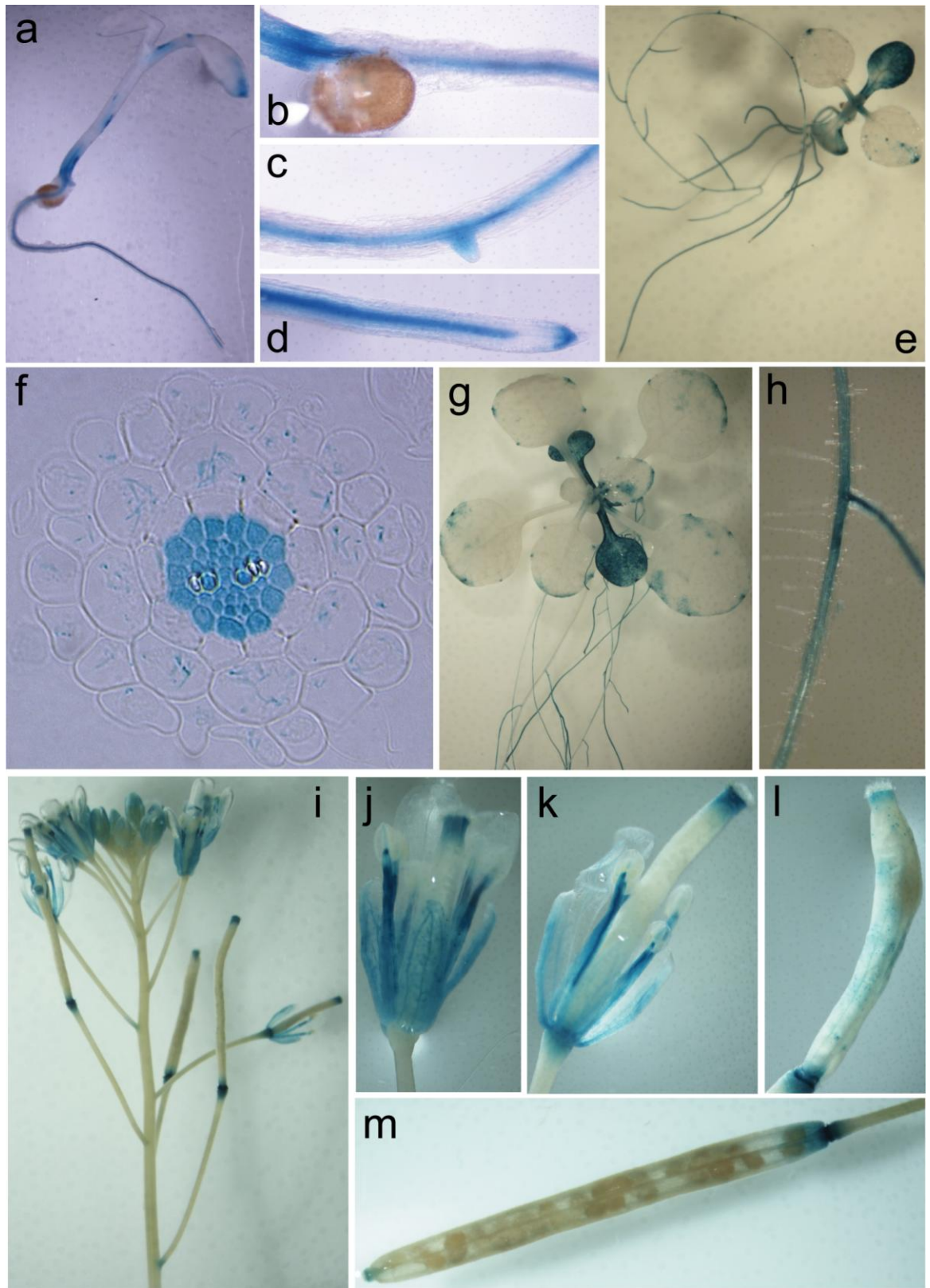
Figure 4.4 Tissue-specific expression of *CML41* in Arabidopsis grown in short-day conditions.
a-d, *proCML41*::*GUS* activity in 5 day-old Arabidopsis seedlings. **e**, *proCML41*::*GUS* expression in 10 day-old Arabidopsis seedlings. **f**, cross-section of 5 day-old Arabidopsis root expressing *proCML41*::*GUS*. **g-h**, 17 day-old Arabidopsis seedlings expressing *proCML41*::*GUS*. **i-l**, 40 day-old *proCML41*::*GUS* flowering plants. **m**, silique of 50 day-old *proCML41*::*GUS* Arabidopsis. **n**, a negative control of GUS histochemical assay on non-*GUS*-transformed seedlings. All Arabidopsis plants were grown in short day conditions. The *proCML41*::*GUS* seedlings were grown on ½ MS agar medium in short day conditions (with 9 hr light/15 hr dark) for 4 weeks before being transferred into soil and grown in long day conditions (with 16 hr light/8 hr dark).
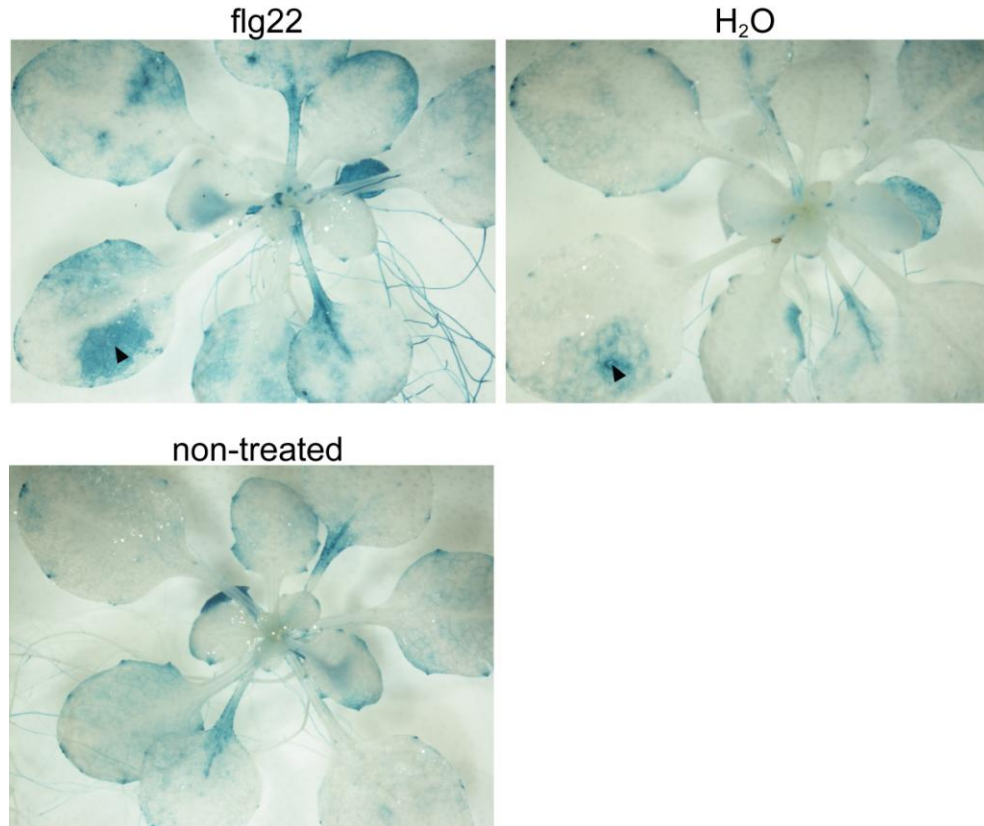
Figure 4.5 GUS activity of *proCML41::GUS* Arabidopsis in response to flg22 infiltration. GUS histochemical staining of 24 day-old *proCML41*::*GUS* Arabidopsis after 4-hr infiltration with either 2 μM flg22 or H_2O, as well as non-infiltrated grown at short-day conditions (with 9 hr light/15 hr dark). '►' points to the infiltration site of flg22 or H_2O into leaf.
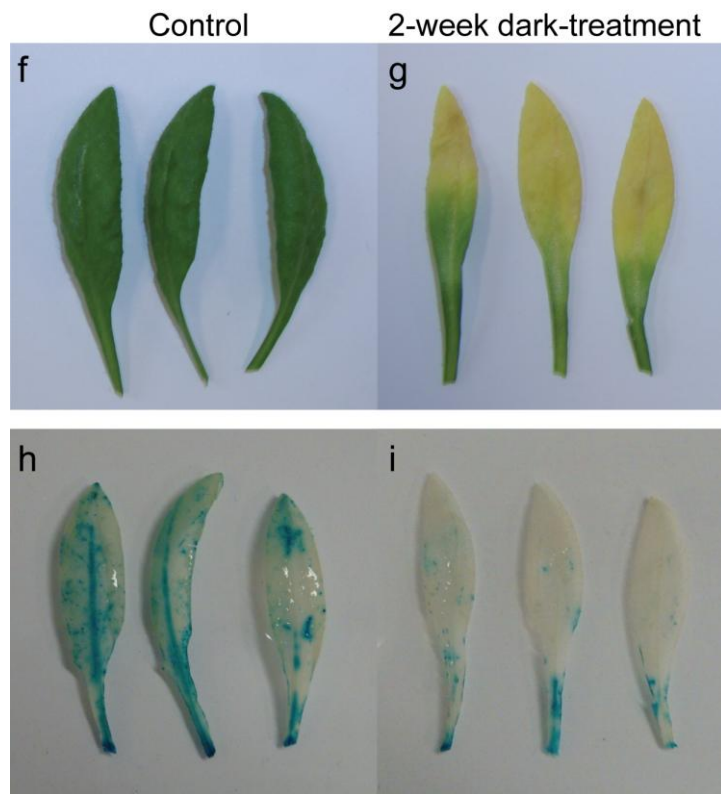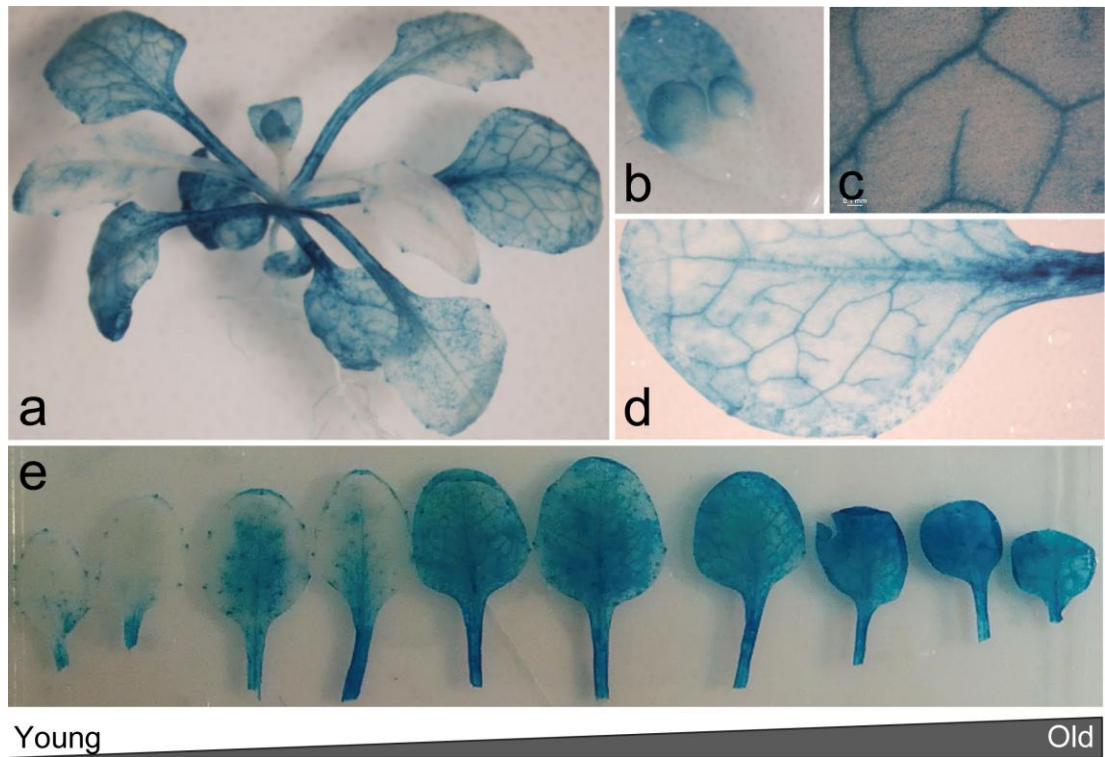
Figure 4.6 Tissue-specific expression of *CML41* in Arabidopsis grown in long day conditions or in short day conditions treated with dark on individual rosette leaf. a, *proCML41*::*GUS* activity

in 24 day old of Arabidopsis seedlings grown in long day conditions (16 hr light/8 hr dark, 22 ºC). **b-e**, zoom-in images of *proCML41*::*GUS* activity in different organs of seedlings in **a**. **e**, *proCML41*::*GUS* activity in detached leaves of plant shown in **a**, aligned from the youngest (on left) to the oldest (on right). **f** and **g**, images of leaves of 8 week old *proCML41*::*GUS* Arabidopsis grown in short-day conditions without dark treatment (**f**) or with 2 week dark treatment (**g**), as shown in an typical example in Figure 4.3. **h** and **i**, GUS activity in those leaves respectively shown in **f** and **g**.

4.3.2 *CML41FL* and *S* expression in transgenic *35S*::*CML41FL, 35S*::*CML41S* and *35S*::*CML41*-amiRNA lines

To investigate the role of *CML41FL* and *S in planta*, I planned to examine Arabidopsis plants through gain and loss of *CML41FL* and *S* expression. To this end, both *CM41FL* and *CML41S* were overexpressed driven by the 2×35S promoter in Arabidopsis via *Agrobacterium*-mediated transformation. The transformants were examined using PCR analysis on their gDNA to confirm the presence of the T-DNA insertion into transfromants before their gene expression were further investigated. Here the PCR amplification indicated that *CML41FL*-OEX-2 and -12, *CML41S*-OEX-3, -4 and -6, *CML41*-amiRNA#1-1, -2 and -8, *CML41*-amiRNA#2-1, -4 and -8 lines all had a T-DNA insertion event, suggesting that they all had been transformed (Figure 4.7). A further analysis by qRT-PCR indicated that *CML41FL* transcript level was dramatically increased by more than 2500- and 4000-fold respectivelyin overexpression lines *CML41FL-OEX-2* and *-12* (*P < 0.0001*) in comparison to control wild-type Col-0 plants, but was not significantly different in *CML41S* overexpression lines compared to controls (*CML41S-OEX-3* and *-6*) (*P > 0.05*) (Figure 4.8A). *CML41S* transcript level was considerably enhanced in *CML41S-OEX-3* by about 14-fold and 28,000-fold in *CML41-OEX-6* compared to wild-type Col-0. Interestingly, CML41S also appeared to have increased in *CML41FL-OEX-2* and *-12,* 260- and 330-fold respectively, as indicated by qRT-PCR (*P < 0.05*) (Figure 4.8A). In Col-0 in standard conditions, the transcript level of *CML41S* was only about 12% of *CML41FL* (Figure 4.8A).
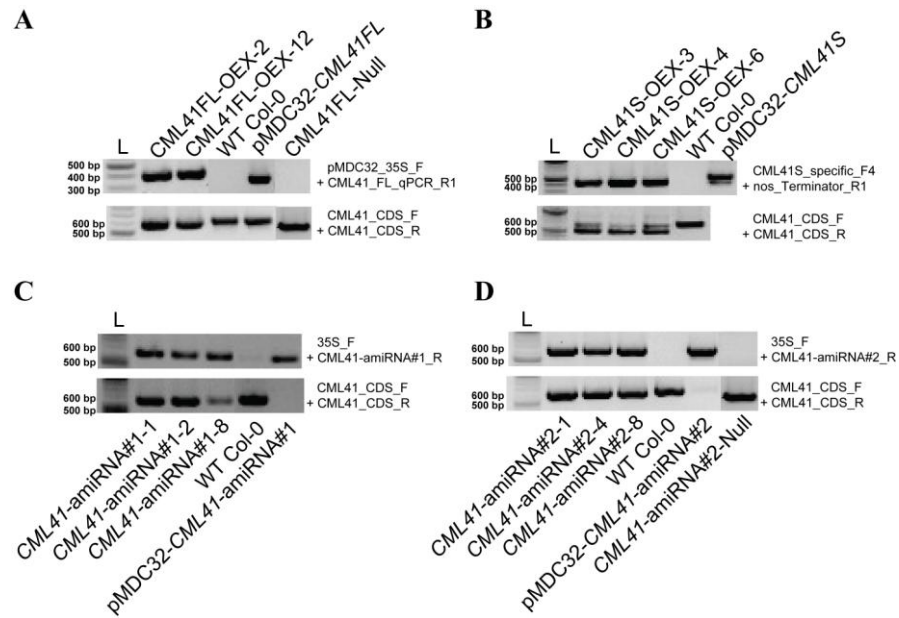
Figure 4.7 PCR amplification to validate the putative Arabidopsis T_1 transformants and wild-type Col-0. PCR amplified fragments from Arabidopsis gDNA for genes of interest derived from the pMDC32 binary vector with primers (listed in Table 4.3) as indicated in the upper panels of **A**, **B**, **C** and **D**; control PCR reactions amplified *CML41* fragments on gDNA of putative T_1 transformants and wide-type Col-0 as templates with CML41_CDS_F/R primers (listed in Table 4.3) as indicated in the lower panels of **A**, **B**, **C** and **D**. **A**, *CML41FL-OEX-2* and *-12* refer to No.2 and 12 putative transformants with *CML41FL* overexpression; *CML4FL*-Null refers to the null line of *CML41FL-OEX* plant. **B**, *CML41S-OEX-3*, *-4* and *-6* refer to No.3, 4 and 6 putative transformants with *CML41S* overexpression. **C**, *CML41*-amiRNA#1-1, -2 and -8 refer to No.1, 2 and 8 putative transformants with *CML41*-amiRNA#1 overexpression. **D**, *CML41*-amiRNA#2-1, -4 and -8 refer to No.1, 4 and 8 putative transformants with *CML41*-amiRNA#2 overexpression; *CML41*-amiRNA#2-Null refers to the null line of *CML41*-amiRNA#2 plant. Wild-type Col-0 gDNA and plasmid DNA of pMDC32 vector containing genes of interest respectively were used as negative and positive controls in **A**, **B**, **C** and **D**, L = DNA marker ladders, 100 bp DNA Ladder (New England Biolabs).
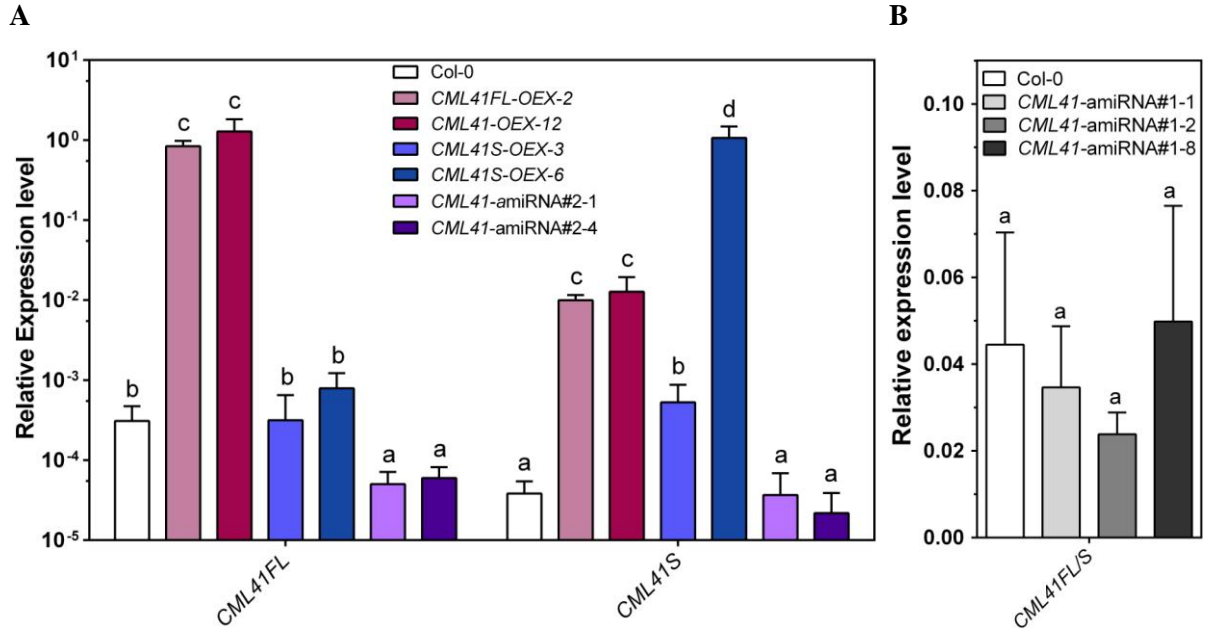
Figure 4.8 *CML41FL* **and** *S* **expression level in** *35S::CML41FL,* *35S::CML41S* **and** *35S::CML41-*
amiRNA Arabidopsis lines and Col-0. qRT-PCR analysis of *CML41FL* and *S* expression with
primer pairs CML41FL_qPCR_F1/R1 and CML41S_qPCR_F1/R3 (listed in Table 4.4) in the leaves
of 5-6 week-old plants grown in BNS in short-day conditions (with 9 hr light/15 hr dark) in **A** or in
the leaves of 5-6 week-old plants grown in BNS in short-day conditions treated with 1 μM flg22 in **B**;
gene expression level was relative to *GAPDH-A* (At3g26650). Mean ± SD, n = 5 plants in **A** and n =
4 plants in **B**, qRT-PCR performed in triplicate; a, b, c and d represent data groups that are not
statistically different, as determined by Student's *t* test, *P < 0.05*.

To abolish *CML41FL* and *S* expression *in planta* the T-DNA Express database
(http://signal.salk.edu/cgi-bin/tdnaexpress) was mined to identify whether any *CML41* T-DNA-
insertion line existed (Alonso et al., 2003). However, no line with a T-DNA inserted into *CML41* was
available in this database, so an alternative approach that employs amiRNA technology to induce
specific gene-silencing in Arabidopsis was used (Schwab et al., 2006; Ossowski et al., 2008). Two
amiRNAs are recommended for one target gene since the chance for a designed amiRNA silencing its
target is around 75% (refers to http://wmd3.weigelworld.org/cgi-
bin/webapp.cgi?page=Help#procedure). Searching for *CML41*-amiRNA#1 and *CML41*-amiRNA#2
targets in WMD3 database indicated that both amiRNAs were specifically targeted to *CML41 mRNA*
and bound to different regions of the genes (to 3'-UTR and C-terminal coding region of *CML41*
mRNA respectively, with an approximate hybridization energy of -36 kcal/mol) (Figure 4.2),

suggesting that overexpression of either amiRNA could be reasonably expected to target both *CML41FL and CML41S* transcripts and silence them simultaneously (Figure 4.2). The overexpression of *CML41*-amiRNA#1 failed to silence either *CML41FL* or *CML41S* in all three *CML41*-amiRNA#1-1, -2 and -8 lines (Figure 4.8B). But the overexpression of *CML41*-amiRNA#2, by contrast, reduced expression of *CML41FL* by up to 84% rather but not *CML41S* in the lines *CML41*-amiRNA#2-1 and -4 in standard conditions (*P < 0.05*) (Figure 4.8A).

4.3.3 Gene expression profiles in transgenic *35S::CML41FL, 35S::CML41S* and *35S::CML41-amiRNA#2* lines

In addition to quantifying *CML41FL* and *S* expression in these overexpression lines, *CAX1* and *CAX3* transcript profiles were also investigated in *CML41FL* and *S-OEX* lines, as I hypothesised that *CML41FL* and *S* might control expression of either of them. However, neither *CAX1* nor *CAX3* transcript levels was altered in leaves of any of these overexpression lines compared to wild-type Col-0 (*P > 0.05*) (Figure 4.9). In addition, some sample hormone- and chemical-response marker genes, including *ARR5* (At3g48100, marker gene for cytokinin – CK), *BR6ox2* (At3g30180, marker gene for BR), *IAA1* (At4g14560, marker gene for auxin – IAA), *SCL3* (At1g50420, marker gene for gibberellins – GA) and *PR1* (At2g14610, marker gene for SA), were not misexpressed by overexpressing either *CML41FL* or *CML41S* (Figure 4.9) (Abel et al., 1995; Penninckx et al., 1996; Taniguchi et al., 1998; Ogawa et al., 2003; Shimada et al., 2003). *CAX3*, *ARR5* and *IAA1* expression did not respond to the knock-down of *CML41FL* in the leaves of *CML41*-amiRNA#2 lines (Figure 4.9B). Additionally, nitric oxide synthase-type gene (*NOA1*) and *ICS1* seemed not to have an altered expression level in *CML41FL* and *S-OEX* lines (*P < 0.05*) (Figure 4.9A).

A
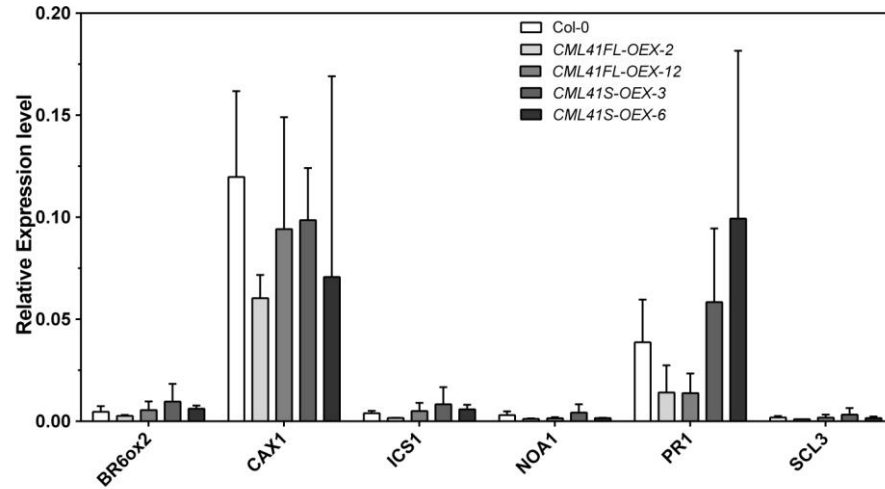
B
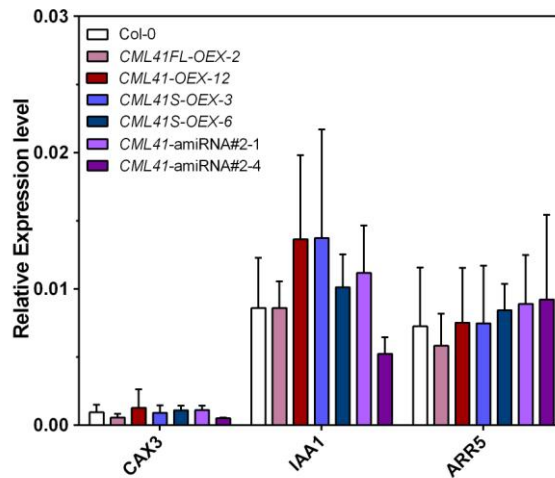
Figure 4.9 Gene transcription profile in *35S*::*CML41FL*, *35S*::*CML41S* lines and Col-0. A, qRT-PCR analysis of gene expression in the leaves of 5-6 week-old *35S*::*CML41FL*, *35S*::*CML41S* lines and Col-0 grown in BNS in short day conditions (with 9 hr light/15 hr dark) with qRT-PCR primers listed in Table 4.4. **B**, qRT-PCR analysis of gene expression in the leaves of 5-6 week-old *35S*::*CML41FL*, *35S*::*CML41S*, *35S*::*CML41-amiRNA#2* lines and Col-0 grown in BNS in short day conditions with qRT-PCR primers listed in Table 4.4. Gene transcript level was relative to *GAPDH-A* (At3g26650). Mean ± SD, **A**, n = 3 plants, **B**, n = 5 plants, qRT-PCR performed in triple-technical replicates, statistical difference was determined by One-way ANOVA, *P < 0.05*.

As the GUS histochemical assay indicated that *CML41* expression could be induced in leaves in short day conditions by flg22 treatment (Figure 4.5), a further investigation of *CML41FL* and *S* transcription following flg22 treatment was performed using qRT-PCR. This was deemed appropriate as a limitation of GUS-reporter assays is that such staining intensities are able to be accumulated over time even if the real-time gene expression is very low, this is because of that GUS is also very stable and not easily degraded in plant cells (Mantis and Tague, 2000). Pre-infiltration of 1 μM flg22 significantly increased both *CML41FL* and *CML41S* transcript level in wild-type Col-0 by about 6- and 2-fold respectively compared to H_2O-control treatment (Figure 4.10A). Similarly, flg22 treatment also significantly up-regulated *CML41FL* by 7- and 18-fold relative to H_2O treatment in *CML41*-amiRNA#2-1 and -4 lines; the transcript level under flg22 in these lines approached that of the basal transcript level of *CML41FL* in H_2O-treated wild-type Col-0, but was still 4 to 5-fold lower in abundance in wild-type Col-0 with flg22 treatment (Figure 4.10A). Although it had a greater mean expression, *CML41S* transcript level was not statistically different between flg22- and H_2O-treated *CML41*-amiRNA#2 lines (Figure 4.10A). Of the other genes examined in *CML41*-amiRNA#2-1 and -4 lines, *Actin2*, *CAX3* and *ACA10* were significantly up-regulated by about 2-, 6- and 5-fold respectively in the wild-type Col-0 by flg22 compared to H_2O treatment (*P < 0.05*); however, although the mean expression of these genes did increase with flg22-treatment in *CML41*-amiRNA#2 lines, there was an insignificant increase in their transcriptional abundance relative to H_2O treatment (*P > 0.05*) (Figure 4.10B). Homologs of *CAX3* and *ACA10, CAX1* and *ACA8*, appeared not to respond to flg22 in by changing their abundance, as they displayed similar transcript levels in flg22- and H_2O-treated *CML41*-amiRNA#2 lines and wild-type plants (*P > 0.05*) (Figure 4.10B). *PR1* had increased abundance after pre-infiltration with flg22 in both the wild-type plants and *CML41*-amiRNA#2 lines (Figure 4.10B).

A

B
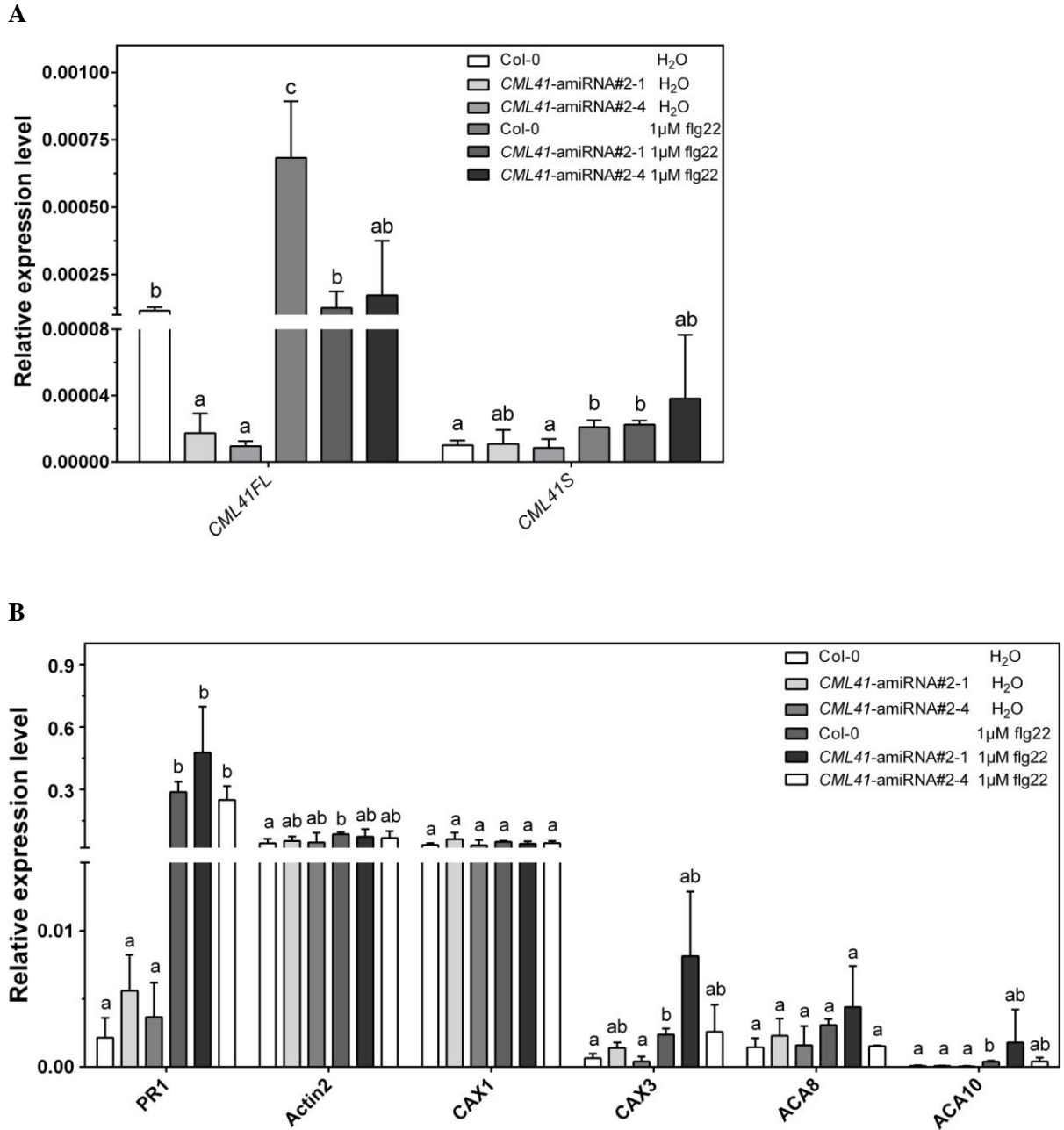
Figure 4.10 Gene expression level in *CML41*-amiRNA#2 lines treated with either flg22 or H₂O.
qRT-PCR analysis of *CML41FL* and *CML41S* expression (**A**) and other gene expression (**B**) in the leaves of 5-6 week-old *35S::CML41-amiRNA#2* lines and wild-type Col-0 grown in BNS in short day conditions (with 9 hr light/15 hr dark) pre-infiltrated by either 1 μM flg22 or H₂O with primer pairs as listed in Table 4.4. Mean ± SD, n = 3 plants, qRT-PCR performed in triple-technical replicates. Gene transcript level was relative to *GAPDH-A* (At3g26650) in both **A** and **B**. a, b and c represent data groups that are not statistically different, as determined by Student's *t* test, *P < 0.05*.

4.3.4 Senescence and growth phenotypes in *CML41FL* and *S-OEX* and amiRNA lines

The transgenic T_2 Arabidopsis lines whose *CML41FL* and *S* misexpression had been validated by qRT-PCR were grown on a BNS agar medium to undergo rapid screening for stress conditions to compare resulting phenotypes with wildtype plants; it was hoped that this might uncover a CML41FL and S-associated phenotype. However, *CML41FL* and *S–OEX* and *CML41*-amiRNA lines had no obvious growth differences compared to wild-type Col-0 plants when they were grown in either a BNS agar medium in short day conditions with or without stresses, such as salt (up to 200 mM NaCl), a high osmotic stress (up to 500 mM mannitol) or a Ca^{2+}-depleted condition (2 mM EGTA) (Figure 4.11A and B). Later, transgenic T_3 Arabidopsis homozygous lines, as well as wild-type Col-0 plants, were grown on a ½ MS agar medium with or without additional $CaCl_2$ supplementation in long day conditions. When grown in a ½ MS medium, the primary-root length of a week-old *CML41FL* and *S-OEX*, *CML41*-amiRNA#2-1 seedlings was similar to that of wild-type Col-0, but the *CML41*-amiRNA#2-4 line whose primary root was 7.704 ± 0.677 mm in length, was significantly shorter than Col-0 primary root (10.085 ± 0.493 mm) (Figure 4.11C and D). The supplement of 12.5 mM $CaCl_2$ increased the primary root length of Col-0 by 16.4% and of *CML41*-amiRNA#2-1 and -4 lines respectively by 25% and 30% (*P < 0.05*); however this amount of $CaCl_2$ had a non-significant effect on the primary root of *CML41FL* and *S-OEX* seedlings (*P > 0.05*) (Figure 4.11C and D). Then, an increase in this $CaCl_2$ supplement to 50 mM notably reduced the primary root growth (by 26.1%) of wild-type Col-0, (up to 36.8% and 44.5%) of *CML41FL OEX-2* and *-12* lines and (27.2% and 36.5%) of *CML41S-OEX-3* and *-6* lines separately, compared to their primary root growth in ½ MS medium without additional $CaCl_2$ (*P < 0.05*). In contrast, the primary-root growth of *CML41*-amiRNA#2 lines was insignificantly impaired by 50 mM Ca^{2+} (Figure 4.11C and D).

When *CML41FL* and *S-OEX*, *CML41*-amiRNA#2 lines and wild-type Col-0 were grown in soil in long day conditions, they had little difference in the their plant size, and no obvious difference was observed at flowering stage (Figure 4.12 A and B)

A

Col-0   *CML41FL-OEX*   Col-0   *CML41S-OEX*

Col-0   *CML41-amiRNA*

B

Col-0   *CML41FL-OEX*   Col-0   *CML41S-OEX*   Col-0   *CML41-amiRNA*

2 mM EGTA

100 mM NaCl

200 mM NaCl

200 mM Mannitol

500 mM Mannitol
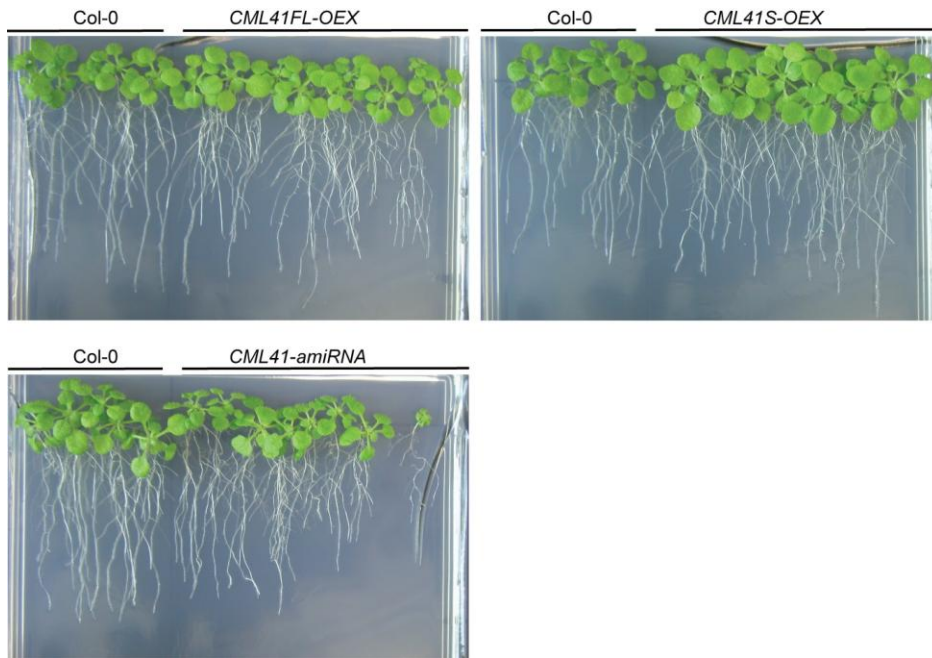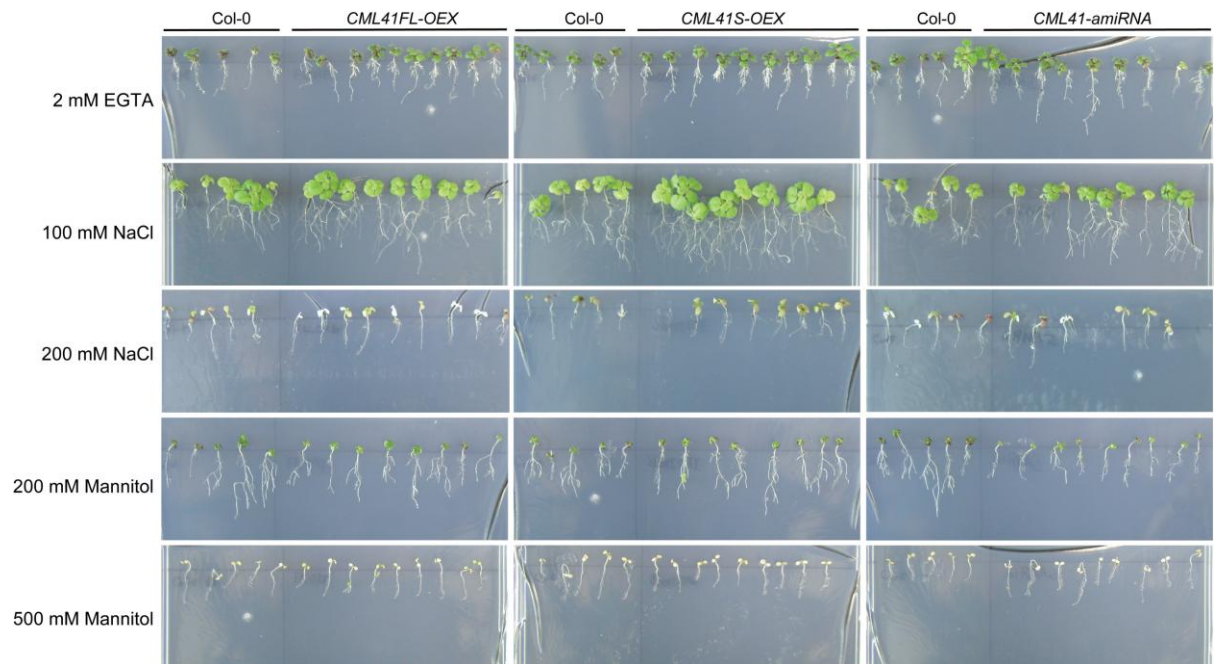
C
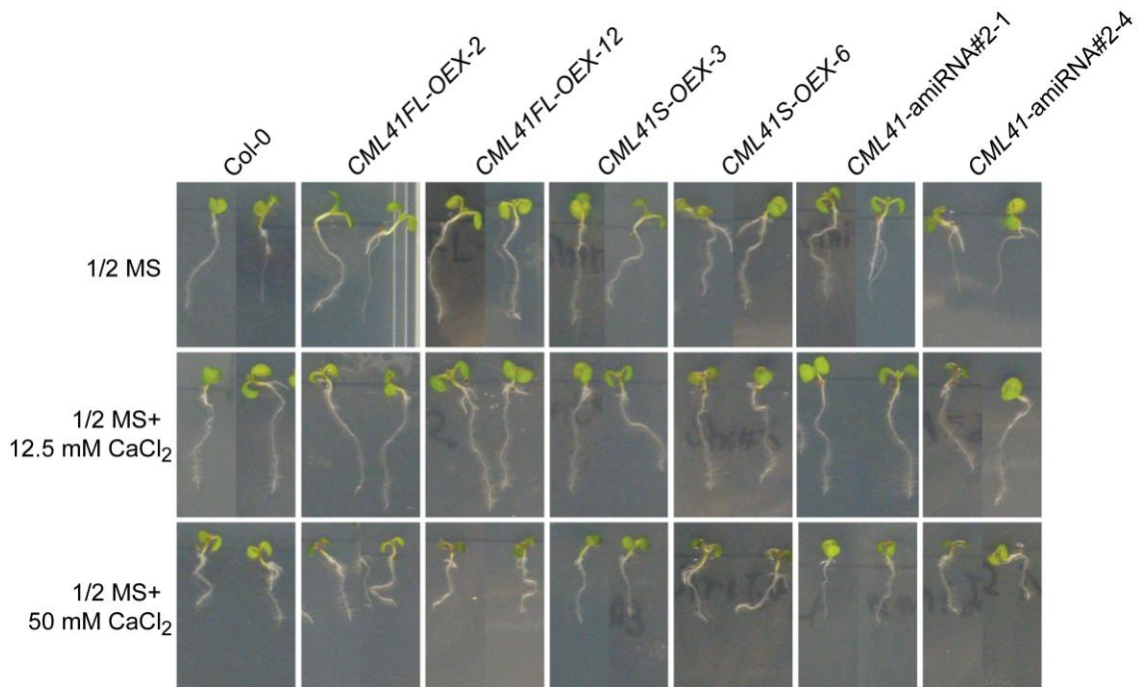
D
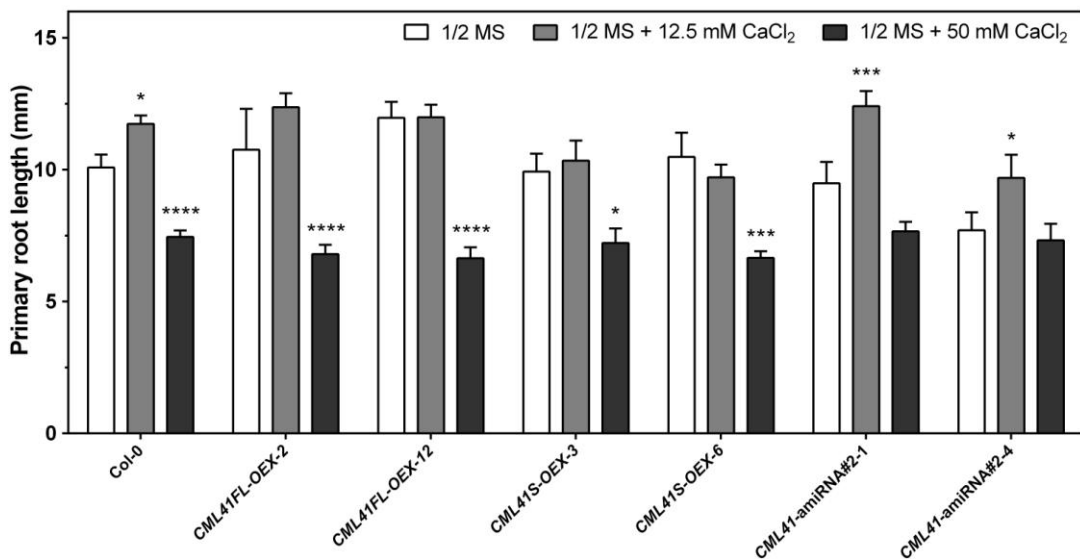
Figure 4.11 Growth measurements of *CML41FL* and *S-OEX*, *CML41*-amiRNA lines and Col-0 on agar medium. A, images of 3 week-old seedlings of *CML41FL* and *S-OEX*, *CML41*-amiRNA lines and Col-0 grown in BNS plus 1.2% (w/v) agar in short day conditions (with 9 hr light/15 hr dark). **B**, images of 3 week-old seedlings of *CML41FL* and *S-OEX*, *CML41*-amiRNA lines and Col-0 grown in BNS plus 1.2% (w/v) agar for one week and transferred to fresh BNS medium with either 2 mM EGTA, 100 mM NaCl, 200 mM NaCl, 200 mM mannitol or 500 mM mannitol for additional 2

weeks in short day conditions. **C**, images of 1-week-old seedlings of *CML41FL* and *S-OEX*, *CML41*-amiRNA lines and Col-0 germinated and grown in ½ MS medium plus 1% (w/v) agar in long day conditions (16 hr light/8 hr dark, 22 ℃) with or without additional $CaCl_2$ supplement as indicated. **D**, the primary root length of transgenic and wild-type seedlings as indicated in **C** quantified by ImageJ, Mean ± SE; Col-0 plants, n = 22-48; *CML41FL-OEX-2*, n = 8-19; *CML41FL-OEX-12*, n = 11-26; *CML41S-OEX-3*, n = 7-12; *CML41S-OEX-6*, n = 7-22; *CML41*-amiRNA#2-1, n = 12-23; *CML41*-amiRNA#2-4, n = 11-17; statistical difference compared the primary-root length within each line in $CaCl_2$-supplemented medium with normal ½ MS medium, and was determined by Two-way ANOVA, *, *** and **** represent *P < 0.05*, *< 0.001* and *< 0.0001* respectively.

A

Col-0   *CML41*-amiRNA#2-1   *CML41*-amiRNA#2-4

CML41FL-OEX-2   *CML41FL-OEX-12*   *CML41S-OEX-3*   *CML41S-O*

B

CML41S-OEX-6   *CML41*-amiRNA#2-1   *CML41*-amiRNA#2-4
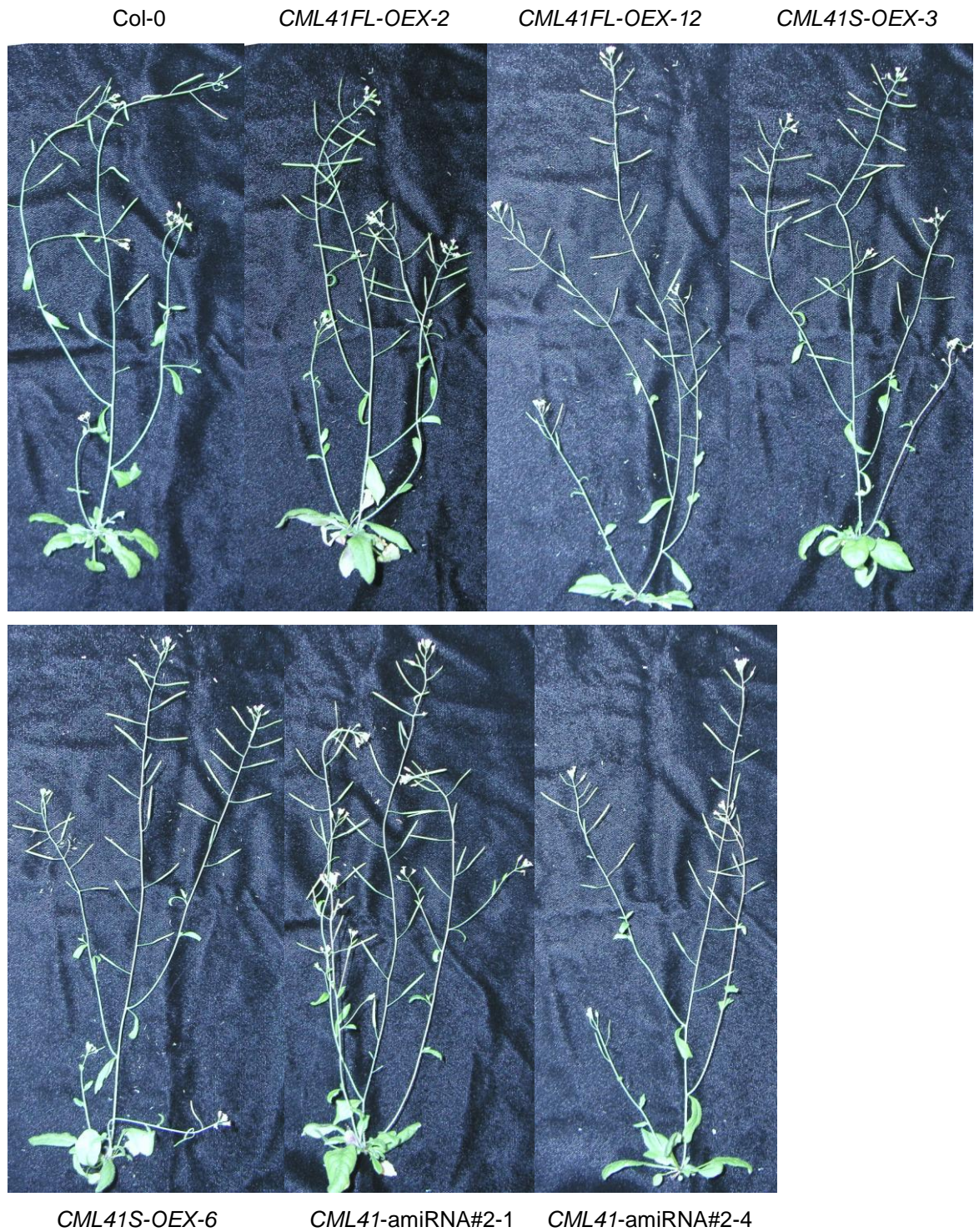
Figure 4.12 Growth of *CML41FL* and *S-OEX*, *CML41*-amiRNA lines and Col-0 in soil. A, images of 4 week-old *CML41FL* and *S-OEX*, *CML41*-amiRNA lines and Col-0 grown in soil in long day conditions (16 hr light/8 hr dark, 22 ºC). **B**, images of 7 week-old flowering *CML41FL* and *S-OEX*, *CML41*-amiRNA lines and Col-0 grown in soil in long day conditions.

A correlation of *CML41* expression with leaf senescence had been investigated in *proCML41*::*GUS* plants grown in short day conditions and results indicated that the senescence (or chlorophyll-breakdown) was linked to suppressed *CML41* expression rather than induced *CML41* expression in rosette leaves at the sites of chlorophyll-breakdown for a dark treatment of 14 days (Figure 4.6f-i). As such, I planned to impose a similar dark treatment with a shorter period (0 d, 2 d and 4 d) on individual rosette leaves of *CML41FL* and *S* overexpression lines, *CML41*-amiRNA#2 (knocked-down) lines and wild-type plants grown in short day conditions. I expected to see a differential degree of senescence within those lines to uncover whether the there was an up- or down-regulation of *CML41FL* and *S* during leaf senescence. All lines possessed similar level of chlorophyll content without dark treatment about 0.548 ± 0.077 µg per mg of fresh tissue across all samples (One-way ANOVA, *P>0.05*) (Figure 4.13). After 2 d and 4 d dark treatments, the chlorophyll level was different across lines. The chlorophyll content in the leaves of Col-0, *CML41FL-OEX-2* and *-12* lines was slightly decreased after 4-day dark treatment but was statistically not significant (reduced from 0.478 ± 0.033 down to 0.407 ± 0.038 µg/mg in Col-0; from 0.511 ± 0.023 down to 0.490 ± 0.033 µg/ mg in *CML41FL-OEX-2*; from 0.533 ± 0.025 down to 0.457 ± 0.054 µg/ mg in *CML41FL-OEX-12*); whereas *CML41S-OEX-3*, *-6* and *CML41*-amiRNA#2-1, -4 lines had a significant reduction of chlorophyll content after 4-day dark treatment (reduced from 0.550 ± 0.064 down to 0.405 ± 0.036 µg/ mg in *CML41S-OEX-3*; from 0.580 ± 0.064 down to 4.22 ± 0.02 µg/ mg in *CML41S-OEX-6*; from 0.629 ± 0.023 down to 0.384 ± 0.053 µg/ mg in *CML41*-amiRNA#2-1; 0.547 ± 0.033 down to 0.412 ± 0.028 µg/ mg in *CML41*-amiRNA#2-4) (Figure 4.13)
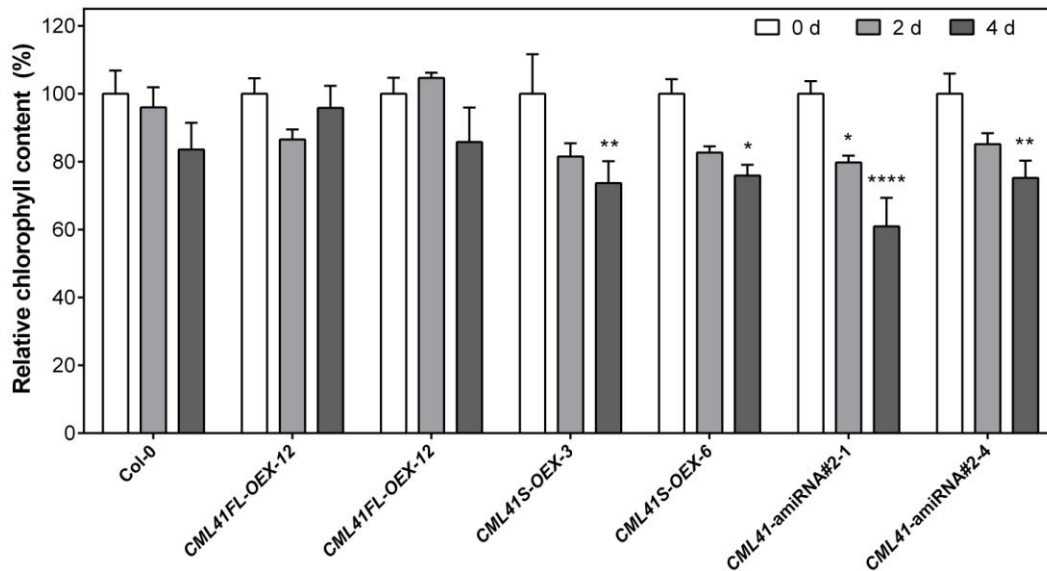
Figure 4.13 Relative leaf chlorophyll content of *CML41FL* and *S-OEX*, *CML41*-amiRNA lines and wild-type Col-0 after dark treatment. The chlorophyll content (in μg per mg of FW) with 2- or 4-d dark treatment is relative to the mean of chlorophyll content without dark treatment (as 100%) within each lines. Mean ± SE, n = 3 plants, statistical difference was determined by Two-way ANOVA, *, ** and **** represent *P < 0.05, < 0.01* and *< 0.0001* respectively.

4.3.5 Callose measurement

Both qRT-PCR analysis and GUS histochemical assays suggested a probable role of *CML41* in response to flg22 in leaves (Figure 4.5 and 4.10A). As an elicitor of *P. syringae* pv. tomato, flg22 can induce callose deposition in leaves (Gómez-Gómez et al., 1999; Zipfel et al., 2004). Callose consists of β-1,3-glucan and can be detected via histochemical aniline-blue staining (Stone et al., 1984; Hückelhoven, 2007). Therein, a comparison of callose deposition in the plants misexpressing *CML41* was made to uncover a role for CML41 in the plants response to flg22. Obviously, the pre-infiltration of 2 μM flg22 induced widespread callose deposition in the leaves of wild-type Col-0, up to 230 ± 25.1 callose spots mm^{-2} leaf area of view compared to a H_2O infiltration of merely about 5 ± 0.9 (Figure 4.14A). Whereas, both *CML41*-amiRNA#2-1 and -4 lines accumulated significantly much less callose respectively, down to 89.6 ± 6.3 and 60 ± 15.3 mm^{-2} leaf area after flg22 treatment (*P < 0.0001*) (Figure 4.14A). Meanwhile, the quantification of callose was also performed in leaves of *CML41FL* and *S-OEX* lines in comparison to Col-0 with H_2O treatment. However, the number of callose deposited in leaves by H_2O infiltration was similar across *CML41FL* and *S-OEX*, *CML41-*

107

amiRNA lines and wild-type Col-0 at an average of 3.3 ± 0.4 callose spots mm^{-2} leaf area across treatments (Figure 4.14A and B).

A

B
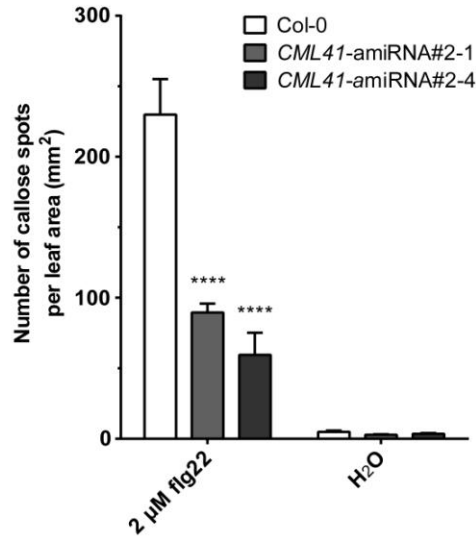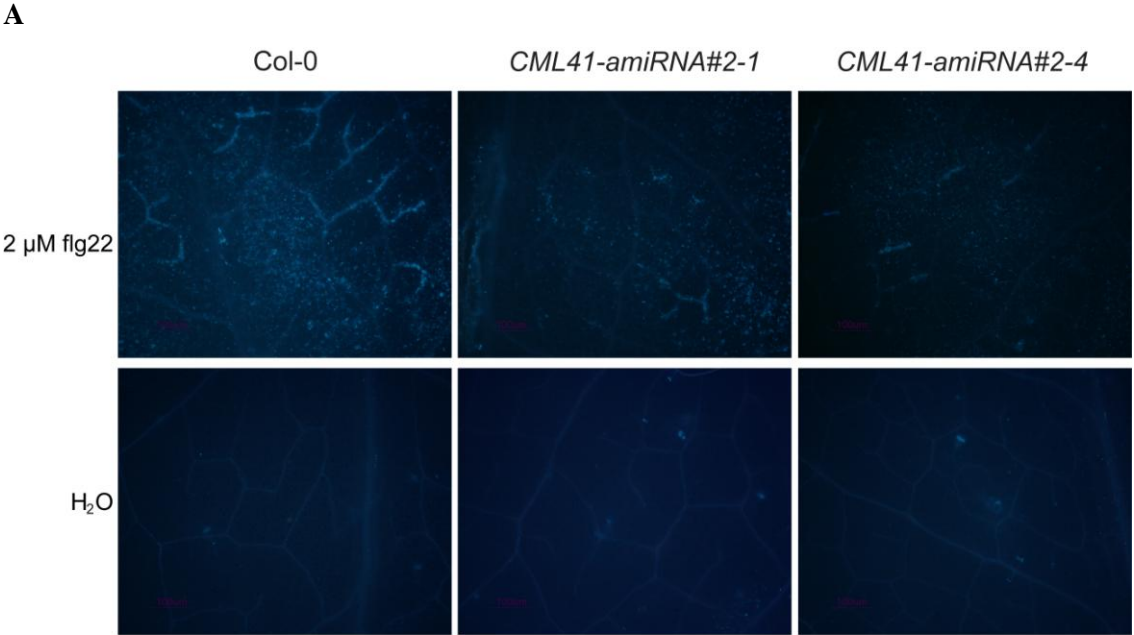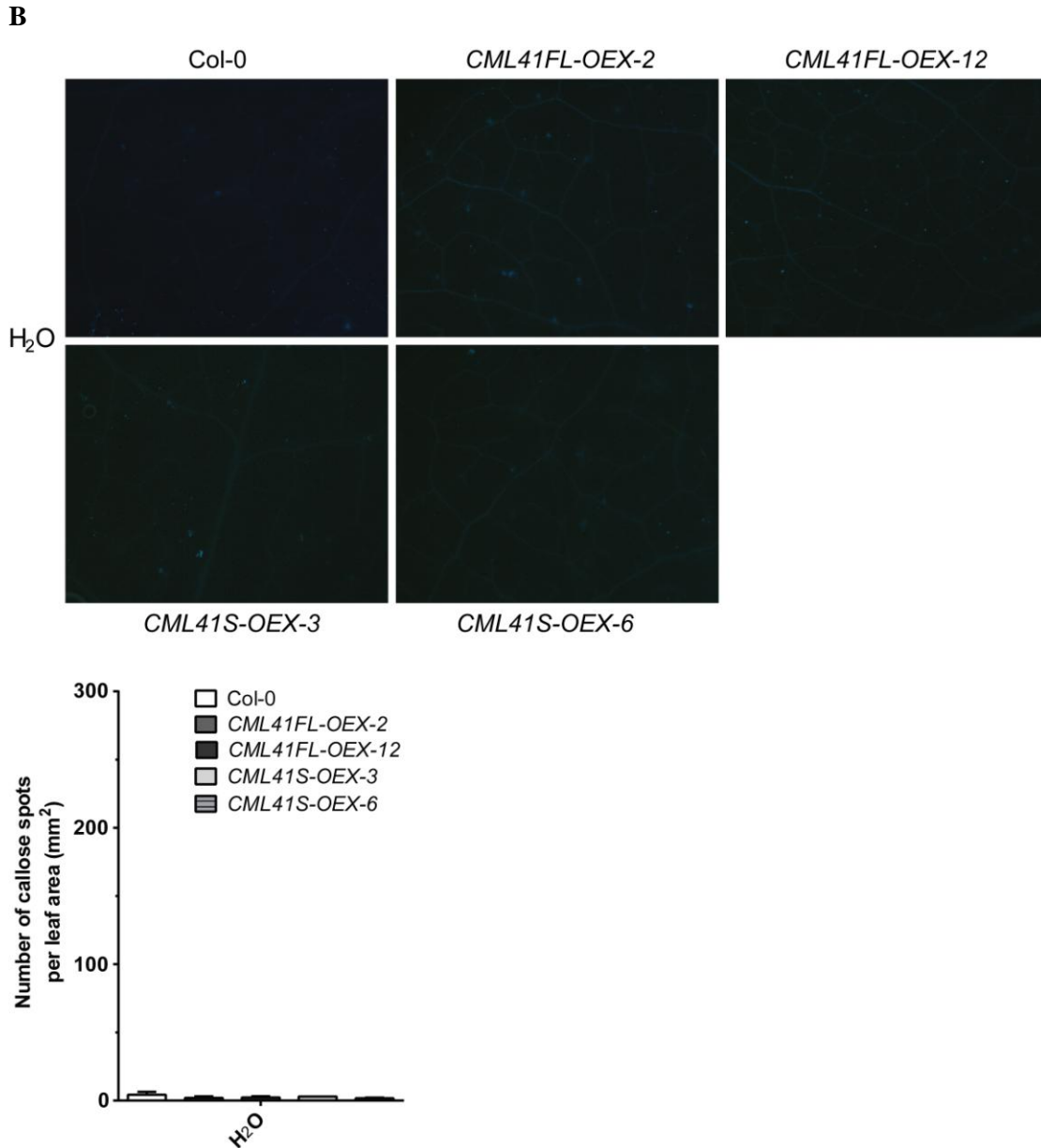
Figure 4.14 Callose deposition in *CML41FL* and *S-OEX*, *CML41*-amiRNA lines and wild-type Col-0. A, callose deposition in the leaves of 4-5 week-old *CML41*-amiRNA#2-1, -4 and Col-0 grown in short day conditions (with 9 hr light/15 hr dark) upon flg22 or H_2O treatment, three separated leaves of six individual plants per lines were pre-infiltrated with either 2 μM flg22 or H_2O for 24 hr before aniline-blue staining, Mean $\pm$ SE, n = 6, statistical difference analysis by One-way ANOVA, *P < 0.0001*. **B**, callose deposition in the leaves of 4-5 week-old *CML41FL* and *S-OEX* lines and Col-0 grown under short-day conditions upon H_2O treatment, single leaves of three individual plants per lines were pre-infiltrated with H_2O for 24 hr before aniline-blue staining, Mean $\pm$ SE, n = 3, statistical difference analysis by One-way ANOVA, *P < 0.05*.

4.4 Discussion

4.4.1 *CML41FL* and *S* expression in *CML41FL* and *S* overexpression lines and *CML41-amiRNA#2* lines

Alternative transcript splicing is a widespread phenomenon in higher eukaryotes and generates proteomic and functional diversity (Graveley, 2001; Brett et al., 2002; Ner-Gaon et al., 2004; Blencowe, 2006). In the case of *AtCML41*, the gene is likely to be transcribed into two transcripts – *CML41FL* and *CML41S*. The overexpression of *CML41FL* increased *CML41FL* transcript abundance in *CML41FL-OEX-2* and *-12* lines and *CML41S* overexpression enhanced *CML41S* expression in *CML41S-OEX-3* and *-6* lines (Figure 4.8A). The overexpression of *CML41-* amiRNA#2 appeared to significantly knock down *CML41FL* expression but not *CML41S*, as indicated by qRT-PCR analysis. This is despite BLAST results of *CML41-*amiRNA#2 suggesting that it should target both *CML41FL* and *S* mRNA; the reason for this is unknown (Figure 4.2 and 4.8A). The overexpression of *CML41-*amiRNA#1 reduced neither *CML41FL* nor *CML41S* expression in plants (Figure 4.8B).

Interestingly, qRT-PCR analysis suggested that *CML41S* expression was also increased by a few hundred-fold in *CML41FL-OEX-2* and *-12* lines. On one hand, this *CML41S* in theory could be truly overexpressed in *CML41FL-OEX-2* and *-12* lines, as alternative splicing occurs on precursor-mRNA (pre-mRNA) at a post-transcriptional level (Reddy, 2007), and the constitutive expression of *CML41FL* could increase *CML41S* mRNA via pre-RNA splicing processing on *CML41* pre-mRNA. On the other hand, it may be a consequence of *CML41S* transcription being over-estimated by qRT-PCR. The quantification of alternative splicing transcripts via qRT-PCR analysis can be achieved by a few approaches involving transcript-specific primers and probes as shown in Figure 4.14 (Vandenbroucke et al., 2001).
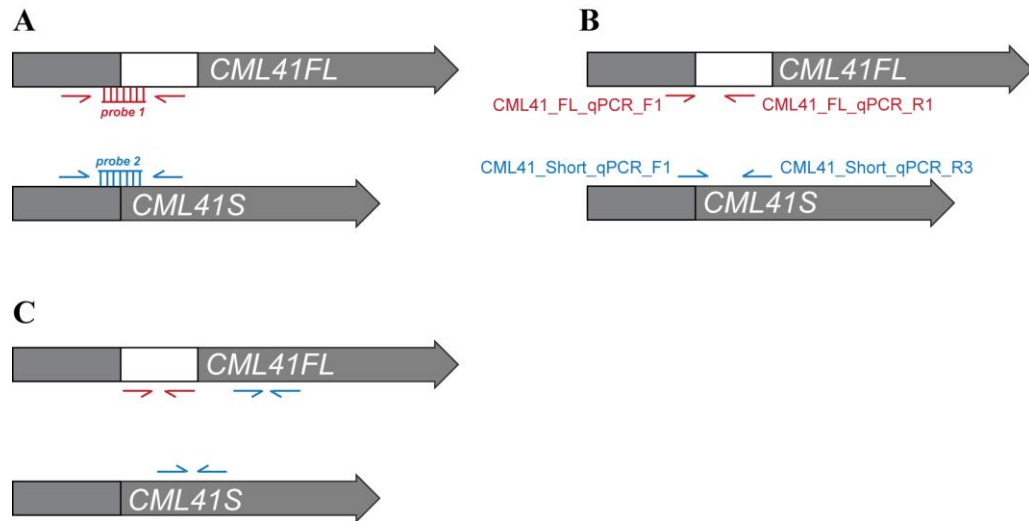
Figure 4.15 Overview of potential approaches to differentiate the alternative splicing transcripts of *CML41* by qRT-PCR analysis. A, distinguish the alternative splicing transcripts by a boundary spanning probe based on Taqman qRT-PCR. **B**, distinguish the alternative splicing transcripts by boundary-spanning/junction-specific primer pairs based on fluorescence-based qRT-PCR. **C**, distinguish the alternative splicing transcripts by quantitative subtraction using two pairs of primers based on fluorescence-based qRT-PCR. Arrows indicate the binding primers; primers in different colours point to different pairs of primers, the primer sets point to the binding site of each primer on the template as indicated in **B**, the blank region points to the splicing region of *CML41* transcript in **A**, **B** and **C**. Adapted from Vandenbroucke et al (2001)

As the SYBR green fluorescence-based qRT-PCR is well established in our lab, two strategies as shown in Figure 4.15B and C were chosen to distinguish *CML41FL* and *CML41S* transcripts. However, as stated (but not clarified) by Vandenbroucke et al (2001) the strategy in Figure 15C is only suitable for equally abundant transcripts between splicing variants. Therefore, the application of a splice junction-specific primer pair CML41S_qPCR_F1/R3 as listed in Table 4.4 was considered appropriate to distinguish the *CML41S* expression in our case, as shown in Figure 4.15B, since *CML41FL* and *CML41S* transcript level was obviously not equally abundant in leaf tissue in normal conditions (Figure 4.5). However, a PCR reaction with 40 cycles, performed on the plasmid DNA containing the *CML41FL* gene as template could amplify a product (data not shown). This presumably occurred because the CML41S_qPCR_F1 primer partially and CML41S_ qPCR_R3 primer perfectly bound *CML41FL* transcripts and together allowed a low-efficiency amplification of a product with the *CML41FL* gene as template. Whether such a low efficiency reaction could detect

CML41S from *CML41FL* as a template in cDNA is yet unknown. But if this is the case, this low-efficiency amplification may affect the quantification of *CML41S* when *CML41FL* is highly overexpressed (up to 4000-fold), and as a result potentially over-estimating *CML41S* expression in *CML41FL* overexpression lines (Figure 4.8A). As such, it is unknown, so far if this *CML41S* expression has been truly up-regulated and/or over-estimated in *CML41FL-OEX-2* and *-12* lines, unless a more accurate and specific method is applied to quantify *CML41S* expression in *CML41FL-OEX* lines, such as a junction-specific Taqman probe as shown in Figure 4.15A (Heid et al., 1996). Altenratively, such an issue could be also addressed through validation at the protein level, such as a Western blot. For instance, an application of anti-GFP antibody to probe GFP protein fused to CML41FL in plants overexpressing *CML41FL* fused with *GFP* gene (*CML41FL-GFP-OEX*), is possibly one way to uncover whether *CML41FL* or both *CML41FL* and *S* are overpressed in *CML41FL-OEX* lines. If a single product was obtained when using an anti-GFP antibody on protein extracts from *CML41FL-GFP-OEX* plants this would indicate solely *CML41FL* being overexpressed in *CML41FL-GFP* plants, if two products were obtained *CML41S* is suggested to be simutaneously overexpressed too. In conclusion, the CML41S_qPCR_F1/R3 primer pair is considered not ideal to quantify *CML41S* expression in *CML41FL*-overexpressed conditions and any difference observed between *CML41FL-OEX* lines and wild-type Col-0 has to be cautiously interpreted with respect to the role of CML41 *in planta*.

4.4.2 The involvement of CML41FL and S in plant growth and senescence

CML41 was highly expressed in the cotyledon of 10 day-old young seedlings and only at the apical regions of leaves of 3-4 week-old plants grown in short-day conditions as indicated by GUS histochemical assays (Figure 4.4e, g and 4.5, non-treated). *CML41* expression increased in leaves in an age-dependent manner in plants grown in long day conditions (Figure 4.6A), where Arabidopsis flowering occurs more quickly (Simpson and Dean, 2002). These results suggest that *CML41* expression in leaves responds to photoperiod (Figure 4.6A). In short day conditions, *CML41* expression tended to be localised to the main vein of 8 week-old plant leaves. The 2-week dark treatment induced chlorophyll degradation and senescence on 8 week-old leaves, and C*ML41* expression was relatively suppressed; it is not clear if this *CML41* suppressed expression was a result of senescence or just a response to dark as a photoperiod treatment (Figure 4.6f-i). Carviel et al (2009) inoculated *P. syringae* into *Arabidopsis* to increase intracellular SA level required for activation of age-related resistance in plants and identified *CML41* as one of age-related resistance-associated genes via analysis of the global gene misexpression profile. In addition, *CML41* was indicated tightly

co-expressed with the senescence-related gene *SAG13*, suggesting that *CML41* misexpression might be linked to somewhat age/senescence phenotype in plants (Figure 2.3) (Swartzberg et al., 2006 and 2011). Thus, I treated the plant leaf with a shorter period of dark. The 4 d dark treatment significantly reduced the chlorophyll content in treated leaves of *CML41S-OEX* and *CML41*-amiRNA#2 lines but not in wild-type Col-0 and *CML41FL-OEX* lines (Figure 4.13). In the *CML41S-OEX* plants, *CML41S* has been specifically overexpressed and in *CML41*-amiRNA#2 lines *CML41FL* has been knocked down (Figure 4.8A). Accordingly, I speculate that CML41FL and S may regulate dark-induced senescence on leaves with CML41FL perhaps negatively regulating senescence whereas CML41S acting in an opposite way; this hypothesis needs further testing. *CML41* was also observed during flowering, suggesting that CML41FL and S might also have some role in this process – something that was not further examined in this thesis (Figure 4.4i-m).

In young seedlings of about 5 to 10 days old, *CML41* was found highly expressed in the vascular tissue of roots (Figure 4.4a, e, f and h), this result coupled with its negative correlation with the major Ca^{2+} transporter gene *CAX1* expression and co-expression with *CAX3* (Figure 2.2) implicates that CML41FL and S may have a role related to Ca^{2+} nutrient uptake or response in plants. The root growth response to serial calcium dilutions has been measured in cotton by Howard and Adams (1965) and discovered that the root growth of cotton is positively correlated with soil calcium nutrient at sub-mM (ranged from 75 µM to 0.5 mM), and the calcium supplementation above 0.5 mM up to 6 mM doesn't further improve the root growth. Gerard (1971) also has measured the influence of various calcium nutrients to the cotton root and found that the calcium supplementation ranged from 7.5 mM to 10 mM leads to the maximum stimulation to the cotton root growth in moderate salt conditions. In my case, the addition of 12.5 mM $CaCl_2$ promoted the primary root growth of wild-type Col-0 (to 12.370 ± 0.534 mm), compared to (10.756 ± 1.553 mm) in normal calcium supply about 300 µM (in ½ MS medium) (Murashige and Skoog, 1962) (Figure 4.11C and D). However, increasing $CaCl_2$ up to 50 mM severely suppressed the primary root growth of the wild-type plants (down to 6.8 ± 0.35 mm), probably attributing to the ionic (about 100 mM Cl^- in ½ MS + 50 $CaCl_2$ medium) and osmotic stress/toxicity to the root growth (Figure 4.11C and D) (Teakle and Tyerman, 2009). The overexpression of *CML41FL* or *CML41S* abolished the primary root response to 12.5 mM, implicating that CML41FL and S may have a role in primary root growth in response to external/environmental calcium nutrients (Figure 4.11C and D). Notably, the knock-down *CML41FL* expression alleviated the inhibition of the primary root growth of *CML41*-amiRNA#2 lines by 50 mM $CaCl_2$, which might be linked to the greater blockage of Cl^- influx by external Ca^{2+} and/or a higher $[Ca^{2+}]_{cyt}$ in *CML41*-amiRNA#2 lines, this has to be determined by further work (Figure 4.11C and D) (Lorenzen et a., 2004; Saleh and Plieth, 2013). However, the details concerning separate contributions

113

of CML41FL and CML41S to these processes are unknown, since the *CML41S* expression profile is not confirmed in *CML41FL-OEX* lines.

4.4.3 CML41FL but not CML41S is involved in callose deposition during PAMP-triggered immunity

A number of studies, including Denoux et al (2008), Carviel et al (2009) and Bricchi et al (2012) have observed *CML41* transcript increased in abundance during pathogen responses. In this chapter, this was validated via a GUS histochemical assay on leaves of *proCML41*::*GUS* plants (Figure 4.5). This suggests a potential connection between CML41 and plant defence to pathogen invasion. Pathogen attack induces plant defence responses by two principal strategies: 1) pathogen-associated molecular pattern (PAMP)-triggered immunity (PTI) initiated by pathogen elicitors (e.g. flg22); and 2) effector-triggered immunity (ETI) initiated by pathogen effectors (Jones and Dangl, 2006). In the case of Arabidopsis response to flg22, PTI is elicited by a Leucine-rich repeats receptor kinase (LRR-RK) Flagellin Sensing 2 (FLS2) directly binding to flg22 and rapidly forming a complex with BRI1 associated receptor kinase (BAK1) to positively regulate PAMP (Gómez-Gómez et al., 2000; Chinchilla et al., 2007; Dodds and Rathjen, 2010; Zipfel and Robatzek, 2010). PTI involves the precipitation of diverse PAMP-activated signalling from the early generation of a Ca^{2+}-signature, an oxidative burst and hormone production (including SA accumulation), and downstream signalling resulting in a production of glucosinolate compound and callose deposition (Chisholm et al., 2006; Hückelhoven, 2007; Clay et al., 2009; Hématy et al., 2009; Zipfel and Robatzek, 2010).

Callose deposition can reflect the severity of a plants' PTI response to various pathogens or their elicitors, reduce symplasmic permeability and prevent pathogen effector transport between host cells (Smart et al., 1986; Gómez-Gómez et al., 1999; Jacobs et al., 2003; Zipfel et al., 2004; Zhang et al., 2007; Luna et al., 2011). Callose measurement revealed that *CML41*-amiRNA lines accumulated significantly less callose in the leaves following infiltration of flg22 than for Col-0 (Figure 4.14A). As *CML41S* expression displayed no difference in between *CML41*-amiRNA#2 lines and wild-type Col-0 regardless of flg22 treatment, this suggested that the lower amount of callose deposited in *CML41*-amiRNA plants induced by flg22 was unlikely to be due to CML41S (Figure 10A). Whereas, *CML41FL* was strongly induced by the infiltration of flg22 up to 6-fold and its expression in *CML41*-amiRNA lines was silenced down-to 10% of its normal level in wild-type plants (Figure 4.10A). Together with callose deposition measurement and qRT-PCR results, this suggested that silencing *CML41FL* is likely to result in a difference of flg22-induced callose deposition in leaves. Additionally, no obvious difference in callose number was observed across *CML41FL* and *S-OEX*, *CML41-*

amiRNA lines and Col-0 with H$_2$O-control treatment, implicating that simply overexpression *CML41FL* was not sufficient to deposit more callose in the leaves (Figure 4.14B). As a consequence, I propose that perhaps CML41FL rather than CML41S is involved in callose deposition during PTI and its involvement probably requires certain Ca^{2+} signatures like flg22/PAMP-triggered Ca^{2+} signalling. It is interesting that unlike the loss-of-function *fls2* mutant line, the *CML41*-amiRNA lines do not show complete abolishment of callose deposition upon flg22 treatment; the callose counts were merely reduced. This may be because the expression of *CML41* amiRNA, and the resulting knockdown of *CML41*, is not reduced to the same degree in every cell. Although this is not a widely reported phenomenon, it is commonly acknowledged that 35S-driven overexpression does not result in equal expression in all cells.

Flg22 seems induced the expression of *Actin2*, *ACA10* and *CAX3* in leaves of wildtype Col-0, compared to control treatment, but this did not occur in *CML41*-amiRNA lines where these three gene expression was not statistically different between flg22 and control treatment, although the mean of their expression in *CML41*-amiRNA lines was higher in flg22-treated leaves than the H$_2$O-treated (Figure. 4.10B) This could be experimental variations that have to been determined by further investigation. *PR1* expression was enhanced by flg22 treatment in both *CML41*-amiRNA#2 lines and wild-type plants, suggesting that PR1 acts independent of or the upstream of CML41FL in flg22-triggered immunity (Figure 4.10B). So far, it is still unknown if any hormone production/regulation participates in CML41FL-regulated signalling pathway or callose deposition during PTI, although marker genes for a few hormone such as CK, BR, IAA and GA were not misexpressed in *CML41FL-OEX* lines (Figure 4.9). In *CML41FL* knock-down plants, a few genes that are perhaps located downstream of CML41FL such as *Actin2*, *ACA10* and *CAX3*.

Chapter 5: Sub-cellular localisation and protein-protein interaction

5.1 Introduction

In the preceding chapter, CML41 was demonstrated to have a likely role in callose deposition during flg22-induced PAMP-triggered immunity. Different CaMs/CMLs decode Ca^{2+}- signatures to achieve similar cellular responses (Dodd et al., 2010). For instance, the transcription factors, CAMTA3 and CBP60g mediate salicylic acid (SA) content during plant immunity response via an interaction with CaM, respectively binding the promoter of Enhanced Disease Susceptibility 1 (*EDS1*) and isochorismate synthase 1 (*ICS1/SID2*) and regulating their expression (Du et al., 2009; Wang et al., 2009; Zhang et al., 2010). However, cytosolic Ca^{2+}-signalling by the vacuolar Ca^{2+} transporters ACA4 and ACA11, whose Ca^{2+}-transport is activated via an interaction with CaM, can be mediated via regulation of the increase in SA content during a plant immunity response (Geisler et al., 2000; Lee et al., 2007; Boursiac et al., 2010). Similarly, CML41FL and S may behave in one of these manners to regulate callose deposition in response to flg22. Interestingly, a nuclear-localised TCP transcription factor member, TCP14 was revealed as an interacting partner with CML41 using an Y2H screen (Arabidopsis Interactome Mapping Consortium, 2011; Rueda-Romero et al., 2012), suggesting that CML41 might contribute to certain gene regulation via interaction with a transcription factor. Therefore, the interaction between CML41FL and S and TCP14 was further investigated in this Chapter. In addition, the subcellular localisation of both proteins was determined, since it is important to confirm whether both proteins are in close spatial proximity in order that they can interact; this is an important step in corroborating Y2H identified targets and investigate whether the interaction is physiologically relevant in plants (Reddy et al., 2011). Furthermore, the subcellular localisation of CML41 on its own is likely to reveal information about its role in the plant. In Chapter 3, I determined that the cleavage of the putative signal peptides did not abolish the ability of CML41 to bind Ca^{2+}. Here, I examined whether the cleavage of the putative signal peptides altered the protein localisation and whether the chloroplastic prediction in Chapter 2 was correct. Also if localisation data sheds more light on the callose deposition phenotype observed in Chapter 4.

5.2 Material and Methods

5.2.1 Gene cloning and plasmid construction

The PCR reactions to amplify the truncated *CML41FL* and *CML41S* without a stop codon (-stop) followed the protocols described in Section 3.2.1 with primers CML41_TNT_F_CACC and CML41_CDS_R-stop (listed in Section 2.2.3 and 3.1). The PCR amplified products were ligated into

the Gateway® entry vector pENTR™/D-TOPO (Invitrogen) by Directional TOPO cloning. As the TCP14 genome sequence has no intron, the PCR to amplify the *TCP14* coding sequence (1470 bp) with or without stop codon was performed on Arabidopsis gDNA as a template with primers TCP14_CDS_F_CACC and TCP14_CDS_R/TCP14_CDS_R-stop (listed in Table 5.1) using Phusion™ Hot Start High-Fidelity DNA polymerase (FINNZYMES). A Directional TOPO cloning reaction was used to ligate these PCR amplification products into the Gateway® entry vector pENTR™/D-TOPO (Invitrogen) following the manufacturers' instructions. The TOPO reactions of *CML41FLΔ*1-46-stop, *CML41SΔ*1-46-stop and *TCP14* were transformed into TOP10 Chemically Competent *E. coli* cells (Invitrogen), while the reaction of *TCP14*-stop was transformed into NEB 5-α F'*I^q* Competent *E. coli* cells (New England Biolabs). The cloning of *CML41FLΔ*1-46-stop and *CML41SΔ*1-46-stop in the entry vector was confirmed by restriction digest using *EcoRI/Nhe*I (New England Biolabs) and sequencing with the primer M13_Forward (see Section 2.2.3). The cloning of *TCP14* and *TCP14*-stop in the entry vector was confirmed by restriction digest using *Ssp*I (New England Biolabs) and sequencing with primers M13_Forward, TCP14_F1_seq (5'-CAACAAGCTGAACCATCTGTAA-3') and TCP14_F2_seq (5'-ATTTCTGGATGGTTGCGG-3') (listed in Section 2.2.3). The recombination of *CML41FL*-stop, *CML41S*-stop, *CML41FLΔ*1-46-stop and *CML41SΔ*1-46-stop from pENTR/D/TOPO CML41 into the expression vector pBS 35S attR-YFP (for sub-cellular localisation through transient expression in Arabidopsis protoplasts) and binary vector pMDC83 were performed using the Gateway® LR Clonase® II Enzyme Mix (Invitrogen). The same experiment was also performed when recombining *CML41FL*-stop, *CML41S*-stop and *TCP14*-stop into the expression vectors pUC-SPYNE/GW, pUC-SPYCE/GW, pGPTVII-Bar.GW-YC, pGPTVII-Hyg.GW-YC and pDuExD7, and recombining *CML41FL*, *CML41S* and *TCP14* into the expression vectors pGPTVII-Bar.YN-GW, pGPTVII-Hyg.YC-GW and pDuExAn6 (see Appendix 7 and 8). Further details of expression vectors are in Appendix 8 these include: pUC-SPYNE/GW and pUC-SPYCE/GW which were used for the split YFP protein-protein interaction assay in Arabidopsis mesophyll protoplasts (Waadt et al., 2008); pGPTVII-Bar.GW-YC, pGPTVII-Hyg.GW-YC, pGPTVII-Bar.YN-GW and pGPTVII-Hyg.YC-GW that were utilised for split YFP protein-protein interaction assays in intact Arabidopsis plants via *Agrobacterium*-mediated transient expression (Walter et al., 2004); pDuExD7 and pDuExAn6 that were used for the split luciferase protein-protein interaction assay in Arabidopsis mesophyll protoplasts (Fujikawa and Kato, 2007).

Table 5.1 Primers used to clone *TCP14* coding sequence from Arabidopsis gDNA. Primer sequence underlined refers to directional cloning sequence used for directional TOPO cloning.

Product name	Primers	Sequence (5'-3')	Tm* (°C)	Product size
TCP14	TCP14_CDS_F_CACC	<u>CACC</u>ATGCAAAAGCCAACATCAAGT	57.5	1474 bp
	TCP14_CDS_R	CTAATCTTGCTGATCCTCCTCAT	57.4	
TCP14-stop	TCP14_CDS_F_CACC	<u>CACC</u>ATGCAAAAGCCAACATCAAGT	57.5	1471 bp
	TCP14_CDS_R-stop	ATCTTGCTGATCCTCCTCATCA	58.6	

*Primer Tm as calculated by NetPrimer (http://www.premierbiosoft.com/netprimer/index.html)

5.2.2 Transient expression in Arabidopsis mesophyll protoplasts

Protoplast isolation and transformation was modified and optimized from the method described by Yoo et al (2007) where W2 solution (4 mM MES, 0.4 M mannitol, 15 mM KCl, 10 mM CaCl$_2$ and 5 mM MgCl$_2$, adjusted to pH 5.7 with KOH) was used to take the place of WI and W5 solution. Arabidopsis plants that were 5-6 weeks old and grown as described in Section 2.2.2 were used for protoplast isolation. In total, 10-20 leaves, consisting of 3-4 leaves from each plant, were cut into 1 mm strips and transferred by dipping both side of the strips into 10 mL of enzyme solution (20 mM MES, 1.5% (w/v) Cellulase R10, 0.4% (w/v) Macerozyme R10, 0.4 M mannitol, 20 mM KCl, 10 mM CaCl$_2$, 0.1% (w/v) BSA, pH = 5.7 by KOH). The enzyme solution with leaf strips was vacuum-infiltrated for 30 min using a desiccator and incubated in the dark at room temperature. After 3 hr incubation, the incubation media was mixed with ice-cold 10 mL W2 solution to stop the reaction. Then transferred and filtered using a 75 µm nylon mesh into a new 50 mL falcon tube. The protoplast solution was centrifuged at $150 \times$ g at 4°C for 2 min followed by one wash in 10 mL ice-cold W2 buffer. Protoplast cells were collected again by centrifugation at $150 \times$ g at 4°C for 2 min to remove the excessive enzyme solution and resuspended in ice-cold W2 solution. Protoplasts (100 µL) were mixed with 10-20 µg plasmid DNA (6-12 kb) and 110 µL PEG solution (30% (w/v) PEG 4000, 0.2 M mannitol and 100 mM CaCl$_2$) and incubated for 5 min at room temperature for protoplast transformation. The transformation reaction was stopped by adding 400 µL W2 solution and collected by centrifugation by $200 \times$ g at room temperature for 4 min. The cell pellet was gently resuspended in 500 µL W2 solution, transferred into a 12-well plate (Iwaki) and incubated in the dark at room temperature for 16-24 hr to allow the gene of interest to be expressed in protoplasts before imaging.

5.2.3 Transient expression in Arabidopsis by Agroinfiltration of leaves

Serial binary vectors of pGPTVII-Bar.YN-GW/GW-YN and pGPTVII-Hyg.YC-GW/GW-YC with different genes of interest (Walter et al., 2004) (see Appendix 7) were transformed into *A. tumefaciens* strain AGL1 using a freeze-thaw method (details see Section 4.2.5). The *Agrobacterium*-mediated transient expression in Arabidopsis followed the method optimised from Lee and Yang (2006) and Kim et al (2009b). In brief, the transformed *Agrobacterium* colonies carrying genes of interest in the binary vector was culture in 5 mL LB media with Rifampicin (25 µg/mL) and Kanamycin (50 µg/mL) at 30 ℃ for 2 d. The saturated *Agrobacterium* culture was diluted 1:10 into 10 mL fresh LB with the same antibiotics and cultured at 30 ℃ for 5-6 hr till its OD at 600 nm reached 0.7-1.0. The bacterial culture was collected by centrifugation at $3000 \times$ g for 5 min, and the cell pellet was resuspended in an equal volume of infiltration medium (0.5% (w/v) D-glucose, 10 mM MES, 10 mM $MgCl_2$, 0.2 mM acetosyringone, 0.1% Triton X-100, pH = 5.8 by KOH). Approximately 0.1-0.3 mL of *Agrobacterium* cell suspension was infiltrated using a 1 mL needless syringe into individual the mature leaf of 5-6 week-old Arabidopsis that was grown in a short day condition as described in Section 2.2.2. Totally, 3 leaves of each plant were infiltrated. In terms of co-expression of two genes, two *Agrobacterium* suspensions that carry different binary vectors were mixed in equal volume together to be infiltrated into the Arabidopsis leaf. Infiltrated Arabidopsis plants were covered with clear polyethylene film for 16 hr in the dark to maintain high humidity. Then the film was removed, and those plants were further grown in short day conditions for another 3-6 d before imaging.

5.2.4 Stable expression of *CML41FL*::*GFP* and *CML41S*::*GFP* in Arabidopsis

The stable expression of *CML41FL* and *CML41S* fused with *GFP* in Arabidopsis using the pMDC83 vector (Curtis and Grossniklaus, 2003) and selection of transgenic Arabidopsis plants followed the protocol described by Harrison et al (2006) (details described in Section 4.2.5-4.2.6). T_1 to T_3 plants were grown hydroponically in short day conditions as described in Section 2.2.2 and used for cell imaging.

5.2.5 Fluorescence live-cell imaging

The fluorescence of fluorescent proteins in transgenic Arabidopsis plants or transiently-expressed in Arabidopsis mesophyll protoplasts was imaged by the confocal laser scanning microscope equipped with a Zeiss Axioskop 2 mot plus LSM5 PASCAL and argon laser (Carl Zeiss) or a Leica SP5 spectral scanning confocal microscope (Leica). Sequential scanning and laser

excitation was used to capture fluorescence via the LSM5 PASCAL from GFP (excitation = 488 nm, emission Band-Pass (BP) = 505-530 nm), YFP (excitation = 514 nm, emission BP = 570-590 nm) propidium iodide/chlorophyll autofluorescence (excitation = 543 nm, emission Long-Pass (LP) = 560 nm), or by using the Leica SP5, YFP (excitation = 514 nm, emission BP = 520-550 nm), chlorophyll autofluorescence (excitation = 488 nm, emission = 640-740 nm). Images were analysed by either LSM 5 Image Examiner (Carl Zeiss) or LAS AF Lite (Leica).

5.2.6 Split luciferase complementation assay

The pDuEx-Bait-Prey expression vectors – pDuExD7 and pDuExAn6 with N- and C-terminal fragments of *Renilla reniformis* luciferase were used to study the potential protein-protein interaction (Fujikawa and Kato, 2007). Transient co-expression of pDuExD7 and pDuExAn6 with genes of interest in Arabidopsis mesophyll protoplasts followed the protocols of Section 5.2.2. Luminescence detection after protoplasts transfection for 24 hr was optimised from the method as described in Hocking (2008) and Fujikawa and Kato (2007). ViviRen Live Cell substrate (60 µM) (Promega) was added to and mixed briefly with W2 solution of transfected protoplasts, 100 µL of which was transferred into individual wells of a 96-well white plate (Greiner bio-one). The protoplast solution was always mixed with substrate for 2 min before the luminescent signal was quantified every 30 sec for 3 mins (at gain = 4095) using FLUOstar Optima multi-mode microplate reader (BMG LABTECH). As the peak luminescence had been observed at 300 sec after the substrate addition by Hocking (2008), the last luminescent reading was used for the analysis.

5.3 Results

5.3.1 Punctate YFP fused to CML41FL and CML41S and cytoplasmic YFP fused to CML41FLΔ1-46 and CML41SΔ1-46 in Arabidopsis mesophyll protoplasts

Plant protoplasts with enzymatic removal of the cell wall are still capable of performing extensive signal transduction events and physiological response to light, hormones, metabolites, biotic and abiotic stresses (Sheen, 2001). One of the likely reasons for this is that many of the cellular proteins are still properly targeted to the appropriate organelles and are still functional in protoplasts. Therefore, plant protoplasts (e.g. Arabidopsis mesophyll protoplasts) are widely used to study protein subcellular localisation via fusion with a fluorescent protein (Yoo et al., 2007). So transient expression of *CML41FL* and *S* in Arabidopsis mesophyll protoplasts fused with fluorescence protein was here deemed a suitable way to investigate their subcellular localisation. Fluorescence of YFP

fused to C-terminus of CML41FL (CML41FL::YFP) always appeared to be in punctate structures in protoplasts (Figure 5.1A). CML41FL and CMLS share the same putative signal-peptide sequence, thus the fluorescence signal of YFP fused to N-terminus of CML41S (YFP::CML41S), also displayed punctate structures similar with CML41FL (Figure 5.1). Nevertheless this YFP fluorescence was unlikely to have arisen from the chloroplasts, since similar punctate YFP was observed in cells expressing *YFP*::*CML41S* in a leaf epidermal cell lacking chloroplasts (Figure 5.1B, panel vi). Compared to published protein localisation in other organelles of Arabidopsis protoplasts, CML41FL and S fused with YFP in punctate structures may indicate targeting to peroxisomes, golgi, endosomes, mitochondria or plastids (Nelson et al., 2007; Geldner et al., 2009; Lamberto et al., 2010).

In Arabidopsis mesophyll protoplasts, the fluorescence of YFP fusion to C-terminus of CML41FLΔ1-46and CML41SΔ1-46 (designated as CML41FLΔ1-46::YFP and CML41SΔ1-46::YFP) exhibited very different subcellular localisation patterns compared to the fusion of YFP to CML41FL and CML41S. Truncation of the putative signal peptide of CML41FL and S resulted in their fused YFP fluorescence extensively in the cytoplasm instead of punctate structures (Figure 5.2). The absence of the first 46 aa likely led to the mistargeting of CML41FL and SΔ1-46 to any specific organelle in Arabidopsis protoplasts.

A

	Brightfield	CML41FL::YFP	Merged

B
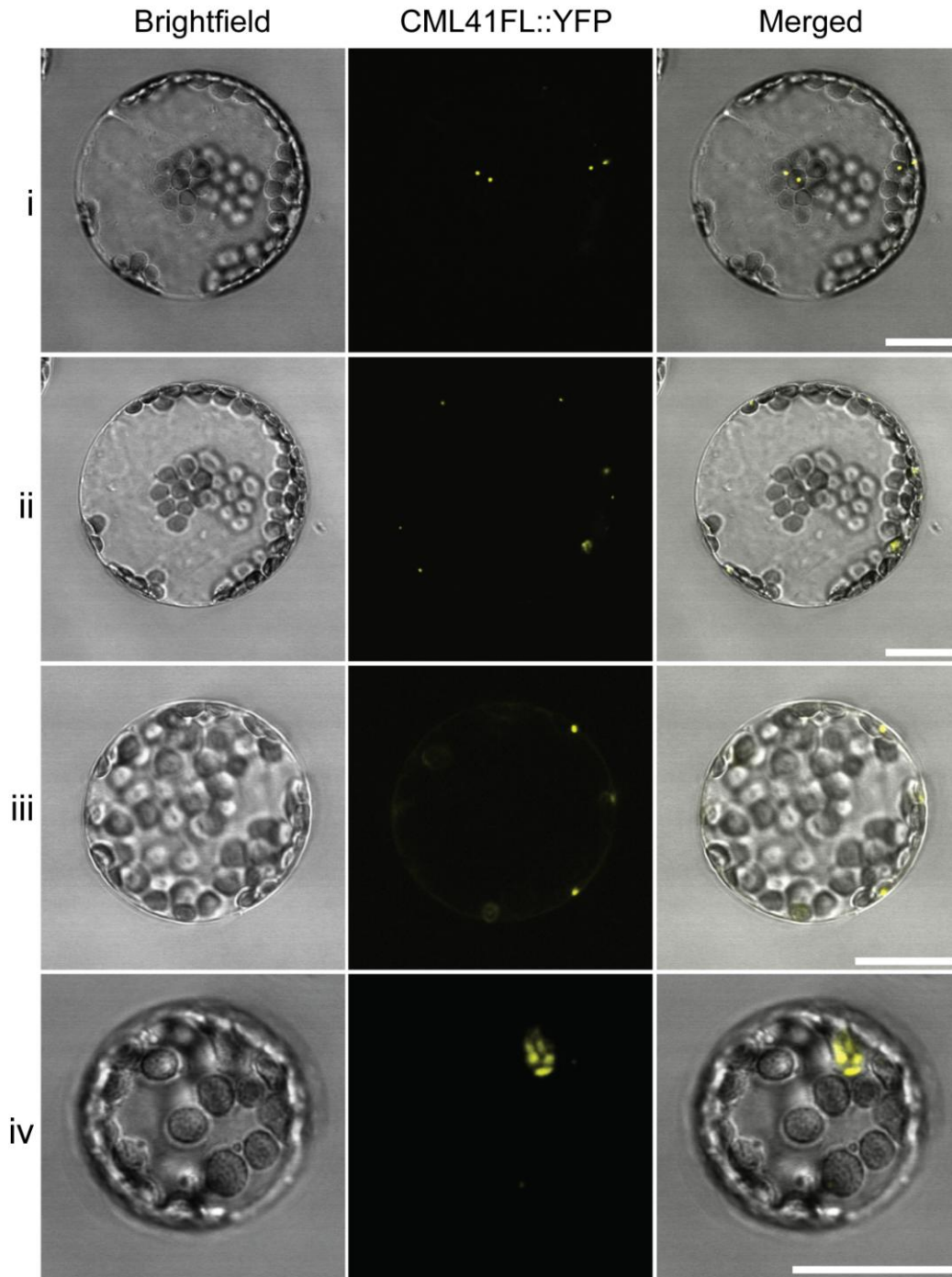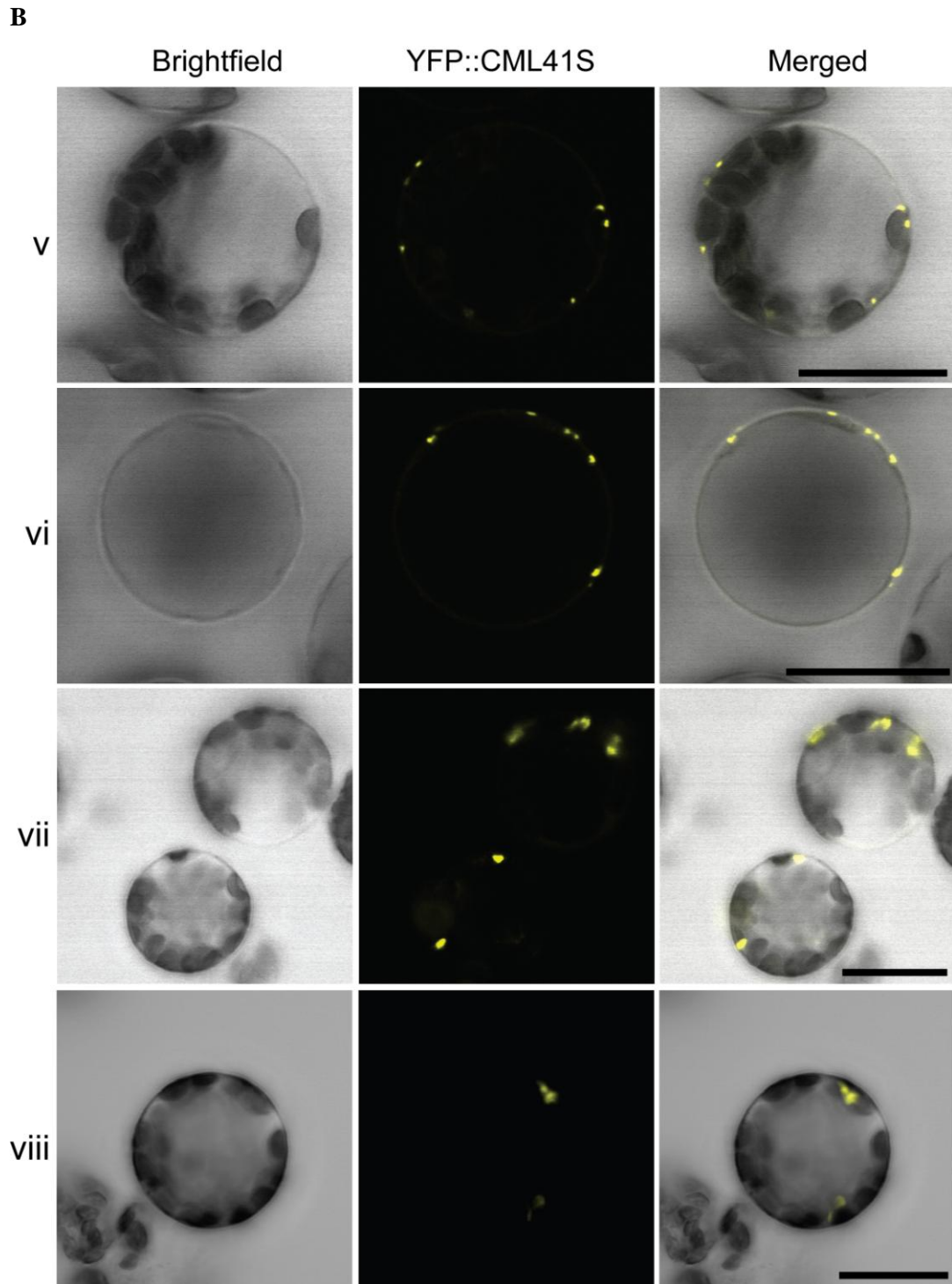
Figure 5.1 Subcellular localisation of CML41FL and S in Arabidopsis mesophyll protoplasts.
Transient expression of *CML41FL*::*YFP* and *YFP*::*CML41S* (driven by 35S promoter) in 5-6 week-old Arabidopsis mesophyll protoplasts. **A**, i-iv panels show confocal images of different protoplasts expressing *CML41FL*::*YFP*. **B**, v-viii panels show confocal images of different protoplasts expressing

YFP::*CML41S*. The fluorescence was captured using sequential scanning for YFP (excitation = 514 nm, emission = 570-590 nm) by LSM5 PASCAL, scale bars = 20 μm.

A
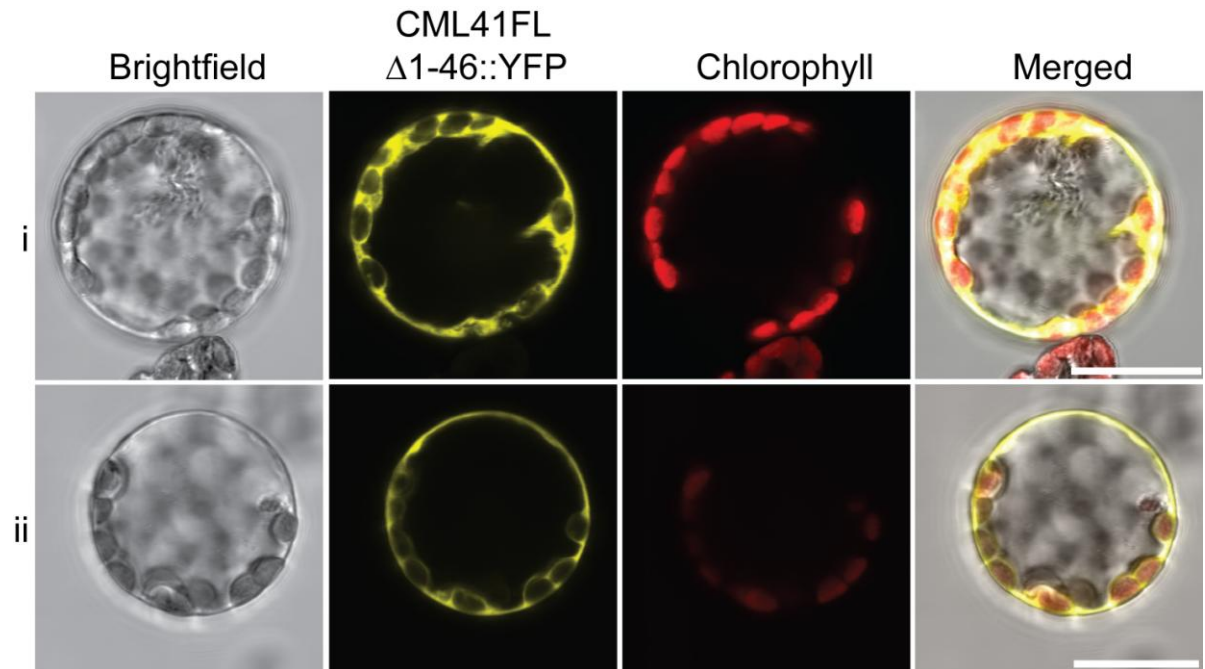
B
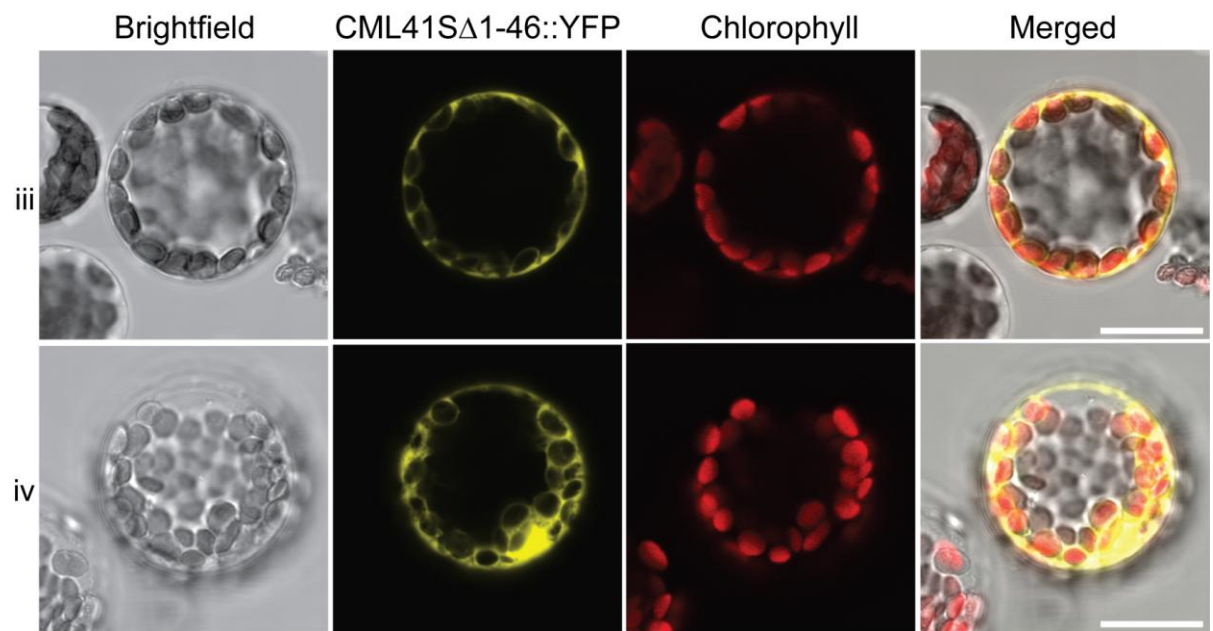
Figure 5.2 Subcellular localisation of CML41FL and SΔ1-46 in Arabidopsis mesophyll protoplasts. Transient expression of *CML41FLΔ1-46::YFP* and *CML41SΔ1-46::YFP* (driven by 35S promoter) in 5-6 week-old Arabidopsis mesophyll protoplasts. **A**, i and ii panels show images of protoplasts expressing *CML41FLΔ1-46::YFP*. **B**, iii and iv panels show images of protoplasts expressing *CML41SΔ1-46::YFP*. The fluorescence was obtained by sequential scanning for YFP (excitation = 514 nm, emission = 520-550 nm) and chlorophyll autofluorescence (excitation = 488 nm, emission = 640-740 nm) by Leica SP5, scale bars = 20 μm.

5.3.2 Dual types of CML41FL and S localisation in stable-transformed Arabidopsis

Protoplasts with loss of cell wall are divergent from their form in plants, even though they still retain many physiological functions. The cell boundary and its related characteristics are lost or interrupted in protoplasts, including plasmodesmata (PD), cell-cell communication and interactions; the study of cell-wall related processes or components may be not interpreted properly in the protoplast system (Sheen, 2001). As a consequence, transient expression in protoplasts is not a perfect system to study all types of protein localisation. Simultaneous expression of a gene fused with a fluorescent gene into intact plant is often applied to verify its protein localisation results obtained in the protoplasts system (Sheen et al., 1995; Sheen, 2001). Thus, *CML41FL* and S fused with *GFP* on their C-teriminus (designated as *CML41FL::GFP* and *CML41S::GFP*) driven by 35S promoter were stably over-expressed in Arabidopsis plants. Roots of transgenic plants were firstly used to examine the subcellular localisation of CML41FL and S. GFP fused to CM41FL was predominantly in the cytoplasm of root tip and the elongation zone, and the plasmolysis of root cells by 10 % (w/v) sucrose show GFP fluorescence clearly in cytoplasm (Figure 5.3A, i-iii). The same cytoplasmic GFP was also observed when fused to CML41S in roots (Figure 5.3B, i and ii). GFP-CML41FL and S were localised to the cytoplasm of roots thorough all developmental stages from initial elongation of the hypocotyl till the flowering stage of Arabidopsis under normal growth conditions (data not shown). Nevertheless, this cytoplasmic CML41FL and S were translocated into punctate structures in the root tip but not in root elongation zone whilst 5-6 week-old Arabidopsis were exposed to nutrient solution with 25 mM $CaCl_2$ for 3 d (Figure 5.3A, iv, v and 5.3B, viii, ix). When zooming into those images, it was clear that this punctate GFP fused to CML41FL and S always appeared in pairs at opposite sides of cells, contiguous with the cell boundary (Figure 5.3A, v and B ix).

A

| | CML41FL::GFP | PI | Fluorescence Merged | Merged |
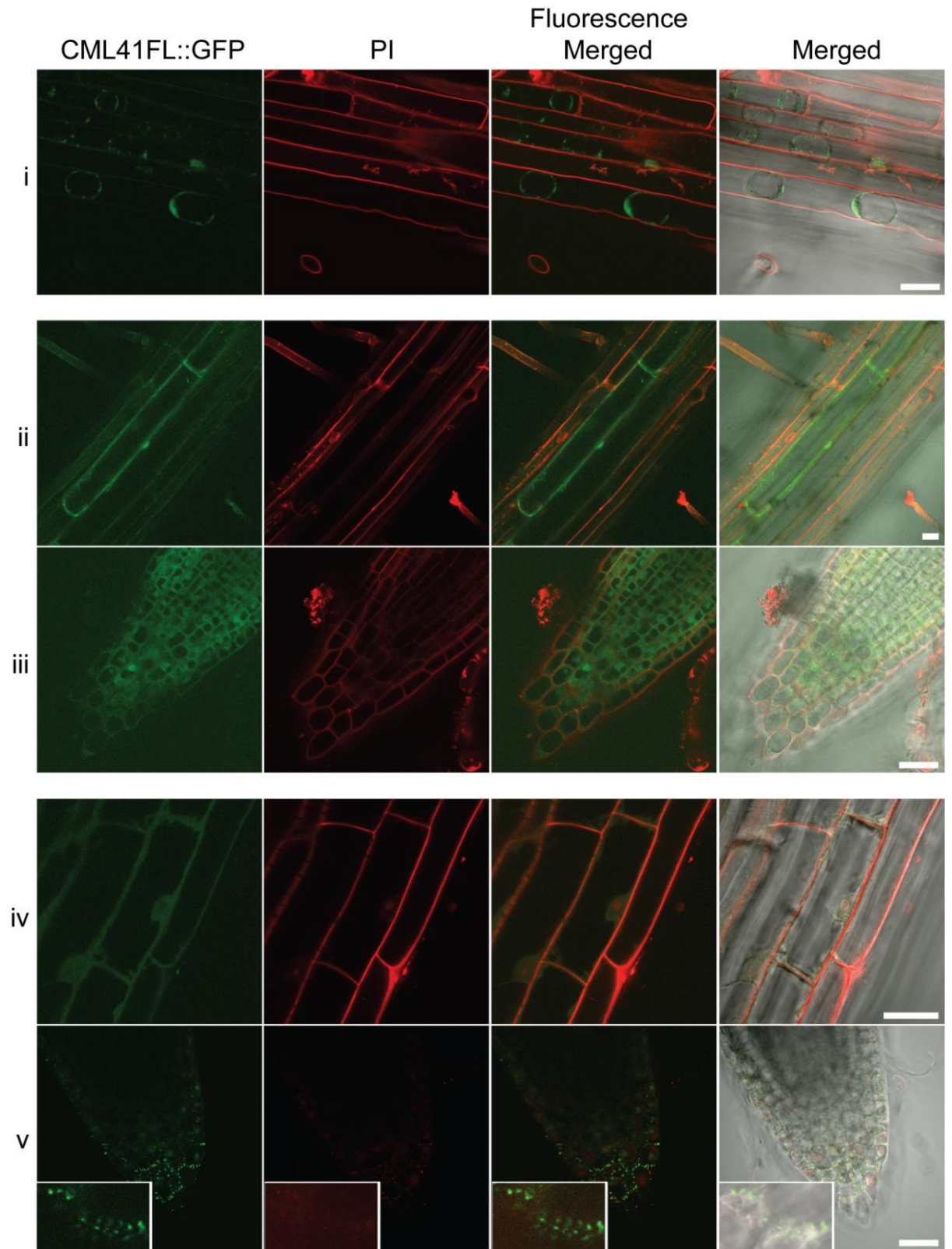
B
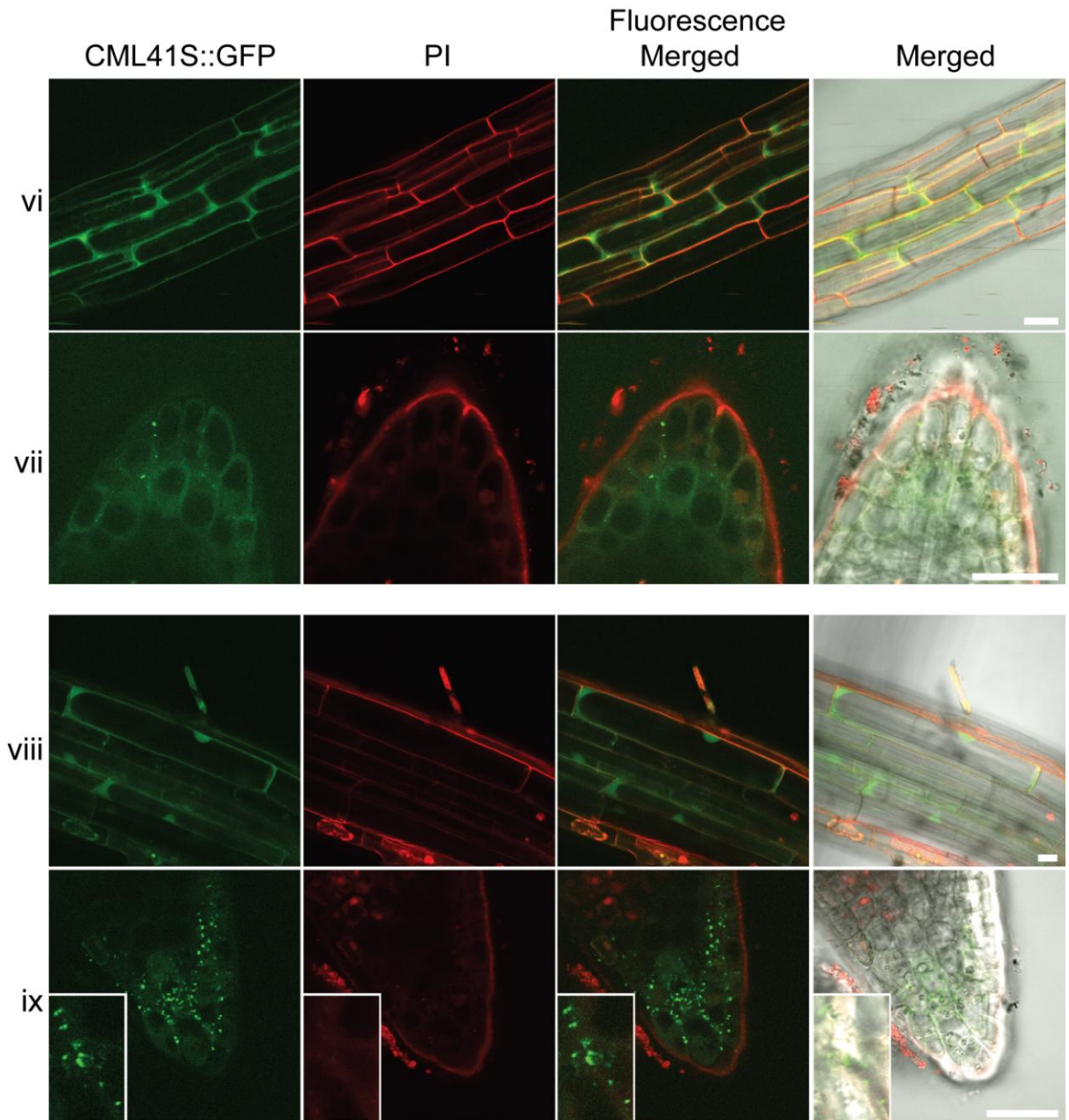
Figure 5.3 Subcellular localisation of CML41FL and S in Arabidopsis roots. Stable expression of *CML41FL*::*GFP* and *CML41S*::*GFP* in Arabidopsis Col-0 plants. **A**, localisation of CML41FL::GFP in Arabidopsis roots, i to v images were the root tissue of 5-6 week-old Arabidopsis expressing *CML41FL*::*GFP*. **B**, localisation of CML41S::GFP in Arabidopsis roots, vi to ix images were the root tissue of 5-6 week-old Arabidopsis expressing *CML41S*::*GFP*. i, ii, iii, vi and vii imaged from Arabidopsis grown at BNS; i imaged from root tissue plasmolysis by 10% (w/v) sucrose; iv, v, viii and ix imaged from Arabidopsis at BNS and treated with 25 mM $CaCl_2$ for 3 d. The fluorescence was captured using sequential scanning for GFP (excitation = 488 nm, emission = 505-530 nm) and PI =

Propidium Iodide (excitation = 534 nm, emission LP = 560 nm) by LSM5 PASCAL, scale bars = 25 μm.

        CML41FL and S also had distinct localisations in leaves. The fluorescence signal of GFP fused to CML41FL and S was always visualised in the cytoplasm in developing young leaves (those had not yet developed an elongated petiole) of 5-6 week-old Arabidopsis plants, and this cytoplasmic GFP of both CML41FL and S gradually changed into a punctate localisation from developing young leaves, mature leaves to old leaves (Figure 5.4). In the old leaves, the CML41FL and S-GFP again exhibited punctate structures in pairs on the opposite sides of epidermal cells but was absent in mature guard cells (Figure 5.4). Additionally, the GFP puncta was absent in the cytoplasm but only present contiguous with the cell boundary; therefore CML41FL and S were possibly targeting a cell-wall related component (Figure 5.4). As a control, overexpression of *GFP* driven by 35S promoter (*35S*::*GFP*) in Arabidopsis plants constantly showed cytosolic-bound GFP localisation in leaf cells thorough all developmental stages, suggesting that the cytoplasmic and punctate GFP pattern was due to different targeting of CML41FL and S in Arabidopsis cells (Figure 5.4 and 5.5).

A

B

C

► Young leaves   ▷ Mature leaves   ► Old leaves
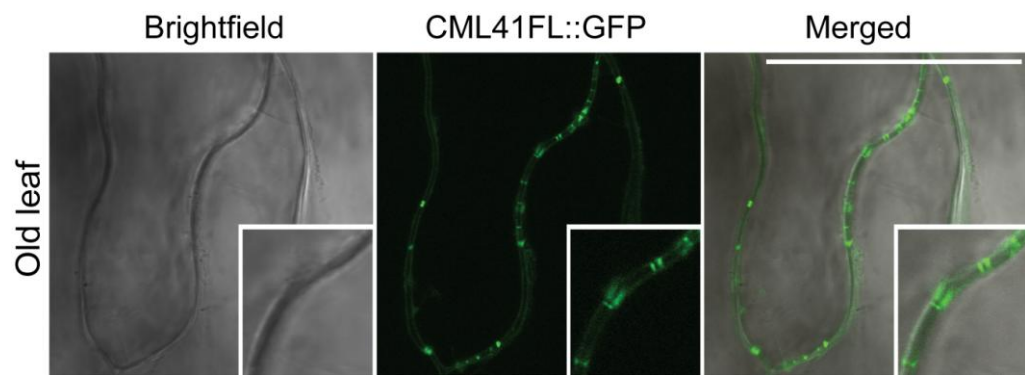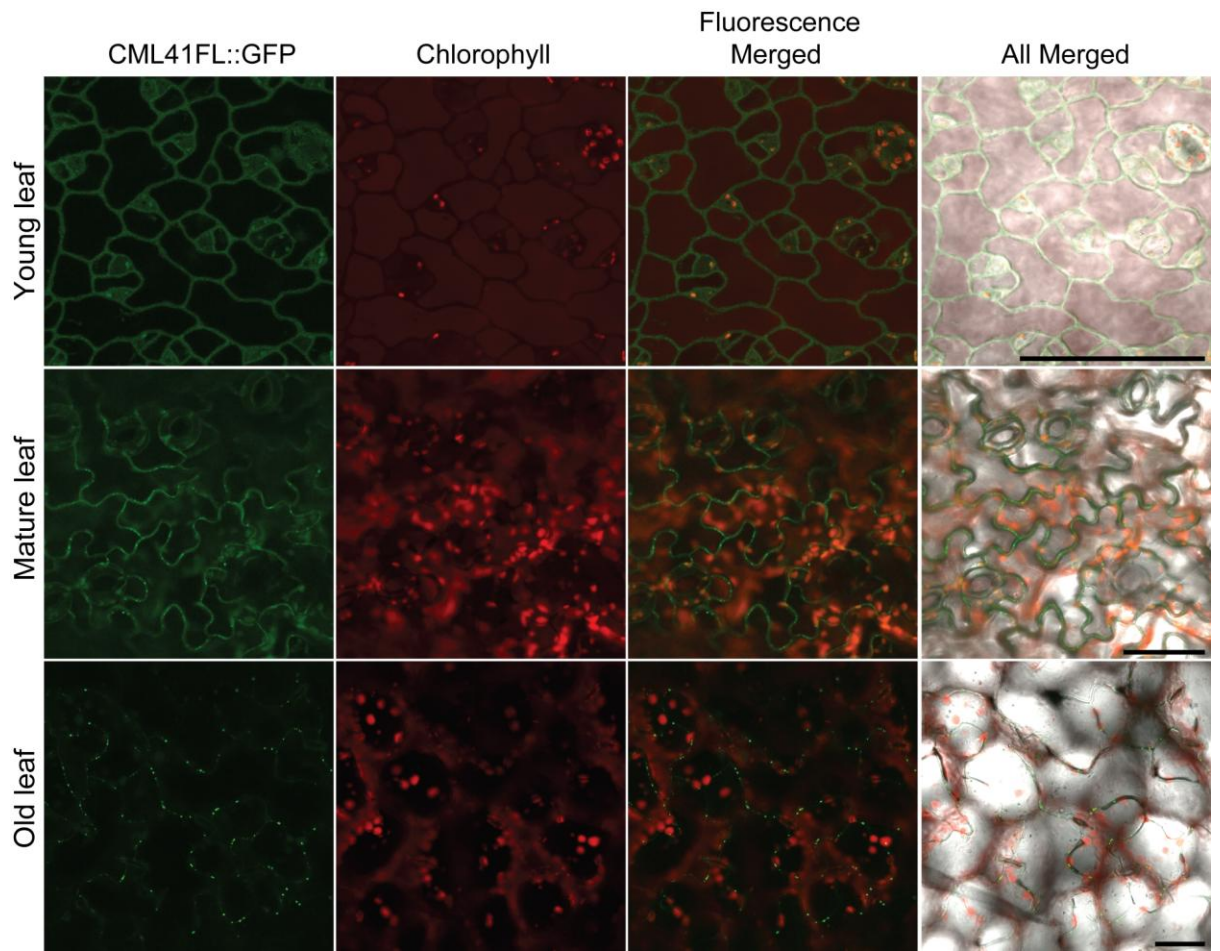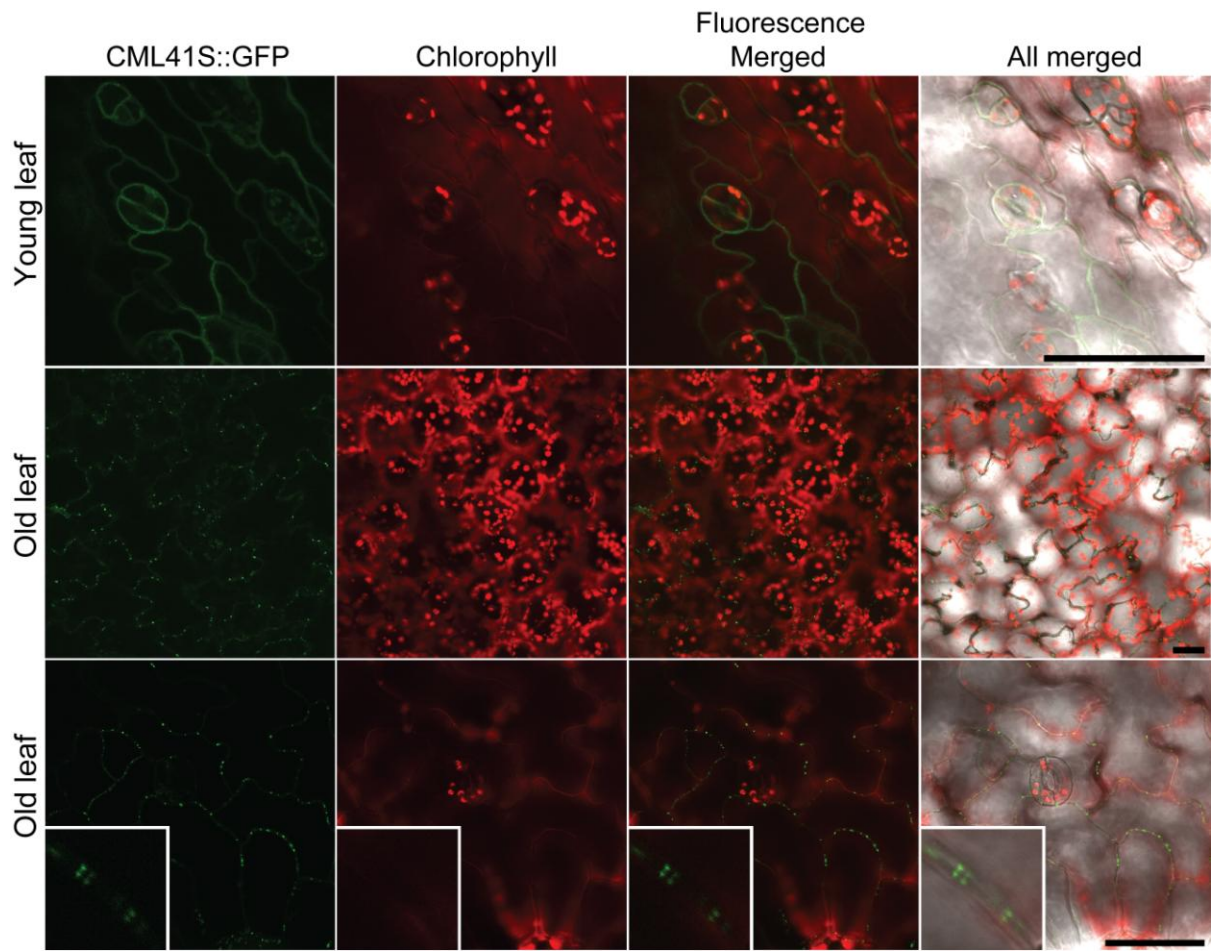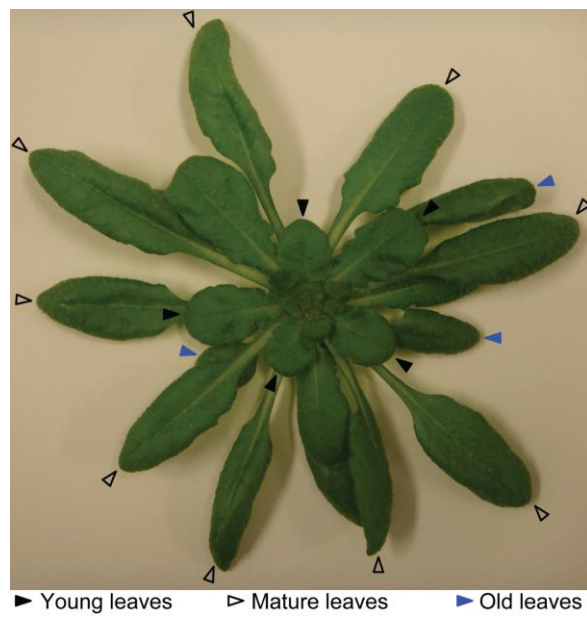
Figure 5.4 Subcellular localisation of CML41FL and S in Arabidopsis rosette leaves. Stable expression of *CML41FL*::*GFP* and *CML41S*::*GFP* in Arabidopsis Col-0 plants. **A**, Localisation of CML41FL::GFP in leaves Arabidopsis grown hydroponically in BNS, **B**, Localisation of CML41S::GFP in leaves of Arabidopsis grown hydroponically in BNS. **C**, Leaves corresponding to young, mature and old leaves used in **A** and **B** are pointed by arrows as indicated. The fluorescence was captured using sequential scanning for GFP (excitation = 488 nm, emission = 505-530 nm) and chlorophyll autofluorescence (excitation = 534 nm, emission LP = 560 nm) by LSM5 PASCAL, scale bars = 50 μm.
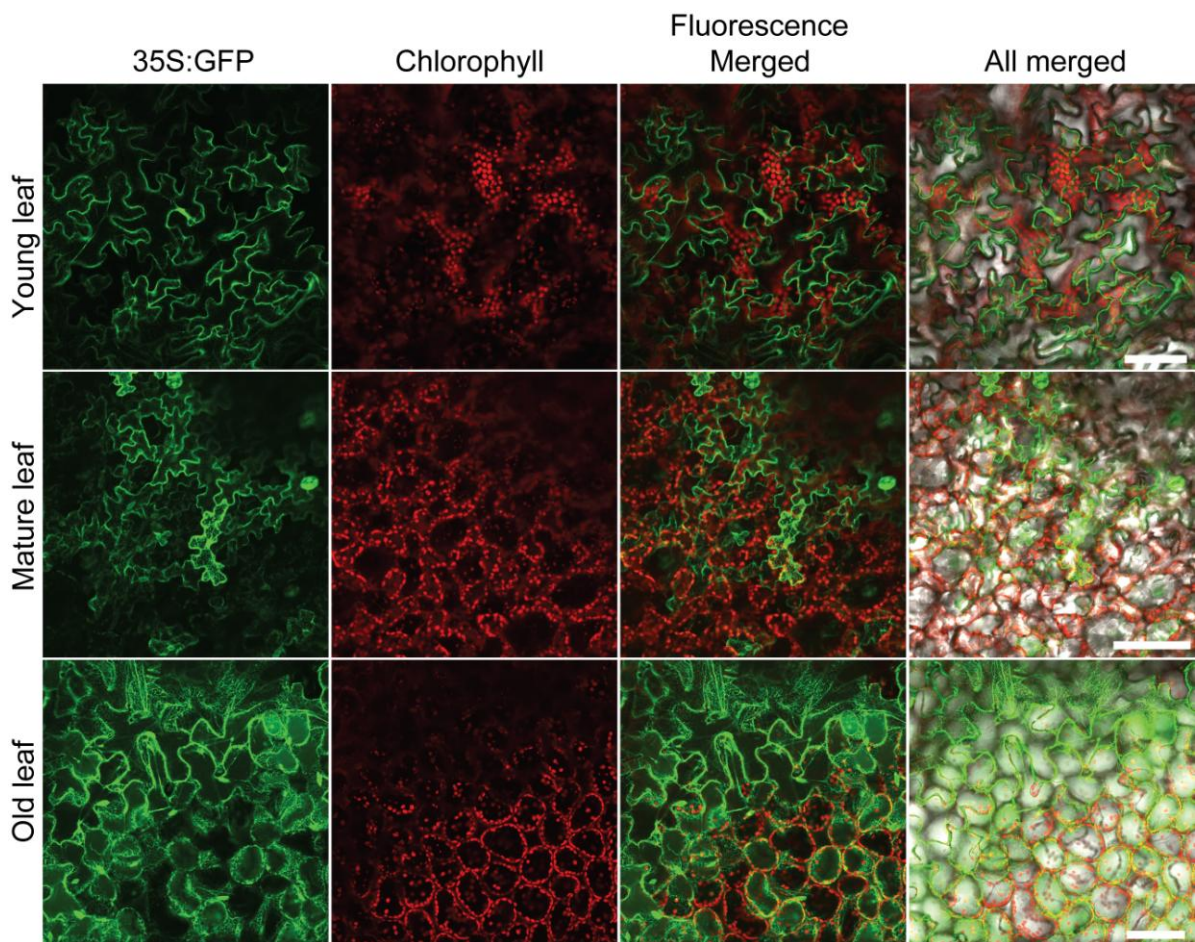
Figure 5.5 Subcellular localisation of free GFP in Arabidopsis rosette leaves. Stable expression of *35S*::*GFP* in Arabidopsis Col-0 plant; localisation of free GFP in leaves of Arabidopsis grown hydroponically in BNS for 5-6 weeks. Leaves corresponding to the young, mature and old leaves used as indicated in Figure 5.4C. The fluorescence captured using sequential scanning for GFP and chlorophyll autofluorescence refers to in Figure 5.4, scale bars = 100 μm.

5.3.3 Protein-protein interaction between CML41FL and S and TCP14

The Y2H system provides a robust tool for the discovery of protein-protein interactions particularly for high-throughput interactome mapping (Uetz et al., 2000; Ito et al., 2001; Causier and Davies, 2002; Parrish et al., 2006; Arabidopsis Interactome Mapping Consortium, 2011, Braun et al., 2013). However, Y2H screens are susceptible to high background noise and high false positive rates, and whilst the bimolecular fluorescent complementation (BiFC) assay or split *Renilla reniformis* luciferase complementation assays are still subject to false positives they provide another line of evidence to confirm the putative interaction between proteins (Uetz et al., 2000; Ito et al., 2001; Fujikawa and Kato, 2007; Morsy et al., 2008; Waadt et al., 2008; Braun et al., 2013). The BiFC and split luciferase complementation assay were employed to further validate the CML41 interaction with the TCP14 target protein, which was discovered in the Arabidopsis interactome map using the Y2H system (Arabidopsis Interactome Mapping Consortium, 2011). BiFC expression vectors – pUC-SPYNE/GW and pUC-SPYCE/GW (with the split N- and C-terminal fragments of YFP fusion to C terminus of protein), were utilized to transiently co-express *CML41LFL / S* and *TCP14* in Arabidopsis mesophyll protoplasts (details see Appendix 7 and 8). The fluorescence given off by the formed YFP complex was visualised in the protoplasts via co-expression of *CML41FL-YFP^N* and *TCP14-YFP^C* and of *TCP14-YFP^N* and *CML41S-YFP^C* (Figure 5.6, Appendix 7 and 8). Co-expression of *CML41S* and *TCP14* resulted in a slightly lower level of YFP fluorescence signal than when *CML41FL* and *TCP14* were co-expressed. The fluorescence of the YFP complex resulting from *CML41FL* and *S* and *TCP14* co-expression was still in punctate structures, whilst this BiFC assays seemed to produce larger number of YFP than the simple expression of *CML41FL*::*YFP* and *YFP*::*CML41S* in protoplasts (Figure 5.1 and 5.6A).

Another approach was used to verify the interaction between CML41FL and S and TCP14 via expressing them fused with the split luciferase gene in Arabidopsis mesophyll protoplasts. Luminescence was detected with very good signal-to-noise ratio that its signal from protein-interaction pair (>20,000 RLU) was at least 10-fold higher than the background noise (only about 2,000 RLU) (Figure 5.6B). Significant luminescence signal was detected from all the protein pairs: CML41LFL-D7::CML41FL/CML41S/TCP14-An6, CML41S-D7::CML41FL/CMLS/TCP14-An6 and TCP14-D7::CML41FL/CML41S/TCP14 as well as positive control 35S::LUC. The CML41FL-D7::TCP14-An6 protein pair showed higher level of luminescence than TCP14-D7::CML41FL-An6 pair (One-way ANOVA, *P < 0.0001*), while the luminescence detected from CML41S-D7::TCP14-

An6 and TCP14-D7::CML41S::An6 was subtly different. Interestingly, the luminescence signals from the protein pairs CML4FL-D7::CML41FL-An6 was the highest, about 2-fold higher than the rest of protein pairs (one-way ANOVA, $P < 0.0001$). Co-expression of Luc^N-CML41FL and S and Luc^C-CML41S-Luc^C also led to high level of luminescence detected (Figure 5.6B).

A
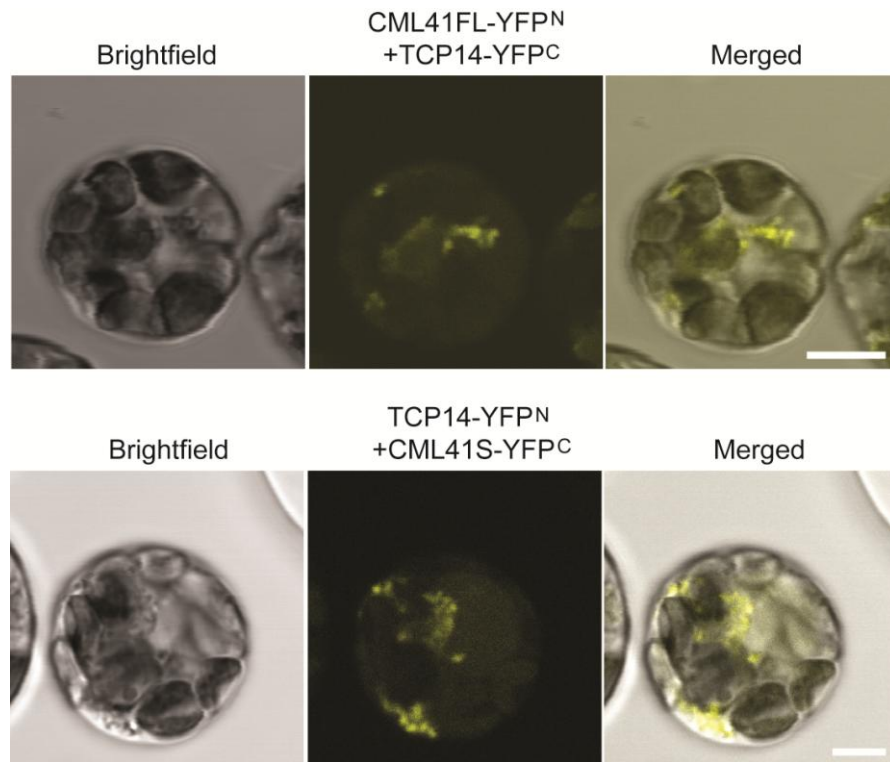
B
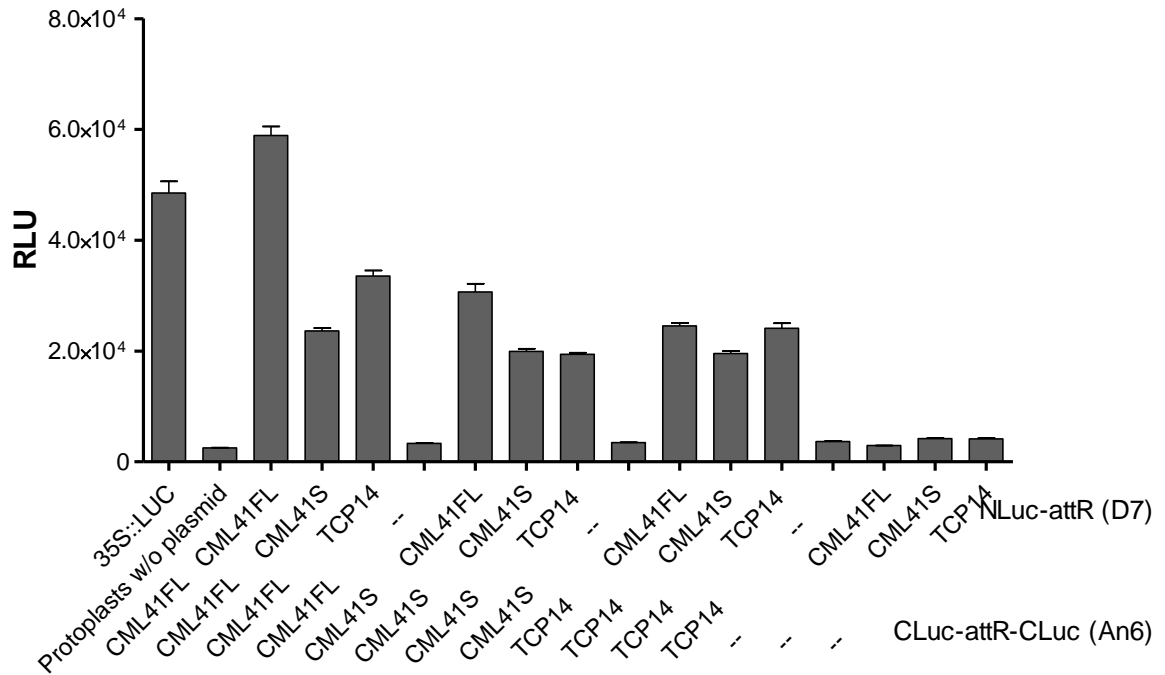
Figure 5.6 CML41FL and S and TCP14 interaction in Arabidopsis mesophyll protoplasts. A, confocal images of 5-6 week-old Arabidopsis mesophyll protoplasts transiently co-expressing pUC-SPYNE/GW-*CML41FL* with pUC-SPYCE/GW-*TCP14* (as indicated *CML41FL-YFP^N + TCP14-YFP^C*) or pUC-SPYCE/GW-*CML41S* with pUC-SPYNE/GW-*TCP14* (as indicated *TCP14-YFP^N + CML41S-YFP^C*); The fluorescence was captured using sequential scanning for YFP refers to Figure 5.2, scale bars = 10 μm. **B**, Luminescence from 5-6 week-old Arabidopsis mesophyll protoplasts transiently co-expressing *CML41FL*, *CML41S* and/or *TCP14* using pDuEX-Bait and -Prey serial vectors (details see Appendix 7 and 8), *35S*::*LUC* and protoplasts without (w/o) plasmids as control, RUL = relative luminescence units, Mean ± SD (n = 3).

As CML41FL and S might potentially have a cell-wall related localisation (Figure 5.4), the interaction between CML41FL and S and TCP14 was determined again using BiFC but in the intact Arabidopsis plants. Serial binary vectors – pGPTVII carrying *CML41FL* and *S* and *TCP14* were transformed into *Agrobacterium*. Different combinations of *CML41FL* and *S* and *TCP14* co-expression fused with split *YFP* were transiently expressed in 5-6 week-old Arabidopsis leaves mediated by *Agrobacterium* infiltration. The fluorescence of the YFP complex formed by the YFP^N-CML41FL + YFP^C-TCP14 protein pair was observed in punctate structures in the Arabidopsis leaf.

These punctate YFP were obviously in pairs positioned on opposite sides of cells (Figure 5.7A). The additional z-serial images of cells on Figure 5.7A (bottom panel) showed a large number of punctate YFP present on two adjacent cells, some of which was also likely attached somewhat on the endoplasmic reticulum (ER) as well (Figure 5.7A and B). YFP fluorescence was also observed when *Agrobacterium* carrying *YFP^N-CML41S* and *TCP14-YFP^C* had been co-infiltrated into the Arabidopsis leaf. This YFP was mainly in cytoplasm, although a few YFP spots were noticed around the cell boundary. Meanwhile, the YFP signal derived from YFP^N-CML41S + TCP14-YFP^C pair was obviously weaker than that from YFP^N-CML41FL + YFP^C-TCP14 pair (Figure 5.7C). Overall, CML41FL probably interacts with TCP14 at similar subcellular localisation to CML41FL-GFP in the Arabidopsis leaf, whereas the interaction between CML41S and TCP14 is obviously not as strong as CML41FL and TCP14 interaction (Figure 5.7A and C).

A

Brightfield

YFP^N-CML41FL
+YFP^C-TCP14

Merged

B

C

| | YFP^N^-CML41S +TCP14-YFP^C^ | |
| Brightfield | | Merged |
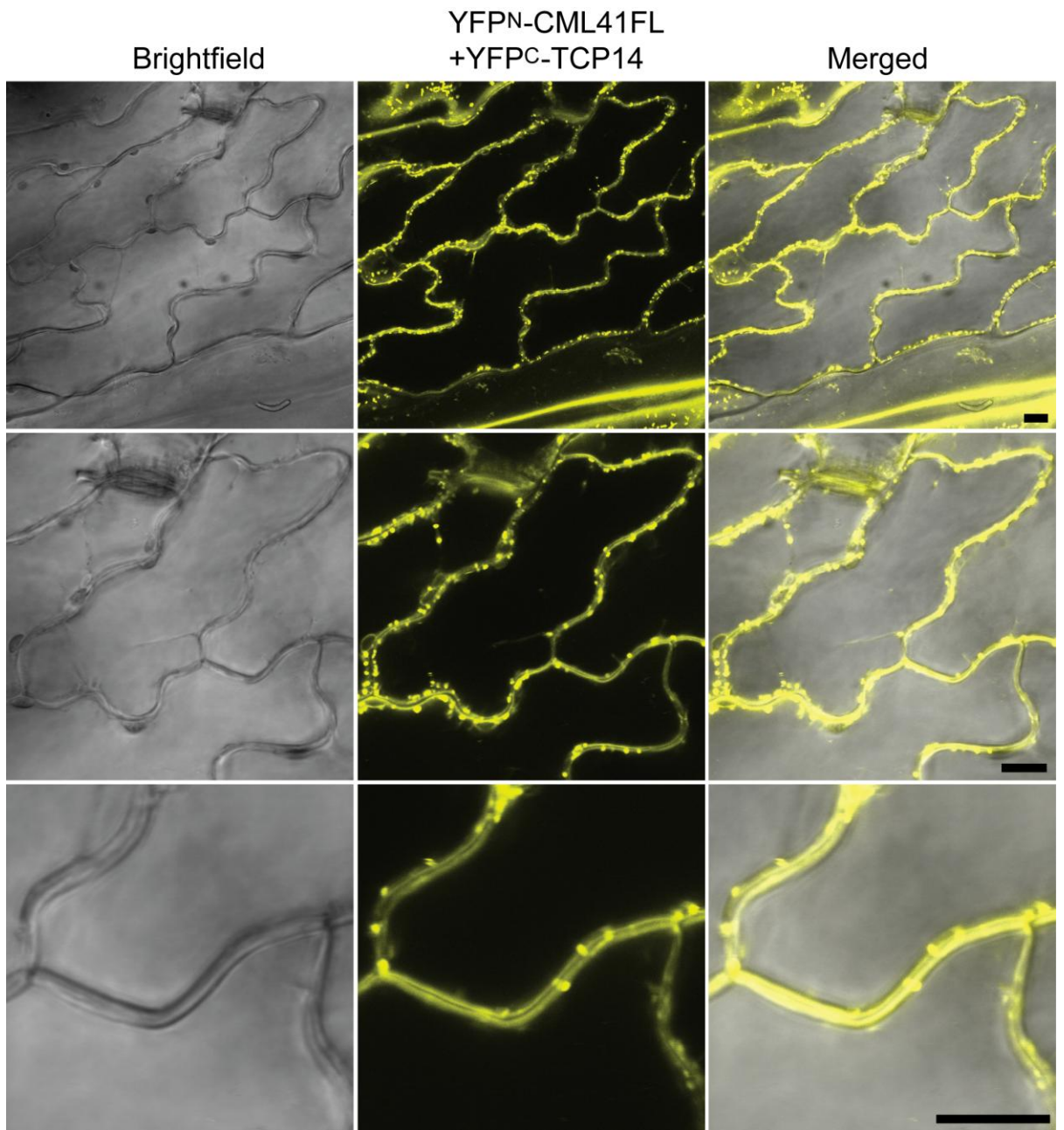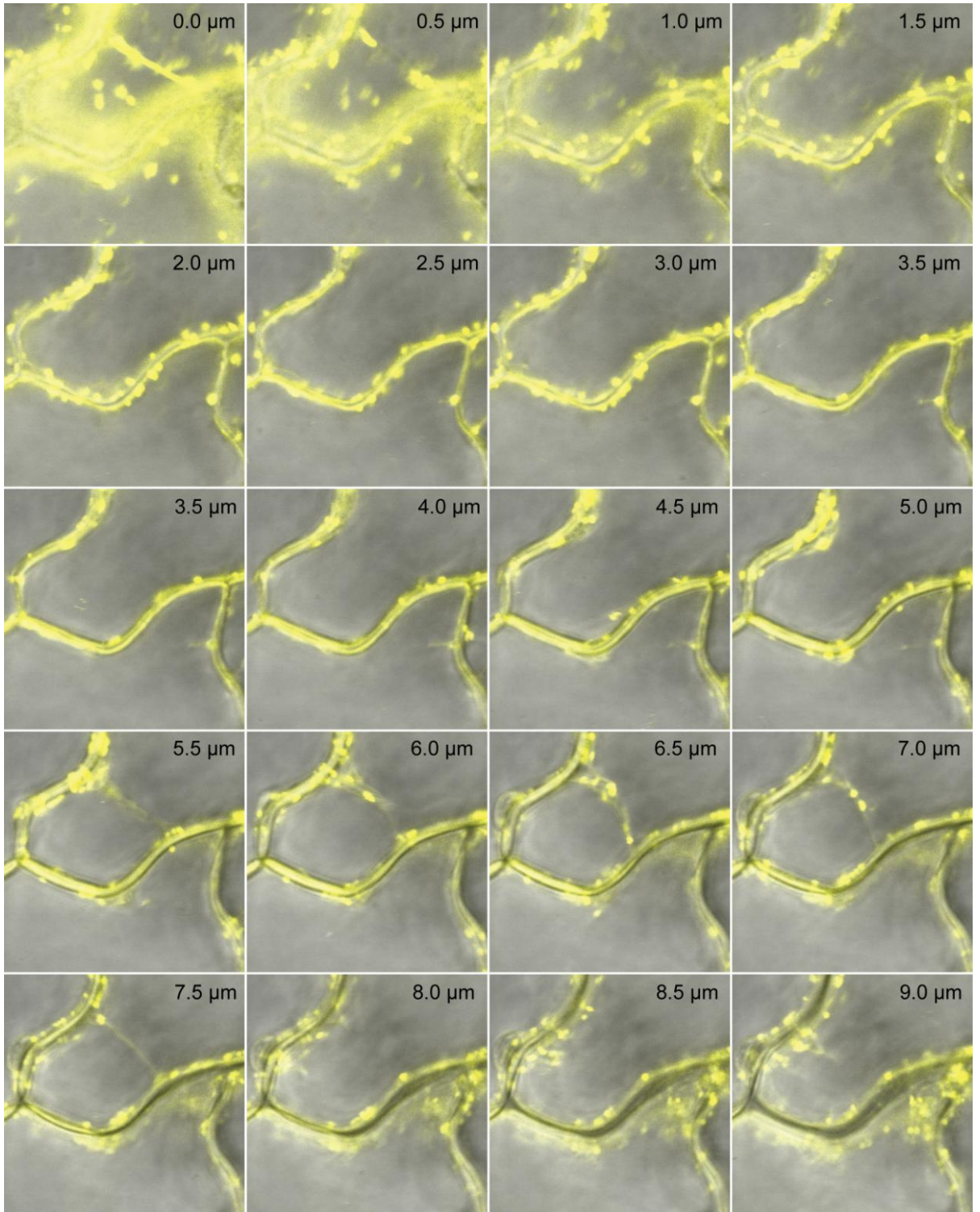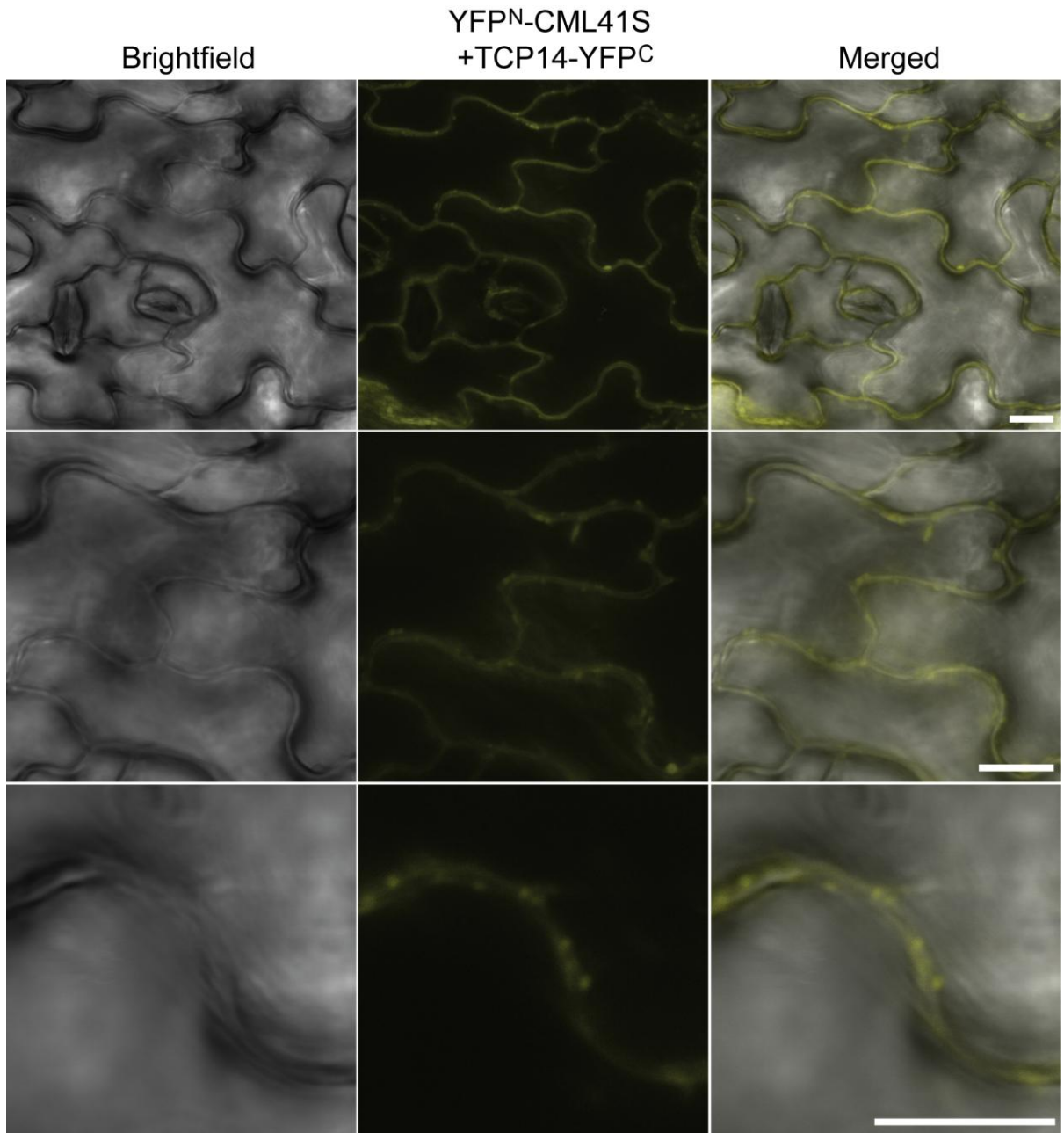
Figure 5.7 CML41FL and S and TCP14 interaction in Arabidopsis leaf. A, images of Arabidopsis leaf with co-infiltration of *Agrobacterium* carrying *YFP^N^-CML41FL* (N-terminal fragment of *YFP* fused to N-terminus of *CML41FL*) and *YFP^C^-TCP14* (C-terminal fragment of *YFP* fused to N-terminus of *TCP14*). **B**, z-serial optical section images of the cell displayed on the bottom panel of **A**. **C**, images of Arabidopsis leaf with co-infiltration of *Agrobacterium* carrying *YFP^N^-CML41S* (N-terminal fragment of *YFP* fused to N-terminus of *CML41S*) and *TCP14-YFP^C^* (C-terminal fragment of

YFP fused to C-terminus of *TCP14*). The fluorescence was captured using sequential scanning for YFP refers to Figure 5.2, scale bars = 10 μm.

5.4 Discussion

5.4.1 CML41FL and S are localised at plasmodesmata

Recently, PD have been successfully isolated from Arabidopsis cell suspension cultures using cell-wall digestion by Fernandez-Calvino et al (2011). The analysis of the PD proteome by Nano LC-MS/MS discovered more than 1,300 PD-localised proteins, about 20% of these were predicted to be localised in chloroplasts by public subcellular-localisation databases (e.g. TargetP and SignalP) (Fernandez-Calvino et al., 2011). This means there is a precedent for proteins with a high chloroplast prediction score, due to the presence of a putative chloroplast transit peptide, actually being localised to the PD. It must be noted that CML41 was not detected in the PD proteome in this study as perhaps it is not in those conditions and the cell-types used in that study. A review by Zambryski (2004) summarised the methods for the identification of PD components, one of which utilizes *cDNA-GFP* expression in plants. The cDNA-GFP displaying punctate fluorescence similar to GFP-CML41FL and S and adjacent to the cell boundary is strongly considered as a PD-specific localisation as shown examples in Figure 5.8A-C. Moreover, the CML41FL and S-GFP punctate localisation was identical with the localisation of GFP/YFP fused to plasmodesmata-located protein 1 (PDLP1, At5g43980), PDLP5 At1g70690 and plasmodesmata callose binding protein 1 (PDCB1, At5g61130) in Arabidopsis, as well as *Melon necrotic virus* pA7 and *Poa semilatent virus* (PSLV, genus *Hordeivirus*) TGBp3 in *N. tabacum* (Gorshkova et al., 2003; Thomas et al., 2008; Simpson et al., 2009; Amari et al., 2010; Genovés et al., 2010; Lee et al., 2011). All of these proteins have been proven to be targeted to PD in plants. Therefore, the equivalent distribution of punctate CML41FL and S-GFP at opposite sides of cell boundary indicates that CML41FL and S are likely to be localised at PD in intact Arabidopsis mature and old leaves as well as in the root tip upon a high calcium treatment (Figure 5.3 and 5.4).

A 30 kDa movement protein (MP) of tobacco mosaic virus (TMV) has been well studied that is targeted on the PD of tobacco and associated with viral movement between cells via interaction with the PD; removal of cell wall restricts the TMV MP to the cytoplasm attached with cytoskeleton of transfected *N. tabacum* protoplasts and TMV MP gradually aggregates at the edge of protoplasts after 48 hr transfection (Wolf et al., 1989; Lucas and Gilbertson, 1994; Heinlein et al., 1995; McLean et al., 1995 and 1997). Similarly, MP-GFP of *Red clover necrotic mosaic virus* (RCNMV) is also

targeted at PD in *Nicotiana benthamiana* epidermal cells at 15-20 hr after viral RNA inoculation but appearing in punctate spots in the cytoplasm and toward the internal surface of *N. benthamiana* protoplasts as shown examples in Figure 5.8D and E (Kaido et al., 2009). Hence, the punctate YFP-CML41FL and CML41S-YFP observed in Arabidopsis mesophyll protoplasts is likely to be the result of CML41FL and S that were not localised at PD but co-localised with cytoskeleton in the cytoplasm of protoplasts and aggregated towards the periphery of cells (Figure 5.1). So the study of cell-wall related components has to be treated with caution when using the protoplast system (Sheen, 2001). Similarly, the investigation of CML41FL and S to target these proteins in the protoplast system for either split YFP or luciferase complementation assay will also be compromised (Figure 5.6).

To validate the signal peptides of CML41FL and S, the truncation of the first 46 residues caused the YFP fusion of CML41FLΔ1-46 or CML41SΔ1-46 to be observed in the cytoplasm of Arabidopsis mesophyll protoplasts (Figure 5.2). This 46-residue truncation did not abolish the Ca^{2+}-binding characteristic of CML41FLΔ1-46 or CML41SΔ1-46 (Figure 3.5). Interestingly, CML41FL and CML41S can be found in the cytoplasm in certain conditions (see Section 5.4.2 below). This suggests that the N-terminal 46 residues of CML41FLΔ1-46 or CML41SΔ1-46 may function as a signal peptide to alter the subcellular localisation of the CML41 proteins, being cleaved to result in a cytosolic localisation and being intact to result in a PD localisation (Figure 3.5 and 5.1-5.2).
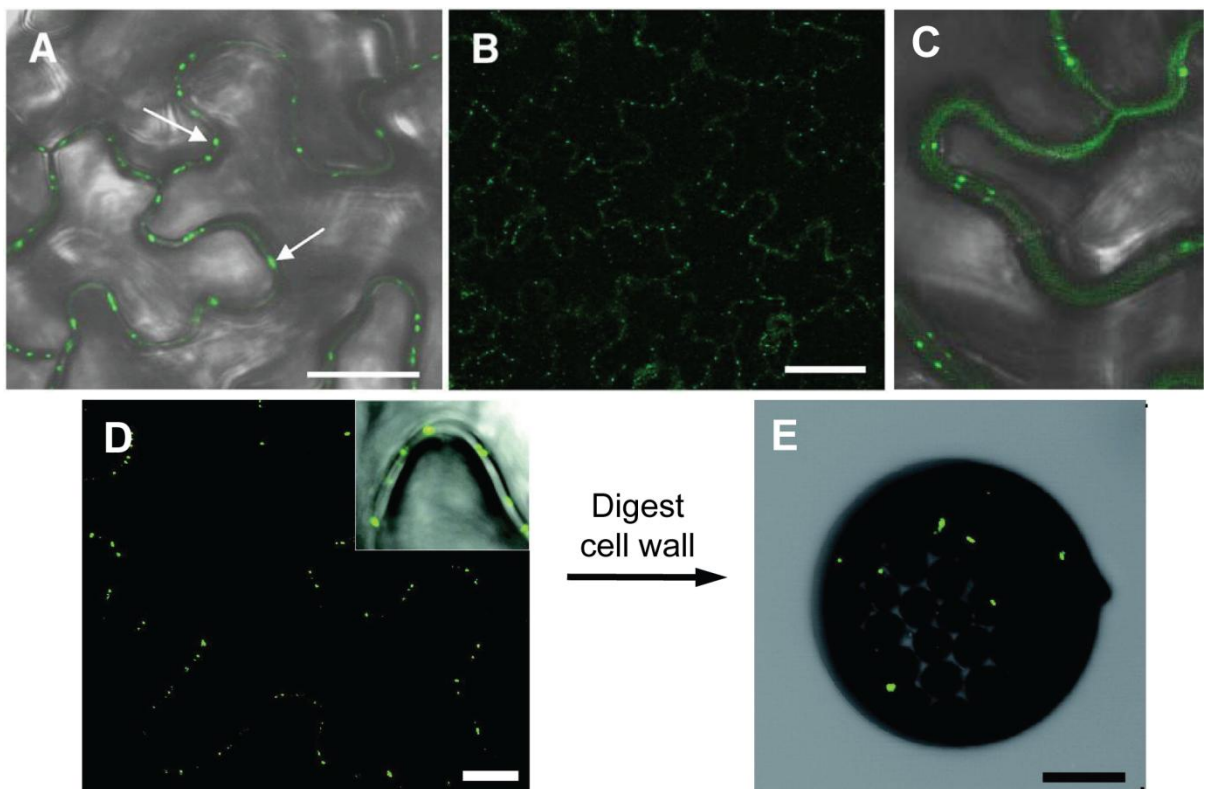
Figure 5.8 Typical GFP fused to PD-localised proteins in plants. A-**C**, confocal images of Arabidopsis epidermal cell expressing *YFP-PDCB1*. **C**, zoom-in image of YFP-PDCB1, YFP exhibits predominantly punctate spots at opposite sides of cell wall in Arabidopsis. **D**, confocal image of RCNMV MP-GFP localization in *N. benthamiana* at 15-20 hr after viral RNA inoculation, RCNMV MP-GFP is targeted at PD. **E**, confocal image of *N. benthamiana* protoplasts isolated from **D**. Images adapted from Simpson et al (2009) and Kaido et al (2009).

5.4.2 Dual patterns of CML41FL and S localisation dependent on developmental stages, organs and calcium treatment

A few Arabidopsis PD-localised proteins discovered by Fernandez-Calvino et al (2011) were validated by fusion with a GFP in Arabidopsis, these include three Receptor-like kinases (RLKs, At1gG56145, At4g21380, and At5g24010) and Tetraspanin 3 (TET3, At3g45600). These were found to be not only localised on the PD but also on the plasma membrane (Fernandez-Calvino et al., 2011). Not surprisingly if they are PD-localised proteins, CML41FL and S appeared not to be targeted to the PD in all circumstances. For instance, GFP-CML41FL and S were observed predominantly in the cytoplasm of root tissue during all developmental stages of Arabidopsis grown in BNS except that CML41FL and S were translocated to the PD in the root tip when the high dose of calcium was added into the Arabidopsis growth solution (Figure 5.3). Cytoplasmic CML41FL and S were observed in very young leaves as well (Figure 5.4). Thus, CML41FL and S are therefore likely to be dual-targeted proteins and are the first CaM/CMLs found in Arabidopsis that have this differential dual-targeting characteristics in a developmental, organ- and Ca^{2+}-dependent manner, although Arabidopsis CaM2, CML9 and CML42 have also been reported to be localised simultaneously within the nucleus and cytoplasm of *N. benthamiana* (Perochon et al., 2010; Vadassery et al., 2012; Fischer et al., 2013).

The common mechanisms for the dual-targeting of proteins is regulated at the transcriptional and translational levels (reviewed in Danpure, 1995; Small et al., 1998; Silva-Filho, 2003). This can result in multiple translation products that either gain or lack the signal polypeptides, achieved by different transcriptional initiation, alternative splicing transcripts or distinct translational initiation (Figure 5.9A and B) (Danpure et al., 1995; Small et al., 1998; Silva-Filho, 2003). In the case of CML41, the dual-targeting characteristics of CML41FL and S seemed not to be regulated at a transcriptional level, as both CML41FL (the non-splicing CML41) and CML41S (the spliced CML41) shared the same dual-targeting localisation in response to similar stimuli (e.g. Ca^{2+}, development) (Figure 5.3 and 5.4). Additionally, no proper second AUG was observed on the N-terminus of mRNA

transcribed from *CML41FL* and *S* CDS, suggesting that CML41FL and S both only have a single translation and their dual-targeting are not regulated at translational level either (Figure 2.5 and 2.7). In fact, a single translation is still able to direct protein dual localisation via post-translation modification (e.g. protein conformational change) (Silva-Filho, 2003; Karniely and Pines, 2005). For instance, a DNA-repair enzyme Apurinic/apyrimidinic endonuclease 1 (Apn1) from *S. cerevisiae* harbours a nuclear targeting signal on the C-terminus and a mitochondrial targeting signal on the N-terminus; the interaction between Apn1 and Pir1 induces Anp1 a conformational change, concealing its C-termina mitochondrial targeting signal and leading it its localisation in the nucleus (Vongsamphanh et al., 2001). In a similar way, CML41FL and S structural conformation at resting cytosolic Ca^{2+} concentration may mask the protein's targeting signal that however might be revealed in the presence of a specific Ca^{2+} signature (Karniely and Pines, 2005). CML41FL and S both can bind Ca^{2+} and their PD localisation occurred in the root tip in the presence of high calcium in the growth solution (Figure 3.5, 3.7 and 5.3). In the high calcium condition, there is likely to be an increased apoplastic and cytoplasmic Ca^{2+} concentration in the root tip since Ca^{2+} entry into the root xylem is restricted to the root tip (White, 2001; review in Chapter 1). So I propose that as Ca^{2+} sensors – CML41FL and S perhaps sense Ca^{2+} signalling in response to a high cytoplasmic or apoplastic Ca^{2+} concentration which induces CML41FL and S a conformational change, exposes their N-terminal PD signal and translocates them from cytosol to PD. Similarly, CML41FL and S PD localisation in mature and old leaves was probably a result of decoding the Ca^{2+}-signalling during Arabidopsis development or senescence (Figure 5. 4). Such PD localisation of CML41FL and S is worth a further validation using other techniques such as immunogold particle labelling of GFP in *CML41FL::GFP* or *CML41S::GPF* expressing plants (as further discussed in Chapter 6).

142
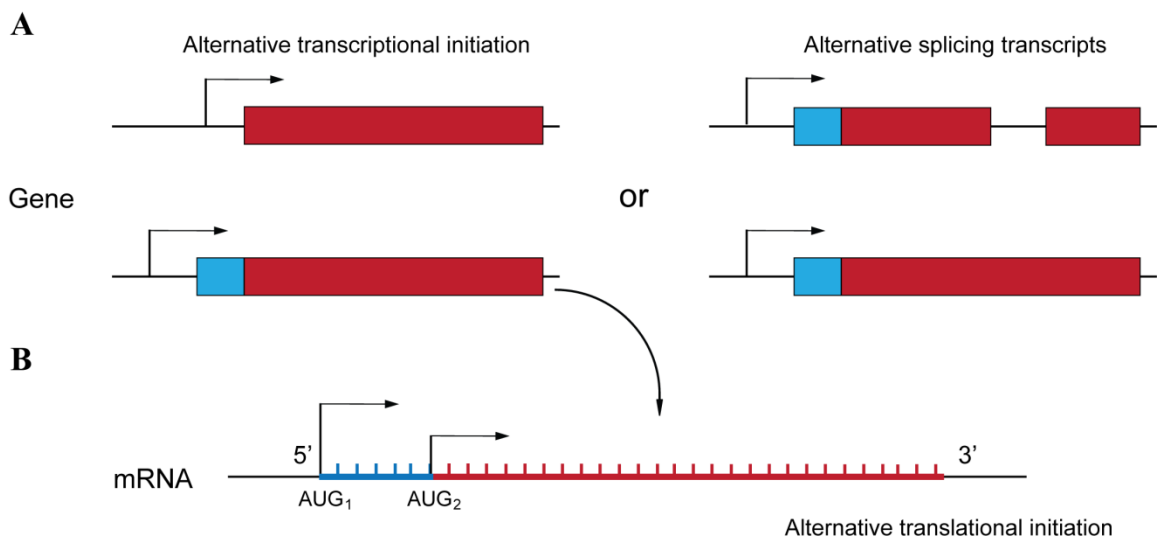
Figure 5.9 Transcriptional and translational regulation of multiple protein products from a single gene. A, multiple transcribed mRNAs produced by either different 5'-end transcriptional initiation or different splicing transcriptions on a single gene, arrows indicate gene transcriptional start-site. **B**, multiple translational start sites from different AUGs on a single mRNA, arrows indicate translational start-site. Adapted from Danpure et al (1995), Small et al (1998), Silva-Filho (2003) and Karniely and Pines (2005).

5.4.3 CML41FL and S interact with TCP14

As discussed above, CML41FL and S PD targeting is proposed to be as a result of a conformational change via the binding Ca^{2+} that exposes a targeting signal on the N-terminus of the protein. Hence, cytosolic CML41FL and S may be considered as the default location when not bound to Ca^{2+} (Silva-Filho, 2003). PD-localised CML41FL and S occurs in the Ca^{2+}-bound state by exposing the hydrophobic region ready to target another protein, then a target proteins such as TCP14, identified via interaction with CML41FL, are co-localised to the PD as well. Consistent with this, the fluorescence of a YFP complex formed via the interaction between CML41FL and TCP14 was clearly observed in punctate structures contiguous with the cell boundary, very much similar to GFP localisation fusion to CML41FL (Figure 5.3A, 5.4A and 5.7A), suggesting that the CML41FL and TCP14 interaction may occur at the PD in leaves. However, the interaction between CML41S and TCP14 was observed comparatively more in the cytoplasm than at the PD (Figure 5.7B). The fluorescence given off by the YFP complex implicates that the interaction between CML41FL and TCP14 was obviously stronger than that between CML41S and TCP14 (Figure 5.7A and C). This was potentially attributed to a structural difference between these two CMLs (Bhattacharya et al., 2004; Gifford et al., 2007). CML41FL has four putative EF-hands, whereas CML41S putatively has only three, which may lead to very different EF-hand domain organisation between them (Figure 5.10 and 5.11) (Gifford et al., 2007). EF-hands usually appear in pairs to bind Ca^{2+} in face-to-face manner and together form a stable four-helix bundle domain to create a hydrophobic surface essential for interaction with targeting protein (Bhattacharya et al., 2004; Gifford et al., 2007). For instance, putative EF-h1::EF-h2 of CML41FL probably creates a hydrophobic surface that CML41S is missing, resulting in the different target selectivity between these two CMLs (Bhattacharya et al., 2004). Following the CML41 and TCP14 interaction identified by Arabidopsis Interactome Mapping Consortium (2011), Valentim et al (2012) predicted the CML41 putative interaction motif to occur in the residues 'SHFDSDGD'. This 'SHFDSDGD' motif is actually present in both CML41FL (of EF-

h1) and CML41S (of New EF-h) (Figure 5.10). As a consequence, I propose that both CML41FL and CML41S can interact with TCP14 because of the presence of the putative 'SHFDSDGD' interaction motif in both of them; however the putative EF-h1::EF-h2 pair may facilitate a more selective/stronger interaction between CML41FL and TCP14 than between TCP14 and CML41S in presence of putative New EF-hand::EF-h3 in a pair (Figure 5.7 and 5.10). Experiments, such as isothermal scanning calorimetry, could be expected to further probe the Ca^{2+}-binding capacity and kinetics of each putative EF hand in CML41FL and S and test our hypothesis (Dobney et al., 2009).

In conclusion, the CML41FL and S interaction with TCP14 as well as their subcellular localisation has been tested in this chapter. Together with the evidence from BiFC, another validation of this protein-protein interaction using other techniques such as immunoprecipiation may provide more convincing results, since CML41FL /S are surprisingly neither nuclear nor chloroplastic proteins and TCP14 previously identified as a nuclear protein but here seems strongly interacting with CML41FL at the PD, the reason for this is unknown (Rueda-Romero et al., 2012; Braun et al., 2013). Futhermore, a transcription factor being targeting to PD is unprecidented. Moreover, CML41FL and S PD-localisation also provides another evidence that neither regulate *CAX1* expression *in planta*.
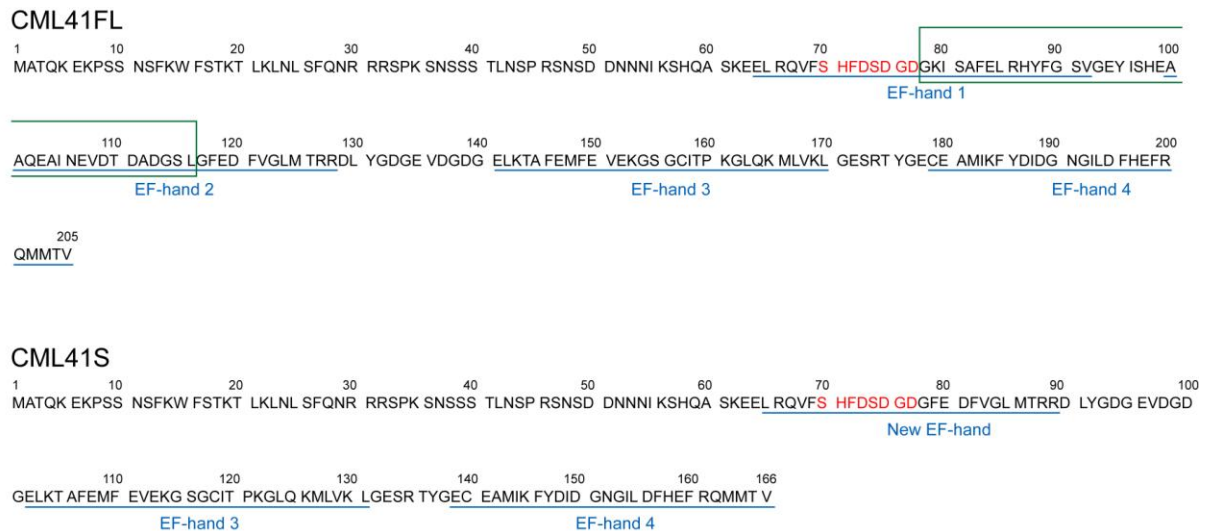
Figure 5.10 Protein sequences of CML41FL and S with EF-hand domain and predicted interaction motif labelled. The residues in red are the putative interaction motif of CML41 as predicted by Valentim et al (2012), the residues in green box are the spliced region of CML41FL into CML41S and the residues underline are the predicted EF-hand motifs by InterProScan (http://www.ebi.ac.uk/Tools/pfa/iprscan/).
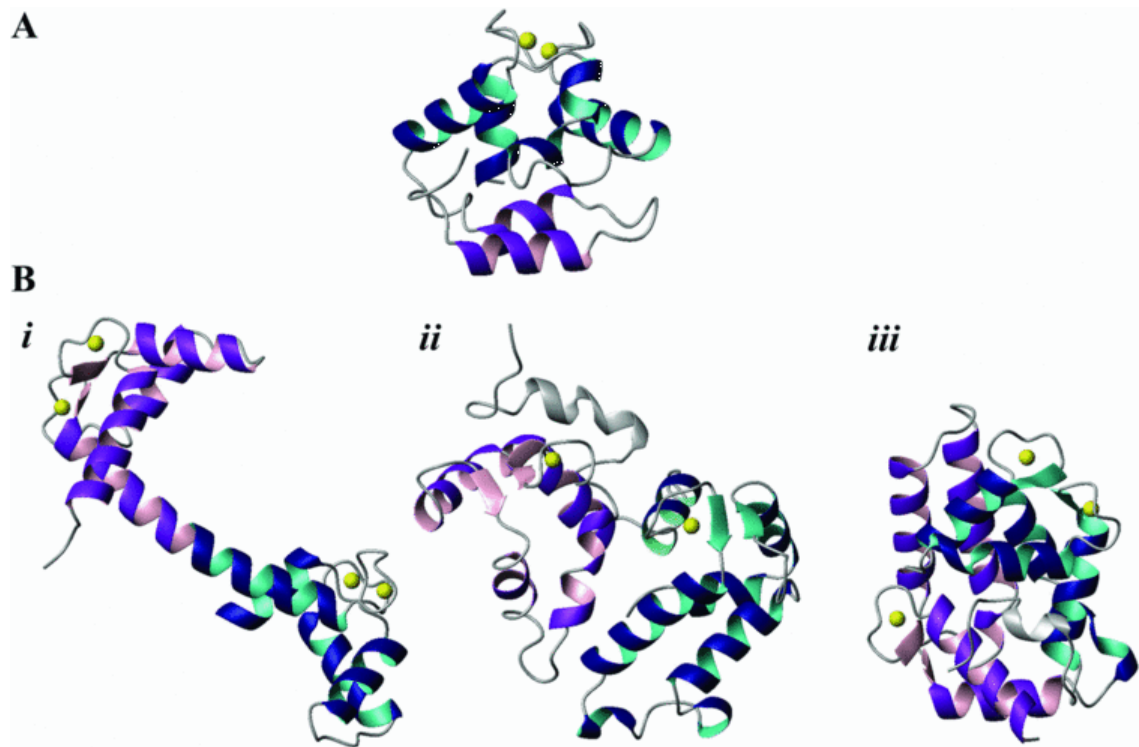
Figure 5.11 EF-hand domain organisations of EF-hand proteins. A, an example of Parvalbumin with three-EF-hands from rat, the EF-hand on the bottom (as indicated in purple) helps stabilise the EF-hand Ca^{2+}-binding pair above (as indicated in blue). **B**, three different arrangements of EF-hands in proteins with four EF-hands: i, two separate domains of a CaM jointed by a dynamic linker; ii, two domains placed tandem on the same protein face; iii, two pairs of EF-hands arranged oppositely to form a compact spherical fold structure. Apdated from Gifford et al (2007).

Chapter 6: General discussion

In this project, I aimed to identify signalling components associated with perturbed calcium storage, or at least the knockout of *CAX1*, with the rationale that this would uncover either transcriptional regulators of *CAX1* or downstream signalling elements dependent upon its proper function. The hope being that this may help develop better strategies for calcium biofortification in plants or at least improve our understanding of Ca^{2+} signalling networks in plants. Candidates were initially identified via analysing the global transcriptional profile in the loss-of-function mutants – *cax1*, *cax3*, *cax1/cax3* and *cax1/sCAX1* as well as the wild-type Col-0 as a control. The Calmodulin-like gene 41 was found to be negatively correlated with *CAX1* misexpression in these mutant lines, and as the most highly misexpressed candidate, it was decided that it would be an interesting gene to functionally characterise. My studies on *CML41* indicate that the misexpression of *CML41* does not control *CAX1* (Chapter 4) and therefore it is likely to function downstream of perturbations in Ca^{2+} signalling caused by *CAX1* misexpression.

Interestingly, it was found that *CML41* is likely to be transcribed into two CDSs – *CML41FL* and *CML41S*. They respectively encode the CML41FL and CML41S protein each with a distinct number of putative EF-hand Ca^{2+}-binding domains but the same signal-peptide sequence (Chapter 2). Both of them have a Ca^{2+}-binding capacity, so the proteins are equipped with the capacity of decoding intracellular Ca^{2+}-signals, and this may also assist with altering their subcellular translocation between cytoplasm and PD via eliciting a conformational change that conceals or reveals a protein targeting signal (Chapter 3 and 5). They are the first calmodulin family members identified as PD components and thereby are expected to participate in very different cellular processes from other published CaMs/CMLs behaving as transcriptional regulators in Arabidopsis (Reddy et al., 2011). Further characterisation *in planta* reveals that CML41FL is likely to participate in the plant in response to pathogen elicitors, CML41FL and S are involved in leaf senescence and regulating primary root growth in response to changes in external Ca^{2+}, and possibly the plant immune response (Chapter 4). The following discussion will further explore the role of this novel Ca^{2+} sensor in Arabidopsis and uncover important questions that remain to be tested with further experiments.

6.1 PD-localised CML41FL involved in callose deposition in PTI

In the Chapter 4 and 5, I observed that CML41 can localise to PD and the reduction in *CML41* expression leads to the reduction of callose deposition at PD. The callose deposition assay was carried out using quantification of allinine blue staining. This is one of several approaches that can be used to measure callose. Ideally, to corroborate this finding alternative techniques should be used

such as immunogold labelling to label the callose deposition upon flg22 treatments with anti-callose (Salnikov et al., 2003). However, the following discussion makes the assumption that CML41 can localised to PD and is involved in callose deposition.

Every living organism has their own approach for intercellular communication (Luca and Lee, 2004). PD as a symplasmic domain has evolved in plants for cell-to-cell communication. A simple PD is comprised of microchannels with a specific structure containing: a plasma membrane-lined cylindrical tunnel bridging neighbouring cells; an appressed ER trapped within the centre of cytoplasmic cylinder; proteinaceous components anchored to both the plasma membrane and ER; and, the cell wall surrounding the plasma membrane to provide physical constrains on the channel via deposition of insoluble glucans such as callose (Figure 6.1) (Luca and Lee, 2004; Maule et al, 2011).
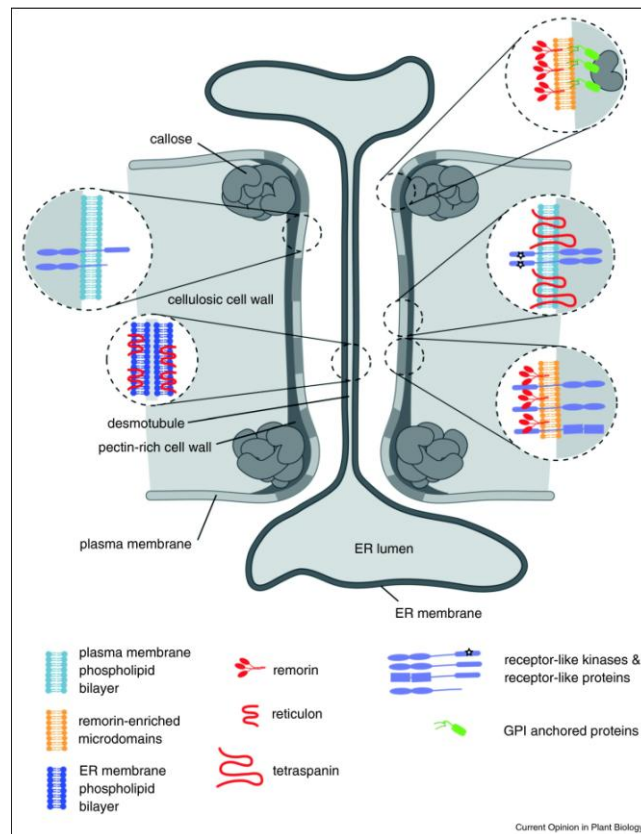
Figure 6.1 Schematic model of a simple PD. Adapted from Maule et al (2011).

Cytoplasmic sleeves act as a gateway traversing the cytoplasm in between cells and are a space of 3-4 nm in diameter bordered by the plasma membrane and ER of PD. This imposes a basal

size-exclusion limit (SEL; ~800 to 1,200 Da) for the passive diffusion of small molecules between cells (e.g. sugar, organic acids) (Roberts and Oparka, 2003; Luca and Lee, 2004; Maule, 2008). PD also have the capacity to mediate cell-to-cell trafficking of macromolecules like RNA and a special class of proteins called non-cell autonomous proteins (NCAPs); the trafficking of NCAPs, of size up to 40 kDa is facilitated by PD via a gated or selective pathway (reviewed in Zambryski and Crawford, 2000; Lucas and Lee, 2004). PD-mediated symplasmic transport coordinates plant development and immunity against viral, fungal and bacterial invasion through its distinctive dynamic structural characteristics (models for pathogen defence by callose deposition at PD is summarised in Figure 6.2A-C) (Zambryski, 2004; Burch-Smith et al., 2011; Lee and Lu, 2011). Callose as a polysaccharide is composed of β-1,3-glucan branched with β-1,6-glucan, and deposited at neck region of PD as shown in Figure 6.1. One of the immune responses to *P. syringae* is callose deposition at PD to reduce PD permeability and restrict bacterial effectors and other unknown signalling molecules movement between cells; this is mediated by a SA-dependent pathway, triggered by *P. syringae* flagellin (e.g. flg22) (Figure 6.2D) (Radford et al., 1998; Chen and Kim, 2009; Dodds and Rathjen, 2010; Luna et al., 2010; Lee and Lu, 2011; Wang et al., 2013).
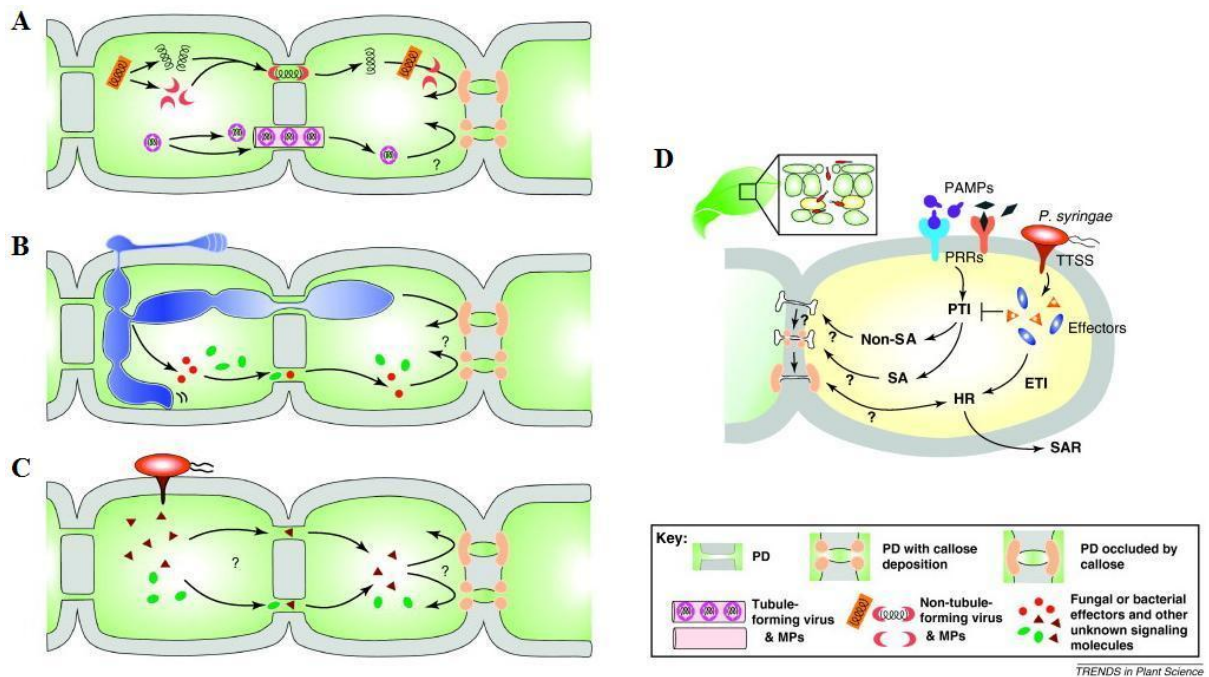
Figure 6.2 Models of callose plug deposition at PD following microbial pathogen invasion. A, virus utilises movement proteins to modulate PD size-exclusion limits to assist with viral cell-to-cell spread. **B**, fungus and effectors move between cells through PD. **C**, bacterial effectors are transported via PD. The plant defence involves the regulation PD permeability via callose plugs reducing

movement of those microbial pathogens as shown in **A**, **B** and **C**. **D**, a hypothetical pathway of PD regulation against bacterial infection. Adapted from Lee and Lu (2011).

Here, I report the expression of both *CML41FL* and *CML41S* is induced by flg22 infiltration into leaves, in this flg22-triggered immune response, knocking down *CML41FL* expression reduces the callose deposition at PD in *CML41*-amiRNA#2 lines; the involvement of CML41S in this process is unknown (Figure 4.5, 4.10A and 4.14A). In addition, PD is the location where CML41FL is present in leaves except in young developing tissues where CML41FL is localised in cytoplasm instead (Figure 5.4). CML41FL has also been demonstrated to be a Ca^{2+} binding protein (Figure 3.6 and 3.8). Accordingly, I speculate that CML41FL probably functions as a Ca^{2+} sensor in translating a PAMP-triggered Ca^{2+} signalling into the regulation of PD callose deposition and PD permeability in the plant innate immunity in response to flg22, for which this CML41FL-PD localisation probably is essential.

6.2 CML41FL differs from other immunity-response CMLs in Arabidopsis

CaMs/CMLs as Ca^{2+} signalling regulators play a critical role in the plants defence against intruders (Reddy et al, 2011). As discussed above, CML41FL is likely to participate in the callose deposition during PTI. In fact, similar to CML41FL, a few other CaMs/CMLs have also been reported to regulate the plant immunity response in Arabidopsis such as CML9, CML24 (TCH2), CML42 and CML43 (reviewed in Cheval et al., 2013, references therein). But each of them, including CML41FL functions in distinct cellular processes during the plant immunity response. CML42 is predominantly localised to the nucleus and cytoplasm, and mediates Ca^{2+}-signalling to negatively modulate JA and the glucosinolate content in plants as a chemical defence against attack by the herbivorous insect *Spodoptera littoralis* (Vadassery et al., 2012). CML43, the closest homologue to CML42 is regulated by *P. syringae* pv. tomato, and *CML43* overexpression facilitates the faster/accelerated activation of Ca^{2+}-signalling regulated hypersensitive-response (HR) in Arabidopsis (Chiasson et al., 2005). CML9, similar to CML41FL, modulates callose deposition during PTI but via a negative regulation of *PR1* expression and perhaps via a switch of GA-dependent signalling elements (Popescu et al., 2007; Leba et al., 2012a and 2012b). CML24 is a touch-induced calmodulin-like protein and important in recognition of PAMP-triggered early signalling in the activation of downstream NO generation and HR against *P. syringae* pv. tomato (Ma et al., 2008). The unique subcellular localisation of CML41FL at the PD is likely to determine its function in different cellular processes during the plants immunity response when compared to the nuclear-localised CML24, CML9 and CML42 (Perochon et al., 2010;

Vadassery et al., 2012; Mohd Noh, 2013). Moreover, the role of CML41FL is likely to be the modulation of symplasmic transport and cell-to-cell communication, whereas the majority of CaMs/CMLs characterised in this response exert their effect via Ca^{2+}-regulated transcriptional regulation (reviewed in Kim et al., 2009a; Reddy et al., 2011; Bender and Snedden, 2013, references therein). However, the details of the pathway controlling CML41FL-regulated Ca^{2+} signalling are far from clear.

6.3 Involvement of CML41FL and S in response to other stresses

CML41 has previously been identified as one of a number of age-related resistance-associated genes (Carviel et al., 2009), and is included in a co-expression network with the senescence-related gene *SAG13* (Figure 2.3) (Swartzberg et al., 2006 and 2011). GUS histochemical assays suggest that dark-induced senescence (after 14 days) imposed in this study is not an effective treatment for stimulating *CML41* expression, but the constitutive expression of *CML41S* and silencing of *CML41FL* both accelerate the dark-triggered chlorophyll breakdown and leaf senescence in plants. This suggests that both CML41FL and S may be involved in the regulation of senescence elicited by changes in photoperiod (Figure 4.6f-i and 4.13). In fact, PCD is induced in plants as a mechanism of resistance to pathogen invasion and produces reactive oxygen species (ROS) that is always followed by the production of callose (Greenberg, 1997; Breusegem and Dat, 2006; Benitez-Alfonso et al., 2011). Indeed, the constitutive expression of *PLDP5* is linked to the over production of callose and an early senescence phenotype in plants (Lee et al., 2011). Presumably, the dark-induced PCD on individual leaves is also related to callose metabolism; however in my case, it still remains obscure whether this dark-triggered senescence is sufficient to invoke the translocation of CML41FL and S between the cytoplasm and PD, and if this CML41FL and S-associated senescence modulates PD permeability via callose deposition.

PD-mediated symplasmic transport regulated by PD closure can be regulated by abiotic stresses, such as exposure to aluminium (Al^{3+}) which induces callose formation to reduce the PD size-exclusion limit (SEL) in epidermal cells of maize roots and then in root cortical cells after the loss of epidermal layers (Sivaguru et al., 2000; Jones et al., 2006; Benitez-Alfonso et al., 2011). In 12.5 mM calcium supplemented conditions, the overexpression of *CML41FL* and *S* reduces the sensitivity of the primary root to external Ca^{2+}, relative to the wild-type Col-0 (Figure 4.11C and D). In response to high external Ca^{2+}, CML41FL and S appears to be translocated from the cytosol to the PD at the root tip of *CML41FL* and *S-GFP* plants, suggesting that the primary root sensitivity to Ca^{2+} perhaps is linked to CML41FL and S targeting to PD (Figure 4.11C, D and 5.3). Moreover, the root Ca^{2+} uptake

involves apoplastic Ca^{2+} influx into the root at the root apical area from soil and then is delivered via the symplasmic pathways into the xylem (White, 2001; White and Broadley, 2003). As such, this translocation of CML41FL and S to PD may reduce the PD permeability at the root tip in response to external high Ca^{2+}, perhaps followed by a decrease in the symplasmic Ca^{2+} transport via PD into root xylem from the root tip. In the presence of high Ca^{2+}, primary root growth of *CML41FL* and *S-OEX* lines displayed relatively lower sensitivity than wild-type plants, presumably as a result of a reduced Ca^{2+} symplasmic delivery into root xylem (Figure 4.11C and D). Nevertheless, the separate contribution by CML41FL and S in this cellular process are yet to be elucidated, but this could be aided by examining the *CML41FL* and *CML41S* expression profile in *CML41FL-OEX* lines (Section 4.4.1). In high $CaCl_2$ conditions (up to 50 mM), the wild-type plants and *CML41FL* and *S-OEX* lines undergo a severe reduction in primary root growth, whereas this growth reduction is suppressed in *CML41*-amiRNA#2 (Figure 4.11C and D). This phenomenon might be a partial consequence of the enhanced Ca^{2+} symplasmic uptake into root xylem via silencing *CML41FL* expression, undergoing a higher $[Ca^{2+}]_{cyt}$/greater Ca^{2+} influx and lowering Cl^- uptake/toxicity in the cells (Lorenzen et a., 2004; Saleh and Plieth, 2013). This hypothesised correlation of CML41 with root symplasmic Ca^{2+} uptake requires further measurement, and the impacts by *CML41* misexpression on leaf calcium content are worthwhile to be tested in plants as well.

6.4 Correlation of CML41 with CAX1

Initially, *CML41* was selected from >1000 misexpressed genes via a microarray analysis as it displayed the strongest negative correlation with *CAX1* expression in the *cax* mutant lines analysed; *CAX1* knock-out was associated with a significant induction of *CML41* expression (Figure 2.1 and 2.3). The misexpression of *CML41FL* and *S*, however did not perturb *CAX1* expression in leaves even under certain stresses (e.g. flg22), this suggests that CML41FL and S are not transcriptional regulators of *CAX1*. Instead CAX1 probably negatively regulates *CML41* expression and CML41FL and S act as the Ca^{2+} sensors downstream of CAX1 (Figure 4.9A and 4.10B). Moreover, *CML41* misexpression in *cax1/cax3* line is significantly alleviated when *cax1/cax3* line are grown with low calcium supplementation (300 µM), where the leaf necrosis of *cax1/cax3* line disappears and its $[Ca^{2+}]_{apo}$ and cell-wall thickness are also reduced to a similar level with wild-type Col-0 (Conn et al., 2011; Gilliham et al., unpublished results). Therefore, *CML41* expression is presumably induced in *cax1*/*cax3* misexpression lines due to either damage to the cell wall or by a perturbation in Ca^{2+}-signalling/$[Ca^{2+}]_{apo}$ as would occur also in response to several biotic and abiotic stresses, as discussed above (Conn et al., 2011). Nevertheless, this explanation is not consistent with *CML41* misexpression

observed in *cax1* mutant line (Figure 2.1), where CAX3 is specifically induced in the leaf mesophyll and believed to functionally compensate for the loss of CAX1 and carryout Ca^{2+} uptake into the mesophyll vacuoles; however neither $[Ca^{2+}]_{apo}$ nor cell-wall thickness is obviously altered in *cax1* line (Conn et al., 2011; Conn et al., unpublished results). In fact, the tonoplast Ca^{2+}/H^+ antiport activity has been observed as decreased by up to 50% in the *cax1* line, suggesting that CAX3 may acquire lower tonoplast Ca^{2+} uptake capacity than CAX1 in leaf mesophyll. This is perhaps due to the absence of certain CAX3 activators in leaf mesophyll, unlike CAX1, or a lower innate Ca^{2+} transport rate and/or affinity, although the de-regulated sCAX1 and sCAX3 (Δ90-CAX3) have similar affinities in *S. cerevisiae* (respectively 10-15 μM and 14 μM) (Hirschi, 1996; Cheng et al., 2003; Manohar et al., 2011). Moreover, *cax1* plants has a ~35% enhanced tonoplast Ca^{2+}-ATPase uptake activity, however Ca^{2+}-ATPases have relative lower capacity for Ca^{2+} transport, therefore this increased Ca^{2+} uptake by Ca^{2+}-ATPase perhaps is not enough to perfectly compensate the reduction (by 50 %) in tonoplast Ca^{2+}/H^+ antiport Ca^{2+} uptake activity, and the overall tonoplast Ca^{2+}-uptake capacity of mesophyll is presumably impaired in *cax1* line (Sze et al., 2000; Geisler et al., 2000; Baxter et al., 2003; Cheng et al., 2003; Hayter and Peterson, 2004). This reduced total tonoplast Ca^{2+}-uptake capacity in the mesophyll of *cax1* plants does not lead to a perceptible $[Ca^{2+}]_{apo}$ increase in *cax1* line (Conn et al., unpublished results). The up-regulation of *CML41* in *cax1* line may be linked to a reduced symplasmic Ca^{2+} transport into root xylem at apical part of roots (as discussed in Section 6.3) and perhaps less Ca^{2+} delivery into leaf apoplasm via xylem, and result in undetectable difference in $[Ca^{2+}]_{apo}$ of *cax1* line from wild-type plants, for which a further investigation is worthwhile (Figure 2.1) (Cheng et al., 2003; Conn et al., 2011). Relative to normal calcium (2 mM) supplementation, *cax1/cax3* line acquires a lower $[Ca^{2+}]_{apo}$ level in the low calcium supplemented environment where *CML41* is not initiated (Conn et al., 2011; Conn et al., unpublished results; Gilliham et al., unpublished results). Alternatively, as CAX3 has a lower transport capacity than CAX1, $[Ca^{2+}]_{cyt}$ signalling is perturbed in not only *cax1/cax3* but also *cax1* and this initiates *CML41* expression. But the phenotypes in *cax1* are not as severe as *cax1/cax3* as the limitation on Ca^{2+} transport characteristics of the tonoplast are not as severe. Moreover, it is noted that *CML41* is also misexpressed in *cax1/sCAX1* line, where *sCAX1* is constitutively expressed and the active sCAX1 constantly moves Ca^{2+} into vacuoles in all cell types of *cax1* plants, however the phenotype of *cax1* line is essentially comparable with wild-type plants (Figure 2.1) (Cheng et al., 2003). This signifies that the regulation of *CML41* as a signalling element probably is interrelated with mesophyll-specific expression of *CAX1* in plants.

I speculate that the reasons behind *CML41* up-regulation in *cax1* and *cax1/cax3* lines may be linked to CML41-associated external calcium nutrient response, possibly in addition to CML41-

mediated pathogen response in plants, and the spatial expression of *CAX1* may be vital for the regulation of *CML41*. Hence, it would be interesting to examine the calcium-sensitive phenotypes and $[Ca^{2+}]_{apo}$ in *cax1* and *cax1/sCAX1* mutant lines overexpressing *CML41*-amiRNA#2 as they may increase in leaves.

A caveat must be raised for using purely gene expression data to form a complete picture of an experimental system. In the discussion above, it is clear that expression differences of Ca^{2+} transporters leads to difference in protein abundance and activity. However we have not yet been able to validate whether differences in

6.5 Remaining questions and future direction

Apart from several questions mentioned above, there are a few additional remaining questions about the CML41FL and S-associated regulation in plant growth, development and adaptation to environmental stimuli, such as:

1) Is *CML41S* transcript really present in Arabidopsis mRNA?

CML41S seems to be the major transcript form of *CML41* in Arabidopsis mesophyll protoplasts, apart from that *CML41FL* has been observed to be the major one in all other conditions tested (Figure 2.4). So I speculate that *CML41S* is very likely present as a splicing variant of *CML41*. However, a further validation is worthwhile to back up this hypothesis, such as a Nothern blot. This could probe RNA directly to detect the presence and absence of certain mRNA spliced transcripts at very low abundance from total RNA (Vandenbroucke et al., 2001). An extension of this question is whether both protein products are produced. This could be tested by Western blot analysis specific antibodies to CML41FL and CML41S.

2) Does CML41FL and S function at PD and require an interaction with another PD-localised protein?

The PD is a membrane-rich structure. A number of known PD protein families acquire transmembrane domains (TMD), such as PDLPs, RLKs, GPI-anchor proteins, and β-1,3-glucanases (Levy et al., 2007; Thomas et al., 2008; Simpson et al., 2009; Fernandez-Calvino et al., 2011), but no transmembrane domain (TMD) has been found in CML41FL based on the prediction from 18 individual database (Figure 6.3). Although as a Ca^{2+} sensor involved in callose deposition in PTI, CML41FL when targeting to PD unlikely acts as an enzyme to stabilise/inhibit callose binding/degradation, instead perhaps it interacts with another PD-localised protein to regulate some

enzymatic process. CML41FL and S share very similar structural characteristics, such as Ca^{2+}-binding ability and a putative targeting signal (Figure 2.6 and 2.8). CML41S function at the PD may also require incorporation with a PD-anchored protein. In fact, eight CaM-binding proteins have been identified from the PD proteome, including two pathogen-related CaM-binding proteins – Mildew resistance locus O 2 (MLO2, At1g11310) and Bcl-2-associated athanogene 6 (BAG6, At2g46240) (Doukhanina et al., 2006, Bai et al., 2008; Lewis et al., 2012). An interaction screen of CML41 and these candidates, under high Ca^{2+} conditions would be worthwhile, as would performing pull-down type experiments using GFP-Trap immunoprecipitation on *CML41-GFP* plants (Roux et al., 2011).

Figure 6.3 Diagram of CML41 (At3g50770) TMD prediction based on 18 individual programs output by ARAMEMNON transmembrane alpha helix prediction. (http://aramemnon.uni-koeln.de/index.ep).

3) Does any interaction CML41FL and S with TCP14 contribute to pathogen defence in PTI?

The interaction between CML41FL and S with TCP14 has been validated in this thesis, however the function of these interaction pairs is still unknown. Analysis of the Arabidopsis interactome data set by Mukhtar et al (2011) revealed that TCP14 interacts with NB-LRR receptor proteins At1g31540 and At1g62630, which contain nucleotide-binding (NB) and leucine-rich repeat (LRR) domains that can recognise the specific pathogen effectors, and with an immune-related

WRKY transcription factor (WRKY36, At1g69810) (Caplan et al., 2008; Dodds and Rathjen, 2010; Arabidopsis Interactome Mapping Consortium, 2011). Mukhtar et al (2011) propose that TCP14 is a key component in a certain subunit within the whole plant-pathogen immune network. In addition to CML41FL function in the PAMP immune response, the interaction of CML41FL and TCP14 might have a role in the plant defence against pathogens. Moreover, the investigation of protein interaction was performed on leaves using *Agrobacterium*-mediated transient expression. In fact, the *A. tumefaciens* mediated transformation involves the activation of PAMP in Arabidopsis via an elicitor named elf18 different from flg22 elicitor of *P. syringae* that is compromising the first 18 aa on the N terminus of bacterial elongation factor Tu (EF-Tu) and precipitated by EFR receptor kinase of Arabidopsis (Kunze et al., 2004; Zipfel et al., 2006; Zipfel, 2008). Both elf18 and flg22 harbour similar signalling pathways and both elicit callose deposition at PD regardless of whether they are recognized by different receptors in the plant, both also increase the expression of *CML41* in plants (Figure 2.8 and 4.10A) (Bittel and Robatzek, 2007; Lu et al., 2009). The stronger/selective interaction between CML41FL with TCP14 than between CML41S and TCP14 observed predominantly at PD hints that this CML41FL and TCP14 interaction might contribute to the modulation of PD, perhaps via callose deposition in the plants defence against pathogens (e.g. *A. tumefaciens*). However, this requires further investigation. For instance, serial pathogen inoculation (e.g. virulent or avirulent strains of *P. syringae* pv. tomato) and real-time ROS measurement on *CML41* knock-down and/or loss-of-function *tcp14* plants, which would be expected to reveal the contribution of the interaction between CML41FL and S with TCP14 in the plant immune response and uncover more details of CML41FL roles in the regulation of callose deposition by flg22 treatment.

4) Are CML41FL and S involved in the regulation of plant development?

The *CML41FL* and *S* expression and CML41FL and S subcellular localisation both exhibit an age-dependent pattern (Figure 4.6 and 5.4), implicating that CML41FL and S are likely to be regulated by developmental signalling. Moreover, macromolecule transport between cells plays a critical role in regulation of plant development, indeed the endogenous NCAPs and RNA trafficking confers the sophisticated regulation of embryonic, vegetative and reproductive development in plants (reviewed in Zambryski et al., 2000; Zambryski, 2004). This cell-to-cell transport of certain NACPs and RNA even involves long-distance signal transport via the phloem between organs, such as the *FLOWERING LOCUS T* (*FT*) encoded FT protein that is synthesized in leaves but is transported via the phloem into the shoot apex to initiate Arabidopsis flowering (Lucas and Lee, 2004; Corbesier et al., 2007; Turgeon and Wolf, 2009) The cell-to-cell transport/communication, including long-distance

transport signals, can be mediated by PD (Lucas and Lee, 2004; Zambryski, 2004; Turgeon and Wolf, 2009). *CML41FL* and *S* expression has been found in the main vein of mature and old leaves where CML41FL and S are targeted to the PD (Figure 4.6 and 5.4). Accordingly, these results suggest that CML41FL and S might sense certain developmental Ca^{2+} signalling to modulate the PD SEL in cells of main vein of leaves and regulate long-distance signal transport during certain plant developmental processes, and perhaps even through the interaction with TCP14 that functions as a regulator of plant leaf shape and internode length (Kieffer et al., 2011)

5) Where are CML41FL and S localised within PD?

CML41FL and S have been identified as the PD components but it is not clear where they are precisely located within PD. A precise localisation within PD will better help understand how CML41 might be associated with PD modulation. For example, the overexpression of either *PDCB1* or *PDLP5* has been found to increase callose accumulation in plants; later PDCB1 and PDLP5 are indicated by immunogold labelling to be localised respectively at neck region of PD and at the central region of PD as shown in Figure 6.4, and their precise localisation at PD helps better understand the difference in their mechanisms of modulating PD closure. PDCB1 directly mediates callose deposition at PD via physically binding callose at the neck region of PD, while PDLP5 being localised at the central region of PD requires an additional unknown factor to indirectly mediate the callose accumulation and involve a positive signalling feedback loop between it and SA in a *EDS1/ICS1/NPR1* dependent manner (Simpson et al., 2009; Lee et al., 2011; Wang et al., 2013). Likewise, more details of CML41FL and S PD localisation would potentially help a further identification of CML41FL and S-mediated signalling pathways in Arabidopsis, potentially to be indicated by immunogold labelling. Meanwhile, this is also expected to provide further evidence to support CML41FL and S PD localisation indicated by cell imaging.
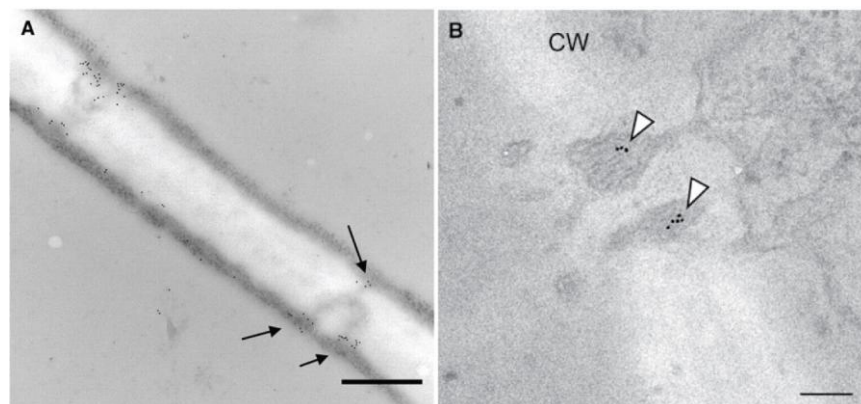
Figure 6.4 PDCB1 and PDLP5 localisation within PD imaged by transmission electron microscopy. The arrows point to the immunogold particles labelling PDCB1 (**A**) and PDPL5-GFP (**B**) *in vivo*. Adapted from Simpson et al (2009) and Lee et al (2011).

6.6 Conclusion

In this thesis, I have reported that a calmodulin-like gene 41 (*CML41*) possibly encodes dual Ca^{2+}- sensors – CML41FL and CML41S that are likely to play a regulatory role in response to biotic stresses, calcium nutrition and leaf senescence. As such, this study discovers novel Ca^{2+}-signalling elements likely to be under the regulation of CAX1 and this has filled knowledge gaps and tested some hypotheses listed in Section 1.5:

i) *CML41* was identified to be negatively correlated with *CAX1* expression in serial *cax1* mutant lines, and CML41 probably acts as a Ca^{2+} sensor/signalling element downstream of CAX1.

ii) The understanding of CML41 roles in plants uncovers a new Ca^{2+}-signalling pathway mediated by CAX1 in participation of plant adaptation to pathogen, sensitivity to environmental calcium supply and dark-stimulated leaf senescence.

iii) The physiological link between cell-specific calcium compartmentation and CML41 (both modulated by CAX1) has not been tested in this study, but both of them rely upon cell-specific expression of *CAX1* in plants, implicating that the cell-type calcium compartmentation in plants might be essential to control Ca^{2+} signalling elements in plants, such as CML41.

Appendix 1. Manuscript of a review: Ca delivery and water flow

Calcium delivery and storage in plant leaves: exploring the link with water flow

Matthew Gilliham, Maclin Dayod, Bradleigh J. Hocking, Bo Xu, Simon J. Conn, Brent N. Kaiser, Roger A. Leigh and Stephen D. Tyerman

Waite Research Institute, School of Agriculture, Food and Wine, University of Adelaide, PMB1, Glen Osmond, SA, 5064, Australia

STATEMENT OF AUTHORSHIP

Xu, B. (Candidature)

Contributed the part of review of Ca transport in plant.

I hereby certify that the statement of contribution is accurate.

Signed………………………………………………..Date…………………………………

Gilliham, M.

Conceived model and review concept, wrote manuscript

I hereby certify that the statement of contribution is accurate and I give permission for the inclusion of the paper in the thesis.

Signed………………………………………………..Date…………………………………

Dayod, M.

Contributed to part of review of Ca transport in plants

I hereby certify that the statement of contribution is accurate and I give permission for the inclusion of the paper in the thesis.

Signed………………………………………………..Date…………………………………

Hocking, B.J.

Contributed to part of review of Ca transport in plants

I hereby certify that the statement of contribution is accurate and I give permission for the inclusion of the paper in the thesis.

Signed………………………………………………..Date…………………………………

Conn, S.J.

Contributed to part of review of Ca transport in plants

I hereby certify that the statement of contribution is accurate and I give permission for the inclusion of the paper in the thesis.

Signed…………………………………………………..Date…………………………………………

Kaiser, B.N.

Conceived model and review concept, edited manuscript

I hereby certify that the statement of contribution is accurate and I give permission for the inclusion of the paper in the thesis.

Signed…………………………………………………..Date…………………………………………

Roger, R.A.

Conceived model and review concept, edited manuscript

I hereby certify that the statement of contribution is accurate and I give permission for the inclusion of the paper in the thesis.

Signed…………………………………………………..Date…………………………………………

Tyerman, S.D.

Conceived model and review concept, wrote manuscript

I hereby certify that the statement of contribution is accurate and I give permission for the inclusion of the paper in the thesis.

Signed…………………………………………………..Date…………………………………………

Gilliham, M., Dayod, M., Hocking, B.J., Xu, B., Conn, S.J., Kaiser, B.N., Leigh, R.A. & Tyerman, S.D. (2011). Calcium delivery and storage in plant leaves: exploring the link with water flow.
Journal of Experimental Botany, 62(7), 2233–2250.

Appendix 2. Manuscript of hydroponic growth method

Protocol: optimising hydroponic growth systems for nutritional and physiological analysis of *Arabidopsis thaliana* and other plants

Simon J Conn[1], Bradleigh Hocking[1,2], Maclin Dayod[1,2], Bo Xu[1,2], Asmini Athman[1,2], Sam Henderson[1,2], Lucy Aukett[1], Vanessa Conn[1,2], Monique K Shearer[1,3], Sigfredo Fuentes[1], Stephen D Tyerman[1,2], Matthew Gilliham[1,2]

[1] School of Agriculture, Food & Wine and The Waite Research Institute, University of Adelaide Waite Campus, PMB1, Glen Osmond, South Australia 5064, Australia

[2] Australian Research Council Centre of Excellence in Plant Energy Biology, Glen Osmond, South Australia 5064, Australia

[3] Australian Centre for Plant Functional Genomics, Waite Research Institute, University of Adelaide, Glen Osmond, South Australia, Australia

Protocol: optimising hydroponic growth systems for nutritional and physiological analysis of
Arabidopsis thaliana and other plants
Plant Methods. 2013. 9:4.

Xu, B. (Candidature)
Developed the rapid screen for selection of transformants and made the video.
I hereby certify that the statement of contribution is accurate.

Signed……………………………………………………..Date…………………………………

Gilliham, M.
Designed the hydroponics system, drafted the manuscript, carried out the IRGA measurements,
performed vMinTEQ design of growth solutions and adapted the system for use of the whole plant
chamber and made the video.
I hereby certify that the statement of contribution is accurate and I give permission for the inclusion
of the paper in the thesis.

Signed……………………………………………………..Date…………………………………

Conn, S.J.
Designed the hydroponics system, drafted the manuscript, and undertook growth assays, SiCSA and
qPCR.
I hereby certify that the statement of contribution is accurate and I give permission for the inclusion
of the paper in the thesis.

Signed……………………………………………………..Date…………………………………

Dayod, M.
Drafted the manuscript, performed vMinTEQ design of growth solutions and adapted the system for
use of the whole plant chamber.
I hereby certify that the statement of contribution is accurate and I give permission for the inclusion
of the paper in the thesis.

Signed………………………………………………………..*Date*…………………………………………

Shearer, M.K.

Developed the pizza tray system

I hereby certify that the statement of contribution is accurate and I give permission for the inclusion of the paper in the thesis.

Signed………………………………………………………..*Date*…………………………………………

Athman, A.

Performed vMinTEQ design of growth solutions and adapted the system for use of the whole plant chamber and made the video

I hereby certify that the statement of contribution is accurate and I give permission for the inclusion of the paper in the thesis.

Signed………………………………………………………..*Date*…………………………………………

Henderson, S

Validated the system for imaging promoter GUS fusions and gene-GFP assays.

I hereby certify that the statement of contribution is accurate and I give permission for the inclusion of the paper in the thesis.

Signed………………………………………………………..*Date*…………………………………………

Conn, V.

Designed and tested qPCR primers

I hereby certify that the statement of contribution is accurate and I give permission for the inclusion of the paper in the thesis.

Signed………………………………………………………..*Date*…………………………………………

Hocking, B.

Performed protoplast isolation and transfection and made the video

I hereby certify that the statement of contribution is accurate and I give permission for the inclusion of the paper in the thesis.

Signed………………………………………………..Date…………………………………

Fuentes, S.

Designed the MATLABW code for quantifying plant rosette cover area for IRGA measurements

I hereby certify that the statement of contribution is accurate and I give permission for the inclusion of the paper in the thesis.

Signed………………………………………………..Date…………………………………

Aukett, L.

Validated the system for imaging promoter GUS fusions and gene-GFP assays.

I hereby certify that the statement of contribution is accurate and I give permission for the inclusion of the paper in the thesis.

Signed………………………………………………..Date…………………………………

Tyerman, S.D.

Contribute to the manuscript writing.

I hereby certify that the statement of contribution is accurate and I give permission for the inclusion of the paper in the thesis.

Signed………………………………………………..Date…………………………………

PLANT METHODS

METHODOLOGY   **Open Access**

Protocol: optimising hydroponic growth systems for nutritional and physiological analysis of *Arabidopsis thaliana* and other plants

Simon J Conn[1], Bradleigh Hocking[1,2], Maclin Dayod[1,2], Bo Xu[1,2], Asmini Athman[1,2], Sam Henderson[1,2], Lucy Aukett[1], Vanessa Conn[1,2], Monique K Shearer[1,3], Sigfredo Fuentes[1], Stephen D Tyerman[1,2] and Matthew Gilliham[1,2*]

Abstract

Background: Hydroponic growth systems are a convenient platform for studying whole plant physiology. However, we found through trialling systems as they are described in the literature that our experiments were frequently confounded by factors that affected plant growth, including algal contamination and hypoxia. We also found the way in which the plants were grown made them poorly amenable to a number of common physiological assays.

Results: The drivers for the development of this hydroponic system were: 1) the exclusion of light from the growth solution; 2) to simplify the handling of individual plants, and 3) the growth of the plant to allow easy implementation of multiple assays. These aims were all met by the use of pierced lids of black microcentrifuge tubes. Seed was germinated on a lid filled with an agar-containing germination media immersed in the same solution. Following germination, the liquid growth media was exchanged with the experimental solution, and after 14-21 days seedlings were transferred to larger tanks with aerated solution where they remained until experimentation. We provide details of the protocol including composition of the basal growth solution, and separate solutions with altered calcium, magnesium, potassium or sodium supply whilst maintaining the activity of the majority of other ions. We demonstrate the adaptability of this system for: gas exchange measurement on single leaves and whole plants; qRT-PCR to probe the transcriptional response of roots or shoots to altered nutrient composition in the growth solution (we demonstrate this using high and low calcium supply); producing highly competent mesophyll protoplasts; and, accelerating the screening of Arabidopsis transformants. This system is also ideal for manipulating plants for micropipette techniques such as electrophysiology or SiCSA.

Conclusions: We present an optimised plant hydroponic culture system that can be quickly and cheaply constructed, and produces plants with similar growth kinetics to soil-grown plants, but with the advantage of being a versatile platform for a myriad of physiological and molecular biological measurements on all plant tissues at all developmental stages. We present 'tips and tricks' for the easy adoption of this hydroponic culture system.

Keywords: Hydroponics, Plant nutrition, Arabidopsis, Gas exchange, ACA2, CAX1, CAX2, VHA-α, Transient transformation

* Correspondence: matthew.gilliham@adelaide.edu.au
[1]School of Agriculture, Food & Wine and The Waite Research Institute, University of Adelaide Waite Campus, PMB1, Glen Osmond, South Australia 5064, Australia
[2]Australian Research Council Centre of Excellence in Plant Energy Biology, Glen Osmond, South Australia 5064, Australia
Full list of author information is available at the end of the article

Introduction

Arabidopsis thaliana (L.) Heynh. (Arabidopsis) has been adopted as a model plant of choice in many laboratories for a variety of reasons. These include a brief life cycle, a small and well-annotated genome, its amenability to tissue culture, the limited cell-layers per cell type (for developing roots), the availability of natural diversity sets and targeted mutants, and the ease at which it can be genetically transformed [1]. The diminutive stature and rosette growth habit of Arabidopsis also means that it does not require a large area to cultivate. At the same time, the size of Arabidopsis has presented considerable challenges for those wanting to perform physiological measurements on intact plants such as gas exchange, hydraulic conductance, or for obtaining single-cell parameters such as turgor pressure and membrane potential. To benefit from the vast molecular resources of Arabidopsis, physiologists have had to adapt measuring equipment and assays to the microscale; these technological challenges have curtailed the use of Arabidopsis as a tractable physiological model [2]. In order to perform such assays whilst providing a flexible experimental platform for manipulation of both the shoot and root environment, the use of hydroponics for research purposes has become common.

Hydroponics, as a convenient means for studying plants in the laboratory and for growing commercial crops, was a term first coined by William F. Gericke in 1929, yet it is a documented technique dating back to the late 17th century [3,4]. Its advantages include the potential for accessibility to all plant tissues and the easy manipulation of the nutrient profile of the growth medium when compared to soil, given the complex interaction of ions with soil particles. Agar or phytagel plates share these advantages but the opportunities for physiological experimentation using this system are limited as seedlings can only be grown for about 2 weeks on plates and plants transpire very little meaning that sucrose is commonly included as a carbon substrate and aseptic culture must be used. A disadvantage of both hydroponics and agar plates is that many species have a different root morphology when compared to soil, including a lack of root hairs, although this is not the case for Arabidopsis [5]. Various hydroponic systems have been developed for the growth of Arabidopsis independently in several laboratories reflecting their need and utility; Araponics©, is an example of a commercially available system [6]. Other hydroponics systems described in the literature have often been designed with a specific purpose in mind, and as a result have not been tested in terms of the ease at which various experimental parameters can be assayed (refer to Table 1 for advantages and disadvantages of each method). Whilst trialling these methods in our laboratory we identified several key limitations with these systems as they are documented in the literature, including: (1) the use of a small holding tank (up to 1 L) to hold the growth solution, reducing scalability [7,8]; (2) the need to sterilise parts of the set-up [8,9], which lengthened and complicated the procedure; (3) the use of rockwool or sponge [7,10-12], which prevented access to the full root system and predisposed the apical meristems to flooding; (4) the use of specialised materials such as a prefabricated seed holder, which increased cost [13]; and the need to transfer plantlets between multiple growth environments [14,15]. While each methodology possessed strengths and was designed to suit its endpoint analysis, we sought to streamline the entire process and provide a universal and fully adaptable system.

One common and significant problem associated with aggregate hydroponics growth systems is the algal contamination of the culture medium [16]. This can occur in the tank, and particularly on rockwool or agar-based plugs, or the plant roots and shoots, due to the use of non-sterile phosphorous-rich medium and the exposure of these components to light. This becomes a problem for physiological studies as algal growth can reduce root nutrient uptake efficiency, plant growth, perturb the composition of the growth solution (nutrients, pH) and induce significant changes to the plant global transcriptome and proteome [16-18]. For this reason alone it is important that hydroponic systems avoid illumination of the growth media if they are to be used in physiological studies.

A major driver for developing this hydroponics system was to be able to manipulate Arabidopsis plants for a variety of assays including single cell sampling and analysis (SiCSA), which requires live plants to be fixed to a flat, hard growth surface [19-22]. The following system allowed us to sample single cells easily for both molecular and ionomic interrogation (the methodology for molecular analysis is outlined in [22]); it would also be ideal for micropipette techniques such as turgor measurement and electrophysiology. After considerable iterative development we present this simple, inexpensive, flexible and robust hydroponics system for the cultivation of Arabidopsis (and other plants), which addresses the above considerations and streamlines the methodology to allow other laboratories to adopt this procedure. In addition, we document how to adapt physiological measuring equipment to this hydroponics system and present some analyses of Arabidopsis plants grown in this hydroponic set-up. These comparisons show that the hydroponic system produces plants with equivalent growth rates to soil-grown plants but provides more flexibility for applying many physiological and molecular analyses of the plant tissues.

Materials
Reagents

- Agar, plant cell culture tested (e.g. Sigma, A7921)
- Nutrient solution stocks (see Additional file 1 for detailed description of growth solutions).

Table 1 Advantages and disadvantages between geoponics, agar plates and three distinct aggregate hydroponics methods for cultivating arabidopsis plants

Parameter	Geoponics (i.e. soil/sand)	Agar plates	Aggregate hydroponics		
			Polystyrene/ Rockwool	Araponics©	This system (Conn *et al.*)
Setup costs	Low	Low	Low	High	Low
Running costs					
Media	Low	Intermediate	Low	Intermediate	Low
Equipment	Low	Intermediate	Low	Intermediate	Low
Footprint	Small	Small	Small	Small-to- Intermediate*	Small
Sterile culture	No	Yes	No	No	No
Batch variability	High	Low	Low	Low	Low
Experimental Flexibility	Low	Intermediate	High	High	High
Contamination (algal, bacterial)	Medium	High	High	Low	Low
Throughput	High	Intermediate	Intermediate	Intermediate	Intermediate
Root entanglement	Yes	Potential	Yes	Yes	No
Developmental window	Mature plants	< 3 week-old seedlings	Mature plants	Mature plants	Mature plants

* Can use either the low or high density trays.
The system presented in this manuscript is regarded as agar-based, aggregate hydroponics. Estimated setup costs for Araponics system is approximately US$4 per plant, while for the system presented in this paper is US$0.81 (based on 140 plants, pricing as per January 2013, http://www.araponics.com).

Equipment

- 1.5 mL microcentrifuge tube, black (e.g. Bioplastics, B74010), 48
- 50 mL polypropylene conical centrifuge tube with flat top screw cap (e.g. BD Biosciences, 352070), 48
- Leather punch, or 15-18G × 1 1/2" hypodermic needles (e.g. Terumo, NN-1838R), 1
- 13 L multistacking container (e.g. Nally, IH305), 1
- 24 well floater microtube rack, blue with hinged lid (Scientific Specialties, 5100-43), 2
- Or, for large scale planting (> 100 seeds) pizza crisper trays with 11 mm holes (e.g. Willow, heavy metal bakeware 34 cm family size) and pot saucer that fits the pizza tray making it light tight (e.g. Reko, 430 mm saucer, RSRSTD430.07), 1 each.
- Plastic support for tubes in hydroponics container, plastic, 1
- Aquarium air pump (e.g. Resun, AC9904), 1
- Freshwater aquarium air stones, 2
- Aquarium tubing, 1.5 m to fit aquarium pump (e.g. Aquaone, 4 mm internal diameter tube)
- Plastic Y-connectors to fit tubing, and clamps to adjust airflow
- Fluorescent lamps 36W/840 cool white (e.g. Osram, 4050300517872).

Equipment setup
Mature plant tank

- Remove the conical base from the 50 mL centrifuge tubes using a hacksaw or band saw, and smooth the cut edges with a metal file to prevent future root

damage. Drill a hole in the centre of 50 mL centrifuge tube lid (11 mm diameter) to support the lip of the plant holder. Forty-eight tubes are required per tank.
- Adhere four plastic strips (20 × 120 × 10 mm) to the inside of an opaque 13 L hydroponics growth container (320 mm × 415 mm × 110 mm) with silicon-based adhesive, 20 mm from the top to support the microcentrifuge tube lid.
- Plastic lids can be made from a rectangular plastic sheet (290 mm × 390 mm × 5 mm). Using a hole-bit drill 48 holes (6 × 8 pattern) of 32 mm diameter to fit the cut 50 mL centrifuge tubes.
- Aeration of each hydroponics tank is provided via a single tube from a 4-outlet aquarium pump (5 W, 540 L.h^{-1} maximum), with a Y-connector fitted inline to permit the use of two freshwater airstones (30 –100 mm) in each tank. These can be anchored onto the base of the tank with silicone adhesive. Use clamps to adjust airflow if necessary.
- Plants in hydroponics tanks can be illuminated as required. For this setup we use 36W/840 cool white fluorescent lamps, 8 lamps per shelf (3 tanks per shelf). Plants are typically grown 210 mm beneath lamps.

Protocol
The general workflow for the Arabidopsis hydroponics system is summarised in Figure 1, Additional File 2, with step-wise written instructions below and is further outlined in a tutorial video (http://www.youtube.com/watch?v=c9neV LaS63c). The total cost to completely establish this system, at current prices, is up to five times less than commercially
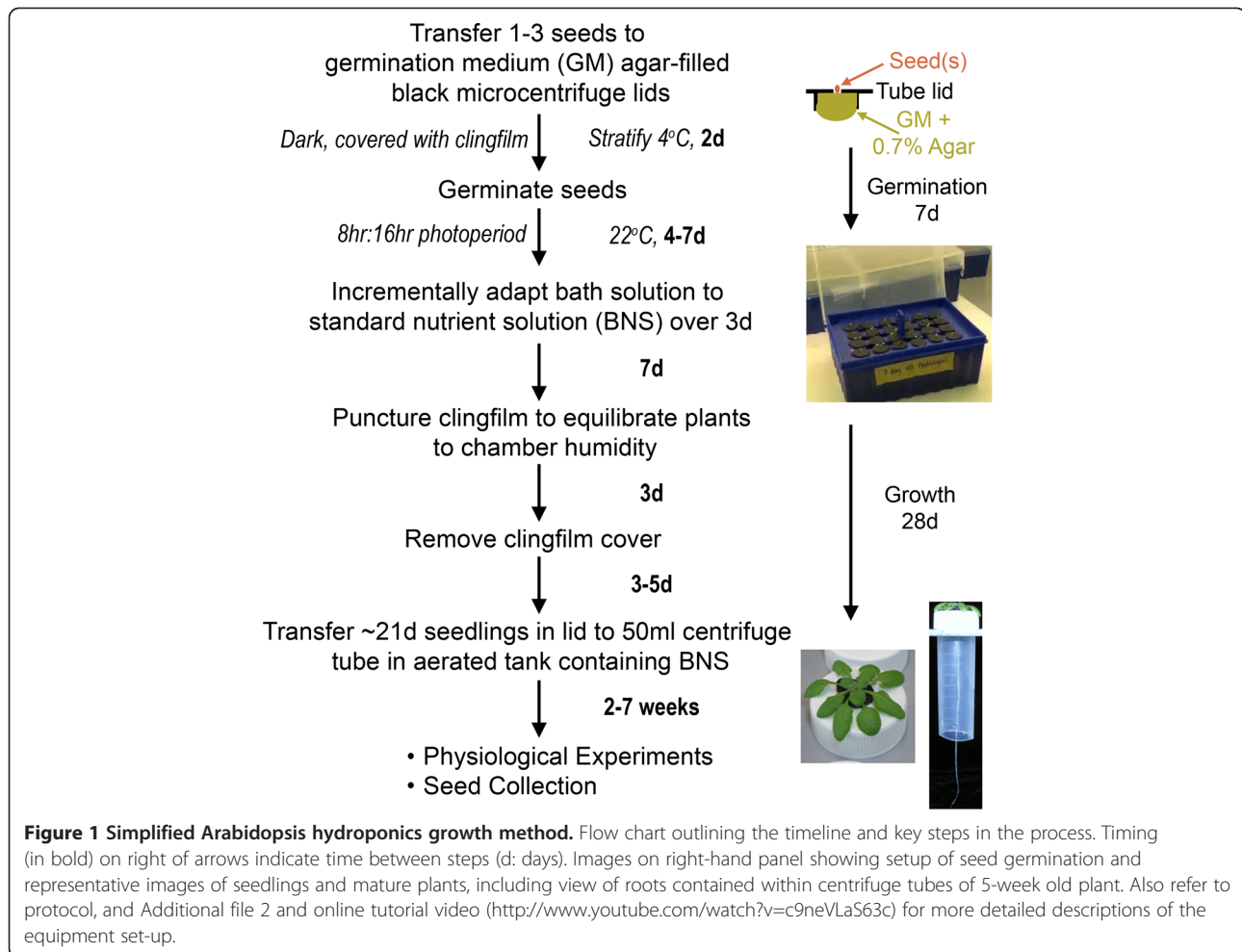
Figure 1 Simplified Arabidopsis hydroponics growth method. Flow chart outlining the timeline and key steps in the process. Timing (in bold) on right of arrows indicate time between steps (d: days). Images on right-hand panel showing setup of seed germination and representative images of seedlings and mature plants, including view of roots contained within centrifuge tubes of 5-week old plant. Also refer to protocol, and Additional file 2 and online tutorial video (http://www.youtube.com/watch?v=c9neVLaS63c) for more detailed descriptions of the equipment set-up.

sourced systems. The ability to reuse the majority of the components further reduces the expense of the system.

Preparing germination lids

1. Prepare 100 mL of germination medium (GM) (recipe Additional file 1) in a autoclavable bottle and add 0.7 g agar (final conc. 0.7% w/v), autoclave and cool slightly. The solution can also be microwaved to dissolve the agar as aseptic culture is not required.
2. Using a leather punch or hypodermic needle, bore a single 1.2 – 1.8mm diameter hole into the centre of a black microcentrifuge tube lid.

NOTE: This design is essential to limit light penetration into the culture medium and in so doing abolishes algal growth and minimises evaporation/water loss from the hydroponic tanks.

3. Cut lids from the microcentrifuge tube base, retaining 1 – 2mm of the hinge, invert lid onto clingfilm or adhesive tape. Once all lids have been

prepared, fill each with ~250-300 μL germination medium agar and leave to solidify for 15 min.

CRITICAL POINT: The hinge of the microcentrifuge lid can be used for easy manipulation of plants with tweezers.

CRITICAL POINT: Ensure the lids are filled such that there is a dome of GM-agar for each lid, but avoid over-flowing as this may cause the lids to sit askew in the germination tank. If the solution escapes through the lid hole, either allow media to cool (55-60°C is ideal) or supplement with additional media.

NOTE: Once finished, the residual GM-agar can be stored at 4°C for 1 month and reused by melting in the microwave as required.

4. Invert lids into floating racks with the agar plug in contact with liquid GM to create the functional seed/seedling/plant holder.

NOTE: Prefabricated 34 cm diameter pizza crisper trays, containing over three hundred holes of 11 mm in diameter, can be used to hold larger batches of plants.

We found it essential that each of the microcentrifuge tube lids sat snugly enough in the holding tray to prevent light penetration into the GM, but loosely enough so they could be easily removed and transferred to another container when required.

Germinating seedlings

5. Using a moistened toothpick, place up to three seeds in the hole of the lid on the agar surface to maximise chances of seed germination. Then, cover the entire container with plastic clingfilm to enhance humidity, leaving at least 10 mm above the plant for growth. Stratify seeds in the dark at 4°C for at least 48 h.
6. Transfer the germination tank into growth cabinets under a 8:16 h, light:dark cycle, with 55% atmospheric humidity, at 22°C and an irradiance of 150 μmol photons $m^{-2}.s^{-1}$ at the plant level. Under these conditions, the roots of these seedlings emerge from the agar plug after 4-7 days.
7. At this stage thin down to a single plant per lid and replace the bath solution incrementally from GM to a standard growth solution (in our case, a modified ¼ Hoagland's solution, hereafter referred to as BNS, refer to Additional file 1 for recipe). On day 1 of the solution change, $^1/_3$ of the GM was replaced with BNS. On day 2, 50% of the existing solution was exchanged with BNS and on day three the entire solution was replaced with BNS.
8. After day 14, puncture holes in the clingfilm to decrease humidity and then remove completely after day 17.

CRITICAL POINT: Do not allow agar plugs to dry out at this stage, this is rarely a problem if using floating racks but it is extremely important to keep the solution level topped up if using pizza or equivalent trays to germinate the seedlings.

Maturing plants

9. When the roots are 40–50 mm in length, approximately 21 days post-germination, plants are the appropriate size to survive transfer into an aerated hydroponics tank. Transfer plants in lids to the modified 50 mL centrifuge tubes, passing the roots through the 11 mm diameter hole drilled in its lid to support the lip of the seedling holder. Then insert this unit into the lid of the tank containing 10 L of growth solution and continue until all 48 positions are filled.

CRITICAL POINT: These holders permit access for the roots to the whole growth media but prevent root entanglement for up to ~7 weeks when grown under short (8 h:16h) photoperiod (Figure 1).

NOTE: If not all 48 plant tubes are filled with plants, unused holes must be covered to exclude light from the growth solution. Use 50 mL centrifuge tube lids without holes or place an intact lid or base of a black microcentrifuge tube within the 11 mm hole if present, or use large pieces of aluminium foil wrapped in plastic clingfilm to cover multiple holes simultaneously.

NOTE: Plants can remain in these 13 L tanks, each holding 48 plants, with weekly solution changes until analysis. After ~3 days in these larger tanks the agar plug dries to form a thin film that separates itself from the root system. This occurs because the agar plug no longer is in contact with the growth solution when the plant holder is placed in the hydroponic tank. As such, this permits full access to the whole of the shoot and/or root system. The plant holder provides a useful handling tool for transferring the seedling to experimental chambers or different solutions, whilst limiting mechanical stress, but could be removed from the plant by cutting the plastic lid in half. This is particularly useful for imaging whole plants for reporter localisation studies.

Sample results
Plant growth and seed collection

Plant growth and development are dynamic processes that can be perturbed by a number of biotic and abiotic factors, including nutrient availability, oxygenation of growth solutions, prevalence of microorganisms, humidity and air temperature [23]. A number of measurements were made to ascertain the physiological state of plants grown in our hydroponics system. Under both soil and hydroponic conditions using the BNS growth solution, plants had vibrant green colouration (total chlorophyll content of 5-week old hydroponics plant leaves was 12.5 ± 0.4 μg.mg-DW^{-1} (mean ± SD) while soil-grown leaves had 12.6 ± 0.6 μg.mg-DW^{-1} (n = 12), both with approximately 2.5:1 of Chl*a*:Chl*b*), and possessed the same growth rates throughout the vegetative growth cycle (3-7 weeks) (Figure 2A). The germination rate of plants grown hydroponically was 5–18% higher than on soil (supplemented with seed raising mix for 20 lines tested), with the greatest increase seen for the *cax1-1/cax3-1* T-DNA insertion line [24]. Once siliques were filled, plants were wrapped in clear, perforated plastic bags and transferred into tanks containing ~2 L water to avoid salt formation on roots, to avoid mould growth and to hasten drying. Siliques dried upon evaporation of the water, with the isolated seeds possessing from 90–100% germination efficiency and unaffected leaf ionomics profile compared to the previous generations (data not shown).

Transient protoplast transformation

A number of studies on promoter responsiveness, cellular localisation and protein-protein interactions can be

Figure 2 Comparisons of Arabidopsis shoot growth kinetics and protoplast transformation efficiency between soil and hydroponics system. A) Shoot biomass during vegetative growth phase of Arabidopsis Col-0 is equivalent between soil-grown and hydroponically-grown plants under short-day photoperiod (8 h:16 h) until seven weeks post-germination. Mean ± SD (n = 6 plants per timepoint, per condition). No significant differences were found between growth conditions at each timepoint using a *t*-test (P < 0.01). **B**) Transfection efficiency of Arabidopsis mesophyll protoplasts were determined by fluorescence microscopy comparing two quantities (5 μg and 10 μg) of two sGFP-expressing plasmids under a single CaMV 35S promoter, pHBT-sGFP(S65T)-NOS (GenBank accession number: EF090408) [25] and pGWB406 (GenBank accession number: AB294430) [37] of 4.2 kb and 12.4 kb, respectively as per Conn *et al.* [20]. For each condition n = 5 independent transformations, each with cell counts > 100 protoplasts. Data presented as the proportion of GFP-expressing cells; Mean + SEM. Asterisks indicate significant difference between soil and hydroponics derived protoplasts within each condition (P < 0.01).

expression of a cytosolic *sGFP* encoded on both a small vector (4 kb) and a large vector (12 kb), and quantifying the proportion of GFP-positive cells. The transfection efficiency of protoplasts derived from hydroponically-grown leaves was consistently higher than that of those derived from soil-grown plants, at least 2-fold higher for the 12 kb vector and 8–26% higher for the smaller vector, depending on DNA input (Figure 2B). Furthermore, as expected, we observed that the transformation efficiency of the larger vector was lower regardless of growth regime. However, for the hydroponically grown plants at least, the rate was sufficiently high at 14–20% to be used as a screening tool for specific applications like subcellular localisation of large membrane transporters. No difference was observed in the average size of protoplasts between methods, or the intracellular localisation of sGFP, yet the total yield of mesophyll protoplasts was consistently 15% above those from soil-grown plants, in part due to more uniform growth enabling the harvest of healthy leaves at consistent stages of development. Combining this higher yield and higher transformation rate, this constitutes an optimised approach for the study of many processes in protoplasts.

Plant nutrition and transcriptional response

We tested a number of plant growth solutions and found that a modified ¼ Hoagland's solution (BNS) was a simple, defined and affordable media, which supported good plant growth and similar nutrition to plants grown in soil obtained from the largest public dataset for Arabidopsis ionomics, the PiiMS database (http://www.ionomicshub. org) (Table 2). Note that the PiiMS soil-grown plants were fed ½-strength Murashige and Skoog (MS) medium. As a result of previously observing growth retardation and stress phenotypes associated with full strength growth solution (i.e. Gamborg's, Hoagland's or MS) we used the more dilute BNS media, as it was sufficient to provide adequate and reproducible growth. The flexibility afforded by creating the growth solution from individual components allowed manipulation of certain nutrients either separately or in combination in order to investigate nutrition-associated genotypes or phenotypes of different Arabidopsis ecotypes or mutant lines [19-21]. The basic recipe plus those with altered (increased or decreased) concentrations of potassium (K), sodium (Na), calcium (Ca) [19,21] and magnesium (Mg) [20] can be found in Additional file 1. In each of these solutions the concentrations of multiple components were altered to keep the activity of most ions the same despite a significant change in the one or two of the ion species. This was performed using the ion activity calculator program vMinteq (KTH) to investigate, as far as possible, ion-specific treatments [19-21].

The ability to isolate the entire root and shoot tissues of plants also enabled quantification of the transcriptional response to altered elemental concentrations in the growth

undertaken in Arabidopsis protoplasts, rather than using the whole plants. Yoo *et al.* [25] presented a technique for transient expression of genes in protoplasts isolated from Arabidopsis mesophyll cells. We trialled a modified version of this protocol on protoplasts isolated from plants grown in soil or our hydroponics system, to detect

Table 2 Comparative ionomics of soil-grown and hydroponically-grown plants

Element	Soil-grown	Hydroponics	Ratio
Na[23]	1,608 ± 219	1,808 ± 120	1.12
Mg[25]	9,402 ± 845	9,876 ± 492	1.05
P[31]	8,449 ± 602	8,225 ± 204	0.97
K[39]	34,214 ± 1874	37,747 ± 1542	1.11
Ca[43]	44,314 ± 3005	38,821 ± 1603	0.86
Micronutrients			
Cr[52]	0	< 4	n.d.
Mn[55]	64 ± 35	116 ± 42	1.82
Fe[56]	85 ± 36	64 ± 20	0.75
Co[59]	3 ± 0.6	< 6	n.d.
Ni[60]	1 ± 0.2	< 7	n.d.
Cu[65]	1 ± 0.5	1.3 ± 0.4	1.10
Zn[66]	65 ± 28	360 ± 108	5.56
Se[77]	2 ± 0.4	< 60	n.d.
Cd[111]	3 ± 1.1	< 2	n.d.

Data presented as dry weight normalised shoot ionomics data obtained by inductively coupled plasma optical emission spectroscopy (ICP-OES) as per [19,20] on 5 week old Col-0 shoots grown in soil (the PiiMS database: soil-grown plants fed ½-strength MS media; n=125 plants) and our hydroponics system (n=12 plants). Ratio compares ionome of hydroponics plants to soil-grown plants showing lines are similar in nutrient content for most elements, excluding Zinc, in the shoot. Detection limit shown for Cr, Co, Ni, Se and Cd, n. d.: not determined as one or both readings were given as a detection limit (note in all these cases the ranges overlap).

media. We adjusted the calcium ion activity (a_{Ca2+}) to 3 levels; 1 mM (BNS), 0.025 mM (Low Calcium Solution, LCS) and 5 mM (High Calcium Solution, HCS) (Additional file 1), whilst keeping the activity of all other ions (except Cl$^-$) similar. We quantified the transcriptional response of

roots and shoots to these solution changes within the epidermal enhancer trap line, KC464 (Columbia-0 background) of: known tonoplast Ca^{2+}/H^+ exchangers (*AtCAX1*, *AtCAX2*) and endoplasmic reticulum-localised autoinhibited Ca^{2+}-ATPase (*AtACA2*) calcium transporter; and vacuolar H^+-ATP synthase subunits (*AtVHA-a2*, *AtVHA-a3*) (Figure 2).

We found that the expression levels of genes matched previous reports, including the higher shoot expression of *AtCAX1* and the higher root expression of both *AtCAX2* and *AtACA2* (Figure 3, Additional file 3) [26,27]. We also confirm the calcium concentration-dependent response of *AtCAX1* seen in previous reports [19,20,28]. Whilst the transcript abundance of *AtACA2* has previously been shown to be unchanged with increased Ca [26,27], we detected that its expression was increased in both shoot and root tissues in LCS. *AtACA2* and *AtCAX2* also showed the opposite transcriptional regulation to *AtCAX1* by LCS (Figure 3A,B). It is conceivable that this may be the result of a greater affinity but lower capacity for Ca ion (Ca^{2+}) transport by *AtACA2* than *AtCAX1* [29,30], so altering the capacity of the vacuole for Ca storage and increasing the role of the ER in this process over the vacuole when Ca is limiting. Likewise, the lower affinity Ca^{2+}-transport capacity of AtCAX2 compared to AtCAX1 [29,30] may also contribute to the lower Ca storage of the vacuole under these conditions [19-21]. The fact that both genes are preferentially expressed in the mesophyll, adds further evidence to suggest that *AtACA2* and *AtCAX2* may play a minor role in leaf Ca compartmentation, as this is where the majority of Ca is stored [19-21,29]. In addition both genes are

Figure 3 Calcium-dependent transcriptional responses of Arabidopsis leaves and roots of hydroponically-grown plants. qPCR performed on RNA isolated from the (**A**) shoots and (**B**) roots (above and below the hypocotyls, respectively) of 5-week old Arabidopsis KC464 plants grown under three different Ca activities (a_{Ca} LCS = 0.025mM; a_{Ca} BNS = 1 mM; a_{Ca} HCS = 5 mM) for seven days. n = 9, from three biological replicates per tissue. Mean + SD. Asterisk indicates significant expression difference from BNS (P < 0.01). qPCR performed as described in Conn *et al.* [19,20] with primers listed in Additional file 3.

transcriptionally upregulated in the double knockout of two vacuolar CAX genes (*cax1/cax3*), therefore *AtACA2* and *AtCAX2* have both been predicted to partially compensate for the loss of the major mechanism to secrete leaf apoplastic Ca [19,21]. The vacuolar ATPase subunits, *AtVHA-a2* and *AtVHA-a3*, were found to show a similar Ca-dependent transcriptional response as *AtCAX1*, which is consistent with the T-DNA insertional mutant of these genes showing similar dwarf growth and lower leaf Ca accumulation phenotypes to the *cax1/cax3* line [19,31]. As such, these results validated the use of these solutions in this hydroponics system.

Figure 4 Gas exchange measurements for Arabidopsis Col-0 measured using the LiCOR extended reach chamber or whole plant chamber whilst growing in hydroponics. A Transpiration or **B** Net CO_2 assimilation/photosynthesis measured using 6-week old plants growing the basal nutrient solution. Individual plants were exposed to light intensity of ~350 µmol m^{-2} s^{-1} at least 30 min prior to the start of measurement. The rosette was allowed to acclimatise inside the Arabidopsis whole rosette or extended reach chamber for at least 10 min before gas exchange data were recorded with reference CO_2 concentration set at 500 µmol mol^{-1}, flow rate at 500 µmol s^{-1} (for the whole plant chamber) or 100 µmol s^{-1} (for the extended reach chamber) light intensity at 350 µmol photons m^{-2} s^{-1} and relative humidity at 56%. Data shown as Mean + SEM of fifteen biological replicates. No significant differences were found between each dataset using a *t*-test (P < 0.01).

Gas exchange measurement of hydroponically grown plants

Measurement of gas exchange for Arabidopsis can be problematic due to the plants' small stature and rosette growth. However, Arabidopsis can be induced to produce a relatively large amount of shoot vegetative biomass in low light conditions (~100 µmol photons.m^{-2}s^{-1}), and when the photoperiod is short (~8-10 h). Leaves of hydroponically grown Arabidopsis plants are relatively clean, compared to soil grown leaves, hence there is no need to wipe the leaves prior to measurement of gas exchange. This avoids any potential mechanical damage to the leaves or the trichomes, which would affect airflow and the extent of the boundary layer across the leaf, which can influence the results of gas exchange measurements. We used a LiCOR 4600-XT InfraRed Gas Analyser (IRGA), with the whole Arabidopsis chamber or extended reach chamber, to take gas exchange measurements as described in the Figure 4 legend and Additional file 2.

To be able to perform these measurements we found it necessary to make all components of the Arabidopsis whole plant chamber airtight – without this, moisture from the hydroponics media compromised the gas exchange measurements. As detailed in Additional file 2, we sealed the plant holding lid into the centrifuge tube lid using teflon air-tight sealing tape. The plant, now held within a centrifuge tube lid, was transferred into an intact centrifuge tube base containing the treatment solution of interest. The centrifuge tube was then sealed into the LiCOR 'cone-tainer' using a 30 mm OD rubber O-ring. This system would allow exclusive measurement of rosette gas exchange for at least 3 h for 6-week old Arabidopsis plants without any detectable reduction in photosynthetic rate during the middle of the photoperiod (Figure 4). Gas exchange measurements were adjusted on the basis of the leaf area contained within: i) the extended reach chamber (LiCOR) estimated by taking a scaled photograph and analysis of the percentage of the leaf within the chamber window using ImageJ (National Institute of Health, NIH) as detailed in [19] or, ii) the whole Arabidopsis plant chamber (LiCOR) by estimating the rosette size using a customised code developed in MATLAB® 2010b (Mathworks Inc., Natick, MA, USA) and the Image Analysis Toolbox® to process scaled photographs semi-automatically. Two codes were used, a semi-automated and an automated code. The latter recognises by colour contrast the Arabidopsis rosette to obtain automatically the cover area. The semi-automated code was used in pictures where this contrast was not detected by the automation algorithm. In this case, a tool was developed to select a region of interest (ROI) corresponding to the rosette manually to extract the cover area. See Additional files 4, 5, 6 for further details of the code and method.

The leaf gas exchange measurements were not significantly different for the hydroponics system using either

the LiCOR whole Arabidopsis plant chamber or the extended leaf chamber (Figure 4). However, it was evident that the whole plant chamber took more consistent readings presumably due to the ability to sum the reading over a larger area and avoiding the need to seal the chamber directly onto the leaf tissue, which can confound results through improper sealing and/or leaf damage. We found that consistent results could be achieved with the extended leaf chamber when leaves were large enough, but the dimensions of the leaf and petiole made the clamping of a large amount of leaf area in the chamber a challenge unless the plant was older than 6 weeks. In contrast plants could be assayed in the whole Arabidopsis chamber from weeks 3-8. It is clear that this system offers potential to be widely used to study leaf gas exchange in a highly controlled manner throughout the majority of Arabidopsis development.

Comments
In our hands
Given the importance of aeration of hydroponics systems for adequate growth [10], several aeration systems were trialled. The media within the tank was aerated either using a standard 4-outlet aquarium pump that constantly bubbled air through airstones or by using an ebb-and-flow system that pumped media between the tank containing the plants and a solution holding reservoir every 60 min. Both systems produced plants that at least qualitatively resembled each other, however, the former technique was markedly simpler to construct and maintain so it was used for all further studies. Oxygenation levels in the constantly aerated plants were sufficient to avoid increased expression of known hypoxia induced genes, *AtWRKY40* and *AtNIP2;1* [32,33], in contrast, transcription of both genes were induced when the media was non-aerated for 7 days (Additional file 7).

Profiling of transgenic plants
The desire to accelerate the analysis of transgenic Arabidopsis plants has led to the design of a number of rapid approaches for selection of transformants. The method commonly used to select transformed Arabidopsis seedlings is by spreading the seeds on suitable growth media such as soil or agar. Soil is commonly used if the selection marker gene is phosphothrinocin, whereas agar is used if the marker gene is kanamycin or hygromycin. Thereafter, the putative transformants are usually transferred into soil for seed collection. The main problem with this method is the potential damage to the fragile root systems of the selected seedlings, which consequently affects their survival rate. We demonstrate that our hydroponic system can be used as an alternative to soil growth for cultivation of transformants selected on agar plates (using phosphothrinocin, kanamycin or

hygromycin) as per Harrison *et al.* [34]. Over 95% of transformants survived transfer using this method, with the collected seed displaying a high germination rate (Additional file 8). However, the real advantage lies in the ability to reliably analyse mature first generation transformants, particularly for root cellular localisation studies and root phenotypes that are impossible with soil- and agar plate- based selection methods.

Adapting the system for other plants
The improved hydroponic system we highlight here can be easily adapted for use with other plants with changes to the diameter of the hole produced in the lid of the microcentrifuge tube. We made holes of up to 6 mm in diameter (suitable for up to 4-week old cucumber and 6 week old tobacco [35]), and also grew *Lotus* spp. seedlings (data not shown). Furthermore, we also adapted the system for use with cereals using the 1.5 mL black microcentrifuge tubes with the bottom 7 mm cut off, this was sufficient to hold the seed, roots and shoots in place and removed the need for agar [36].

Conclusions
We demonstrate the quality and versatility of our hydroponics system by profiling and comparing with soil-grown plants and previous hydroponics reports many parameters throughout the growth of Arabidopsis, including biomass, ionomics and transcriptomics. We present this hydroponics growth system as an adaptable system for characterising the entire Arabidopsis plant and other plants by a variety of physiological and molecular biological methods, superior to and more inexpensive than many techniques currently in use.

Additional files

> **Additional file 1: Growth solutions used in this manuscript.**
>
> **Additional file 2: Detailed flowchart of plant preparation for gas exchange measurements.**
>
> **Additional file 3: qPCR primers used in this manuscript.**
>
> **Additional file 4: Details on the code developed for MATLAB® for estimating Arabidopsis rosette size.**
>
> **Additional file 5: Code developed in MATLAB used to estimate Arabidopsis rosette size.**
>
> **Additional file 6: Excel file with extra columns needed to alter LiCOR gas exchange measurements for different size rosettes.**
>
> **Additional file 7: Aerated hydroponics produce plants with no apparent oxygen transcriptional stress response.**
>
> **Additional file 8: Flow-chart and images of post-selection growth of Arabidopsis transformants.**

Abbreviations
SiCSA: Single cell sampling and analysis; qPCR: Quantitative real-time RT-PCR; GFP: Green fluorescent protein; GSP: Gene-specific primer; UAS: Upstream activation sequence; Ca: Calcium; K: Potassium; Mg: Magnesium; Na: Sodium; a_{Ca}: Calcium activity; GM: Germination medium; BNS: Basal nutrient solution;

LCS: Low calcium solution; HCS: High calcium solution; CAX: Calcium proton exchanger.

Authors' contributions
SC and MG designed the hydroponics system. SC, MD and MG drafted the manuscript. SC undertook growth assays, SiCSA and qPCR. MG carried out the IRGA measurements. BH performed protoplast isolation and transfection. BX developed the rapid screen for selection of transformants. MS developed the pizza tray system. MG performed vMinTEQ design of growth solutions and adapted the system for use of the whole plant chamber with MD and AA. SF designed the MATLAB® code for quantifying plant rosette cover area for IRGA measurements. VC designed and tested qPCR primers. SH and LA validated the system for imaging promoter GUS fusions and gene-GFP assays. BH, AA, BX and MG made the video. All authors read and approved the final manuscript.

Author details
[1]School of Agriculture, Food & Wine and The Waite Research Institute, University of Adelaide Waite Campus, PMB1, Glen Osmond, South Australia 5064, Australia. [2]Australian Research Council Centre of Excellence in Plant Energy Biology, Glen Osmond, South Australia 5064, Australia. [3]Australian Centre for Plant Functional Genomics, Glen Osmond, South Australia 5064, Australia.

References
1. Initiative TAG: **Analysis of the genome sequence of the flowering plant** *Arabidopsis thaliana*. *Nature* 2000, **408**:796–815.
2. Rhee SY: **Bioinformatic resources, challenges, and opportunities using Arabidopsis as a model organism in a post-genomic era.** *Plant Physiol* 2000, **124**:1460–1464.
3. Hershey DR: **Solution culture hydroponics: history & inexpensive equipment.** *Am. Biol. Teacher* 1994, **56**:111–118.
4. Jones JB Jr: **Hydroponics: Its history and use in plant nutrition studies.** *J. Plant Nutr.* 1982, **5**:1003–1030.
5. Ahn SJ, Shin R, Schachtman DP: **Expression of *KT/KUP* genes in Arabidopsis and the role of root hairs in K$^+$ uptake.** *Plant Physiol* 2004, **134**:1135–1145.
6. *Araponics: hydroponic growing system for Arabidopsis thaliana.* 2010. http://www.araponics.com/.
7. Robison MM, Smid MPL, Wolyn DJ: **High-quality and homogeneous** *Arabidopsis thaliana* **plants from a simple and inexpensive method of hydroponic cultivation.** *Can J Bot* 2006, **84**:1009–1012.
8. Arteca RN, Arteca JM: **A novel method for growing** *Arabidopsis thaliana* **plants hydroponically.** *Physiol Plant* 2000, **108**:188–193.
9. Schlesier B, Bréton F, Mock H-P: **A hydroponic culture system for growing** *Arabidopsis thaliana* **plantlets under sterile conditions.** *Plant Mol Biol Rep* 2003, **21**:449–456.
10. Smeets K, Ruytinx J, Van Belleghem F, Semane B, Lin D, Vangronsveld J, Cuypers A: **Critical evaluation and statistical validation of a hydroponic culture system for** *Arabidopsis thaliana*. *Plant Physiol Biochem* 2008, **46**:212–218.
11. Huttner D, Bar-Zvi D: **An improved, simple, hydroponic method for growing** *Arabidopsis thaliana*. *Plant Mol Biol Rep* 2003, **21**:59–63.
12. Gibeaut DM, Hulett J, Cramer GR, Seemann JR: **Maximal biomass of** *Arabidopsis thaliana* **using a simple, low-maintenance hydroponic method and favorable environmental conditions.** *Plant Physiol* 1997, **115**:317–319.
13. Tocquin P, Corbesier L, Havelange A, Pieltain A, Kurtem E, Bernier G, Périlleux C: **A novel high efficiency, low maintenance, hydroponic system for synchronous growth and flowering of** *Arabidopsis thaliana*. *BMC Plant Biol* 2003, **3**:2.
14. Berezin I, Elazar M, Gaash R, Avramov-Mor M, Shaul O: **The use of hydroponic growth systems to study the root and shoot ionome of** *Arabidopsis thaliana*. In *Hydroponics - A Standard Methodology for Plant Biological Researches*. Edited by Asao T. InTech; 2012.
15. Hermans C, Verbruggen N: **Physiological characterization of Mg deficiency in** *Arabidopsis thaliana*. *J Exp Bot* 2005, **56**:2153–2161.
16. Coosemans J: **Control of algae in hydroponic systems.** *ISHS Acta Hort* 1995, **382**:263–268.
17. Boller T, Felix G: **A renaissance of elicitors: perception of microbe-associated molecular patterns and danger signals by pattern-recognition receptors.** *Annu Rev Plant Biol* 2009, **60**:379–406.
18. Huang C, Verrillo F, Renzone G, Arena S, Rocco M, Scaloni A, Marra M: **Response to biotic and oxidative stress in** *Arabidopsis thaliana:* **analysis of variably phosphorylated proteins.** *J Proteomics* 2011, **74**:1934–1949.
19. Conn SJ, Gilliham M, Athman A, Schreiber AW, Baumann U, Moller I, Cheng N-H, Stancombe MA, Hirschi KD, Webb AAR, Burton R, Kaiser BN, Tyerman SD, Leigh RA: **Cell-specific vacuolar calcium storage mediated by** *CAX1* **regulates apoplastic calcium concentration, gas exchange, and plant productivity in Arabidopsis.** *Plant Cell* 2011, **23**:240–257.
20. Conn SJ, Conn V, Tyerman SD, Kaiser BN, Leigh RA, Gilliham M: **Magnesium transporters, MGT2/MRS2-1 and MGT3/MRS2-5, are important for magnesium partitioning within** *Arabidopsis thaliana* **mesophyll vacuoles.** *New Phytol* 2011, **190**:583–594.
21. Gilliham M, Athman A, Tyerman SD, Conn SJ: **Cell-specific compartmentation of mineral nutrients is an essential mechanism for optimal plant productivity–another role for TPC1?** *Plant Signal Behav* 2011, **6**:1656–1661.
22. Roy SJ, Conn SJ, Mayo GM, Athman A, Gilliham M: **Transcriptomics on small samples.** In *Methods in Molecular Biology: Plant Salt Tolerance*. Edited by Shabala S, Cuin TA. New Jersey, USA: Humana Press; 2012.
23. Mündermann L, Erasmus Y, Lane B, Coen E, Prusinkiewicz P: **Quantitative modeling of Arabidopsis development.** *Plant Physiol* 2005, **139**:960–968.
24. Cheng N-H, Pittman JK, Shigaki T, Lachmansingh J, LeClere S, Lahner B, Salt DE, Hirschi KD: **Functional association of Arabidopsis CAX1 and CAX3 is required for normal growth and ion homeostasis.** *Plant Physiol* 2005, **138**:2048–2060.
25. Yoo S-D, Cho Y-H, Sheen J: **Arabidopsis mesophyll protoplasts: a versatile cell system for transient gene expression analysis.** *Nat Protocols* 2007, **2**:1565–1572.
26. Hirschi KD: **Expression of Arabidopsis *CAX1* in tobacco: altered calcium homeostasis and increased stress sensitivity.** *Plant Cell* 1999, **11**:2113–2122.
27. Edmond C, Shigaki T, Ewert S, Nelson MD, Connorton JM, Chalova V, Noordally Z, Pittman JK: **Comparative analysis of CAX2-like cation transporters indicates functional and regulatory diversity.** *Biochem J* 2009, **418**:145–154.
28. Maathuis FJM, Filatov V, Herzyk P, Krijger G, Axelsen K, Chen S, Green BJ, Li Y, Madagan KL, Sánchez-Fernández R, Forde BG, Palmgren MG, Rea PA, Williams LE, Sanders D, Amtmann A: **Transcriptome analysis of root transporters reveals participation of multiple gene families in the response to cation stress.** *Plant J* 2003, **35**:675–692.
29. Conn S, Gilliham M: **Comparative physiology of elemental distributions in plants.** *Ann Bot* 2010, **105**:1081–1102.
30. Korenkov V, Hirschi K, Crutchfield JD, Wagner GJ: **Enhancing tonoplast Cd/H antiport activity increases Cd, Zn, and Mn tolerance, and impacts root/shoot Cd partitioning in** *Nicotiana tabacum* L. *Planta* 2007, **226**:1379–1387.
31. Krebs M, Beyhl D, Görlich E, Al-Rasheid KA, Marten I, Stierhof YD, Hedrich R, Schumacher K: **Arabidopsis V-ATPase activity at the tonoplast is required for efficient nutrient storage but not for sodium accumulation.** *Proc Natl Acad Sci USA* 2010, **107**:3251–3256.
32. Liu F, Vantoai T, Moy LP, Bock G, Linford LD, Quackenbush J: **Global transcription profiling reveals comprehensive insights into hypoxic response in Arabidopsis.** *Plant Physiol* 2005, **137**:1115–1129.
33. Vlad F, Spano T, Vlad D, Daher FB, Ouelhadj A, Fragkostefanakis S, Kalaitzis P: **Involvement of Arabidopsis prolyl 4 hydroxylases in hypoxia, anoxia and mechanical wounding.** *Plant Signal Behav* 2007, **2**:368–369.

34. Harrison SJ, Mott EK, Parsley K, Aspinall S, Gray JC, Cottage A: **A rapid and robust method of identifying transformed** *Arabidopsis thaliana* **seedlings following floral dip transformation.** *Plant Methods* 2006, **2**:19.

35. Casal JJ, Ballare CL, Tourn M, Sanchez RA: **Anatomy, growth and survival of a long-hypocotyl mutant of** *Cucumus sativus* **deficient in phytochrome B.** *Ann Bot* 2012, **73**:569–575.

36. Munns R, James RA, Xu B, Athman A, Conn SJ, Jordans C, Byrt CS, Hare RA, Tyerman SD, Tester M, Plett D, Gilliham M: **Wheat grain yield on saline soils is improved by an ancestral Na$^+$ transporter gene.** *Nat Biotech* 2012, **30**:360–364.

37. Nakagawa T, Suzuki T, Murata S, Nakamura S, Hino T, Maeo K, Tabata R, Kawai T, Tanaka K, Niwa Y, Watanabe Y, Nakamura K, Kimura T, Ishiguro S: **Improved Gateway binary vectors: high-performance vectors for creation of fusion constructs in transgenic analysis of plants.** *Biosci Biotechnol Biochem* 2007, **71**:2095–2100.

Appendix 3. Manuscript of *TmHKT1;5-A*

Wheat grain yield on saline soils is improved by an ancestral Na^{+} transporter gene

Rana Munns[1,2,8], Richard A James[1,8], Bo Xu[3-5,8], Asmini Athman[3,5], Simon J Conn[3], Charlotte Jordans[3], Caitlin S Byrt[1,3,4,6], Ray A Hare[7], Stephen D Tyerman[3,5], Mark Tester[3,4], Darren Plett[3,4], Matthew Gilliham[3,5]

[1] CSIRO Plant Industry, Canberra, Australian Capital Territory, Australia.

[2] School of Plant Biology, University of Western Australia, Crawley, Western Australia, Australia.

[3] School of Agriculture, Food and Wine and Waite Research Institute, University of Adelaide, Glen Osmond, South Australia, Australia.

[4] Australian Centre for Plant Functional Genomics, Waite Research Institute, University of Adelaide, Glen Osmond, South Australia, Australia.

[5] Australian Research Council Centre of Excellence in Plant Energy Biology, Waite Research Institute, University of Adelaide, Glen Osmond, South Australia, Australia.

[6] Australian Research Council Centre of Excellence in Plant Cell Walls, Waite Research Institute, University of Adelaide, Glen Osmond, South Australia, Australia.

[7] NSW Department of Primary Industries, Tamworth, New South Wales, Australia.

[8] These authors have contributed equally to this work.

Wheat grain yield on saline soils is improved by an ancestral Na$^+$ transporter gene

Nature Biotechnology. 2012. 30(4): 360-364.

Xu, B. (Candidature)

Performed all *Xenopus*, yeast and protoplast experiments.

I hereby certify that the statement of contribution is accurate.

Signed………………………………………………..Date…………………………………

Munns, R.

Conceived the project and planned experiments, supervised the research and wrote the manuscript.

I hereby certify that the statement of contribution is accurate and I give permission for the inclusion of the paper in the thesis.

Signed………………………………………………..Date…………………………………

James, R.A.

Conceived the project and planned experiments, performed field research and wrote the manuscript.

I hereby certify that the statement of contribution is accurate and I give permission for the inclusion of the paper in the thesis.

Signed………………………………………………..Date…………………………………

Tester, M.

Conceived the project and planned experiments.

I hereby certify that the statement of contribution is accurate and I give permission for the inclusion of the paper in the thesis.

Signed………………………………………………..Date…………………………………

Plett, D.

Conceived the project and planned experiments and wrote the manuscript.

I hereby certify that the statement of contribution is accurate and I give permission for the inclusion of the paper in the thesis.

Signed……………………………………………………..Date…………………………………….

Gilliham M.

Conceived the project and planned experiments, supervised the research and wrote the manuscript.

I hereby certify that the statement of contribution is accurate and I give permission for the inclusion of the paper in the thesis.

Signed……………………………………………………..Date…………………………………….

Byrt, C.S.

Performed wheat genotyping.

I hereby certify that the statement of contribution is accurate and I give permission for the inclusion of the paper in the thesis.

Signed……………………………………………………..Date…………………………………….

Tyerman, S.D.

Assisted with electrophysiology experiments.

I hereby certify that the statement of contribution is accurate and I give permission for the inclusion of the paper in the thesis.

Signed……………………………………………………..Date…………………………………….

Conn, S.J.

Performed *in situ* PCR and qPCR

I hereby certify that the statement of contribution is accurate and I give permission for the inclusion of the paper in the thesis.

Signed……………………………………………………..Date…………………………………….

Athman, A.

Performed *in situ* PCR and qPCR

I hereby certify that the statement of contribution is accurate and I give permission for the inclusion of the paper in the thesis.

Signed……………………………………………………..Date…………………………………………

Jordans, C.

Performed *in situ* PCR

I hereby certify that the statement of contribution is accurate and I give permission for the inclusion of the paper in the thesis.

Signed……………………………………………………..Date…………………………………………

Hare, R.A.

Conceived the project and planned experiments.

I hereby certify that the statement of contribution is accurate and I give permission for the inclusion of the paper in the thesis.

Signed……………………………………………………..Date…………………………………………

Munns, R., James, R.A., Xu, B., Athman, A., Conn, S.J., Jordans, C., Byrt, C.S., Hare, R.A., Tyerman, S.D., Tester, M., Plett, D. & Gilliham, M. (2012). Wheat grain yield on saline soils is improved by an ancestral Na$^+$ transporter gene. *Nature Biotechnology, 30*(4), 360-364.

Appendix 4. Full list of misexpression gene (log (2) ≥ 1) in *cax1*, *cax3*, *cax1/cax3* and *cax1/sCAX1* lines, compared to wildtype Col-0 plants

-3.0   1:1   3.0

cax1   cax3   cax1/cax3   cax1/sCAX1

Gene	Description
At5g13330	AP2 domain-containing transcription factor family protein
At2g44940	"AP2 domain-containing transcription factor TINY, putative"
At3g50260	"AP2 domain-containing transcription factor, putative"
At1g01250	"AP2 domain-containing transcription factor, putative"
At1g64380	"AP2 domain-containing transcription factor, putative"
At3g61630	"AP2 domain-containing transcription factor, putative"
At1g77640	"AP2 domain-containing transcription factor, putative"
At5g50915	basic helix-loop-helix (bHLH) family protein
At2g18300	basic helix-loop-helix (bHLH) family protein
At3g47640	basic helix-loop-helix (bHLH) family protein
At5g67110	basic helix-loop-helix (bHLH) family protein
At1g51140	basic helix-loop-helix (bHLH) family protein
At3g61950	basic helix-loop-helix (bHLH) family protein
At3g07340	basic helix-loop-helix (bHLH) family protein
At5g48560	basic helix-loop-helix (bHLH) family protein
At2g42280	basic helix-loop-helix (bHLH) family protein
At4g00050	basic helix-loop-helix (bHLH) family protein
At4g34590	bZIP transcription factor family protein
At1g76650	calcium-binding EF hand family protein
At5g39670	calcium-binding EF hand family protein
At3g47480	calcium-binding EF hand family protein
At3g01830	"calmodulin-related protein, putative"
At3g02310	developmental protein SEPALLATA2 / floral homeotic protein (AGL4) (SEP2)
At1g13260	DNA-binding protein RAV1 (RAV1)
At2g36080	"DNA-binding protein, putative"
At3g55560	DNA-binding protein-related
At5g25190	"ethylene-responsive element-binding protein, putative"
At1g72360	"ethylene-responsive element-binding protein, putative"
At1g67970	"heat shock factor protein, putative (HSF5)"
At4g18880	heat shock transcription factor 21 (HSF21)
At3g61890	homeobox-leucine zipper protein 12 (HB-12) / HD-ZIP transcription factor 12
At2g46680	homeobox-leucine zipper protein 7 (HB-7) / HD-ZIP transcription factor 7
At1g62990	homeodomain transcription factor (KNAT7)
At5g49330	myb family transcription factor
At5g67300	myb family transcription factor
At4g37180	myb family transcription factor
At2g38090	myb family transcription factor
At1g74650	myb family transcription factor (cY13)
At1g63910	myb family transcription factor (MYB103)
At2g47190	myb family transcription factor (MYB2)
At3g27812	myb family transcription factor (MYB3) (MYB21)
At4g34990	myb family transcription factor (MYB32)
At4g38620	myb family transcription factor (MYB4)
At5g26655	myb family transcription factor (MYB4) (MYB86)
At5g12870	myb family transcription factor (MYB46)
At1g18710	myb family transcription factor (MYB47)
At1g18570	myb family transcription factor (MYB51)
At4g01680	myb family transcription factor (MYB55)
At1g09540	myb family transcription factor (MYB61)
At4g22680	myb family transcription factor (MYB85)
At1g01010	no apical meristem (NAM) family protein
At1g02220	no apical meristem (NAM) family protein
At1g34180	no apical meristem (NAM) family protein
At1g52890	no apical meristem (NAM) family protein
At2g17040	no apical meristem (NAM) family protein
At3g04070	no apical meristem (NAM) family protein
At5g18270	no apical meristem (NAM) family protein
At5g13180	no apical meristem (NAM) family protein
At1g69490	no apical meristem (NAM) family protein
At2g46770	no apical meristem (NAM) family protein

Continued

Gene	Description
At1g32770	no apical meristem (NAM) family protein
At4g28500	no apical meristem (NAM) family protein
At1g28470	no apical meristem (NAM) family protein
At1g27360	squamosa promoter-binding protein-like 11 (SPL11)
At2g42200	squamosa promoter-binding protein-like 9 (SPL9)
At3g02150	"TCP family transcription factor, putative"
At3g06160	transcriptional factor B3 family protein
At4g31800	WRKY family transcription factor
At2g30250	WRKY family transcription factor
At5g07100	WRKY family transcription factor
At2g38470	WRKY family transcription factor
At5g22570	WRKY family transcription factor
At3g01970	WRKY family transcription factor
At4g01720	WRKY family transcription factor
At5g49520	WRKY family transcription factor
At4g23810	WRKY family transcription factor
At1g62300	WRKY family transcription factor
At2g25000	WRKY family transcription factor
At5g13080	WRKY family transcription factor
At5g46350	WRKY family transcription factor
At2g44745	WRKY family transcription factor
At5g25830	zinc finger (GATA type) family protein
At3g15050	calmodulin-binding family protein
At3g59690	calmodulin-binding family protein
At4g00820	calmodulin-binding protein-related
At3g51920	calmodulin-9 (CAM9)
At2g41410	"calmodulin, putative"
At4g33050	calmodulin-binding family protein
At4g31000	calmodulin-binding protein
At2g26190	calmodulin-binding family protein
At2g41100	" calmodulin-related protein 3, touch-induced (TCH3)"
At1g73800	calmodulin-binding protein
At1g73805	calmodulin-binding protein
At5g26920	calmodulin-binding protein
At3g50770	"calmodulin-related protein, putative"
At5g57630	"CBL-interacting protein kinase 21, putative (CIPK21)"
At5g10930	CBL-interacting protein kinase 5 (CIPK5)
At1g01140	CBL-interacting protein kinase 9 (CIPK9)
At5g18470	curculin-like (mannose-binding) lectin family protein
At2g30500	kinase interacting family protein
At1g67520	lectin protein kinase family protein
At5g60280	lectin protein kinase family protein
At1g53070	legume lectin family protein
At2g13790	leucine-rich repeat family protein / protein kinase family protein
At1g34420	leucine-rich repeat family protein / protein kinase family protein
At5g25930	leucine-rich repeat family protein / protein kinase family protein
At4g08850	leucine-rich repeat family protein / protein kinase family protein
At1g51790	"leucine-rich repeat protein kinase, putative"
At1g51860	"leucine-rich repeat protein kinase, putative"
At1g51800	"leucine-rich repeat protein kinase, putative"
At1g51890	"leucine-rich repeat protein kinase, putative"
At1g79620	"leucine-rich repeat transmembrane protein kinase, putative"
At4g18640	"leucine-rich repeat transmembrane protein kinase, putative"
At3g03770	"leucine-rich repeat transmembrane protein kinase, putative"
At4g22730	"leucine-rich repeat transmembrane protein kinase, putative"
At1g74360	"leucine-rich repeat transmembrane protein kinase, putative"
At5g45800	"leucine-rich repeat transmembrane protein kinase, putative"
At2g31880	"leucine-rich repeat transmembrane protein kinase, putative"
At1g35710	"leucine-rich repeat transmembrane protein kinase, putative"
At2g19190	"senescence-responsive receptor-like serine/threonine kinase, putative (SIRK)"
At4g08470	"mitogen-activated protein kinase, putative"
At1g01560	"MAPK, putative (MPK11)"
At5g43910	pfkB-type carbohydrate kinase family protein
At1g14370	protein kinase (APK2a)
At2g40120	protein kinase family protein
At1g09440	protein kinase family protein
At1g24030	protein kinase family protein
At1g56720	protein kinase family protein
At5g39420	protein kinase family protein
At2g18890	protein kinase family protein
At5g11410	protein kinase family protein
At5g58350	protein kinase family protein
At4g23300	protein kinase family protein
At5g58940	protein kinase family protein
At1g70520	protein kinase family protein
At2g32800	protein kinase family protein
At4g23190	protein kinase family protein
At1g70530	protein kinase family protein
At4g25390	protein kinase family protein
At2g31010	protein kinase family protein

Continued

				Gene ID	Description
				At2g34340	protein kinase family protein
				At4g23240	protein kinase family protein
				At4g04490	protein kinase family protein
				At5g25440	protein kinase family protein
				At4g23220	protein kinase family protein
				At4g11890	protein kinase family protein
				At4g23150	protein kinase family protein
				At4g04500	protein kinase family protein
				At2g45910	protein kinase family protein / U-box domain-containing protein
				At5g65530	"protein kinase, putative"
				At5g02290	"protein kinase, putative"
				At5g47070	"protein kinase, putative"
				At2g39660	"protein kinase, putative"
				At3g46280	protein kinase-related
				At3g22060	receptor protein kinase-related
				At4g23140	receptor-like protein kinase 5 (RLK5)
				At4g23310	"receptor-like protein kinase, putative"
				At3g45860	"receptor-like protein kinase, putative"
				At5g38210	serine/threonine protein kinase family protein
				At1g66880	serine/threonine protein kinase family protein
				At5g38240	"serine/threonine protein kinase, putative"
				At1g21240	"wall-associated kinase, putative"
				At2g46600	"calcium-binding protein, putative"
				At5g04220	C2 domain-containing protein (sytC)
				At1g21550	"calcium-binding protein, putative"
				At2g38170	calcium exchanger (CAX1)
				At3g51860	"cation exchanger, putative (CAX3)"
				At1g64170	"cation/hydrogen exchanger, putative (CHX16)"
				At4g23700	"cation/hydrogen exchanger, putative (CHX17)"
				At1g27770	Ca(2+)-ATPase isoform 1 (ACA1) / plastid envelope ATPase 1 (PEA1)
				At3g57330	"Ca2+-ATPase, putative (ACA11)"
				At5g57110	Ca(2+)-ATPase isoform 8 (ACA8)
				At4g29900	"Ca2+-ATPase, putative (ACA10)"
				At3g22910	"Ca(2+)-ATPase, putative (ACA13)"
				At3g63380	"Ca(2+)-ATPase, putative (ACA12)"
				At4g14610	---
				At4g04410	---
				At2g04460	---
				At5g20410	"MGDG synthase, putative"
				At5g23020	2-isopropylmalate synthase 2 (IMS2)
				At5g09290	"inositol polyphosphate 1-phosphatase, putative"
				At5g64000	"3'(2'),5'-bisphosphate nucleotidase, putative"
				At3g55360	3-oxo-5-alpha-steroid 4-dehydrogenase family protein
				At1g65060	4-coumarate--CoA ligase 3 / 4-coumaroyl-CoA synthase 3 (4CL3)
				At1g06570	4-hydroxyphenylpyruvate dioxygenase (HPD)
				At3g28510	AAA-type ATPase family protein
				At3g50930	AAA-type ATPase family protein
				At3g28540	AAA-type ATPase family protein
				At3g55110	ABC transporter family protein
				At1g71330	ABC transporter family protein
				At3g47780	ABC transporter family protein
				At3g21080	ABC transporter-related
				At4g01130	"acetylesterase, putative"
				At2g26400	acireductone dioxygenase (ARD/ARD') family protein
				At3g12110	actin 11 (ACT11)
				At2g16700	actin-depolymerizing factor 5 (ADF5)
				At3g05020	"acyl carrier protein 1, chloroplast (ACP-1)"
				At4g33790	"acyl CoA reductase, putative"
				At4g28390	"ADP, ATP carrier protein, mitochondrial, putative "
				At3g08860	"alanine--glyoxylate aminotransferase, putative"
				At3g47800	aldose 1-epimerase family protein
				At1g34040	alliinase family protein
				At4g25000	"alpha-amylase, putative / 1,4-alpha-D-glucan glucanohydrolase, putative"
				At1g32350	"alternative oxidase, putative"
				At4g21120	amino acid permease family protein
				At1g77690	"amino acid permease, putative"
				At2g41190	amino acid transporter family protein
				At2g24600	ankyrin repeat family protein
				At1g10340	ankyrin repeat family protein
				At3g15400	"anther development protein, putative"
				At1g24520	anther-specific protein agp1
				At3g01700	arabinogalactan-protein (AGP11)
				At4g26320	arabinogalactan-protein (AGP13)
				At5g56540	arabinogalactan-protein (AGP14)
				At2g22470	arabinogalactan-protein (AGP2)
				At5g10430	arabinogalactan-protein (AGP4)
				At1g35230	arabinogalactan-protein (AGP5)
				At3g20865	"arabinogalactan-protein, putative (AGP)"
				At5g53250	"arabinogalactan-protein, putative (AGP22)"
				At3g57690	"arabinogalactan-protein, putative (AGP23)"
				At2g27880	"argonaute protein, putative / AGO, putative"

Continued

Gene ID	Description
At2g?7???	oligopeptide protein, putative / HS-?, putative
At4g36030	armadillo/beta-catenin repeat family protein
At5g67340	armadillo/beta-catenin repeat family protein / U-box domain-containing protein
At2g03200	aspartyl protease family protein
At4g04460	aspartyl protease family protein
At1g25510	aspartyl protease family protein
At1g49050	aspartyl protease family protein
At5g10760	aspartyl protease family protein
At2g38940	At1g76430
At2g29120	At2g24730
At1g60810	ATP citrate-lyase -related
At3g42640	"ATPase, plasma membrane-type, putative / proton pump, putative"
At1g30410	"ATP-binding cassette transport protein, putative"
At4g17280	auxin-responsive family protein
At5g50760	auxin-responsive family protein
At1g16510	auxin-responsive family protein
At4g27260	auxin-responsive GH3 family protein
At5g13320	auxin-responsive GH3 family protein
At5g54510	"auxin-responsive GH3 protein, putative (DFL-1)"
At4g12980	"auxin-responsive protein, putative"
At5g47530	"auxin-responsive protein, putative"
At2g04850	auxin-responsive protein-related
At3g12955	auxin-responsive protein-related
At1g33960	avirulence-responsive protein / avirulence induced gene (AIG1)
At5g39720	avirulence-responsive protein-related / avirulence induced gene (AIG) protein-related
At1g69840	band 7 family protein
At3g01290	band 7 family protein
At1g35310	Bet v I allergen family protein
At4g15210	"beta-amylase (BMY1) / 1,4-alpha-D-glucan maltohydrolase"
At2g32290	"beta-amylase, putative / 1,4-alpha-D-glucan maltohydrolase, putative"
At1g78950	"beta-amyrin synthase, putative"
At4g28250	"beta-expansin, putative (EXPB3)"
At3g13790	beta-fructosidase (BFRUCT1) / beta-fructofuranosidase / cell wall invertase
At3g52600	"beta-fructosidase, putative / beta-fructofuranosidase, putative"
At3g52370	beta-Ig-H3 domain-containing protein / fasciclin domain-containing protein
At2g35860	beta-Ig-H3 domain-containing protein / fasciclin domain-containing protein
At1g04220	"beta-ketoacyl-CoA synthase, putative"
At4g21590	"bifunctional nuclease, putative"
At1g68290	"bifunctional nuclease, putative"
At5g15530	biotin carboxyl carrier protein 2 (BCCP2)
At3g61190	BON1-associated protein 1 (BAP1)
At3g50750	brassinosteroid signalling positive regulator-related
At3g50480	broad-spectrum mildew resistance RPW8 family protein
At1g23140	C2 domain-containing protein
At4g00700	C2 domain-containing protein
At1g09070	"C2 domain-containing protein / src2-like protein, putative"
At1g67990	"caffeoyl-CoA 3-O-methyltransferase, putative"
At4g26220	"caffeoyl-CoA 3-O-methyltransferase, putative"
At1g67980	"caffeoyl-CoA 3-O-methyltransferase, putative"
At1g08450	calreticulin 3 (CRT3)
At5g04180	carbonic anhydrase family protein
At1g58180	carbonic anhydrase family protein / carbonate dehydratase family protein
At2g20870	"cell wall protein precursor, putative"
At4g18780	"cellulose synthase, catalytic subunit (IRX1)"
At5g17420	"cellulose synthase, catalytic subunit (IRX3)"
At5g44030	"cellulose synthase, catalytic subunit (IRX5)"
At1g02205	CER1 protein
At1g02200	CER1 protein
At1g02190	"CER1 protein, putative"
At5g57800	"CER1 protein, putative (WAX2)"
At5g13930	chalcone synthase / naringenin-chalcone synthase
At3g55120	chalcone-flavanone isomerase / chalcone isomerase (CHI)
At5g05270	chalcone-flavanone isomerase family protein
At1g02360	"chitinase, putative"
At2g43620	"chitinase, putative"
At2g43570	"chitinase, putative"
At3g22840	chlorophyll A-B binding family protein / early light-induced protein (ELIP)
At2g40100	chlorophyll A-B binding protein (LHCB4.3)
At4g03320	chloroplast protein import component-related
At2g23910	cinnamoyl-CoA reductase-related
At4g27430	COP1-interacting protein 7 (CIP7)
At3g43670	"copper amine oxidase, putative"
At3g48970	copper-binding family protein
At3g22640	cupin family protein
At4g34490	cyclase-associated protein (cap1)
At4g01010	"cyclic nucleotide-regulated ion channel, putative (CNGC13)"
At4g18930	cyclic phosphodiesterase
At3g45130	"(S)-2,3-epoxysqualene mutase, putative"
At3g23470	cyclopropane-fatty-acyl-phospholipid synthase family protein
At4g35350	"cysteine endopeptidase, papain-type (XCP1)"
At5g47550	"cysteine protease inhibitor, putative / cystatin, putative"

Continued

Gene ID	Description
At1g06260	"cysteine proteinase, putative"
At3g49340	"cysteine proteinase, putative"
At3g22460	"O-acetylserine (thiol)-lyase, putative / O-acetylserine sulfhydrylase, putative"
At2g32720	"cytochrome b5, putative"
At2g30750	"cytochrome P450 71A12, putative (CYP71A12)"
At3g26210	"cytochrome P450 71B23, putative (CYP71B23)"
At2g45570	"cytochrome P450 76C2, putative (CYP76C2) (YLS6)"
At3g28740	cytochrome P450 family protein
At2g46960	cytochrome P450 family protein
At5g44620	cytochrome P450 family protein
At3g20100	cytochrome P450 family protein
At4g39480	cytochrome P450 family protein
At4g39510	cytochrome P450 family protein
At3g26230	cytochrome P450 family protein
At2g29090	cytochrome P450 family protein
At3g26220	cytochrome P450 family protein
At1g57750	"cytochrome P450, putative"
At1g63710	"cytochrome P450, putative"
At3g10570	"cytochrome P450, putative"
At4g12310	"cytochrome P450, putative"
At1g01600	"cytochrome P450, putative"
At4g37370	"cytochrome P450, putative"
At1g33720	"cytochrome P450, putative"
At5g57220	"cytochrome P450, putative"
At2g27660	DC1 domain-containing protein
At2g44380	DC1 domain-containing protein
At2g17740	DC1 domain-containing protein
At5g25610	dehydration-responsive protein (RD22)
At5g15800	developmental protein SEPALLATA1 / floral homeotic protein (AGL2) (SEP1)
At1g61720	dihydroflavonol 4-reductase (dihydrokaempferol 4-reductase) family (BAN)
At3g23110	disease resistance family protein
At3g25010	disease resistance family protein
At2g32680	disease resistance family protein
At2g32660	disease resistance family protein / LRR family protein
At3g24900	disease resistance family protein / LRR family protein
At5g04720	"disease resistance protein (CC-NBS-LRR class), putative"
At4g33300	"disease resistance protein (CC-NBS-LRR class), putative"
At1g33560	"disease resistance protein (CC-NBS-LRR class), putative"
At3g48090	disease resistance protein (EDS1)
At1g61100	"disease resistance protein (TIR class), putative"
At1g57630	"disease resistance protein (TIR class), putative"
At2g32140	"disease resistance protein (TIR class), putative"
At1g72890	"disease resistance protein (TIR-NBS class), putative"
At4g16990	"disease resistance protein (TIR-NBS class), putative"
At1g66090	"disease resistance protein (TIR-NBS class), putative"
At1g63750	"disease resistance protein (TIR-NBS-LRR class), putative"
At5g41740	"disease resistance protein (TIR-NBS-LRR class), putative"
At3g13650	disease resistance response protein-related/ dirigent protein-related
At4g23690	disease resistance-responsive family protein / dirigent family protein
At4g11210	disease resistance-responsive family protein / dirigent family protein
At1g64160	disease resistance-responsive family protein / dirigent family protein
At5g03170	DNAJ heat shock N-terminal domain-containing protein
At4g09350	DNAJ heat shock N-terminal domain-containing protein
At1g72070	DNAJ heat shock N-terminal domain-containing protein
At5g38900	DSBA oxidoreductase family protein
At1g52250	dynein light chain type 1 family protein
At4g24510	eceriferum protein (CER2)
At3g54150	embryo-abundant protein-related
At5g62210	embryo-specific protein-related
At4g24260	"endo-1,4-beta-glucanase, putative / cellulase, putative"
At1g64390	"endo-1,4-beta-glucanase, putative / cellulase, putative"
At2g24170	"endomembrane protein 70, putative"
At3g57510	endo-polygalacturonase (ADPG1)
At3g24360	enoyl-CoA hydratase/isomerase family protein
At4g25940	epsin N-terminal homology (ENTH) domain-containing protein
At4g37150	"esterase, putative"
At1g08310	esterase/lipase/thioesterase family protein
At1g06160	"ethylene-responsive factor, putative"
At1g07000	exocyst subunit EXO70 family protein
At1g02790	"exopolygalacturonase / galacturan 1,4-alpha-galacturonidase (PGA3) / pectinase"
At3g07850	"exopolygalacturonase / galacturan 1,4-alpha-galacturonidase / pectinase"
At1g27440	exostosin family protein
At3g45970	expansin family protein (EXPL1)
At2g18660	expansin family protein (EXPR3)
At2g03090	"expansin, putative (EXP15)"
At3g55500	"expansin, putative (EXP16)"
At5g39280	"expansin, putative (EXP23)"
At3g29030	"expansin, putative (EXP5)"
At3g28270	expressed protein
At3g28750	expressed protein

Continued

Gene	Description
At3g01240	expressed protein
At1g68875	expressed protein
At1g72110	expressed protein
At4g23496	expressed protein
At5g37300	expressed protein
At1g09610	expressed protein
At5g22430	expressed protein
At2g31930	expressed protein
At1g30250	expressed protein
At4g27435	expressed protein
At1g33800	expressed protein
At5g39880	expressed protein
At5g01360	expressed protein
At2g41610	expressed protein
At4g14695	expressed protein
At5g61720	expressed protein
At3g50220	expressed protein
At1g68600	expressed protein
At3g22540	expressed protein
At5g67210	expressed protein
At3g28830	expressed protein
At4g09990	expressed protein
At5g61340	expressed protein
At3g26110	expressed protein
At4g19430	expressed protein
At3g25130	expressed protein
At3g28790	expressed protein
At3g55420	expressed protein
At5g59305	expressed protein
At1g07120	expressed protein
At4g27030	expressed protein
At3g28980	expressed protein
At3g21710	expressed protein
At5g62140	expressed protein
At2g17300	expressed protein
At3g62730	expressed protein
At4g11760	expressed protein
At5g47635	expressed protein
At1g79420	expressed protein
At5g57785	expressed protein
At2g40480	expressed protein
At3g23090	expressed protein
At4g20050	expressed protein
At5g20270	expressed protein
At1g23060	expressed protein
At1g14345	expressed protein
At5g06930	expressed protein
At1g30260	expressed protein
At1g29050	expressed protein
At5g60720	expressed protein
At1g35180	expressed protein
At3g04960	expressed protein
At1g77870	expressed protein
At4g24130	expressed protein
At3g21190	expressed protein
At1g64360	expressed protein
At2g42900	expressed protein
At1g78170	expressed protein
At1g17090	expressed protein
At3g56260	expressed protein
At5g04470	expressed protein
At2g28870	expressed protein
At3g06035	expressed protein
At4g26260	expressed protein
At1g64980	expressed protein
At1g28375	expressed protein
At5g01790	expressed protein
At5g02440	expressed protein
At4g14380	expressed protein
At2g34150	expressed protein
At3g54260	expressed protein
At5g23530	expressed protein
At5g15740	expressed protein
At2g40435	expressed protein
At4g00440	expressed protein
At3g26960	expressed protein
At5g58260	expressed protein
At1g03820	expressed protein
At5g27290	expressed protein
At5g64900	expressed protein

Continued

				At3g52360	expressed protein
				At2g28410	expressed protein
				At4g27840	expressed protein
				At5g59350	expressed protein
				At5g40830	expressed protein
				At4g18425	expressed protein
				At3g57320	expressed protein
				At1g27300	expressed protein
				At1g12020	expressed protein
				At1g10990	expressed protein
				At3g07780	expressed protein
				At1g17710	expressed protein
				At4g25170	expressed protein
				At3g51890	expressed protein
				At5g05300	expressed protein
				At5g15860	expressed protein
				At1g13990	expressed protein
				At1g49000	expressed protein
				At3g27210	expressed protein
				At5g44820	expressed protein
				At5g12340	expressed protein
				At4g05590	expressed protein
				At4g38560	expressed protein
				At5g57760	expressed protein
				At1g14780	expressed protein
				At1g16850	expressed protein
				At5g12420	expressed protein
				At5g18310	expressed protein
				At1g63720	expressed protein
				At5g44810	expressed protein
				At5g42050	expressed protein
				At1g68620	expressed protein
				At3g14060	expressed protein
				At4g31980	expressed protein
				At1g10690	expressed protein
				At1g21520	expressed protein
				At4g32870	expressed protein
				At3g03020	expressed protein
				At4g31240	expressed protein
				At5g07820	expressed protein
				At1g59590	expressed protein
				At3g63010	expressed protein
				At5g64870	expressed protein
				At1g15790	expressed protein
				At2g30990	expressed protein
				At3g13062	expressed protein
				At3g49210	expressed protein
				At1g80130	expressed protein
				At5g16030	expressed protein
				At1g13340	expressed protein
				At5g10695	expressed protein
				At5g16080	expressed protein
				At2g28400	expressed protein
				At1g05575	expressed protein
				At1g23840	expressed protein
				At1g62840	expressed protein
				At4g39670	expressed protein
				At1g05340	expressed protein
				At5g50200	expressed protein
				At1g19020	expressed protein
				At4g16000	expressed protein
				At1g52200	expressed protein
				At1g19380	expressed protein
				At4g23610	expressed protein
				At1g67920	expressed protein
				At5g08240	expressed protein
				At2g41730	expressed protein
				At2g23120	expressed protein
				At5g39520	expressed protein
				At1g65490	expressed protein
				At2g35290	expressed protein
				At1g65510	expressed protein
				At1g76960	expressed protein
				At2g18690	expressed protein
				At4g23880	expressed protein
				At1g14870	expressed protein
				At1g65500	expressed protein
				At1g13470	expressed protein
				At4g27450	expressed protein
				At3g26470	expressed protein

175

Continued

				Gene ID	Description
				At5g25260	expressed protein
				At3g60420	expressed protein
				At3g13950	expressed protein
				At3g18250	expressed protein
				At5g52900	expressed protein
				At2g32210	expressed protein
				At1g15010	expressed protein
				At1g72060	expressed protein
				At2g32190	expressed protein
				At2g44240	expressed protein
				At1g26410	FAD-binding domain-containing protein
				At1g26380	FAD-binding domain-containing protein
				At4g20860	FAD-binding domain-containing protein
				At1g26420	FAD-binding domain-containing protein
				At1g30700	FAD-binding domain-containing protein
				At1g26390	FAD-binding domain-containing protein
				At1g75880	family II extracellular lipase 1 (EXL1)
				At1g75900	family II extracellular lipase 3 (EXL3)
				At1g75910	family II extracellular lipase 4 (EXL4)
				At1g75930	family II extracellular lipase 6 (EXL6)
				At1g20120	"family II extracellular lipase, putative"
				At2g24450	fasciclin-like arabinogalactan family protein
				At5g60490	fasciclin-like arabinogalactan-protein (FLA12)
				At4g12730	fasciclin-like arabinogalactan-protein (FLA2)
				At2g04780	fasciclin-like arabinogalactan-protein (FLA7)
				At2g45470	fasciclin-like arabinogalactan-protein (FLA8)
				At5g44130	"fasciclin-like arabinogalactan-protein, putative"
				At1g06120	fatty acid desaturase family protein
				At1g01120	fatty acid elongase 3-ketoacyl-CoA synthase 1 (KCS1)
				At2g46720	"fatty acid elongase 3-ketoacyl-CoA synthase, putative"
				At5g27920	F-box family protein
				At5g25350	F-box family protein
				At1g63090	F-box family protein / SKP1 interacting partner 3-related
				At3g16250	ferredoxin-related
				At5g07800	flavin-containing monooxygenase family protein / FMO family protein
				At1g62540	flavin-containing monooxygenase family protein / FMO family protein
				At5g07990	flavonoid 3'-monooxygenase / transparent testa 7 protein (TT7)
				At5g08640	flavonol synthase 1 (FLS1)
				At5g63580	"flavonol synthase, putative"
				At4g18960	floral homeotic protein AGAMOUS (AG)
				At1g69120	floral homeotic protein APETALA1 (AP1) / agamous-like MADS box protein (AGL7)
				At3g54340	floral homeotic protein APETALA3 (AP3)
				At5g20240	floral homeotic protein PISTILLATA (PI)
				At1g65480	flowering locus T protein (FT)
				At1g24150	formin homology 2 domain-containing protein / FH2 domain-containing protein
				At4g26530	"fructose-bisphosphate aldolase, putative"
				At3g28340	"galactinol synthase, putative"
				At1g53290	galactosyltransferase family protein
				At4g12960	gamma interferon responsive lysosomal thiol reductase family protein / GILT family protein
				At4g12890	gamma interferon responsive lysosomal thiol reductase family protein / GILT family protein
				At1g58430	GDSL-motif lipase/hydrolase family protein
				At2g42990	GDSL-motif lipase/hydrolase family protein
				At4g26790	GDSL-motif lipase/hydrolase family protein
				At2g04570	GDSL-motif lipase/hydrolase family protein
				At5g33370	GDSL-motif lipase/hydrolase family protein
				At5g45960	GDSL-motif lipase/hydrolase family protein
				At3g48460	GDSL-motif lipase/hydrolase family protein
				At1g54790	GDSL-motif lipase/hydrolase family protein
				At3g62020	germin-like protein (GLP10)
				At3g05930	germin-like protein (GLP8)
				At4g14630	germin-like protein (GLP9)
				At5g26696	"germin-like protein, putative"
				At5g38910	"germin-like protein, putative"
				At1g66350	gibberellin regulatory protein (RGL1)
				At3g03450	"gibberellin response modulator, putative"
				At5g59845	gibberellin-regulated family protein
				At1g61800	"glucose-6-phosphate/phosphate translocator, putative"
				At5g51950	glucose-methanol-choline (GMC) oxidoreductase family protein
				At1g12570	glucose-methanol-choline (GMC) oxidoreductase family protein
				At4g16590	glucosyltransferase-related
				At5g18170	glutamate dehydrogenase 1 (GDH1)
				At5g07440	glutamate dehydrogenase 2 (GDH2)
				At3g04110	glutamate receptor family protein (GLR1.1) (GLR1)
				At3g07520	glutamate receptor family protein (GLR1.4)
				At2g29110	glutamate receptor family protein (GLR2.8) (GLUR9)
				At1g15045	glutamine amidotransferase-related
				At5g37600	"glutamine synthetase, putative"
				At3g62930	glutaredoxin family protein
				At4g15690	glutaredoxin family protein
				At1g03850	glutaredoxin family protein

Continued

At5g18170	glutamate dehydrogenase 1 (GDH1)
At5g07440	glutamate dehydrogenase 2 (GDH2)
At3g04110	glutamate receptor family protein (GLR1.1) (GLR1)
At3g07520	glutamate receptor family protein (GLR1.4)
At2g29110	glutamate receptor family protein (GLR2.8) (GLUR9)
At1g15045	glutamine amidotransferase-related
At5g37600	"glutamine synthetase, putative"
At3g62930	glutaredoxin family protein
At4g15690	glutaredoxin family protein
At1g03850	glutaredoxin family protein
At4g15700	glutaredoxin family protein
At4g15680	glutaredoxin family protein
At2g29470	"glutathione S-transferase, putative"
At1g02930	"glutathione S-transferase, putative"
At1g69930	"glutathione S-transferase, putative"
At1g74590	"glutathione S-transferase, putative"
At3g20520	glycerophosphoryl diester phosphodiesterase family protein
At4g13890	"glycine hydroxymethyltransferase, putative"
At5g17650	glycine/proline-rich protein
At4g18280	glycine-rich cell wall protein-related
At5g07530	glycine-rich protein (GRP17)
At5g07550	glycine-rich protein (GRP19)
At5g07560	glycine-rich protein (GRP20)
At5g51210	glycine-rich protein / oleosin
At5g56100	glycine-rich protein / oleosin
At3g18660	glycogenin glucosyltransferase (glycogenin)-related
At4g33340	glycogenin glucosyltransferase (glycogenin)-related
At4g33330	glycogenin glucosyltransferase (glycogenin)-related
At3g16920	glycoside hydrolase family 19 protein
At1g19170	glycoside hydrolase family 28 protein / polygalacturonase (pectinase) family protein
At3g42950	glycoside hydrolase family 28 protein / polygalacturonase (pectinase) family protein
At1g61810	glycosyl hydrolase family 1 protein
At3g60140	glycosyl hydrolase family 1 protein
At1g75940	glycosyl hydrolase family 1 protein / anther-specific protein ATA27
At4g08160	glycosyl hydrolase family 10 protein
At3g04010	glycosyl hydrolase family 17 protein
At3g57260	glycosyl hydrolase family 17 protein
At4g19810	glycosyl hydrolase family 18 protein
At5g09730	glycosyl hydrolase family 3 protein
At3g62710	glycosyl hydrolase family 3 protein
At5g11920	glycosyl hydrolase family 32 protein
At4g35010	glycosyl hydrolase family 35 protein
At5g34940	glycosyl hydrolase family 79 N-terminal domain-containing protein
At1g19940	glycosyl hydrolase family 9 protein
At2g32990	glycosyl hydrolase family 9 protein
At2g43660	glycosyl hydrolase family protein 17
At4g24040	"glycosyl hydrolase family protein 37 / trehalase, putative"
At1g02310	glycosyl hydrolase family protein 5
At5g03760	glycosyl transferase family 2 protein
At1g60140	glycosyl transferase family 20 protein / trehalose-phosphatase family protein
At2g37090	glycosyl transferase family 43 protein
At4g36890	glycosyl transferase family 43 protein
At5g54690	glycosyl transferase family 8 protein
At1g19300	glycosyl transferase family 8 protein
At1g53100	glycosyltransferase family 14 protein / core-2/I-branching enzyme family protein
At5g19580	glyoxal oxidase-related
At5g02230	haloacid dehalogenase-like hydrolase family protein
At2g41250	haloacid dehalogenase-like hydrolase family protein
At2g35980	harpin-induced family protein (YLS9) / HIN1 family protein / harpin-responsive family protein
At2g35960	harpin-induced family proteinharpin-responsive family protein
At5g06320	harpin-induced family protein NDR1/HIN1-like protein 3
At1g65690	harpin-induced protein-related / HIN1-related / harpin-responsive protein-related
At2g40130	heat shock protein-related
At5g52750	heavy-metal-associated domain-containing protein
At5g52760	heavy-metal-associated domain-containing protein
At4g35060	heavy-metal-associated domain-containing protein / copper chaperone (CCH)-related
At1g22990	heavy-metal-associated domain-containing protein / copper chaperone (CCH)-related
At1g69720	heme oxygenase 3 (HO3)
At5g26340	"hexose transporter, putative (STP13/MSS1)"
At4g08150	homeobox protein knotted-1 like 1 (KNAT1)
At1g62360	homeobox protein SHOOT MERISTEMLESS (STM)
At2g35210	human Rev interacting-like family protein / hRIP family protein
At5g58310	"hydrolase, alpha/beta fold family protein"
At4g12830	"hydrolase, alpha/beta fold family protein"
At5g39220	"hydrolase, alpha/beta fold family protein"
At3g05890	hydrophobic protein (RCI2B) / low temperature and salt responsive protein (LTI6B)
At5g14380	hydroxyproline-rich glycoprotein family protein
At2g34870	hydroxyproline-rich glycoprotein family protein
At2g21140	hydroxyproline-rich glycoprotein family protein
At5g37950	hypothetical protein

Continued

Gene ID	Description
At1g51250	hypothetical protein
At5g14090	hypothetical protein
At1g59930	hypothetical protein
At4g18010	inositol polyphosphate 5-phosphatase II (IP5PII)
At4g39800	inositol-3-phosphate synthase isozyme 1/ IPS 1
At4g25830	integral membrane family protein
At3g14380	integral membrane family protein
At4g15610	integral membrane family protein
At3g45870	integral membrane family protein / nodulin MtN21-related
At4g15750	invertase/pectin methylesterase inhibitor family protein
At2g47050	invertase/pectin methylesterase inhibitor family protein
At1g10770	invertase/pectin methylesterase inhibitor family protein
At4g02250	invertase/pectin methylesterase inhibitor family protein
At5g50030	invertase/pectin methylesterase inhibitor family protein
At1g23205	invertase/pectin methylesterase inhibitor family protein
At2g47670	invertase/pectin methylesterase inhibitor family protein
At5g20740	invertase/pectin methylesterase inhibitor family protein
At3g47380	invertase/pectin methylesterase inhibitor family protein
At1g74710	isochorismate synthase 1 (ICS1) / isochorismate mutase
At1g75280	"isoflavone reductase, putative"
At5g54670	kinesin-like protein C (KATC)
At5g05390	"laccase, putative / diphenol oxidase, putative"
At2g38080	"laccase, putative / diphenol oxidase, putative"
At5g60020	"laccase, putative / diphenol oxidase, putative"
At5g01190	"laccase, putative / diphenol oxidase, putative"
At2g29130	"laccase, putative / diphenol oxidase, putative"
At1g80160	lactoylglutathione lyase family protein / glyoxalase I family protein
At5g21100	"L-ascorbate oxidase, putative"
At4g39830	"L-ascorbate oxidase, putative"
At4g02380	late embryogenesis abundant 3 family protein / LEA3 family protein
At4g25110	latex-abundant family protein (AMC2) / caspase family protein
At5g04200	"latex-abundant protein, putative (AMC9) / caspase family protein"
At5g14930	leaf senescence-associated protein (SAG101)
At5g03350	legume lectin family protein
At5g12940	leucine-rich repeat family protein
At3g17640	leucine-rich repeat family protein
At2g33080	leucine-rich repeat family protein
At2g25440	leucine-rich repeat family protein
At2g45800	LIM domain-containing protein
At5g66630	LIM domain-containing protein
At5g66640	LIM domain-containing protein-related
At5g18630	lipase class 3 family protein
At5g24210	lipase class 3 family protein
At3g48080	lipase class 3 family protein / disease resistance protein-related
At5g59320	lipid transfer protein 3 (LTP3)
At5g59310	lipid transfer protein 4 (LTP4)
At3g08770	lipid transfer protein 6 (LTP6)
At3g51590	"lipid transfer protein, putative"
At1g16530	LOB domain protein 3 / lateral organ boundaries domain protein 3 (LBD3)
At4g37540	LOB domain protein 39 / lateral organ boundaries domain protein 39 (LBD39)
At1g02340	long hypocotyl in far-red 1 (HFR1)
At1g49430	long-chain-fatty-acid--CoA ligase / long-chain acyl-CoA synthetase
At2g47240	long-chain-fatty-acid--CoA ligase family protein / long-chain acyl-CoA synthetase family protein
At1g78970	"lupeol synthase (LUP1) / 2,3-oxidosqualene-triterpenoid cyclase"
At1g78960	"lupeol synthase, putative / 2,3-oxidosqualene-triterpenoid cyclase, putative"
At1g66960	"lupeol synthase, putative / 2,3-oxidosqualene-triterpenoid cyclase, putative"
At1g25530	"lysine and histidine specific transporter, putative"
At5g40780	"lysine and histidine specific transporter, putative"
At5g06300	lysine decarboxylase family protein
At4g09960	MADS-box protein (AGL11)
At2g03710	MADS-box protein (AGL3)
At1g24260	MADS-box protein (AGL9)
At4g23400	major intrinsic family protein / MIP family protein
At4g39330	"mannitol dehydrogenase, putative"
At4g36670	"mannitol transporter, putative"
At5g17700	MATE efflux family protein
At2g04100	MATE efflux family protein
At1g24140	matrixin family protein
At4g21830	methionine sulfoxide reductase domain-containing protein / SelR domain-containing protein
At1g27920	microtubule associated protein (MAP65/ASE1) family protein
At1g20350	"mitochondrial import inner membrane translocase subunit Tim17, putative"
At3g13400	multi-copper oxidase type I family protein
At3g13390	multi-copper oxidase type I family protein
At1g55570	multi-copper oxidase type I family protein
At5g48450	multi-copper oxidase type I family protein
At3g62150	"multidrug resistant (MDR) ABC transporter, putative"
At2g31900	myosin family protein
At3g56480	myosin heavy chain-related
At1g04600	"myosin, putative"
At2g28760	NAD-dependent epimerase/dehydratase family protein

Continued

|				Gene ID	Description
				At3g59845	"NADP-dependent oxidoreductase, putative"
				At5g38000	"NADP-dependent oxidoreductase, putative"
				At3g51240	naringenin 3-dioxygenase / flavanone 3-hydroxylase (F3H)
				At5g11790	Ndr family protein
				At1g69850	nitrate transporter (NTL1)
				At3g21670	nitrate transporter (NTP3)
				At2g17660	"nitrate-responsive NOI protein, putative"
				At5g22300	nitrilase 4 (NIT4)
				At2g39210	nodulin family protein
				At2g39510	nodulin MtN21 family protein
				At4g28040	nodulin MtN21 family protein
				At5g50790	nodulin MtN3 family protein
				At2g16060	non-symbiotic hemoglobin 1 (HB1) (GLB1)
				At1g44130	"nucellin protein, putative"
				At2g34410	O-acetyltransferase family protein
				At5g46340	O-acetyltransferase-related
				At5g42760	O-methyltransferase N-terminus domain-containing protein
				At4g11650	osmotin-like protein (OSM34)
				At3g60290	"oxidoreductase, 2OG-Fe(II) oxygenase family protein"
				At3g19010	"oxidoreductase, 2OG-Fe(II) oxygenase family protein"
				At5g20400	"oxidoreductase, 2OG-Fe(II) oxygenase family protein"
				At5g24530	"oxidoreductase, 2OG-Fe(II) oxygenase family protein"
				At4g10500	"oxidoreductase, 2OG-Fe(II) oxygenase family protein"
				At3g01440	oxygen evolving enhancer 3 (PsbQ) family protein
				At1g14150	oxygen evolving enhancer 3 (PsbQ) family protein
				At4g25860	oxysterol-binding family protein
				At1g27380	p21-rho-binding domain-containing protein
				At5g47350	palmitoyl protein thioesterase family protein
				At2g26560	"patatin, putative"
				At1g78780	pathogenesis-related family protein
				At2g14610	pathogenesis-related protein 1 (PR-1)
				At1g75040	pathogenesis-related protein 5 (PR-5)
				At4g25780	"pathogenesis-related protein, putative"
				At5g40020	pathogenesis-related thaumatin family protein
				At3g01420	"pathogen-responsive alpha-dioxygenase, putative"
				At1g69440	PAZ domain-containing protein / piwi domain-containing protein
				At3g01270	pectate lyase family protein
				At5g55720	pectate lyase family protein
				At5g15110	pectate lyase family protein
				At4g13710	pectate lyase family protein
				At1g57590	"pectinacetylesterase, putative"
				At2g47040	pectinesterase family protein
				At5g07410	pectinesterase family protein
				At5g49180	pectinesterase family protein
				At3g62170	pectinesterase family protein
				At5g07430	pectinesterase family protein
				At2g43050	pectinesterase family protein
				At3g59010	pectinesterase family protein
				At3g17060	pectinesterase family protein
				At3g05610	pectinesterase family protein
				At4g02330	pectinesterase family protein
				At1g56100	pectinesterase inhibitor domain-containing protein
				At3g26630	pentatricopeptide (PPR) repeat-containing protein
				At2g37130	peroxidase 21 (PER21) (P21) (PRXR5)
				At3g49120	peroxidase 33 (PER33) (P33) (PRXCA) / neutral peroxidase C (PERC)
				At4g16270	peroxidase 40 (PER40) (P40)
				At5g42180	peroxidase 64 (PER64) (P64) (PRXR4)
				At1g44970	"peroxidase, putative"
				At5g47000	"peroxidase, putative"
				At5g64110	"peroxidase, putative"
				At5g64120	"peroxidase, putative"
				At3g10340	"phenylalanine ammonia-lyase, putative"
				At1g73600	"phosphoethanolamine N-methyltransferase 3, putative (NMT3)"
				At3g05630	"phospholipase D, putative (PLDP2)"
				At2g38110	phospholipid/glycerol acyltransferase family protein
				At3g18850	phospholipid/glycerol acyltransferase family protein
				At3g52430	phytoalexin-deficient 4 protein (PAD4)
				At5g15630	phytochelatin synthetase family protein / COBRA cell expansion protein COBL4
				At5g60950	phytochelatin synthetase-related
				At5g02200	phytochrome A specific signal transduction component-related
				At2g22860	phytosulfokines 2 (PSK2)
				At1g32100	"pinoresinol-lariciresinol reductase, putative"
				At1g19610	"plant defensin-fusion protein, putative (PDF1.4)"
				At2g02100	"plant defensin-fusion protein, putative (PDF2.2)"
				At2g02140	"plant defensin-fusion protein, putative (PDF2.6)"
				At1g22480	plastocyanin-like domain-containing protein
				At1g72230	plastocyanin-like domain-containing protein
				At5g20230	plastocyanin-like domain-containing protein
				At5g26330	"plastocyanin-like domain-containing protein / mavicyanin, putative"
				At5g45880	pollen Ole e 1 allergen and extensin family protein

Continued

At1g29140	pollen Ole e 1 allergen and extensin family protein
At3g07820	polygalacturonase 3 (PGA3) / pectinase
At1g80170	"polygalacturonase, putative / pectinase, putative"
At1g60590	"polygalacturonase, putative / pectinase, putative"
At5g48140	"polygalacturonase, putative / pectinase, putative"
At2g24240	potassium channel tetramerisation domain-containing protein
At2g38360	prenylated rab acceptor (PRA1) family protein
At1g21310	proline-rich extensin-like family protein
At2g16630	proline-rich family protein
At5g12880	proline-rich family protein
At4g19200	proline-rich family protein
At5g43580	"protease inhibitor, putative"
At1g66850	protease inhibitor/seed storage/lipid transfer protein (LTP) family protein
At5g38170	protease inhibitor/seed storage/lipid transfer protein (LTP) family protein
At5g38160	protease inhibitor/seed storage/lipid transfer protein (LTP) family protein
At1g48750	protease inhibitor/seed storage/lipid transfer protein (LTP) family protein
At3g53980	protease inhibitor/seed storage/lipid transfer protein (LTP) family protein
At1g55260	protease inhibitor/seed storage/lipid transfer protein (LTP) family protein
At3g22600	protease inhibitor/seed storage/lipid transfer protein (LTP) family protein
At4g12470	protease inhibitor/seed storage/lipid transfer protein (LTP) family protein
At5g55450	protease inhibitor/seed storage/lipid transfer protein (LTP) family protein
At2g38860	proteaseI (pfpI)-like protein (YLS5)
At1g34750	"protein phosphatase 2C, putative / PP2C, putative"
At3g10940	protein phosphatase-related
At5g62730	proton-dependent oligopeptide transport (POT) family protein
At1g68570	proton-dependent oligopeptide transport (POT) family protein
At1g22570	proton-dependent oligopeptide transport (POT) family protein
At5g46050	proton-dependent oligopeptide transport (POT) family protein
At3g48650	"pseudogene, At14a-related protein"
At2g15040	"pseudogene, disease resistance protein-related"
At2g24160	"pseudogene, leucine rich repeat protein family"
At4g13900	"pseudogene, similar to NLOD"
At1g57990	purine permease-related
At1g08340	"rac GTPase activating protein, putative"
At3g51300	Rac-like GTP-binding protein (ARAC11) / Rho-like GTP-binding protein (ROP1)
At1g61566	rapid alkalinization factor (RALF) family protein
At1g28270	rapid alkalinization factor (RALF) family protein
At3g25170	rapid alkalinization factor (RALF) family protein
At3g25165	rapid alkalinization factor (RALF) family protein
At1g73640	Ras-related GTP-binding family protein
At5g03530	Ras-related GTP-binding family protein
At5g23750	remorin family protein
At5g37970	S-adenosyl-L-methionine:carboxyl methyltransferase family protein
At2g36880	"S-adenosylmethionine synthetase, putative"
At1g22180	SEC14 cytosolic factor family protein / phosphoglyceride transfer family protein
At2g21540	"SEC14 cytosolic factor, putative / phosphoglyceride transfer protein, putative"
At3g60540	sec61beta family protein
At1g03550	secretory carrier membrane protein (SCAMP) family protein
At2g23810	senescence-associated family protein
At1g22160	senescence-associated protein-related
At5g22980	"serine carboxypeptidase III, putative"
At4g12910	serine carboxypeptidase S10 family protein
At2g22970	serine carboxypeptidase S10 family protein
At2g12480	serine carboxypeptidase S10 family protein
At3g63470	"serine carboxypeptidase, putative"
At2g38900	"serine protease inhibitor, potato inhibitor I-type family protein"
At3g07130	serine/threonine protein phosphatase family protein
At3g12000	"S-locus related protein SLR1, putative (S1)"
At5g45380	sodium:solute symporter family protein
At2g37970	SOUL heme-binding family protein
At3g56230	speckle-type POZ protein-related
At2g45130	SPX (SYG1/Pho81/XPR1) domain-containing protein
At5g24150	"squalene monooxygenase 1,1 / squalene epoxidase 1,1 (SQP1,1)"
At1g32900	"starch synthase, putative"
At2g03760	"steroid sulfotransferase, putative"
At2g23680	"stress-responsive protein, putative"
At3g57010	strictosidine synthase family protein
At1g74020	strictosidine synthase family protein
At1g74010	strictosidine synthase family protein
At3g51440	strictosidine synthase family protein
At5g59130	subtilase family protein
At4g21650	subtilase family protein
At1g01900	subtilase family protein
At2g39850	subtilase family protein
At1g32940	subtilase family protein
At3g19930	sugar transport protein (STP4)
At3g52400	"syntaxin, putative (SYP122)"
At5g44630	terpene synthase/cyclase family protein
At1g61680	terpene synthase/cyclase family protein
At1g35290	thioesterase family protein

Continued

Gene ID	Description
At1g45145	thioredoxin H-type 5 (TRX-H-5) (TOUL)
At4g01870	tolB protein-related
At2g20145	Toll-Interleukin-Resistance (TIR) domain-containing protein
At1g49450	transducin family protein / WD-40 repeat family protein
At1g24530	transducin family protein / WD-40 repeat family protein
At5g23940	transferase family protein
At1g65450	transferase family protein
At5g67160	transferase family protein
At5g23970	transferase family protein
At5g42830	transferase family protein
At1g65445	transferase-related
At2g45290	"transketolase, putative"
At2g23360	transport protein-related
At5g53550	"transporter, putative"
At1g79410	transporter-related
At2g29350	"tropinone reductase, putative / tropine dehydrogenase, putative"
At1g72290	trypsin and protease inhibitor family protein / Kunitz family protein
At1g73260	trypsin and protease inhibitor family protein / Kunitz family protein
At2g43510	"trypsin inhibitor, putative"
At5g23860	tubulin beta-8 chain (TUB8) (TUBB8)
At4g00760	two-component responsive regulator family protein / response regulator family protein
At4g28680	"tyrosine decarboxylase, putative"
At2g20340	"tyrosine decarboxylase, putative"
At1g05000	tyrosine specific protein phosphatase family protein
At1g69523	UbiE/COQ5 methyltransferase family protein
At5g40630	ubiquitin family protein
At3g18710	U-box domain-containing protein
At1g66160	U-box domain-containing protein
At4g15490	UDP-glucoronosyl/UDP-glucosyl transferase family protein
At3g46670	UDP-glucoronosyl/UDP-glucosyl transferase family protein
At2g29730	UDP-glucoronosyl/UDP-glucosyl transferase family protein
At3g21760	UDP-glucoronosyl/UDP-glucosyl transferase family protein
At4g01070	UDP-glucoronosyl/UDP-glucosyl transferase family protein
At1g05680	UDP-glucoronosyl/UDP-glucosyl transferase family protein
At3g53150	UDP-glucoronosyl/UDP-glucosyl transferase family protein
At1g22400	UDP-glucoronosyl/UDP-glucosyl transferase family protein
At2g30140	UDP-glucoronosyl/UDP-glucosyl transferase family protein
At4g10955	"UDP-glucose 4-epimerase, putative "
At4g10960	"UDP-glucose 4-epimerase, putative "
At5g39320	"UDP-glucose 6-dehydrogenase, putative"
At5g15490	"UDP-glucose 6-dehydrogenase, putative"
At5g59290	UDP-glucuronic acid decarboxylase (UXS3)
At1g31070	UDP-N-acetylglucosamine pyrophosphorylase-related
At3g20210	"vacuolar processing enzyme, putative / asparaginyl endopeptidase, putative"
At4g20110	"vacuolar sorting receptor, putative"
At1g51270	"vesicle-associated membrane protein, putative / VAMP, putative"
At1g51280	"vesicle-associated membrane protein, putative / VAMP, putative"
At1g76970	VHS domain-containing protein / GAT domain-containing protein
At5g46780	VQ motif-containing protein
At2g22880	VQ motif-containing protein
At3g22160	VQ motif-containing protein
At1g78410	VQ motif-containing protein
At4g10270	wound-responsive family protein
At5g57560	endo-xyloglucan transferase (TCH4)
At3g25050	"endo-xyloglucan transferase, putative"
At3g44990	"endo-xyloglucan transferase, putative"
At2g14620	"endo-xyloglucan transferase, putative"
At4g25810	"endo-xyloglucan transferase, putative (XTR6)"
At4g14130	"endo-xyloglucan transferase, putative (XTR7)"
At3g28210	zinc finger (AN1-like) family protein
At3g45260	zinc finger (C2H2 type) family protein
At2g28710	zinc finger (C2H2 type) family protein
At5g57520	zinc finger (C2H2 type) family protein (ZFP2)
At5g47610	zinc finger (C3HC4-type RING finger) family protein
At1g72220	zinc finger (C3HC4-type RING finger) family protein
At3g10910	zinc finger (C3HC4-type RING finger) family protein
At1g72200	zinc finger (C3HC4-type RING finger) family protein
At4g30400	zinc finger (C3HC4-type RING finger) family protein
At2g42350	zinc finger (C3HC4-type RING finger) family protein
At4g33940	zinc finger (C3HC4-type RING finger) family protein

Appendix 5. Growth measurement of homozygote T-DNA insertion lines listed in Table 2.2 under ionic stresses

Homozygous T-DNA lines of SALK_049022C (*bHLH122*), SALK_066615 (*ANAC047*), SALK_107191C (*CML44*), SALK_061769C (*LRR-RLK*) and SALK_090958C (*bHLH064*), were identified using the primer sets shown in Appendix 6. Together with *cax1*, *cax1/cax3* and wild-type Col-0, these SALK lines were grown hydroponically following the methods described in Section 2.2.2 for 2 weeks, and transferred into BNS plus 1 mM $MnCl_2$ / 25 mM $MgCl_2$, or Ca^{2+}-depleted BNS for another week in short-day conditions (9 hr light/15 hr dark, 22 ºC).

1 mM $MnCl_2$

25 mM $MgCl_2$

Ca depleted
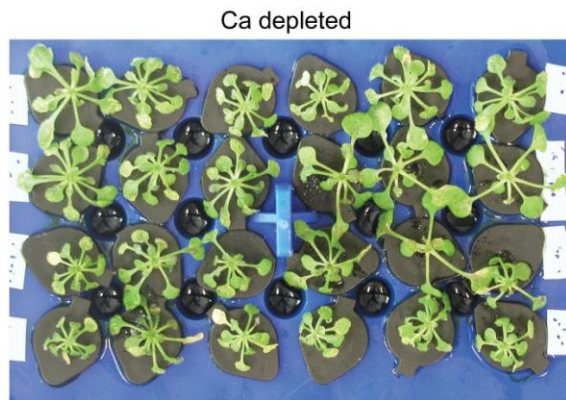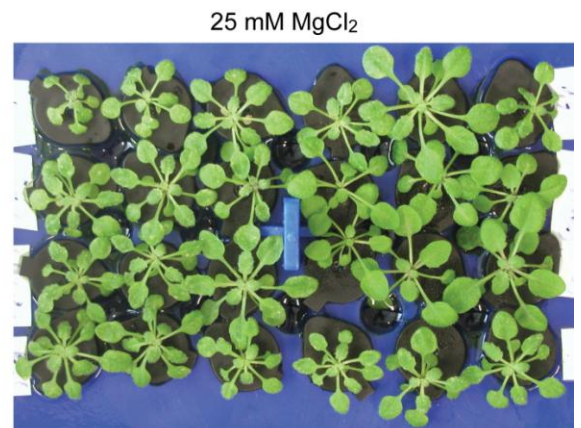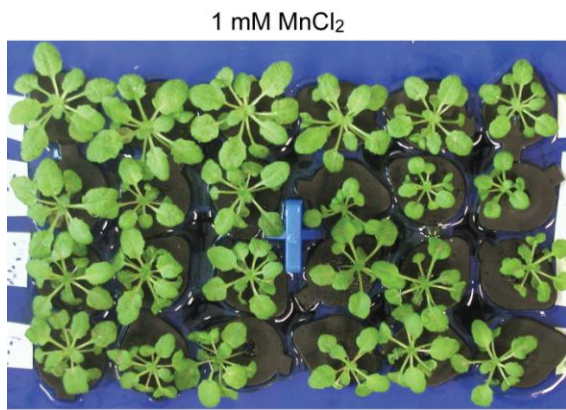
SALK_049022C	SALK_090958C
SALK_066615	*cax1/cax3*
SALK_107191C	*cax1*
SALK_061769C	Col-0

The T-DNA lines of SALK_041710C (*CML35*), SALK_141414 (*bHLH137*) and SALK_001597 (*ANAC016*) (homozygote identified using primer sets as shown in Appendix 6) together with wild-type Col-0, were grown hydroponically following method as described in Section 2.2.2 for 3 weeks, and transferred into low (300 µM), normal (2 mM) and high (25 mM) calcium conditions for 2 weeks in short-day conditions (9 hr light/15 hr dark, 22 ℃).
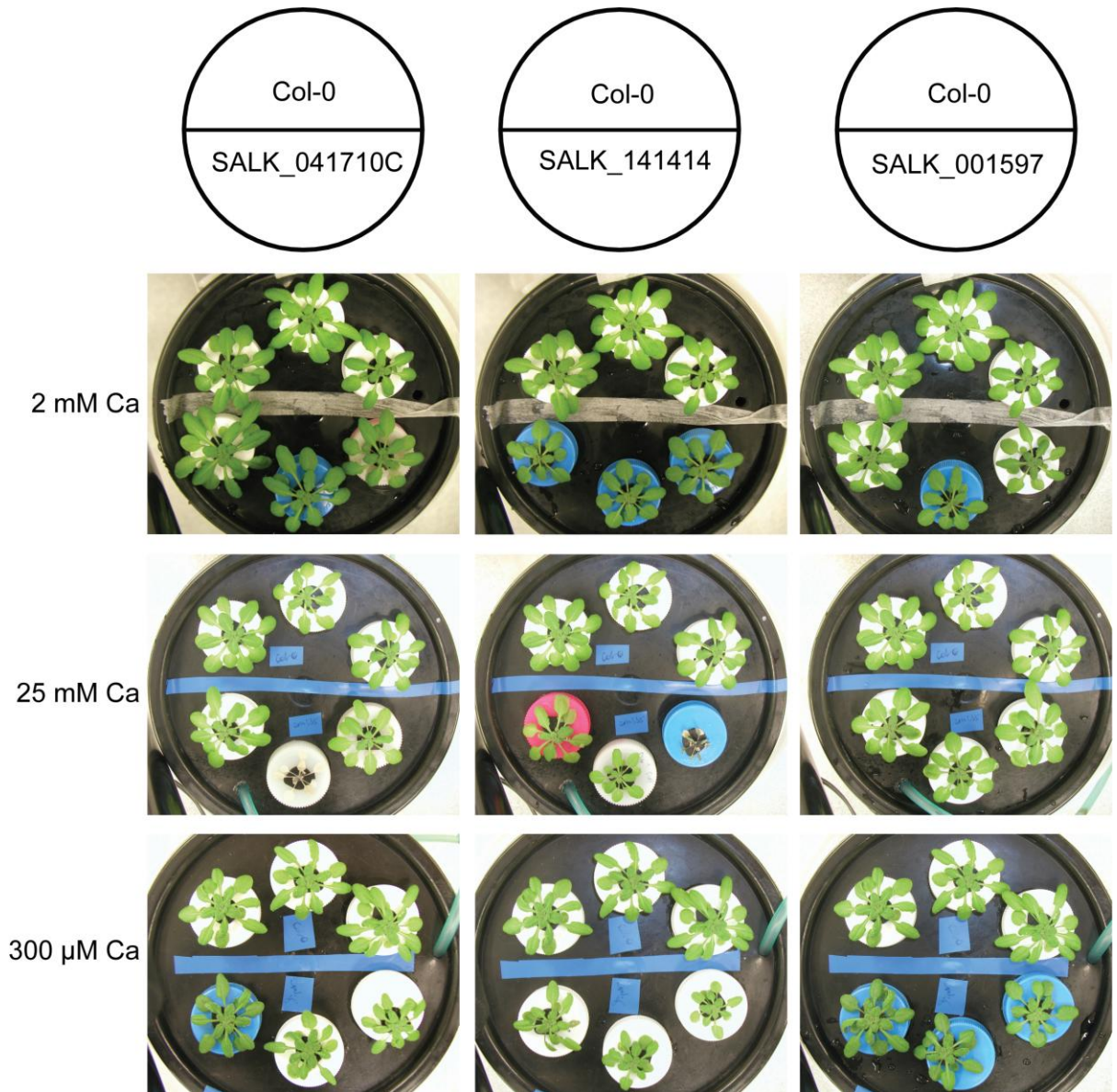
Appendix 6. Primers used to screen homozygote T-DNA insertion lines listed in Table 2.2

All the T-DNA insertion lines have been identified as homozygous lines before undergoing the hydroponic growth test in Appendix 5

T-DNA lines	Gene locus	Gene	Left border Primer (LP, 5'-3')	Right border Primer (RP, 5'-3')	Tm* (ºC)	BP¶+RP product size	LP+BP Product size
SALK_001597C	At1g34180	*ANAC016*	CTGATGAGAACTGGCTCCTTG	TCTCAATGAAATCCCAGATGC	57	492-792 bp	90 bp
SALK_066615	At3g04070	*ANAC047*	TTGAAACGGAAATTTTGTGTTC	GCTCTGTTTGGTCTTGCTCC	57	529-829 bp	1187 bp
SALK_090958C	At2g18300	*bHLH064*	TGTTCATAAGGACATGCCCAC	TGCTGTTGTTGCTGTTGTACC	57	480-780 bp	931 bp
SALK_049022C	At1g51140	*bHLH122*	TTCCTCCAAAACCTCCCATAC	AAAAATGTTAACGTGGTCCCC	58	554-854 bp	1134 bp
SALK_141414C	At5g50915	*bHLH137*	GCCTTCCCTGTTACCTATTCG	TCTAACATAAATTACCCGCCG	57	435-735 bp	149 bp
SALK_041710C	At2g41410	*CML35*	AAAAGGCTCATGCAAATGTTG	TTCAAGGCTGATACAACCACC	57	574-874 bp	1196 bp
SALK_107191C	At1g21550	*CML44*	TTCACAGGGAAAAATCCACTG	TCGAATCATTCTCCCACAATC	57	568-868 bp	1151 bp
SALK_061769C	At4g08850	*LRR-RLK*	TCCCCAATCTCACTTTTGTTG	GAAGGGATTTTGCCTGATAGC	57	642-942 bp	1282 bp

*Primer Tm as calculated by NetPrimer (http://www.premierbiosoft.com/netprimer/index.html)

¶BP = left Border Primer of the T-DNA insertion (5'-ATTTTGCCGATTTCGGAAC-3') and Tm = 57.7 ºC.
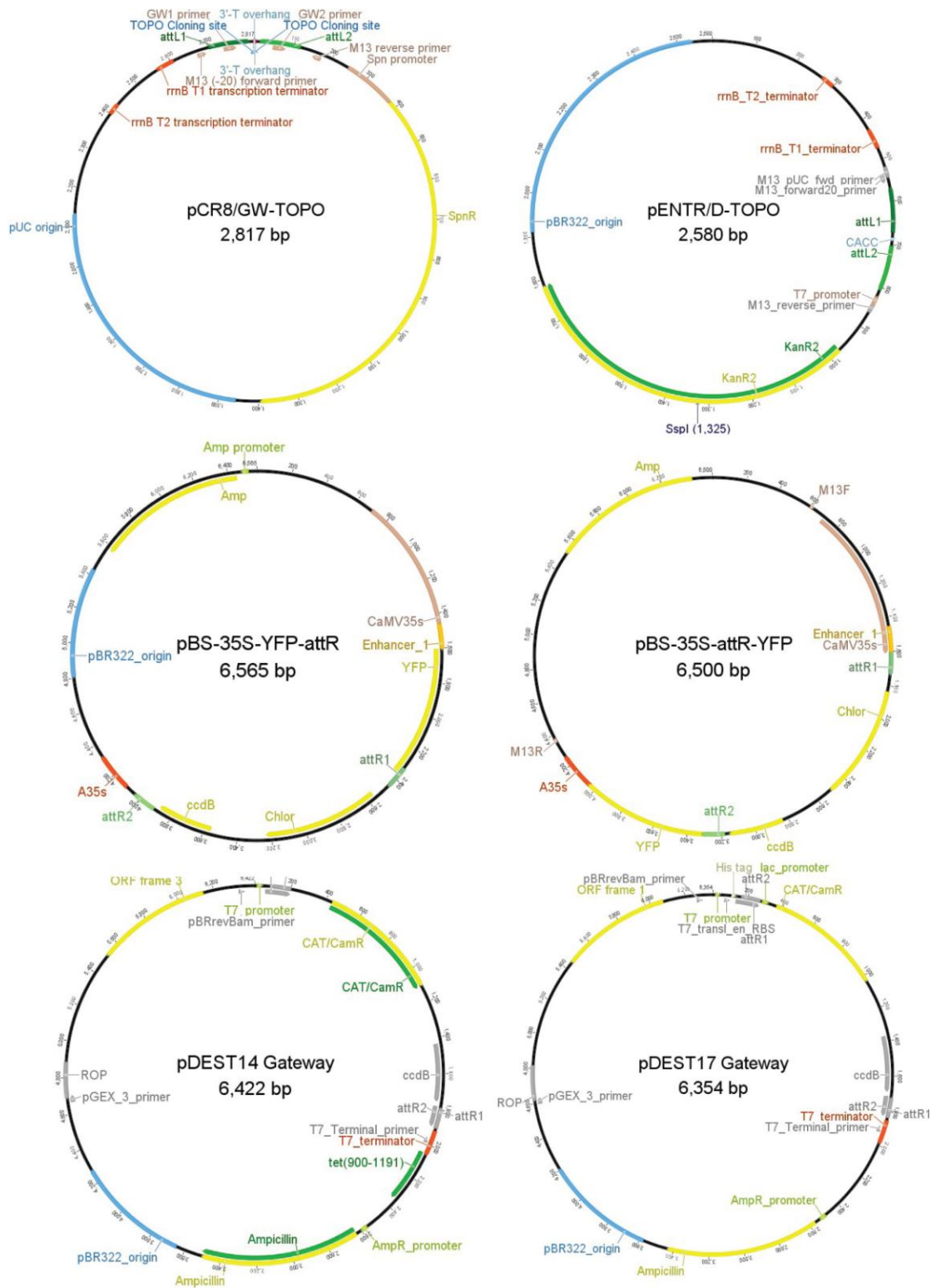
Appendix 7. List of generated PCR cloning products, entry clones and LR-recombinant destination vectors

PCR products	Entry clones	LR-recombinant destination vectors	Description
CML41FL	pCR8/GW/TOPO-*CML41FL*	pDEST565	Protein expression vector of *E. coli* with 6×His-GST tag fused on Gateway (GW) N-terminal site
		pDEST566	
		pDuExAn6	
		pGPTVII-Bar.YN-GW	Plant transient expression vector with YFP fused on GW N-terminal site
		pGPTVII-Hyg.YC-GW	
		pMDC32	
CML41FL-stop	pCR8/GW/TOPO-*CML41FL*-stop	pBS 35S attR-YFP	Binary vector with N-terminal fragment of YFP (YFP^N) fused on GW N-terminal site and with basta selection in plant
		pDuExD7	
		pGPTVII-Bar.GW-YN	
		pGPTVII-Hyg.GW-YC	Binary vector with GFP fused on GW C-terminal site and with hygromycin-B selection in plant
		pMDC83	
		pUC-SPYNE/GW	Plant expression vector with C-terminal fragment of YFP (YFP^C) fused on GW C-terminal site
		pUC-SPYCE/GW	
CML41S	pENTR/D/TOPO-*CML41S*	pDEST565	
		pDEST566	Plant transient expression vector with YFP fused on GW C-terminal site
		pBS 35S attR-YFP	
		pDuExAn6	Binary vector with YFP^C fused on GW N-terminal site and with hygromycin-B selection in plant
		pGPTVII-Bar.YN-GW	
		pGPTVII-Hyg.YC-GW	
		pMDC32	Plant expression vector with two C-terminal fragments of *Renilla reniformis* luciferase (Luc^C) fused on GW N-and C-terminal site separately
CML41S-stop	pENTR/D/TOPO-*CML41S*-stop	pDuExD7	
		pGPTVII-Bar.GW-YN	
		pGPTVII-Hyg.GW-YC	Binary vector with YFP^C fused on GW C-terminal site and with hygromycin-B selection in plant
		pMDC83	
		pUC-SPYCE/GW	
		pUC-SPYNE/GW	

Continued

CML41FLΔ1-46	pENTR/D/TOPO-*CML41FLΔ1-46*	pDEST14	Protein expression vector of *E. coli* with tag-free and GW site
		pDEST17	
		pDEST565	Protein expression vector of *E. coli* with 6×His-MBP tag fused on GW N-terminal site
		pDEST566	
CML41SΔ1-46	pENTR/D/TOPO-*CML41SΔ1-46*	pDEST14	
		pDEST17	Protein expression vector of *E. coli* with 6×His tag fused on GW N-terminal site
		pDEST565	
		pDEST566	
CML41FLΔ1-46-stop	pENTR/D/TOPO-*CML4FLΔ1-46*-stop	pBS 35S attR-YFP	Plant expression vector with N-terminal fragment of *Renilla reniformis* luciferase (Luc^N) fused on GW N-terminal site
CML41SΔ1-46-stop	pENTR/D/TOPO-*CML41SΔ1-46*-stop	pBS 35S attR-YFP	
TCP14	pENTR/D/TOPO-*TCP14*	pDuExAn6	
		pGPTVII-Bar.YN-GW	Binary vector with YFP^N fused on GW N-terminal site and with basta selection in plant
		pGPTVII-Hyg.YC-GW	
TCP14-stop	pENTR/D/TOPO-*TCP14*-stop	pDuExD7	
		pGPTVII-Bar.GW-YN	
		pGPTVII-Hyg.GW-YC	Plant expression vector with YFP^C fused on GW C-terminal site
		pUC-SPYCE/GW	
		pUC-SPYNE/GW	
CML41-amiRNA#1	pCR8/GW/TOPO-*CML41-amiRNA#1*	pMDC32	Binary vector with GW site, 2×35S promoter driven gene expression and hygromycin-B selection in plants
CML41-amiRNA#2	pCR8/GW/TOPO-*CML41-amiRNA#2*	pMDC32	
proCML41	pCR8/GW/TOPO-*proCML41*	pMDC162	Binary vector with GW site, *GUS* gene driven by the promoter from entry clone and with hygromycin-B selection in plants

Appendix 8. Map of entry and LR-recombinant expression vectors listed in Appendix 7

Continued

pDEST565 Gateway
8,932 bp

pDEST566 Gateway
9,367 bp

pUC-SPYNE/GW cassette B
6,466 bp

pUC-SPYCE/GW cassette B
6,252 bp

pDuExAn6
7,315 bp

pDuExD7
8,643 bp
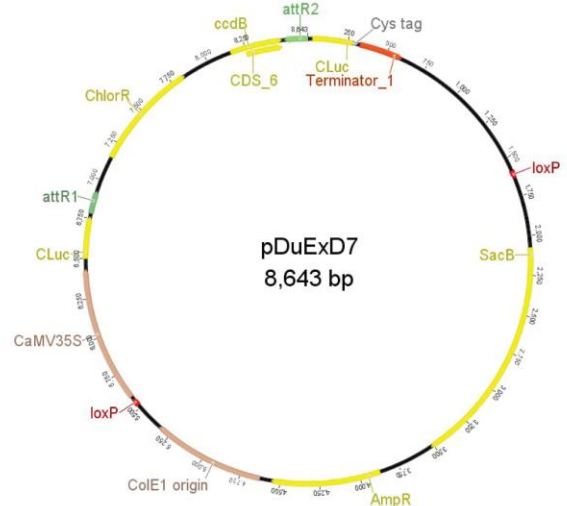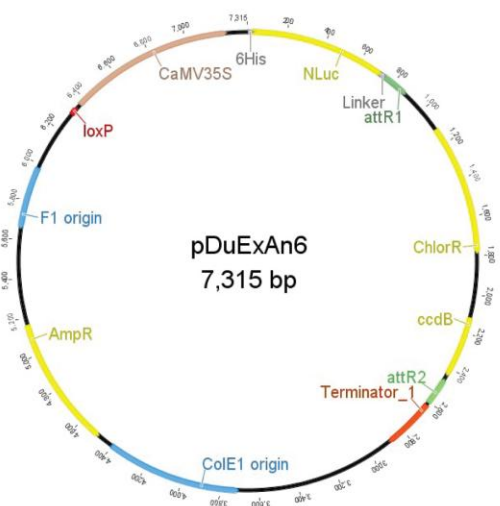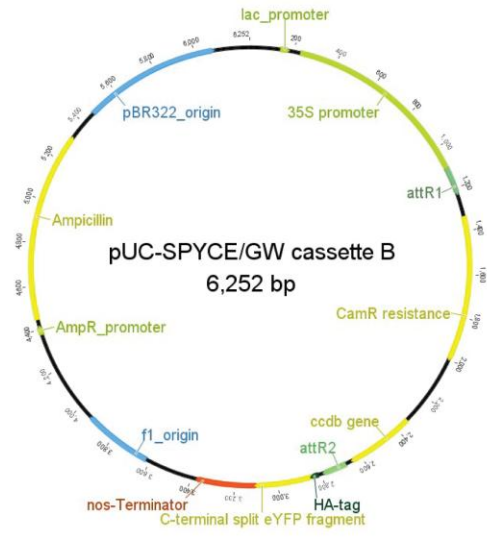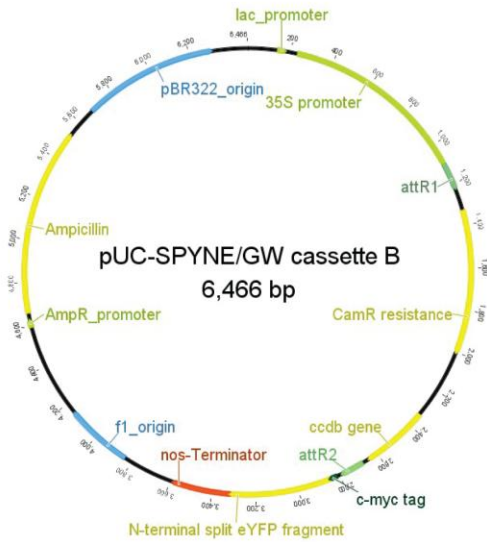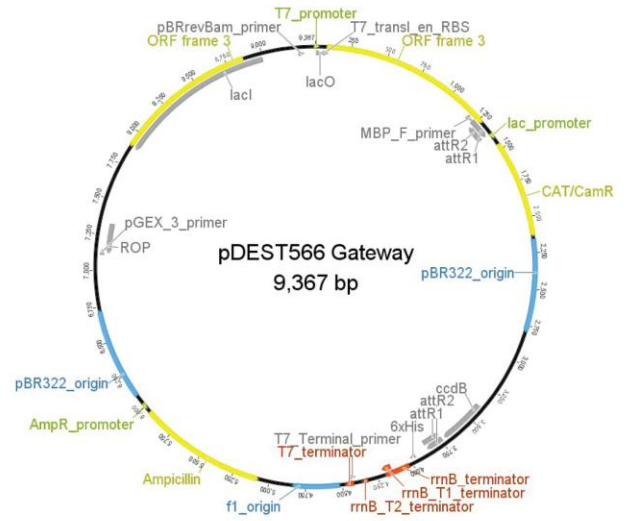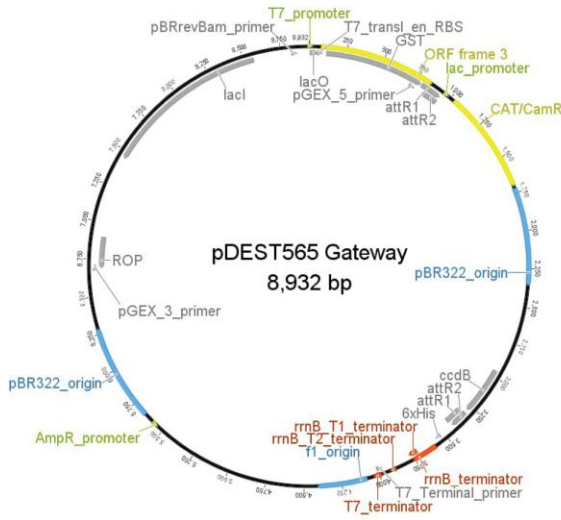
Continued
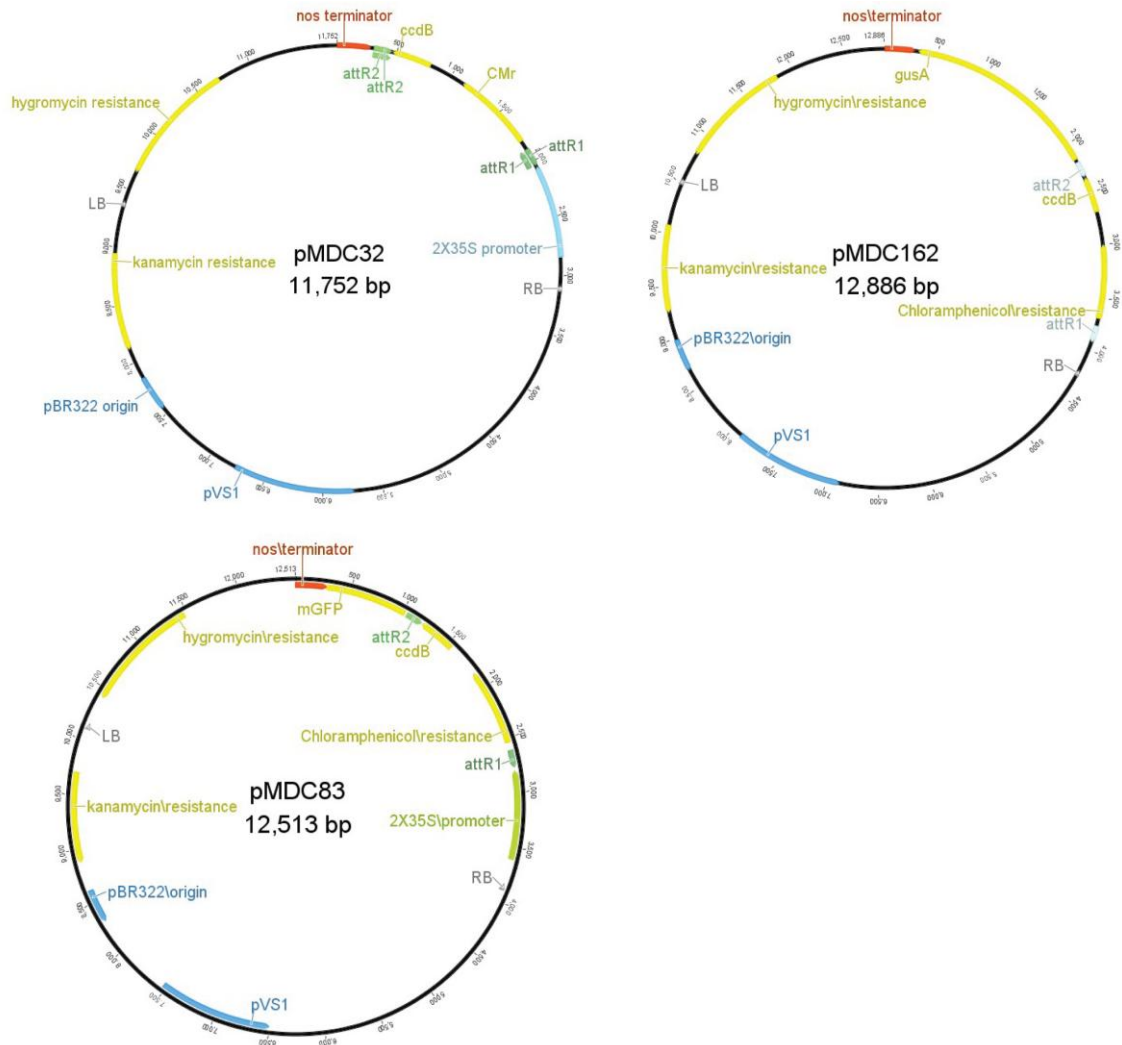
Vector map of pGPTVII-Bar.GW-YC, pGPTVII-Hyg.GW-YC, pGPTVII-Bar.YN-GW and pGPTVII-Hyg.YC-GW are not available on public database, thereby not listed here.

Appendix 9. Nucleotide sequence of *CML41FL* and *S* and amino-acid sequence of CML41FL and S in FASTA format

CML41FL **CDS nucleotide sequence (618 bp)**

ATGGCAACTCAAAAAGAGAAACCTTCCTCCAATTCTTTCAAATGGTTTTCCACCAAAACC
TTAAAGTTAAACCTTAGTTTCCAAAACCGACGAAGATCACCAAAATCAAACTCTTCGTCA
ACCTTAAACTCTCCAAGAAGCAACAGTGATGACAACAACAACATAAAGAGTCACCAGGC
CTCCAAAGAAGAGCTCCGTCAAGTCTTCAGCCATTTCGACAGCGACGGCGACGGTAAGA
TCTCAGCCTTTGAGCTCAGACATTACTTCGGCTCTGTCGGTGAGTATATATCTCACGAGG
CAGCTCAAGAGGCGATAAACGAAGTTGACACTGACGCAGACGGGTCTCTAGGGTTTGAG
GACTTTGTTGGATTGATGACAAGAAGAGATCTTTACGGTGACGGTGAAGTTGATGGCGA
TGGAGAGTTGAAGACAGCGTTTGAGATGTTCGAGGTGGAAAAAGGATCAGGCTGCATAA
CACCAAAGGGTTTGCAAAAGATGCTTGTGAAGTTAGGGGAATCAAGAACGTACGGAGAG
TGTGAAGCCATGATAAAGTTTTACGATATAGATGGTAATGGAATTCTTGATTTTCATGAG
TTTCGTCAAATGATGACGGTTTAG

CML41S **CDS nucleotide sequence (501 bp)**

ATGGCAACTCAAAAAGAGAAACCTTCCTCCAATTCTTTCAAATGGTTTTCCACCAAAACC
TTAAAGTTAAACCTTAGTTTCCAAAACCGACGAAGATCACCAAAATCAAACTCTTCGTCA
ACCTTAAACTCTCCAAGAAGCAACAGTGATGACAACAACAACATAAAGAGTCACCAGGC
CTCCAAAGAAGAGCTCCGTCAAGTCTTCAGCCATTTCGACAGCGACGGCGACGGGTTTG
AGGACTTTGTTGGATTGATGACAAGAAGAGATCTTTACGGTGACGGTGAAGTTGATGGC
GATGGAGAGTTGAAGACAGCGTTTGAGATGTTCGAGGTGGAAAAAGGATCAGGCTGCAT
AACACCAAAGGGTTTGCAAAAGATGCTTGTGAAGTTAGGGGAATCAAGAACGTACGGAG
AGTGTGAAGCCATGATAAAGTTTTACGATATAGATGGTAATGGAATTCTTGATTTTCATG
AGTTTCGTCAAATGATGACGGTTTAG

CML41FL amino-acid sequence (205 aa)

MATQKEKPSSNSFKWFSTKTLKLNLSFQNRRRSPKSNSSSTLNSPRSNSDDNNNIKSHQASKE
ELRQVFSHFDSDGDGKISAFELRHYFGSVGEYISHEAAQEAINEVDTDADGSLGFEDFVGLM

TRRDLYGDGEVDGDGELKTAFEMFEVEKGSGCITPKGLQKMLVKLGESRTYGECEAMIKFY
DIDGNGILDFHEFRQMMTV

CML41S amino-acid sequence (166 aa)

MATQKEKPSSNSFKWFSTKTLKLNLSFQNRRRSPKSNSSSTLNSPRSNSDDNNNIKSHQASKE
ELRQVFSHFDSDGDGFEDFVGLMTRRDLYGDGEVDGDGELKTAFEMFEVEKGSGCITPKGL
QKMLVKLGESRTYGECEAMIKFYDIDGNGILDFHEFRQMMTV

Appendix 10. Full list of CML41 expression in 261 perturbations created by Genevestigator

Dataset: 290 perturbations (sample selection: AT-SAMPLES-1)
1 gene (gene selection: AT-GENES-1)

● AT3G50770

261 of 2213 perturbations fulfilled the filter criteria

Filter values for ● AT3G50770

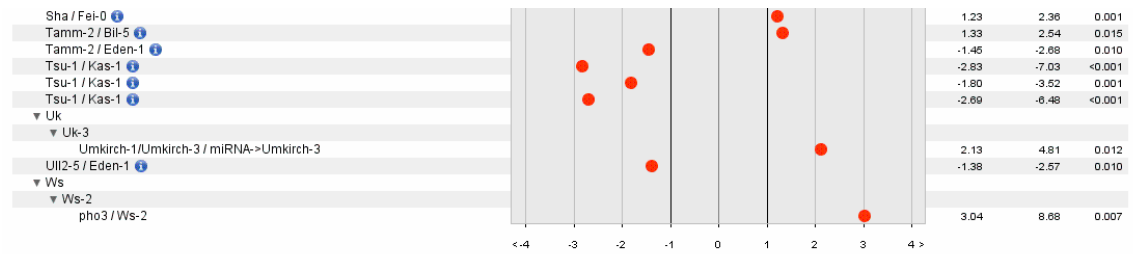| Arabidopsis thaliana (261)	Log(2)-ratio	Fold-Change	p-value
▼ Biotic			
B. cinerea / non-infected rosette leaf samples	3.04	14.01	0.006
B. graminis (ataf1-1) / non-infected rosette leaf samples	2.01	4.04	<0.001
B. graminis (Col-0) / non-infected rosette leaf samples	1.38	2.55	0.005
B. tabaci type B / non-infected rosette tissue samples	3.57	11.86	<0.001
CaLCuV / non-infected rosette leaf samples	3.02	8.09	0.001
E. cichoracearum (pmr4-1) / non-infected pmr4-1 samples	1.67	3.11	0.002
G. cichoracearum study 2 (18h) / non-infected whole rosette samples (Col-0)	1.26	2.53	0.004
G. cichoracearum study 2 (36h) / non-infected whole rosette samples (Col-0)	1.77	3.47	<0.001
G. cichoracearum study 2 (96h) / non-infected whole rosette samples (Col-0)	1.14	2.26	0.001
G. cichoracearum study 3 (18h) / non-infected whole rosette samples (edr1)	1.70	3.13	0.004
G. cichoracearum study 3 (36h) / non-infected whole rosette samples (edr1)	2.46	5.50	0.001
G. cichoracearum study 3 (96h) / non-infected whole rosette samples (edr1)	1.39	2.55	0.014
G. orontii study 6 (Col-0) / untreated rosette leaf samples (Col-0)	1.95	4.61	0.008
G. orontii study 6 (Col-0) / untreated rosette leaf samples (Col-0)	1.89	4.42	0.009
G. orontii study 6 (eds16-1) / untreated rosette leaf samples (eds16-1)	1.47	2.84	<0.001
G. orontii study 6 (eds16-1) / untreated rosette leaf samples (eds16-1)	1.24	2.41	<0.001
H. arabidopsidis (4dpi + 6dpi) / mock treated cotyledon samples	1.96	4.01	0.039
H. arabidopsidis study 4 (rpp4) / untreated seedling samples (rpp4)	2.60	5.91	0.016
H. arabidopsidis study 5 (rpp4) / untreated seedling samples (rpp4)	3.80	13.54	0.008
P. infestans (12h) / mock treated leaf samples (12h)	4.17	18.29	<0.001
P. infestans (6h) / mock treated leaf samples (6h)	4.68	25.50	<0.001
P. syringae pv. maculicola (Col-0) / mock treated leaf samples (Col-0)	4.56	22.35	<0.001
P. syringae pv. phaseolicola (24h) / mock inoculated leaf samples (24h)	1.07	2.10	<0.001
P. syringae pv. phaseolicola (6h) / mock inoculated leaf samples (6h)	0.98	2.03	0.025
P. syringae pv. syringae (OE7a-1) / non-infected leaf samples (OE7a-1)	3.30	9.83	0.003
P. syringae pv. syringae study 2 (Col-0) / P. syringae pv. syringae (Col-0)	1.42	2.68	0.004
P. syringae pv. syringae study 2 (OE7a-1) / non-infected leaf samples (OE7a-1)	3.36	10.22	0.002
P. syringae pv. tomato study 11 (penta) / untreated leaf disc samples (penta)	1.16	2.15	0.026
P. syringae pv. tomato study 12 (atgsnor1-1) / untreated leaf tissue samples (at...	3.68	13.60	0.018
P. syringae pv. tomato study 12 (Col-0) / untreated leaf tissue samples (Col-0)	3.59	11.83	0.005
P. syringae pv. tomato study 12 (sid2) / untreated leaf tissue samples (sid2)	4.60	23.97	0.003
P. syringae pv. tomato study 15 (DC3000) / P. syringae pv. tomato study 13 (DC...	1.10	2.18	0.006
P. syringae pv. tomato study 2 (DC3000 avrRpm1) / P. syringae pv. tomato study...	1.02	2.00	0.006
P. syringae pv. tomato study 3 (DC3000 avrRpm1) / mock inoculated leaf sampl...	2.12	4.44	<0.001
P. syringae pv. tomato study 3 (DC3000 hrcC-) / mock inoculated leaf samples (...	1.71	3.35	0.002
P. syringae pv. tomato study 3 (DC3000) / mock inoculated leaf samples (24h)	2.51	5.75	<0.001
P. syringae pv. tomato study 5 (Col-0) / non-infected leaf samples (Col-0)	3.13	7.11	0.018
P. syringae pv. tomato study 5 (gh3.5-1D) / non-infected leaf samples (gh3.5-1D)	3.47	11.14	<0.001
P. syringae pv. tomato study 8 (DC3000) / mock inoculated leaf samples	3.41	10.26	0.008
R. solani (AG8) / mock inoculated whole plant samples	1.90	4.25	0.026
TuMV (zone 0) / leaf sap treated leaf samples	2.05	4.76	0.023
▼ Chemical			
antimycin A (AOX1a:LUC) / mock treated shoot samples (AOX1a:LUC)	1.58	2.99	<0.001
benzothiadiazole (Col-0) / mock treated rosette tissue samples (Col-0)	2.44	5.41	<0.001
benzothiadiazole (mil4) / mock treated rosette tissue samples (mil4)	2.98	7.51	0.002
benzothiadiazole study 2 / mock treated rosette tissue samples (mil4oe)	2.97	7.72	<0.001
cloransulam-methyl (24h) / mock treated leaf samples (24h)	3.37	10.30	<0.001
clothianidin (4d) / mock treated Col-0 rosette leaf samples (4d)	2.09	4.41	0.035
CMP (24h) / solvent treated root culture samples (24h)	4.35	20.97	<0.001
CMP (4h) / solvent treated root culture samples (4h)	2.68	6.58	<0.001
cycloheximide / mock treated seedlings	4.29	19.67	<0.001
cycloheximide study 4 (pBeaconRFP_GR-ABI3) / mock treated root protoplast s...	1.20	2.27	0.007
dexamethasone study 5 (ORS1-DEX) / mock treated rosette samples (ORS1-D...	1.46	2.71	0.050
DFPM (Col-0) / solvent treated seedling samples (Col-0)	2.65	6.95	0.029
fenclorim (24h) / solvent treated root culture samples (24h)	3.16	9.12	<0.001
fenclorim (4h) / solvent treated root culture samples (4h)	1.00	2.00	0.007
imazapyr (24h) / mock treated leaf samples (24h)	2.35	5.12	<0.001
imidacloprid (4d) / mock treated Col-0 rosette leaf samples (4d)	3.38	10.75	0.014
Na2S (Col-0) / untreated Col-0 rosette leaf samples	1.52	2.88	<0.001
Na2S (des1-1) / untreated des1-1 rosette leaf samples	-3.41	-10.61	<0.001
ozone / air treated seedlings	2.77	7.01	<0.001
ozone study 3 (agb1-2 gpa1-4) / fresh air treated leaf samples (agb1-2 gpa1-4)	2.34	3.58	0.031
ozone study 3 (Col-0) / fresh air treated leaf samples (Col-0)	2.00	3.25	0.029
paclobutrazol study 4 (p35S:HF-RPL18) / untreated p35S:HF-RPL18 rosette sa...	1.60	3.02	0.005
phenanthrene / untreated Col plant samples	1.33	2.51	<0.001
primisulfuron-methyl (24h) / mock treated leaf samples (24h)	4.05	16.35	<0.001
sulfometuron methyl (24h) / mock treated leaf samples (24h)	4.11	17.32	<0.001
syringolin study 2 / solvent treated leaf samples (syl_404_bc2)	-2.46	-5.57	0.011
uniconazole study 2 (pkl) / solvent treated seed samples (pkl)	1.07	2.11	<0.001
▼ Elicitor			
EF-Tu (elf18) study 3 (Col-0) / mock treated seedling samples (Col-0)	0.96	2.01	0.031
EF-Tu (elf18) study 3 (ein2-1) / mock treated seedling samples (ein2-1)	1.46	2.89	0.023
EF-Tu (elf18) study 4 (Col-0) / mock treated seedling samples (Col-0)	2.03	4.09	<0.001
EF-Tu (elf18) study 4 (ein2-1) / mock treated seedling samples (ein2-1)	1.23	2.37	0.010
FLG22 study 11 (2h) / FLG22 study 11 (0h)	-1.07	-2.06	0.006
FLG22 study 5 (35S:miR393) / untreated leaf disc samples (35S:miR393)	1.87	3.70	0.044
Pep2 (bak1-3) / mock treated seedling samples (bak1-3)	2.03	3.71	0.016
Pep2 (Col-0) / mock treated seedling samples (Col-0)	1.75	3.44	0.003
Pep2 (ein2-1) / mock treated seedling samples (ein2-1)	1.61	3.05	0.003
Pep2 study 2 (bak1-3) / mock treated seedling samples (bak1-3)	3.72	11.84	0.001
Pep2 study 2 (Col-0) / mock treated seedling samples (Col-0)	3.31	10.11	<0.001

Continued

▼ Hormone			
2,4-D + trichostatin A (Ler) / 2,4-D study 2 (Ler)	1.99	3.92	0.017
ABA study 6 (Col-0) / untreated plant samples (Col-0)	1.87	3.62	<0.001
ABA study 6 (srk2cf) / untreated plant samples (srk2cf)	1.07	2.08	0.003
IAA study 7 (C24) / untreated seedling samples (C24)	-1.26	-2.46	0.038
MeJa study 5 (gai) / untreated leaf disc samples (gai)	-4.42	-26.61	0.006
MeJa study 5 (Ler) / untreated leaf disc samples (Ler)	-2.40	-5.63	0.013
MeJa study 5 (penta) / untreated leaf disc samples (penta)	-1.54	-3.02	0.010
OPDA study 2 (Col-0) / solvent treated (Col-0) seedlings	2.90	6.67	0.006
OPDA study 2 (tga2-5-6) / solvent treated (tga2-5-6) seedlings	3.63	11.21	0.002
salicylic acid study 11 (dsr1) / mock treated seedling samples (dsr1)	1.97	3.93	0.003
salicylic acid study 11 (JC66) / mock treated seedling samples (JC66)	2.32	4.88	0.002
salicylic acid study 3 / mock treated seedlings	4.10	17.29	0.001
salicylic acid study 7 (npr1-1 sni1 ssn2-1) / solvent treated whole plant samples...	2.59	6.03	<0.001
salicylic acid study 8 (Col-0) / mock treated leaf samples (Col-0)	1.04	2.07	<0.001
zeatin study 3 (ARR22ox) / untreated whole plant samples (ARR22ox)	2.05	4.15	<0.001
▼ Light intensity			
dark / 21°C (140-200min) / moderate light / 21°C (140-200min)	1.27	2.47	0.001
dark / 21°C (220-280min) / moderate light / 21°C (220-280min)	1.47	2.77	<0.001
dark / 21°C (300-360min) / moderate light / 21°C (300-360min)	1.60	3.10	0.009
dark / 21°C (640 and 1280min) / moderate light / 21°C (640 and 1280min)	1.65	3.09	0.027
dark / 32°C (220-280min) / dark / 21°C (220-280min)	1.18	2.29	0.001
dark / 32°C (300-360min) / dark / 21°C (300-360min)	1.60	2.99	<0.001
high light study 7 (atwrky40) / untreated leaf samples (atwrky40)	-1.37	-2.58	<0.001
▼ Light quality			
red study 3 (1h) / dark grown seedlings (Col-0)	-1.01	-2.09	0.025
red study 3 (45h) / dark grown seedlings (Col-0)	-1.33	-2.61	0.002
UV filtered WG295 (1h) / seedlings irradiated with 327nm cut-off (1h)	1.03	2.01	0.006
UV filtered WG295 (6h) / seedlings irradiated with 327nm cut-off (6h)	2.23	4.64	0.017
UV unfiltered max-310nm (1h) / seedlings irradiated with 327nm cut-off (1h)	1.54	2.88	0.001
UV unfiltered max-310nm (6h) / seedlings irradiated with 327nm cut-off (6h)	5.19	35.99	0.003
UV-B (Col-0) / shift LD to CL (Col-0)	2.76	5.71	0.015
UV-B (sng1-1) / shift LD to CL (sng1-1)	2.37	5.18	0.001
UV-B (tt4(C1)) / shift LD to CL (tt4(C1))	3.13	6.97	0.014
▼ Nutrient			
iron deficiency study 13 (bhlh100 bhlh101) / untreated bhlh100 bhlh101 shoot s...	1.22	2.46	0.023
low nitrogen / high nitrogen treated rosette samples	2.32	5.01	<0.001
N depletion (Col-0) / Seedlings grown under N-replete condition (Col-0)	3.43	10.56	<0.001
nitrate starvation / untreated seedlings	4.04	14.63	0.002
P deficiency study 4 (shoot) / mock treated Col-0 shoot samples	-1.08	-2.10	0.032
P deficiency study 5 (6h) / mock treated root samples (6h)	1.83	4.19	0.042
▼ Other			
callus formation study 3 (7d + 1d) / untreated hypocotyl samples (7d)	2.09	4.30	<0.001
▼ Photoperiod			
circadian / ethanol / MG132 study 2 (Col-0) / circadian / ethanol / MG132 (Col-0)	-1.89	-3.70	<0.001
circadian / MG132 study 2 (Alc::TOC1) / circadian / MG132 (Alc::TOC1)	-1.16	-2.24	0.003
long day (Col-0) / short day study 2 (Col-0)	-3.93	-15.44	<0.001
long day (cs26) / short day study 2 (cs26)	2.90	7.53	<0.001
night extension (late) / untreated rosette samples	1.80	3.31	0.007
▼ Stress			
cold study 15 (p35S:HF-RPL18) / total RNA (untreated p35S:HF-RPL18)	1.37	2.80	0.035
cold study 16 (p35S:HF-RPL18) / polysomal RNA (untreated p35S:HF-RPL18)	1.17	2.28	0.004
cold study 6 (Can) / 20°C/18°C treated rosette samples (Can)	1.63	3.06	0.004
cold study 6 (Ler) / 20°C/18°C treated rosette samples (Ler)	-1.88	-3.71	<0.001
cold study 6 (Te) / 20°C/18°C treated rosette samples (Te)	1.48	2.86	0.010
drought study 13 (Tamm-2) / mock treated Tamm-2 rosette leaf samples	-1.41	-2.66	0.016
drought study 7 (Col-0) / untreated plant samples (Col-0)	-1.70	-3.26	0.007
drought study 7 (srk2cf) / untreated plant samples (srk2cf)	-1.57	-2.99	0.005
heat study 5 / untreated plant samples	1.25	2.40	0.038
light/drought (aox1a(sail)) / untreated leaf samples (aox1a(sail))	3.34	10.09	0.003
osmotic (late) / untreated green tissue samples (late)	1.16	2.76	0.017
salt study 4 (Ws) / Hoagland solution watered Ws leaf samples	1.10	2.12	0.029
submergence study 2 (24h) / rosette samples of Col-0 shifted to darkness (24h)	2.23	4.76	0.014
submergence study 2 (7h) / rosette samples of Col-0 shifted to darkness (7h)	3.50	11.32	0.004
wounding (late) / untreated green tissue samples (late)	1.42	2.71	<0.001
▼ Genetic Background			
Ag-0 / Bil-5 ⓘ	1.72	3.52	0.040
Ag-0 / Omo2-3 ⓘ	1.59	3.25	0.042
▼ Bay-0			
Bay-0 parent / C24 ⓘ	1.32	2.44	0.008
Bay-0 parent / Col-0 ⓘ	1.36	2.54	0.003
Bay-0 parent / Fei-0 ⓘ	1.06	2.09	0.002
Bl-1 / C24 ⓘ	-1.44	-2.74	0.007
▼ Bla			
Bla-1 / Bla-1/Hh-0	-3.55	-11.64	<0.001
Bur-0 / Ws-2 ⓘ	1.36	2.54	0.012
▼ C24			
C24 / Bur-0 ⓘ	1.24	2.39	0.010
C24 / Col-0 ⓘ	1.36	2.69	0.019
C24 / Col-0 ⓘ	1.59	3.08	0.003
C24 / Col-0 ⓘ	1.56	2.96	<0.001
C24 / Fei-0 ⓘ	1.36	2.71	0.016
C24 / Fei-0 ⓘ	1.49	2.85	0.019
C24_CAB2::LUC_CaMV35S::AEQ / toc1-1 ⓘ	-1.20	-2.31	0.025
CIBC-17 / Ws-2 ⓘ	1.56	3.20	0.047
▼ Col			
▼ Col(gl1)			
▼ Col(gl1) pRD29A::LUC			
sta1-1 / Col(gl1) pRD29A::LUC	1.60	3.02	0.024
▼ pCBF3::LUC			
ice1 / pCBF3::LUC ⓘ	1.63	3.20	0.048
ice1 / pCBF3::LUC ⓘ	1.14	2.22	0.037
▼ Col-0			
35S-AtMYB44 / Col-0 ⓘ	-2.33	-5.21	0.032
35S::amiR-mads-2(MIR319a)_strong / Col-0	1.52	2.88	0.003
abi4-102 / Col-0 ⓘ	1.14	2.20	<0.001
abi4-102 / Col-0 ⓘ	1.91	4.52	0.045
abi4-102 vtc2-1 / Col-0	1.68	3.62	0.015

Continued

ahk3/ahk4 / Col-0	1.22	2.33	0.001
Alc::TOC1 / Col-0 ⓘ	-1.40	-2.63	0.001
Alc::TOC1 / Col-0 ⓘ	-1.02	-2.03	0.002
arf6-2 arf8-3 / Col ⓘ	-1.55	-2.81	0.036
ARR21Cox / Col-0	3.00	7.99	<0.001
ARR22ox / Col-0 ⓘ	1.07	2.09	0.008
ARR22ox / Col-0 ⓘ	2.25	4.77	<0.001
atcesA6 / atcesA4	1.70	3.20	0.018
atgsnor1-3 / Col-0 ⓘ	-1.07	-2.10	0.001
atwrky40 / Col-0	1.23	2.36	<0.001
AtWRKY63 OE1 / Col-0 ⓘ	1.71	3.34	0.001
cax1-1 cax3-1 / Col-0	3.79	13.73	<0.001
cs26 / Col-0 ⓘ	4.68	25.98	<0.001
cs26 / Col-0 ⓘ	-2.15	-4.48	<0.001
dcl3-1 / Col-0	1.24	2.32	0.004
des1-1 / Col-0 ⓘ	4.07	16.82	<0.001
des1-1 / Col-0 ⓘ	1.01	2.03	0.003
efr-1 / Col-0 ⓘ	-1.32	-2.33	0.038
flu / Col-0	1.42	2.68	<0.001
flu/over-tAPX / Col-0	1.55	2.94	0.010
gh3.5-1D / Col-0 ⓘ	-1.25	-2.40	0.011
gun4-1 / Col-0 ⓘ	-1.97	-3.91	0.002
HSP90(RNAi-A1) / Col-0	-1.04	-2.12	0.021
K16331 / BIG	1.93	3.99	0.015
▼ lecrk-VI.2-1			
35S:LecRK-VI.2 / Col-0	3.66	12.61	<0.001
mkk1/mkk2 / Col-0	4.00	16.00	<0.001
myb21-5 myb24-5 / Col ⓘ	-2.18	-4.87	0.001
myb3r1-1 myb3r4-1 / Col-0	1.18	2.16	0.037
npr1-1 sni1 brca2a / npr1-1 sni1 ⓘ	1.01	2.01	0.001
npr1-1 sni1 ssn2-1 / npr1-1 sni1 ⓘ	-2.53	-5.79	<0.001
nudt7-1 / Col-0	2.69	7.92	0.013
nudt7-1 eds1-2 / nudt7-1	-3.08	-10.40	0.008
nudt7-1 sid2-1 / nudt7-1 eds1-2	4.92	30.95	<0.001
nudt7-1 sid2-1 / Col-0	4.53	23.57	<0.001
nudt7-1 sid2-1 eds1-2 / nudt7-1	-3.01	-9.78	0.010
nudt7-1 sid2-1 eds1-2 / nudt7-1 sid2-1	-4.85	-29.10	<0.001
OE7a-1 / Col-0 ⓘ	-1.67	-3.19	<0.001
pad4 / npr1-1	-2.48	-4.44	0.022
pad4 / pad2	-2.25	-3.78	0.029
pad4 / ein2	-2.09	-3.39	0.038
pad4 / Col-0	-2.66	-5.00	0.017
pepr1-1 pepr2-3 / Col-0 ⓘ	-1.66	-3.09	0.015
pepr1-1 pepr2-3 / Col-0 ⓘ	-2.34	-5.04	0.002
pifq / Col-0 ⓘ	-1.32	-2.59	<0.001
pmr4-1 / Col-0 ⓘ	-1.25	-2.38	0.007
pmr5;pmr6 / Col-0	1.16	2.28	0.017
psad1-1 / Col-0	-2.69	-7.02	0.019
psad1-1/stn7-1 / Col-0	-2.57	-6.39	0.006
rpp4 / Col-0 ⓘ	2.12	4.21	0.031
sid2 / pad4	2.73	5.31	0.017
sph1 / Col-0 ⓘ	1.84	3.66	0.003
sph1 / Col-0 ⓘ	1.10	2.14	0.027
tbf1 / Col-0 ⓘ	-1.08	-2.11	0.001
vtc2-1 / Col-0 ⓘ	2.09	4.87	0.014
▼ Col-1			
immutans / Col-1	3.43	10.80	<0.001
Col-2 / NFA-10 ⓘ	-1.79	-3.28	0.041
ein2-1 / Col-0 ⓘ	-1.15	-2.19	0.007
Eden-1 / Bil-5 ⓘ	2.00	4.64	0.034
Eden-1 / Bil-5 ⓘ	1.75	3.38	0.002
Got-22 / Eden-1 ⓘ	-1.18	-2.25	0.016
Hh-0 / Bla-1/Hh-0	-3.24	-9.37	<0.001
▼ Ler			
ckh2-1 / Ler ⓘ	1.21	2.32	0.005
gai / penta ⓘ	-1.07	-2.06	0.016
▼ Ler-0			
ctr1 / Ler	-2.52	-5.56	0.006
elo3 / Ler-0	1.57	2.96	<0.001
mpk4: ctr1 / Ler	1.26	2.40	0.003
Ler-1 / CIBC-17 ⓘ	-1.26	-2.39	0.045
Ler-1 / NFA-10 ⓘ	-2.28	-5.44	0.032
Ler-1 / NFA-10 ⓘ	-1.58	-3.16	0.016
phyABCDE / Ler ⓘ	1.46	2.86	0.011
phyABCDE / Ler ⓘ	1.49	2.92	0.029
phyABDE / Ler ⓘ	2.14	4.49	0.001
phyABDE / Ler ⓘ	1.97	3.94	<0.001
rga-delta17 / empty cassette ⓘ	2.51	5.69	<0.001
Mir-0 / Mir-0/Se-0	-4.19	-17.95	<0.001
NFA-10 / Ws-2 ⓘ	1.97	4.07	0.011
NFA-10 / Ts-1 ⓘ	1.23	2.51	0.027
▼ not specified strain			
▼ C24 x Col-0			
C24 x Col-0 F1 hybrid / C24	-1.65	-3.15	<0.001
edr1 / Col-0 ⓘ	1.02	2.17	0.019
edr1 / Col-0 ⓘ	1.46	2.68	0.005
edr1 / Col-0 ⓘ	1.71	3.44	0.002
edr1 / Col-0 ⓘ	1.27	2.45	0.007
QK / Ws ⓘ	-1.28	-2.44	0.021
vip3 / n.s	1.19	2.29	0.031
Omo2-3 / Eden-1 ⓘ	-1.63	-3.12	0.002
Se-0 / Mir-0/Se-0	-4.24	-18.94	<0.001
Sha / C24 ⓘ	-1.38	-2.66	0.004
Sha / Col-0 ⓘ	1.63	3.36	0.027
Sha / Col-0 ⓘ	0.99	2.02	0.033
Sha / Col-0 ⓘ	1.06	2.08	0.006
Sha / Fei-0 ⓘ	1.63	3.39	0.024

Continued

Sha / Fei-0	1.23	2.36	0.001
Tamm-2 / Bil-5	1.33	2.54	0.015
Tamm-2 / Eden-1	-1.45	-2.68	0.010
Tsu-1 / Kas-1	-2.83	-7.03	<0.001
Tsu-1 / Kas-1	-1.80	-3.52	0.001
Tsu-1 / Kas-1	-2.69	-6.48	<0.001
▼ Uk			
▼ Uk-3			
Umkirch-1/Umkirch-3 / miRNA->Umkirch-3	2.13	4.81	0.012
Ull2-5 / Eden-1	-1.38	-2.57	0.010
▼ Ws			
▼ Ws-2			
pho3 / Ws-2	3.04	8.68	0.007

created with GENEVESTIGATOR

195

References

Abel, S., Nguyen, M. D., & Theologis, A. (1995). The *PS-IAA4/5*-like family of early auxin-inducible mRNAs in *Arabidopsis thaliana*. *Journal of Molecular Biology*, *251*(4), 533-549.

Åkesson, A., Persson, S., Love, J., Boss, W. F., Widell, S., & Sommarin, M. (2005). Overexpression of the Ca^{2+}-binding protein calreticulin in the endoplasmic reticulum improves growth of tobacco cell suspensions (*Nicotiana tabacum*) in high-Ca^{2+} medium. *Physiologia Plantarum*, *123*(1), 92-99.

Amari, K., Boutant, E., Hofmann, C., Schmitt-Keichinger, C., Fernandez-Calvino, L., Didier, P., Lerich, A., Mutterer, J., Thomas, C. L., Heinlein, M., Mély, Y., Maule, A. J., & Ritzenthaler, C. (2010). A family of plasmodesmal proteins with receptor-like properties for plant viral movement proteins. *PLoS Pathogens*, *6*(9), e1001119.

Ali, R., Ma, W., Lemtiri-Chlieh, F., Tsaltas, D., Leng, Q., von Bodman, S., & Berkowitz, G. A. (2007). Death don't have no mercy and neither does calcium: *Arabidopsis* CYCLIC NUCLEOTIDE GATED CHANNEL 2 and innate immunity. *Plant Cell*, *19*(3), 1081-1095.

Ali, R., Zielinski, R. E., & Berkowitz, G. A. (2006). Expression of plant cyclic nucleotide-gated cation channels in yeast. *Journal of Experimental Botany*, *57*(1), 125-138.

Alonso, J. M., Stepanova, A. M., Leisse, T. J., Kim, C. J., Chen, H., Shinn, P., Stevenson, D. K., Zimmerman, J., Barajas, P., Cheuk, R., Gadrinab, C., Heller, C., Jeske, A., Koesema, E., Meyers, C. C., Parker, H., Prednis, L., Ansari, Y., Choy, N., Deen, H., Geralt, M., Hazari, N., Hom, E., Karnes, M., Mulholland, C., Ndubaku, R., Schmidt, I., Guzman, P., Aguilar-Henonin, L., Schmid, M., Weigel, D., Carter, D. E., Marchand, T., Risseeuw, E., Brogden, D., Zeko, A., Crosby, W. L., Berry, C. C., & Ecker J. R. (2003) Genome-wide insertional mutagenesis of *Arabidopsis thaliana*. *Science*, *301*(5633), 653-657.

Arabidopsis Interactome Mapping Consortium. (2011). Evidence for network evolution in an *Arabidopsis* interactome map. *Science*, *333*(6042), 601-607.

Babini, E., Bertini, I., Capozzi, F., Luchinat, C., Quattrone, A., & Turano, M. (2005). Principal component analysis of the conformational freedom within the EF-hand superfamily. *Journal of Proteome Research*, *4*(6), 1961-1971.

Bai, Y., Pavan, S., Zheng, Z., Zappel, N. F., Reinstädler, A., Lotti, C., Giovanni, C. D., Ricciardi, L., Lindhout, P., Visser, R., Theres, K., & Panstruga, R. (2008). Naturally occurring broad-spectrum powdery mildew resistance in a Central American tomato accession is caused by loss of *mlo* function. *Molecular Plant-Microbe Interactions*, *21*(1), 30-39.

Balagué, C., Lin, B., Alcon, C., Flottes, G., Malmström, S., Köhler, C., Neuhaus, G., Pelletier, G., Gaymard, F., & Roby, D. (2003). HLM1, an essential signaling component in the

hypersensitive response, is a member of the cyclic nucleotide–gated channel ion channel family. *Plant Cell*, *15*(2), 365-379.

Baneyx, F., & Mujacic, M. (2004). Recombinant protein folding and misfolding in *Escherichia coli*. *Nature Biotechnology*, *22*(11), 1399-1408.

Barber SA. (1995). *Soil nutrient bioavailability: a mechanistic approach*, (2nd edn). Wiley, New York.

Baxter, I., Hosmani, P. S., Rus, A., Lahner, B., Borevitz, J. O., Muthukumar, B. Mickelbart, M. V., Schreiber L., Franke R. B., & Salt, D. E. (2009). Root suberin forms an extracellular barrier that affects water relations and mineral nutrition in *Arabidopsis*. *PLoS Genetics*, *5*(5), e1000492.

Baxter, I., Tchieu, J., Sussman, M. R., Boutry, M., Palmgren, M. G., Gribskov, M., Harper, J. F., & Axelsen, K. B. (2003). Genomic comparison of P-type ATPase ion pumps in *Arabidopsis* and rice. *Plant Physiology*, *132*(2), 618-628.

Baxter, J., Moeder, W., Urquhart, W., Shahinas, D., Chin, K., Christendat, D., Kang, H. G., Angelova, M., Kato, N., & Yoshioka, K. (2008). Identification of a functionally essential amino acid for *Arabidopsis* cyclic nucleotide gated ion channels using the chimeric *AtCNGC11/12* gene. *Plant Journal*, *56*(3), 457-469.

Bender, K. W., & Snedden, W. A. (2013). Calmodulin-related proteins step out from the shadow of their namesake. *Plant Physiology*, doi:10.1104/pp.113.221069

Benitez-Alfonso, Y., Jackson, D., & Maule, A. (2011). Redox regulation of intercellular transport. *Protoplasma*, *248*(1), 131-140.

Berridge, M. J., Bootman, M. D., & Roderick, H. L. (2003). Calcium signalling: dynamics, homeostasis and remodelling. *Nature Reviews in Molecular Cell Biology*, *4*(7), 517-529.

Berridge, M. J., Lipp, P., & Bootman, M. D. (2000). The versatility and universality of calcium signalling. *Nature Reviews in Molecular Cell Biology*, *1*(1), 11-21.

Beyhl, D., Hörtensteiner, S., Martinoia, E., Farmer, E. E., Fromm, J., Marten, I., & Hedrich, R. (2009). The *fou2* mutation in the major vacuolar cation channel TPC1 confers tolerance to inhibitory luminal calcium. *Plant Journal*, *58*(5), 715-723.

Bhatia, V. (2008). Dietary calcium intake-a critical reappraisal. *The Indian Journal of Medical Research*, *127*(3), 269.

Bhattacharya, S., Bunick, C. G., & Chazin, W. J. (2004). Target selectivity in EF-hand calcium binding proteins. *Biochimica et Biophysica Acta (BBA)-Molecular Cell Research*, *1742*(1), 69-79.

Bittel, P., & Robatzek, S. (2007). Microbe-associated molecular patterns (MAMPs) probe plant immunity. *Current Opinion in Plant Biology*, *10*(4), 335-341.

Blencowe, B. J. (2006). Alternative splicing: new insights from global analyses. *Cell*, *126*(1), 37-47.

Bock, K. W., Honys, D., Ward, J. M., Padmanaban, S., Nawrocki, E. P., Hirschi, K. D., Twell, D., & Sze, H. (2006). Integrating membrane transport with male gametophyte development and function through transcriptomics. *Plant Physiology*, *140*(4), 1151-1168.

Bonaventure, G., Gfeller, A., Proebsting, W. M., Hörtensteiner, S., Chételat, A., Martinoia, E., & Farmer, E. E. (2007). A gain-of-function allele of *TPC1* activates oxylipin biogenesis after leaf wounding in *Arabidopsis*. *Plant Journal*, *49*(5), 889-898.

Bonza, M. C., Morandini, P., Luoni, L., Geisler, M., Palmgren, M. G., & De Michelis, M. I. (2000). *At-ACA8* encodes a plasma membrane-localized calcium-ATPase of *Arabidopsis* with a calmodulin-binding domain at the N terminus. *Plant Physiology*, *123*(4), 1495-1506.

Bornhorst, J. A., & Falke, J. J. (2000). Purification of proteins using polyhistidine affinity tags. *Methods in Enzymology*, *326*, 245-254.

Boursiac, Y., Lee, S. M., Romanowsky, S., Blank, R., Sladek, C., Chung, W. S., & Harper, J. F. (2010). Disruption of the vacuolar calcium-ATPases in *Arabidopsis* results in the activation of a salicylic acid-dependent programmed cell death pathway. *Plant Physiology*, *154*(3), 1158-1171.

Braun, P., Aubourg, S., Van Leene, J., De Jaeger, G., & Lurin, C. (2013). Plant protein interactomes. *Annual Review of Plant Biology*, *64*, 161-187.

Brett, D., Pospisil, H., Valcárcel, J., Reich, J., & Bork, P. (2002). Alternative splicing and genome complexity. *Nature Genetics*, *30*(1), 29-30.

Breusegem, F. V., & Dat, J. F. (2006). Reactive oxygen species in plant cell death. *Plant Physiology*, *141*(2), 384-390.

Bricchi, I., Bertea, C. M., Occhipinti, A., Paponov, I. A., & Maffei, M. E. (2012). Dynamics of membrane potential variation and gene expression induced by *Spodoptera littoralis*, *Myzus persicae*, and *Pseudomonas syringae* in *Arabidopsis*. *PloS One*, *7*(10), e46673.

Bullock, R. M. (1952). A study of some inorganic compounds and growth promoting chemicals in relation to fruit cracking in Bing cherries at maturity. *American Society for Horticultural Science*, *59*, 243-253.

Burch-Smith, T. M., Stonebloom, S., Xu, M., & Zambryski, P. C. (2011). Plasmodesmata during development: re-examination of the importance of primary, secondary, and branched plasmodesmata structure versus function. *Protoplasma*, *248*(1), 61-74.

Caplan, J., Padmanabhan, M., & Dinesh-Kumar, S. P. (2008). Plant NB-LRR immune receptors: from recognition to transcriptional reprogramming. *Cell Host & Microbe*, *3*(3), 126-135.

Carter, C., Pan, S., Zouhar, J., Avila, E. L., Girke, T., & Raikhel, N. V. (2004). The vegetative vacuole proteome of *Arabidopsis thaliana* reveals predicted and unexpected proteins. *Plant Cell*, *16*(12), 3285-3303.

Carviel, J. L., Al-Daoud, F. A. D. I., Neumann, M., Mohammad, A., Provart, N. J., Moeder, W., Yoshioka, K., & Cameron, R. K. (2009). Forward and reverse genetics to identify genes involved in the age-related resistance response in *Arabidopsis thaliana*. *Molecular Plant Pathology*, *10*(5), 621-634.

Catalá, R., Santos, E., Alonso, J. M., Ecker, J. R., Martínez-Zapater, J. M., & Salinas, J. (2003). Mutations in the Ca^{2+}/H^+ transporter CAX1 increase CBF/DREB1 expression and the cold-acclimation response in *Arabidopsis*. *Plant Cell*, *15*(12), 2940-2951.

Causier, B., & Davies, B. (2002). Analysing protein-protein interactions with the yeast two-hybrid system. *Plant Molecular Biology*, *50*(6), 855-870.

Cerana, M., Bonza, M. C., Harris, R., Sanders, D., & Michelis, M. I. (2006). Abscisic acid stimulates the expression of two isoforms of plasma membrane Ca^{2+}-ATPase in *Arabidopsis thaliana* seedlings. *Plant Biology*, *8*(5), 572-578.

Chan, C. W., Wohlbach, D. J., Rodesch, M. J., & Sussman, M. R. (2008). Transcriptional changes in response to growth of *Arabidopsis* in high external calcium. *FEBS Letters*, *582*(6), 967-976.

Chen, X. Y., & Kim, J. Y. (2009). Callose synthesis in higher plants. *Plant Signaling & Behavior*, *4*(6), 489-492.

Cheng, N. H., & Hirschi, K. D. (2003). Cloning and characterization of CXIP1, a novel PICOT domain-containing *Arabidopsis* protein that associates with CAX1. *Journal of Biological Chemistry*, *278*(8), 6503-6509.

Cheng, N. H., Liu, J. Z., Nelson, R. S., & Hirschi, K. D. (2004a). Characterization of CXIP4, a novel *Arabidopsis* protein that activates the H^+/Ca^{2+} antiporter, CAX1. *FEBS Letters*, *559*(1), 99-106.

Cheng, N. H., Pittman, J. K., Barkla, B. J., Shigaki, T., & Hirschi, K. D. (2003). The *Arabidopsis cax1* mutant exhibits impaired ion homeostasis, development, and hormonal responses and reveals interplay among vacuolar transporters. *Plant Cell*, *15*(2), 347-364.

Cheng, N. H., Pittman, J. K., Shigaki, T., & Hirschi, K. D. (2002). Characterization of CAX4, an *Arabidopsis* H^+/cation antiporter. *Plant physiology*, *128*(4), 1245-1254.

Cheng, N. H., Pittman, J. K., Shigaki, T., Lachmansingh, J., LeClere, S., Lahner, B., Salt, D. E., & Hirschi, K. D. (2005). Functional association of *Arabidopsis* CAX1 and CAX3 is required for normal growth and ion homeostasis. *Plant Physiology*, *138*(4), 2048-2060.

Cheng, N. H., Pittman, J. K., Zhu, J. K., & Hirschi, K. D. (2004b). The protein kinase SOS2 activates the *Arabidopsis* H$^+$/Ca^{2+} antiporter CAX1 to integrate calcium transport and salt tolerance. *Journal of Biological Chemistry*, *279*(4), 2922-2926.

Cheval, C., Aldon, D., Galaud, J. P., & Ranty, B. (2013). Calcium/calmodulin-mediated regulation of plant immunity. *Biochimica et Biophysica Acta (BBA)-Molecular Cell Research*, *1833*(7), 1766-1771.

Chiasson, D., Ekengren, S. K., Martin, G. B., Dobney, S. L., & Snedden, W. A. (2005). Calmodulin-like proteins from *Arabidopsis* and tomato are involved in host defense against *Pseudomonas syringae* pv. tomato. *Plant Molecular Biology*, *58*(6), 887-897.

Chigri, F., Flosdorff, S., Pilz, S., Kölle, E., Dolze, E., Gietl, C., & Vothknecht, U. C. (2012). The *Arabidopsis* calmodulin-like proteins AtCML30 and AtCML3 are targeted to mitochondria and peroxisomes, respectively. *Plant Molecular Miology*, *78*(3), 211-222.

Chin, K., Moeder, W., Abdel-Hamid, H., Shahinas, D., Gupta, D., & Yoshioka, K. (2010). Importance of the αC-helix in the cyclic nucleotide binding domain for the stable channel regulation and function of cyclic nucleotide gated ion channels in *Arabidopsis*. *Journal of Experimental Botany*, *61*(9), 2383-2393.

Chinchilla, D., Zipfel, C., Robatzek, S., Kemmerling, B., Nürnberger, T., Jones, J. D., Felix, G., & Boller, T. (2007). A flagellin-induced complex of the receptor FLS2 and BAK1 initiates plant defence. *Nature*, *448*(7152), 497-500.

Chisholm, S. T., Coaker, G., Day, B., & Staskawicz, B. J. (2006). Host-microbe interactions: shaping the evolution of the plant immune response. *Cell*, *124*(4), 803-814.

Cho, D., Kim, S. A., Murata, Y., Lee, S., Jae, S. K., Nam, H. G., & Kwak, J. M. (2009). De-regulated expression of the plant glutamate receptor homolog AtGLR3. 1 impairs long-term Ca^{2+}-programmed stomatal closure. *Plant Journal*, *58*(3), 437-449.

Cho, D., Villiers, F., Kroniewicz, L., Lee, S., Seo, Y. J., Hirschi, K. D., Leonhardt, N., & Kwak, J. M. (2012). Vacuolar CAX1 and CAX3 influence auxin transport in guard cells via regulation of apoplastic pH. *Plant physiology*, *160*(3), 1293-1302.

Choi, J., Huh, S. U., Kojima, M., Sakakibara, H., Paek, K. H., & Hwang, I. (2010). The Cytokinin-activated transcription factor ARR2 promotes plant immunity via TGA3/NPR1-dependent salicylic acid signaling in *Arabidopsis*. *Developmental Cell*, *19*(2), 284-295.

Cholewa, E., & Peterson, C. A. (2004). Evidence for symplastic involvement in the radial movement of calcium in onion roots. *Plant Physiology*, *134*(4), 1793-1802.

Christopher, D., Borsics, T., Yuen, C., Ullmer, W., Andème-Ondzighi, C., Andres, M., Kang B. H., & Staehelin, L. A. (2007). The cyclic nucleotide gated cation channel AtCNGC10 traffics

from the ER via Golgi vesicles to the plasma membrane of *Arabidopsis* root and leaf cells. *BMC Plant Biology*, *7*(1), 48.

Clark, G., Konopka-Postupolska, D., Hennig, J., & Roux, S. (2010). Is annexin 1 a multifunctional protein during stress responses?. *Plant Signaling & Behavior*, *5*(3), 303-307.

Clarkson, D. T. (1993). Roots and the delivery of solutes to the xylem. *Philosophical Transactions of the Royal Society of London. Series B: Biological Sciences*, *341*(1295), 5-17.

Clay, N. K., Adio, A. M., Denoux, C., Jander, G., & Ausubel, F. M. (2009). Glucosinolate metabolites required for an *Arabidopsis* innate immune response. *Science*, *323*(5910), 95-101.

Clough, S. J., Fengler, K. A., Yu, I. C., Lippok, B., Smith, R. K., & Bent, A. F. (2000). The *Arabidopsis dnd1* "defense, no death" gene encodes a mutated cyclic nucleotide-gated ion channel. *Proceedings of the National Academy of Sciences*, *97*(16), 9323-9328.

Conn, S. J., Berninger, P., Broadley, M. R., & Gilliham, M. (2012). Exploiting natural variation to uncover candidate genes that control element accumulation in *Arabidopsis thaliana*. *New Phytologist*, *193*(4), 859-866.

Conn, S. J., Hocking, B., Dayod, M., Xu, B., Athman, A., Henderson, S., Aukett, L., Vanessa, Conn., Shearer, M. K., Fuentes, S., Tyerman, S. D., & Gilliham, M. (2013) Protocol: optimising hydroponic growth systems for nutritional and physiological analysis of *Arabidopsis thaliana* and other plants. *Plant Method*, 9, 4

Conn, S. J., & Gilliham, M. (2010). Comparative physiology of elemental distributions in plants. *Annals of Botany*, *105*(7), 1081-1102.

Conn, S. J., Gilliham, M., Athman, A., Schreiber, A. W., Baumann, U., Moller, I., Cheng, N. H., Stancombe, M. A., Hirschi, K. D., Webb, A. A. R., Burton, R., Kaiser, B. N., Tyerman, S. D., & Leigh, R. A. (2011). Cell-specific vacuolar calcium storage mediated by CAX1 regulates apoplastic calcium concentration, gas exchange, and plant productivity in *Arabidopsis*. *Plant Cell*, *23*(1), 240-257.

Corbesier, L., Vincent, C. , Jang, S., Fornara, F., Fan, Q., Searle, I., Giakountis, A., Farrona, S., Gissot, L., Turnbull, C., & Coupland, G. (2007). FT protein movement contributes to long-distance signaling in floral induction of *Arabidopsis*. *Science*, *316*(5827), 1030-1033.

Cosgrove, D. J. (2005). Growth of the plant cell wall. *Nature Reviews in Molecular Cell Biology*, *6*(11), 850-861.

Currier, H. B., & Strugger, S. (1956). Aniline blue and fluorescence microscopy of callose in bulb scales of *Allium cepa* L. *Protoplasma*, *45*(4), 552-559.

Curtis, M. D., & Grossniklaus, U. (2003). A gateway cloning vector set for high-throughput functional analysis of genes in planta. *Plant Physiology*, *133*(2), 462-469.

de Freitas, S. T., Padda, M., Wu, Q., Park, S., & Mitcham, E. J. (2011). Dynamic alternations in cellular and molecular components during blossom-end rot development in tomatoes expressing *sCAX1*, a constitutively active Ca^{2+}/H$^+$ antiporter from *Arabidopsis*. *Plant physiology*, *156*(2), 844-855.

de Silva, D. L. R., Honour, S. J., & Mansfield, T. A. (1996). Estimations of apoplastic concentrations of K$^+$ and Ca^{2+} in the vicinity of stomatal guard cells. *New Phytologist*, *134*(3), 463-469.

Dadacz-Narloch, B., Beyhl, D., Larisch, C., López-Sanjurjo, E. J., Reski, R., Kuchitsu, K., Müller, T. D., Becker, D., Schönknecht, G., & Hedrich, R. (2011). A novel calcium binding site in the slow vacuolar cation channel TPC1 senses luminal calcium levels. *Plant Cell*, *23*(7), 2696-2707.

Danpure, C. J. (1995). How can the products of a single gene be localized to more than one intracellular compartment?. *Trends in Cell Biology*, *5*(6), 230-238.

Daudi, A., Cheng, Z., O'Brien, J. A., Mammarella, N., Khan, S., Ausubel, F. M., & Bolwell, G. P. (2012). The apoplastic oxidative burst peroxidase in *Arabidopsis* is a major component of pattern-triggered immunity. *Plant Cell*, *24*(1), 275-287.

Day, I. S., Reddy, V. S., Shad Ali, G., & Reddy, A. S. (2002). Analysis of EF-hand-containing proteins in *Arabidopsis*. *Genome Biology*, *3*(10), 1-24.

Dayod, M., Tyerman, S. D., Leigh, R. A., & Gilliham, M. (2010). Calcium storage in plants and the implications for calcium biofortification. *Protoplasma*, *247*(3-4), 215-231.

Delk, N. A., Johnson, K. A., Chowdhury, N. I., & Braam, J. (2005). CML24, regulated in expression by diverse stimuli, encodes a potential Ca^{2+} sensor that functions in responses to abscisic acid, daylength, and ion stress. *Plant Physiology*, *139*(1), 240-253.

Denoux, C., Galletti, R., Mammarella, N., Gopalan, S., Werck, D., De Lorenzo, G., Ferrari, S., Ausubel, F. M., & Dewdney, J. (2008). Activation of defense response pathways by OGs and Flg22 elicitors in *Arabidopsis* seedlings. *Molecular Plant*, *1*(3), 423-445.

Dickinson, D. B., & McCollum, J. P. (1964). Cellulase in tomato fruits. *Nature,* 203, 525 - 526

Dobney, S., Chiasson, D., Lam, P., Smith, S. P., & Snedden, W. A. (2009). The calmodulin-related calcium sensor CML42 plays a role in trichome branching. *Journal of Biological Chemistry*, *284*(46), 31647-31657.

Dodd, A. N., Kudla, J., & Sanders, D. (2010). The language of calcium signaling. *Annual Review of Pant Biology*, *61*, 593-620.

Dodds, P. N., & Rathjen, J. P. (2010). Plant immunity: towards an integrated view of plant–pathogen interactions. *Nature Reviews in Genetics*, *11*(8), 539-548.

Doukhanina, E. V., Chen, S., van der Zalm, E., Godzik, A., Reed, J., & Dickman, M. B. (2006). Identification and functional characterization of the BAG protein family in *Arabidopsis thaliana*. *Journal of Biological Chemistry*, *281*(27), 18793-18801.

Du, L., Ali, G. S., Simons, K. A., Hou, J., Yang, T., Reddy, A. S. N., & Poovaiah, B. W. (2009). Ca^{2+}/calmodulin regulates salicylic-acid-mediated plant immunity. *Nature*, *457*(7233), 1154-1158.

Du, L., & Poovaiah, B. W. (2005). Ca^{2+}/calmodulin is critical for brassinosteroid biosynthesis and plant growth. *Nature*, *437*(7059), 741-745.

Edmond, C., Shigaki, T., Ewert, S., Nelson, M., Connorton, J., Chalova, V., Noordally, Z., & Pittman, J. (2009). Comparative analysis of CAX2-like cation transporters indicates functional and regulatory diversity. *Biochemical Journal*, *418*, 145-154.

Eisen, M. B., Spellman, P. T., Brown, P. O., & Botstein, D. (1998). Cluster analysis and display of genome-wide expression patterns. *Proceedings of the National Academy of Sciences*, *95*(25), 14863-14868.

Emanuelsson, O., Brunak, S., von Heijne, G., & Nielsen, H. (2007). Locating proteins in the cell using TargetP, SignalP and related tools. *Nature Protocols*, *2*(4), 953-971.

Esposito, D., & Chatterjee, D. K. (2006). Enhancement of soluble protein expression through the use of fusion tags. *Current Opinion in Biotechnology*, *17*(4), 353-358.

Fernandez-Calvino, L., Faulkner, C., Walshaw, J., Saalbach, G., Bayer, E., Benitez-Alfonso, Y., & Maule, A. (2011). *Arabidopsis* plasmodesmal proteome. *PLoS One*, *6*(4), e18880.

Finn, B. E., Evenäs, J., Drakenberg, T., Waltho, J. P., Thulin, E., & Forsén, S. (1995). Calcium-induced structural changes and domain autonomy in calmodulin. *Nature Structural & Molecular Biology*, *2*(9), 777-783.

Frey, N. F. D., Mbengue, M., Kwaaitaal, M., Nitsch, L., Altenbach, D., Häweker, H., Lozano-Duran, R., Njo M. F., Beeckman, T., Huettel, B., Borst, J. W., Panstruga, R., & Robatzek, S. (2012). Plasma membrane calcium ATPases are important components of receptor-mediated signaling in plant immune responses and development. *Plant physiology*, *159*(2), 798-809.

Frietsch, S., Wang, Y. F., Sladek, C., Poulsen, L. R., Romanowsky, S. M., Schroeder, J. I., & Harper, J. F. (2007). A cyclic nucleotide-gated channel is essential for polarized tip growth of pollen. *Proceedings of the National Academy of Sciences*, *104*(36), 14531-14536.

Fischer, C., Kugler, A., Hoth, S., & Dietrich, P. (2013). An IQ domain mediates the interaction with calmodulin in a plant cyclic nucleotide-gated channel. *Plant and Cell Physiology*, *54*(4), 573-584.

Fujikawa, Y., & Kato, N. (2007). Split luciferase complementation assay to study protein–protein interactions in *Arabidopsis* protoplasts. *Plant Journal*, *52*(1), 185-195.

Furuichi, T., Cunningham, K. W., & Muto, S. (2001). A putative two pore channel AtTPC1 mediates Ca^{2+} flux in *Arabidopsis* leaf cells. *Plant and Cell Physiology*, *42*(9), 900-905.

Furuichi, T., Iida, H., Sokabe, M., & Tatsumi, H. (2012). Expression of *Arabidopsis MCA1* enhanced mechanosensitive channel activity in the *Xenopus laevis* oocyte plasma membrane. *Plant Signaling & Behavior*, *7*(8), 1022-1026.

Galletti, R., Denoux, C., Gambetta, S., Dewdney, J., Ausubel, F. M., De Lorenzo, G., & Ferrari, S. (2008). The AtrbohD-mediated oxidative burst elicited by oligogalacturonides in *Arabidopsis* is dispensable for the activation of defense responses effective against *Botrytis cinerea*. *Plant Physiology*, *148*(3), 1695-1706.

Gao, F., Han, X., Wu, J., Zheng, S., Shang, Z., Sun, D., Zhou, R., & Li, B. (2012). A heat-activated calcium-permeable channel–*Arabidopsis* cyclic nucleotide-gated ion channel 6–is involved in heat shock responses. *Plant Journal*, *70*(6), 1056-1069.

Garrigos, M., Deschamps, S., Viel, A., Lund, S., Champeil, P., Møller, J. V., & Maire, M. L. (1991). Detection of Ca^{2+}-binding proteins by electrophoretic migration in the presence of Ca^{2+} combined with $^{45}Ca^{2+}$ overlay of protein blots. *Analytical Biochemistry*, *194*(1), 82-88.

Geisler, M., Frangne, N., Gomès, E., Martinoia, E., & Palmgren, M. G. (2000). The *ACA4* gene of *Arabidopsis* encodes a vacuolar membrane calcium pump that improves salt tolerance in yeast. *Plant Physiology*, *124*(4), 1814-1827.

Geldner, N., Dénervaud-Tendon, V., Hyman, D. L., Mayer, U., Stierhof, Y. D., & Chory, J. (2009). Rapid, combinatorial analysis of membrane compartments in intact plants with a multicolor marker set. *Plant Journal*, *59*(1), 169-178.

Genger, R. K., Jurkowski, G. I., McDowell, J. M., Lu, H., Jung, H. W., Greenberg, J. T., & Bent, A. F. (2008). Signaling pathways that regulate the enhanced disease resistance of *Arabidopsis* "defense, no death" mutants. *Molecular Plant-Microbe Interactions*, *21*(10), 1285-1296.

Genovés, A., Navarro, J. A., & Pallás, V. (2010). The intra-and intercellular movement of *Melon necrotic spot virus* (MNSV) depends on an active secretory pathway. *Molecular Plant-Microbe Interactions*, *23*(3), 263-272.

George, L., Romanowsky, S. M., Harper, J. F., & Sharrock, R. A. (2008). The ACA10 Ca^{2+}-ATPase regulates adult vegetative development and inflorescence architecture in *Arabidopsis*. *Plant Physiology*, *146*(2), 716-728.

Gerard, C. J. (1971). Influence of osmotic potential, temperature, and calcium on growth of plant roots. *Agronomy Journal*, *63*(4), 555-558.

Gfeller, A., Baerenfaller, K., Loscos, J., Chételat, A., Baginsky, S., & Farmer, E. E. (2011). Jasmonate controls polypeptide patterning in undamaged tissue in wounded *Arabidopsis* leaves. *Plant Physiology*, *156*(4), 1797-1807.

Gifford, J., Walsh, M., & Vogel, H. (2007). Structures and metal-ion-binding properties of the Ca^{2+}-binding helix-loop-helix EF-hand motifs. *Biochemical Journal*, *405*, 199-221.

Gilliham, M., Athman, A., Tyerman, S. D., & Conn, S. J. (2011a). Cell-specific compartmentation of mineral nutrients is an essential mechanism for optimal plant productivity–another role for TPC1?. *Plant Signaling & Behavior*, *6*(11), 1656-1661.

Gilliham, M., Dayod, M., Hocking, B. J., Xu, B., Conn, S. J., Kaiser, B. N., Roger, A. L., & Tyerman, S. D. (2011b). Calcium delivery and storage in plant leaves: exploring the link with water flow. *Journal of Experimental Botany*, *62*(7), 2233-2250.

Gobert, A., Park, G., Amtmann, A., Sanders, D., & Maathuis, F. J. (2006). *Arabidopsis thaliana* cyclic nucleotide gated channel 3 forms a non-selective ion transporter involved in germination and cation transport. *Journal of Experimental Botany*, *57*(4), 791-800.

Gómez-Gómez, L., & Boller, T. (2000). FLS2: An LRR receptor–like kinase involved in the perception of the bacterial elicitor flagellin in *Arabidopsis*. *Molecular cell*, *5*(6), 1003-1011.

Gómez-Gómez, L., Felix, G., & Boller, T. (1999). A single locus determines sensitivity to bacterial flagellin in *Arabidopsis thaliana*. *Plant Journal*, *18*(3), 277-284.

Gopalakrishna, R., & Anderson, W. B. (1982). Ca^{2+}-induced hydrophobic site on calmodulin: Application for purification of calmodulin by phenyl-Sepharose affinity chromatography. *Biochemical and Biophysical Sesearch Communications*, *104*(2), 830-836.

Gorecka, K. M., Thouverey, C., Buchet, R., & Pikula, S. (2007). Potential role of annexin *AnnAt1* from *Arabidopsis thaliana* in pH-mediated cellular response to environmental stimuli. *Plant and Cell Physiology*, *48*(6), 792-803.

Gorshkova, E. N., Erokhina, T. N., Stroganova, T. A., Yelina, N. E., Zamyatnin, A. A., Kalinina, N. O., Schiemann, J., Solovyev, A. G., & Morozov, S. Y. (2003). Immunodetection and fluorescent microscopy of transgenically expressed hordeivirus TGBp3 movement protein reveals its association with endoplasmic reticulum elements in close proximity to plasmodesmata. *Journal of General Virology*, *84*(4), 985-994.

Guo, K. M., Babourina, O., Christopher, D. A., Borsics, T., & Rengel, Z. (2008). The cyclic nucleotide-gated channel, AtCNGC10, influences salt tolerance in *Arabidopsis*. *Physiologia Plantarum*, *134*(3), 499-507.

Guo, K. M., Babourina, O., Christopher, D. A., Borsic, T., & Rengel, Z. (2010). The cyclic nucleotide-gated channel AtCNGC10 transports Ca^{2+} and Mg^{2+} in *Arabidopsis*. *Physiologia Plantarum*, *139*(3), 303-312.

Graveley, B. R. (2001). Alternative splicing: increasing diversity in the proteomic world. *Trends in Genetics*, *17*(2), 100-107.

Greenberg, J. T. (1997). Programmed cell death in plant-pathogen interactions. *Annual Review of Blant Biology*, *48*(1), 525-545.

Grennan, A. K. (2006). Genevestigator. Facilitating web-based gene-expression analysis. *Plant Physiology*, *141*(4), 1164-1166.

Guéguen, L., & Pointillart, A. (2000). The bioavailability of dietary calcium. *Journal of the American College of Nutrition*, *19*(sup2), 119S-136S.

Han, N., Shao, Q., Bao, H., & Wang, B. (2011). Cloning and characterization of a Ca^{2+}/H^+ Antiporter from *Halophyte Suaeda salsa* L. *Plant Molecular Biology Reporter*, *29*(2), 449-457.

Harper, J. F., Hong, B., Hwang, I., Guo, H. Q., Stoddard, R., Huang, J. F., Palmgren, M. G., & Sze, H. (1998). A novel calmodulin-regulated Ca^{2+}-ATPase (ACA2) from Arabidopsis with an N-terminal autoinhibitory domain. *Journal of Biological Chemistry*, *273*(2), 1099-1106.

Harrison, S. J., Mott, E. K., Parsley, K., Aspinall, S., Gray, J. C., & Cottage, A. (2006). A rapid and robust method of identifying transformed *Arabidopsis thaliana* seedlings following floral dip transformation. *Plant Methods*, *2*(1), 19.

Hayter, M. L., & Peterson, C. A. (2004). Can Ca^{2+} fluxes to the root xylem be sustained by Ca^{2+}-ATPases in exodermal and endodermal plasma membranes?. *Plant Physiology*, *136*(4), 4318-4325.

Hedrich, R., & Marten, I. (2011). TPC1–SV channels gain shape. *Molecular Plant*, *4*(3), 428-441.

Heid, C. A., Stevens, J., Livak, K. J., & Williams, P. M. (1996). Real time quantitative PCR. *Genome research*, *6*(10), 986-994.

Heinlein, M., Epel, B. L., Padgett, H. S., & Beachy, R. N. (1995). Interaction of tobamovirus movement proteins with the plant cytoskeleton. *Science*, *270*(5244), 1983-1985.

Hématy, K., Cherk, C., & Somerville, S. (2009). Host–pathogen warfare at the plant cell wall. *Current Opinion in Plant Biology*, *12*(4), 406-413.

Hirschi, K. D. (1999). Expression of *Arabidopsis CAX1* in tobacco: altered calcium homeostasis and increased stress sensitivity. *Plant Cell, 11*(11), 2113-2122.

Hirschi, K. D. (2004). The calcium conundrum. both versatile nutrient and specific signal. *Plant Physiology*, *136*(1), 2438-2442.

Hirschi, K. D. (2008). Nutritional improvements in plants: time to bite on biofortified foods. *Trends in Plant Science*, *13*(9), 459-463.

Hirschi, K. D. (2009). Nutrient biofortification of food crops. *Annual Review of Nutrition*, *29*, 401-421.

Hirschi, K. D., Korenkov, V. D., Wilganowski, N. L., & Wagner, G. J. (2000). Expression of *Arabidopsis CAX2* in tobacco altered metal accumulation and increased manganese tolerance. *Plant Physiology*, *124*(1), 125-134.

Hirschi, K. D., Zhen, R. G., Cunningham, K. W., Rea, P. A., & Fink, G. R. (1996). CAX1, an H^+/Ca^{2+} antiporter from *Arabidopsis*. *Proceedings of the National Academy of Sciences*, *93*(16), 8782-8786.

Hochuli, E., Bannwarth, W., Döbeli, H., Gentz, R., & Stüber, D. (1988). Genetic approach to facilitate purification of recombinant proteins with a novel metal chelate adsorbent. *Nature Biotechnology*, *6*(11), 1321-1325.

Hocking, B. (2008) The *Arabidopsis* Ca^{2+}/H^+ exchangers, AtCAX1 and AtCAX3, are shown by co-localisation, interaction and complementation to participate in plant Ca^{2+} homeostasis. Masters thesis, University of Adelaide, Adelaide.

Höfgen, R., & Willmitzer, L. (1988). Storage of competent cells for *Agrobacterium* transformation. *Nucleic Acids Research*, *16*(20), 9877-9877.

Hong, B., Ichida, A., Wang, Y., Gens, J. S., Pickard, B. G., & Harper, J. F. (1999). Identification of a calmodulin-regulated Ca^{2+}-ATPase in the endoplasmic reticulum. *Plant Physiology*, *119*(4), 1165-1176.

Hörtensteiner, S. (2006). Chlorophyll degradation during senescence. *Annual Review of Plant Biology*, *57*, 55-77.

Howard, D. D., & Adams, F. (1965). Calcium requirement for penetration of subsoils by primary cotton roots. *Soil Science Society of America Journal*, *29*(5), 558-562.

Hrabak, E. M., Chan, C. W., Gribskov, M., Harper, J. F., Choi, J. H., Halford, N., Kudla, J., Luan, S., Nimmo, H. G., Sussman, M. R., Thomas, M., Walker-Simmons, K., Zhu, J. K., & Harmon, A. C. (2003). The *Arabidopsis* CDPK-SnRK superfamily of protein kinases. *Plant Physiology*, *132*(2), 666-680.

Hruz, T., Laule, O., Szabo, G., Wessendorp, F., Bleuler, S., Oertle, L., Widmayer, P., Gruissem, W., & Zimmermann, P. (2008). Genevestigator v3: a reference expression database for the meta-analysis of transcriptomes. *Advances in Bioinformatics*, dx.doi.org/10.1155/2008/420747

Huang, L., Berkelman, T., Franklin, A. E., & Hoffman, N. E. (1993). Characterization of a gene encoding a Ca^{2+}-ATPase-Like protein in the plastid envelope. *Proceedings of the National Academy of Science,* (91), 10066–10070.

Hückelhoven, R. (2007). Cell wall-associated mechanisms of disease resistance and susceptibility. *Annual Review of Phytopathology*, *45*, 101-127.

Hunter, S., Apweiler, R., Attwood, T. K., Bairoch, A., Bateman, A., Binns, D., Bork, P., Das, U., Daugherty, L., Duquenne, L., Finn, R. D., Gough, J., Haft, D., Hulo, N., Kahn, D., Kelly, E., Laugraud, A., Letunic, I., Lonsdale, D., Lopez, R., Madera, M., Maslen, J., McAnulla, C., McDowall, J., Mistry, J., Mitchell, A., Mulder, N., Natale, D., Orengo, C., Quinn, A. F., Selengut, J. D., Sigrist, C. J. A., Thimma, M., Thomas, P. D., Valentin, F., Wilson, D., Wu, C. H., & Yeats, C. (2009). InterPro: the integrative protein signature database. *Nucleic Acids Research*, *37*(suppl 1), D211-D215.

Hunter, S., Jones, P., Mitchell, A., Apweiler, R., Attwood, T. K., Bateman, A., Bernard, T., Binns, D., Bork, P., Burge, S., de Castro, E., Coggill, P., Corbett, M., Das, U., Daugherty, L., Duquenne, L., Finn, R. D., Fraser, M., Gough, J Haft, D., Hulo, N., Kahn, D., Kelly, E., Letunic, I., Lonsdale, D., Lopez, R., Madera, M., Maslen, J., McAnulla, C., McDowall, J., McMenamin, C., Mi, H., Mutowo-Muellenet, P., Mulder, N., Natale, D., Orengo, C., Pesseat, S., Punta, M., Quinn, A. F., Rivoire, C., Sangrador-Vegas, A., Selengut, J. D., Sigrist, C. J. A., Scheremetjew, M., Tate, J., Thimmajanarthanan, M., Thomas, P. D., Wu, C. H., Yeats C., & Yong, S. Y. (2012). InterPro in 2011: new developments in the family and domain prediction database. *Nucleic Acids Research*, *40*(D1), D306-D312.

Irizarry, R. A., Hobbs, B., Collin, F., Beazer-Barclay, Y. D., Antonellis, K. J., Scherf, U., & Speed, T. P. (2003). Exploration, normalization, and summaries of high density oligonucleotide array probe level data. *Biostatistics*, *4*(2), 249-264.

Islam, M. M., Munemasa, S., Hossain, M. A., Nakamura, Y., Mori, I. C., & Murata, Y. (2010). Roles of AtTPC1, vacuolar two pore channel 1, in *Arabidopsis* stomatal closure. *Plant and Cell Physiology*, *51*(2), 302-311.

Ito, T., Chiba, T., Ozawa, R., Yoshida, M., Hattori, M., & Sakaki, Y. (2001). A comprehensive two-hybrid analysis to explore the yeast protein interactome. *Proceedings of the National Academy of Sciences*, *98*(8), 4569-4574.

Jacobs, A. K., Lipka, V., Burton, R. A., Panstruga, R., Strizhov, N., Schulze-Lefert, P., & Fincher, G. B. (2003). An *Arabidopsis* callose synthase, GSL5, is required for wound and papillary callose formation. *Plant Cell*, *15*(11), 2503-2513.

Jarvis, M. C., Logan, A. S., & Duncan, H. J. (1984). Tensile characteristics of collenchyma cell walls at different calcium contents. *Physiologia Plantarum*, *61*(1), 81-86.

Jefferson, R. A., Kavanagh, T. A., & Bevan, M. W. (1987). GUS fusions: beta-glucuronidase as a sensitive and versatile gene fusion marker in higher plants. *EMBO Journal*, *6*(13), 3901.

Jia, X. Y., He, L. H., Jing, R. L., & Li, R. Z. (2009). Calreticulin: conserved protein and diverse functions in plants. *Physiologia Plantarum*, *136*(2), 127-138.

Jones, D. L., Blancaflor, E. B., Kochian, L. V., & Gilroy, S. (2006). Spatial coordination of aluminium uptake, production of reactive oxygen species, callose production and wall rigidification in maize roots. *Plant, Cell & Environment*, *29*(7), 1309-1318.

Jones, J. D., & Dangl, J. L. (2006). The plant immune system. *Nature*, *444*(7117), 323-329.

Jurkowski, G. I., Smith Jr, R. K., Yu, I. C., Ham, J. H., Sharma, S. B., Klessig, D. F., Fengler, K. A., & Bent, A. F. (2004). *Arabidopsis DND2*, a second cyclic nucleotide-gated ion channel gene for which mutation causes the "defense, no death" phenotype. *Molecular Plant-Microbe Interactions*, *17*(5), 511-520.

Kaido, M., Tsuno, Y., Mise, K., & Okuno, T. (2009). Endoplasmic reticulum targeting of the *Red clover necrotic mosaic virus* movement protein is associated with the replication of viral RNA1 but not that of RNA2. *Virology*, *395*(2), 232-242.

Kanter, U., Hauser, A., Michalke, B., Dräxl, S., & Schäffner, A. R. (2010). Caesium and strontium accumulation in shoots of *Arabidopsis thaliana*: genetic and physiological aspects. *Journal of Experimental Botany*, *61*(14), 3995-4009.

Kapust, R. B., & Waugh, D. S. (1999). *Escherichia coli* maltose-binding protein is uncommonly effective at promoting the solubility of polypeptides to which it is fused. *Protein Science*, *8*(8), 1668-1674.

Karley, A. J., Leigh, R. A., & Sanders, D. (2000). Where do all the ions go? The cellular basis of differential ion accumulation in leaf cells. *Trends in Plant Science*, *5*(11), 465-470.

Karniely, S., & Pines, O. (2005). Single translation–dual destination: mechanisms of dual protein targeting in eukaryotes. *EMBO Reports*, *6*(5), 420-425.

Keech, O., Pesquet, E., Ahad, A., Askne, A., Nordvall, D. A. G., Vodnala, S. M., Tuominen, H., Hurry, V., Dizengremel, P., & Gardestroem, P. (2007). The different fates of mitochondria and chloroplasts during dark-induced senescence in *Arabidopsis* leaves. *Plant, Cell & Environment*, *30*(12), 1523-1534.

Kieffer, M., Master, V., Waites, R., & Davies, B. (2011). TCP14 and TCP15 affect internode length and leaf shape in *Arabidopsis*. *Plant Journal*, *68*(1), 147-158.

Kim, K. M. (2012) Major character analysis of *CAX1* (cation exchanger 1) transgenic rice plants *in vivo*. *Korean Journal of Crop Science*, *54*, 375-383.

Kim, K. M., Park, Y. H., Kim, C. K., Hirschi, K., & Sohn, J. K. (2005). Development of transgenic rice plants overexpressing the *Arabidopsis* H$^+$/Ca^{2+} antiporter *CAX1* gene. *Plant Cell Reports*, *23*(10-11), 678-682.

Kim, M. C., Chung, W. S., Yun, D. J., & Cho, M. J. (2009a). Calcium and calmodulin-mediated regulation of gene expression in plants. *Molecular Plant*, *2*(1), 13-21.

Kim, M. J., Baek, K., & Park, C. M. (2009b). Optimization of conditions for transient *Agrobacterium*-mediated gene expression assays in *Arabidopsis*. *Plant Cell Reports*, *28*(8), 1159-1167.

Kim, S. A., Kwak, J., Jae, S. K., Wang, M. H., & Nam, H. (2001). Overexpression of the *AtGluR2* gene encoding an *Arabidopsis* homolog of mammalian glutamate receptors impairs calcium utilization and sensitivity to ionic stress in transgenic plants. *Plant and Cell Physiology*, *42*(1), 74-84.

Köhler, C., Merkle, T., & Neuhaus, G. (1999). Characterisation of a novel gene family of putative cyclic nucleotide-and calmodulin-regulated ion channels in *Arabidopsis thaliana*. *Plant Journal*, *18*(1), 97-104.

Köhler, C., Merkle, T., Roby, D., & Neuhaus, G. (2001). Developmentally regulated expression of a cyclic nucleotide-gated ion channel from *Arabidopsis* indicates its involvement in programmed cell death. *Planta*, *213*(3), 327-332.

Köhler, C., & Neuhaus, G. (2000). Characterisation of calmodulin binding to cyclic nucleotide-gated ion channels from *Arabidopsis thaliana*. *FEBS Letters*, *471*(2), 133-136.

Kolukisaoglu, Ü., Weinl, S., Blazevic, D., Batistic, O., & Kudla, J. (2004). Calcium sensors and their interacting protein kinases: genomics of the *Arabidopsis* and rice CBL-CIPK signaling networks. *Plant Physiology*, *134*(1), 43-58.

Konopka-Postupolska, D., Clark, G., Goch, G., Debski, J., Floras, K., Cantero, A., Fijolek, B., Roux, S., & Hennig, J. (2009). The role of annexin 1 in drought stress in *Arabidopsis*. *Plant Physiology*, *150*(3), 1394-1410.

Korenkov, V., Hirschi, K., Crutchfield, J. D., & Wagner, G. J. (2007). Enhancing tonoplast Cd/H antiport activity increases Cd, Zn, and Mn tolerance, and impacts root/shoot Cd partitioning in *Nicotiana tabacum* L. *Planta*, *226*(6), 1379-1387.

Korenkov, V., King, B., Hirschi, K., & Wagner, G. J. (2009). Root-selective expression of *AtCAX4* and *AtCAX2* results in reduced lamina cadmium in field-grown *Nicotiana tabacum* L. *Plant Biotechnology Journal*, *7*(3), 219-226.

Kretsinger, R. H., & Nockolds, C. E. (1973). Carp muscle calcium-binding protein II. Structure determination and general description. *Journal of Biological Chemistry*, *248*(9), 3313-3326.

Kudla, J., Batistič, O., & Hashimoto, K. (2010). Calcium signals: the lead currency of plant information processing. *Plant Cell*, *22*(3), 541-563.

Kugler, A., Köhler, B., Palme, K., Wolff, P., & Dietrich, P. (2009). Salt-dependent regulation of a CNGC channel subfamily in *Arabidopsis*. *BMC Plant Biology*, *9*(1), 140.

Kunze, G., Zipfel, C., Robatzek, S., Niehaus, K., Boller, T., & Felix, G. (2004). The N terminus of bacterial elongation factor Tu elicits innate immunity in *Arabidopsis* plants. *Plant Cell*, *16*(12), 3496-3507.

Kushwaha, R., Singh, A., & Chattopadhyay, S. (2008). Calmodulin 7 plays an important role as transcriptional regulator in *Arabidopsis* seedling development. *Plant Cell*, *20*(7), 1747-1759.

Kuśnierczyk, A., Tran, D., Winge, P., Jørstad, T., Reese, J., Troczyńska, J., & Bones, A. (2011). Testing the importance of jasmonate signalling in induction of plant defences upon cabbage aphid (*Brevicoryne brassicae*) attack. *BMC Genomics*, *12*(1), 423.

Lamberto, I., Percudani, R., Gatti, R., Folli, C., & Petrucco, S. (2010). Conserved alternative splicing of *Arabidopsis* transthyretin-like determines protein localization and S-allantoin synthesis in peroxisomes. *Plant Cell*, *22*(5), 1564-1574.

Laohavisit, A., Shang, Z., Rubio, L., Cuin, T. A., Véry, A. A., Wang, A., Mortimer, J. C., Macpherson, N., Coxon, K. M., Battery, N. H., Brownlee, C., Park, O. K., Sentenac, H., Shabala, S., Web, A. A. R., & Davies, J. M. (2012). *Arabidopsis* annexin1 mediates the radical-activated plasma membrane Ca^{2+}-and K^+-permeable conductance in root cells. *Plant Cell*, *24*(4), 1522-1533.

LaPorte, D. C., Wierman, B. M., & Storm, D. R. (1980). Calcium-induced exposure of a hydrophobic surface on calmodulin. *Biochemistry*, *19*(16), 3814-3819.

Leba, L. J., Cheval, C., Ortiz-Martín, I., Ranty, B., Beuzón, C. R., Galaud, J. P., & Aldon, D. (2012a). CML9, an *Arabidopsis* calmodulin-like protein, contributes to plant innate immunity through a flagellin-dependent signalling pathway. *Plant Journal*, *71*(6), 976-989.

Leba, L. J., Perochon, A., Cheval, C., Ranty, B., Galaud, J. P., & Aldon, D. (2012b). CML9, a multifunctional *Arabidopsis thaliana* calmodulin-like protein involved in stress responses and plant growth?. *Plant Signaling & Behavior*, *7*(9), 1121-1124.

Lee, J. Y., & Lu, H. (2011). Plasmodesmata: the battleground against intruders. *Trends in Plant Science*, *16*(4), 201-210.

Lee, J. Y., Wang, X., Cui, W., Sager, R., Modla, S., Czymmek, K., Zybaliov, B., van Wijk, K., Zhang, C., Lu, H., & Lakshmanan, V. (2011). A plasmodesmata-localized protein mediates

crosstalk between cell-to-cell communication and innate immunity in *Arabidopsis*. *Plant Cell*, *23*(9), 3353-3373.

Lee, M. W., & Yang, Y. (2006). Transient expression assay by agroinfiltration of leaves. In *Arabidopsis Protocols* (pp. 225-229). Humana Press.

Lee, S. M., Kim, H. S., Han, H. J., Moon, B. C., Kim, C. Y., Harper, J. F., & Chung, W. S. (2007). Identification of a calmodulin-regulated autoinhibited Ca^{2+}-ATPase (ACA11) that is localized to vacuole membranes in *Arabidopsis*. *FEBS Letters*, *581*(21), 3943-3949.

Legius, E., Proesmans, W., Eggermont, E., Vandamme-Lombaerts, R., Bouillon, R., & Smet, M. (1989). Rickets due to dietary calcium deficiency. *European Journal of Pediatrics*, *148*(8), 784-785.

Leng, Q., Mercier, R. W., Hua, B. G., Fromm, H., & Berkowitz, G. A. (2002). Electrophysiological analysis of cloned cyclic nucleotide-gated ion channels. *Plant Physiology*, *128*(2), 400-410.

Lorenzen, I., Aberle, T., & Plieth, C. (2004). Salt stress-induced chloride flux: a study using transgenic *Arabidopsis* expressing a fluorescent anion probe. *Plant Journal*, *38*(3), 539-544.

Levy, A., Erlanger, M., Rosenthal, M., & Epel, B. L. (2007). A plasmodesmata-associated β-1, 3-glucanase in *Arabidopsis*. *Plant Journal*, *49*(4), 669-682.

Lewis, J. D., Wan, J., Ford, R., Gong, Y., Fung, P., Nahal, H., Wang, P. W., Desveaux, D., & Guttman, D. S. (2012). Quantitative interactor screening with next-generation sequencing (QIS-Seq) identifies *Arabidopsis thaliana* MLO2 as a target of the *Pseudomonas syringae* type III effector HopZ2. *BMC Genomics*, *13*(1), 8.

Liu, T. Y., Aung, K., Tseng, C. Y., Chang, T. Y., Chen, Y. S., & Chiou, T. J. (2011). Vacuolar Ca^{2+}/H^{+} transport activity is required for systemic phosphate homeostasis involving shoot-to-root signaling in *Arabidopsis*. *Plant Physiology*, *156*(3), 1176-1189.

Lohmeier-Vogel, E. M., Kerk, D., Nimick, M., Wrobel, S., Vickerman, L., Muench, D. G., & Moorhead, G. B. (2008). *Arabidopsis At5g39790* encodes a chloroplast-localized, carbohydrate-binding, coiled-coil domain-containing putative scaffold protein. *BMC Plant Biology*, *8*(1), 120.

Lu, X., Tintor, N., Mentzel, T., Kombrink, E., Boller, T., Robatzek, S., Schulze-Lefert, P., & Saijo, Y. (2009). Uncoupling of sustained MAMP receptor signaling from early outputs in an *Arabidopsis* endoplasmic reticulum glucosidase II allele. *Proceedings of the National Academy of Sciences*, *106*(52), 22522-22527.

Lucas, W. J., & Gilbertson, R. L. (1994). Plasmodesmata in relation to viral movement within leaf tissues. *Annual Review of Phytopathology*, *32*(1), 387-415.

Lucas, W. J., & Lee, J. Y. (2004). Plasmodesmata as a supracellular control network in plants. *Nature Reviews in Molecular Cell Biology*, *5*(9), 712-726.

Lucca, N., & León, G. (2012). *Arabidopsis ACA7*, encoding a putative auto-regulated Ca2+-ATPase, is required for normal pollen development. *Plant Cell Reports*, *31*(4), 651-659.

Luna, E., Pastor, V., Robert, J., Flors, V., Mauch-Mani, B., & Ton, J. (2011). Callose deposition: a multifaceted plant defence response. *Molecular Plant-Microbe Interactions*, *24*(2), 183-193.

Ma, W., Ali, R., & Berkowitz, G. A. (2006). Characterization of plant phenotypes associated with loss-of-function of *AtCNGC1*, a plant cyclic nucleotide gated cation channel. *Plant Physiology and Biochemistry*, *44*(7), 494-505.

Ma, W., Smigel, A., Tsai, Y. C., Braam, J., & Berkowitz, G. A. (2008). Innate immunity signaling: cytosolic Ca^{2+} elevation is linked to downstream nitric oxide generation through the action of calmodulin or a calmodulin-like protein. *Plant Physiology*, *148*(2), 818-828.

Ma, W., Smigel, A., Walker, R. K., Moeder, W., Yoshioka, K., & Berkowitz, G. A. (2010). Leaf senescence signaling: The Ca^{2+}-conducting *Arabidopsis* cyclic nucleotide gated channel 2 acts through nitric oxide to repress senescence programming. *Plant Physiology*, *154*(2), 733-743.

Maathuis, F. J., Filatov, V., Herzyk, P., C Krijger, G., B Axelsen, K., Chen, S, Brian, J. G., Li, Y., Madagan, K. L., Sánchez-Fernádez, R., Forde, B. G., Palmgren, M. G., Rea, P. A., Willihams, L. E., Sanders, D., & Amtmann, A. (2003). Transcriptome analysis of root transporters reveals participation of multiple gene families in the response to cation stress. *Plant Journal*, *35*(6), 675-692.

MacRobbie, E. A. (2006a). Control of volume and turgor in stomatal guard cells. *Journal of Membrane Biology*, *210*(2), 131-142.

MacRobbie, E. A. (2006b). Osmotic effects on vacuolar ion release in guard cells. *Proceedings of the National Academy of Sciences*, *103*(4), 1135-1140.

Manohar, M., Shigaki, T., Mei, H., Park, S., Marshall, J., Aguilar, J., & Hirschi, K. D. (2011). Characterization of *Arabidopsis* Ca^{2+}/H^+ exchanger CAX3. *Biochemistry*, *50*(28), 6189-6195.

Mantis, J., & Tague, B. W. (2000). Comparing the utility of β-glucuronidase and green fluorescent protein for detection of weak promoter activity in *Arabidopsis thaliana*. *Plant Molecular Biology Reporter*, *18*(4), 319-330.

Marschner, H. (1995). *Mmineral nutrition of higher plants*. Academic Press, London.

Maule, A. J. (2008). Plasmodesmata: structure, function and biogenesis. *Current Opinion in Plant Biology*, *11*(6), 680-686.

Maule, A. J., Benitez-Alfonso, Y., & Faulkner, C. (2011). Plasmodesmata–membrane tunnels with attitude. *Current Opinion in Plant Biology*, *14*(6), 683-690.

Maune, J. F., Klee, C. B., & Beckingham, K. (1992). Ca^{2+} binding and conformational change in two series of point mutations to the individual Ca^{2+}-binding sites of calmodulin. *Journal of Biological Chemistry*, *267*(8), 5286-5295.

McAinsh, M. R., & Pittman, J. K. (2009). Shaping the calcium signature. *New Phytologist*, *181*(2), 275-294.

McCormack, E., & Braam, J. (2003). Calmodulins and related potential calcium sensors of *Arabidopsis*. *New Phytologist*, *159*(3), 585-598.

McCormack, E., Tsai, Y. C., & Braam, J. (2005). Handling calcium signaling: *Arabidopsis* CaMs and CMLs. *Trends in Plant Science*, *10*(8), 383-389.

McLean, B. G., Hempel, F. D., & Zambryski, P. C. (1997). Plant intercellular communication via plasmodesmata. *Plant Cell*, *9*(7), 1043-1054.

McLean, B. G., Zupan, J., & Zambryski, P. C. (1995). Tobacco mosaic virus movement protein associates with the cytoskeleton in tobacco cells. *Plant Cell*, *7*(12), 2101-2114.

Mei, H., Cheng, N. H., Zhao, J., Park, S., Escareno, R. A., Pittman, J. K., & Hirschi, K. D. (2009). Root development under metal stress in *Arabidopsis thaliana* requires the H^+/cation antiporter CAX4. *New Phytologist*, *183*(1), 95-105.

Meyerhoff, O., Müller, K., Roelfsema, M. R. G., Latz, A., Lacombe, B., Hedrich, R., Dietrich, P., & Becker, D. (2005). AtGLR3. 4, a glutamate receptor channel-like gene is sensitive to touch and cold. *Planta*, *222*(3), 418-427.

Michard, E., Lima, P. T., Borges, F., Silva, A. C., Portes, M. T., Carvalho, J. E., Gilliham, M., Liu, L. H., Obermeyer, G., & Feijó, J. A. (2011). Glutamate receptor–like genes form Ca^{2+} channels in pollen tubes and are regulated by pistil D-serine. *Science*, *332*(6028), 434-437.

Mohd Noh, N. I. (2013) Characterization of the function of Calmodulin-like (CML) 23 and CML24 in the *Arabidopsis thaliana* circadian clock. *International Conference on Arabidopsis Research*, POS-TUE-175.

Monihan, S. M. (2011) The *Arabidopsis* Calcineurin B-Like 10 calcium sensor couples environmental signals to developmental responses. PhD Thesis, The University of Arizona, USA.

Morris, J., Hawthorne, K. M., Hotze, T., Abrams, S. A., & Hirschi, K. D. (2008). Nutritional impact of elevated calcium transport activity in carrots. *Proceedings of the National Academy of Sciences*, *105*(5), 1431-1435.

Morsy, M., Gouthu, S., Orchard, S., Thorneycroft, D., Harper, J. F., Mittler, R., & Cushman, J. C. (2008). Charting plant interactomes: possibilities and challenges. *Trends in Plant Science*, *13*(4), 183-191.

Mousavi, S. A. R., Chauvin, A., Pascaud, F., Kellenberger, S., & Farmer, E. E. (2013) *GLUTAMATE RECEPTOR-LIKE* genes mediate leaf-to-leaf wound signalling. *Nature*, *500*, 422-426.

Mukhtar, M. S., Carvunis, A. R., Dreze, M., Epple, P., Steinbrenner, J., Moore, J., Tasan, M., Galli, M., Hao, T., Nishimura1, M. T., Pevzner, S. J., Donovan, S. E., Ghamsari, L., Santhanam, B., Romero, V., Poulin, M. M., Gebreab, F., Gutierrez, B. J., Tam, S., Monachello, D., Boxem, M., Harbort, C. J., McDonald, N., Gai, L., Chen, H., He, Y., European Union Effectoromics Consortium, Vandenhaute, J., Roth, F. G., Hill, D. E., Ecker, J. R., Vidal, M., Beynon, J., Braun, P., & Dangl, J. L. (2011). Independently evolved virulence effectors converge onto hubs in a plant immune system network. *Science*, *333*(6042), 596-601.

Munns, R., James, R. A., Xu, B., Athman, A., Conn, S. J., Jordans, C., Byrt, C. S., Hare, R. A., Tyerman, S. D., Tester, M., Plett, D., & Gilliham, M. (2012). Wheat grain yield on saline soils is improved by an ancestral Na$^+$ transporter gene. *Nature Biotechnology*, *30*(4), 360-364.

Murashige, T., & Skoog, F. (1962). A revised medium for rapid growth and bio assays with tobacco tissue cultures. *Physiologia Plantarum*, *15*(3), 473-497.

Nakagawa, Y., Katagiri, T., Shinozaki, K., Qi, Z., Tatsumi, H., Furuichi, T., Kishigami, A., Sokabe, M., Kojima, I., Sato, S., Kato, T., Tabata, S., Iida, K., Terashima, A., Nakano, M., Ikeda, M., Yamanaka, T., & Iida, H. (2007). *Arabidopsis* plasma membrane protein crucial for Ca^{2+} influx and touch sensing in roots. *Proceedings of the National Academy of Sciences*, *104*(9), 3639-3644.

Nagae, M., Nozawa, A., Koizumi, N., Sano, H., Hashimoto, H., Sato, M., & Shimizu, T. (2003). The crystal structure of the novel calcium-binding protein AtCBL2 from *Arabidopsis thaliana*. *Journal of Biological Chemistry*, *278*(43), 42240-42246.

Nakayama, S., Kawasaki, H., & Kretsinger, R. (2000). Evolution of EF-hand proteins. In *Calcium Homeostasis* (pp. 29-58). Springer Berlin Heidelberg.

Nallamsetty, S., & Waugh, D. S. (2007). A generic protocol for the expression and purification of recombinant proteins in *Escherichia coli* using a combinatorial His$_6$-maltose binding protein fusion tag. *Nature Protocols*, *2*(2), 383-391.

Nelson, B. K., Cai, X., & Nebenführ, A. (2007). A multicolored set of in vivo organelle markers for co-localization studies in *Arabidopsis* and other plants. *Plant Journal*, *51*(6), 1126-1136.

Nelson, M. R., & Chazin, W. J. (1998). Structures of EF-hand Ca^{2+}-binding proteins: diversity in the organization, packing and response to Ca^{2+} binding. *Biometals*, *11*(4), 297-318.

Ner-Gaon, H., Halachmi, R., Savaldi-Goldstein, S., Rubin, E., Ophir, R., & Fluhr, R. (2004). Intron retention is a major phenomenon in alternative splicing in *Arabidopsis*. *Plant Journal*, *39*(6), 877-885.

Obayashi, T., Hayashi, S., Saeki, M., Ohta, H., & Kinoshita, K. (2009). ATTED-II provides coexpressed gene networks for *Arabidopsis*. *Nucleic Acids Research*, *37*(suppl 1), D987-D991.

Obayashi, T., & Kinoshita, K. (2010). Coexpression landscape in ATTED-II: usage of gene list and gene network for various types of pathways. *Journal of Plant Research*, *123*(3), 311-319.

Ogawa, M., Hanada, A., Yamauchi, Y., Kuwahara, A., Kamiya, Y., & Yamaguchi, S. (2003). Gibberellin biosynthesis and response during *Arabidopsis* seed germination. *Plant Cell*, *15*(7), 1591-1604.

Ossowski, S., Schwab, R., & Weigel, D. (2008). Gene silencing in plants using artificial microRNAs and other small RNAs. *Plant Journal*, *53*(4), 674-690.

Ozawa, M., & Muramatsu, T. (1993). Reticulocalbin, a novel endoplasmic reticulum resident Ca^{2+}-binding protein with multiple EF-hand motifs and a carboxyl-terminal HDEL sequence. *Journal of Biological Chemistry*, *268*(1), 699-705.

Park, H. C., Park, C. Y., Koo, S. C., Cheong, M. S., Kim, K. E., Kim, M. C., Lim, C. O., Lee, S. Y., Yun, D. J., & Chung, W. S. (2010). AtCML8, a calmodulin-like protein, differentially activating CaM-dependent enzymes in *Arabidopsis thaliana*. *Plant Cell Reports*, *29*(11), 1297-1304.

Park, S., Cheng, N. H., Pittman, J. K., Yoo, K. S., Park, J., Smith, R. H., & Hirschi, K. D. (2005a). Increased calcium levels and prolonged shelf life in tomatoes expressing *Arabidopsis* H^+/Ca^{2+} transporters. *Plant Physiology*, *139*(3), 1194-1206.

Park, S., Elless, M. P., Park, J., Jenkins, A., Lim, W., Chambers, I. V., & Hirschi, K. D. (2009). Sensory analysis of calcium-biofortified lettuce. *Plant Biotechnology Journal*, *7*(1), 106-117.

Park, S., Kang, T. S., Kim, C. K., Han, J. S., Kim, S., Smith, R. H., Pike, L. M., & Hirschi, K. D. (2005b). Genetic manipulation for enhancing calcium content in potato tuber. *Journal of Agricultural and Food Chemistry*, *53*(14), 5598-5603.

Park, S., Kim, C. K., Pike, L. M., Smith, R. H., & Hirschi, K. D. (2004). Increased calcium in carrots by expression of an *Arabidopsis* H^+/Ca^{2+} transporter. *Molecular Breeding*, *14*(3), 275-282.

Parrish, J. R., Gulyas, K. D., & Finley Jr, R. L. (2006). Yeast two-hybrid contributions to interactome mapping. *Current Opinion in Biotechnology*, *17*(4), 387-393.

Patrick, J. W. (1997). Phloem unloading: sieve element unloading and post-sieve element transport. *Annual Review of Plant Biology*, *48*(1), 191-222.

Peiter, E., Maathuis, F. J., Mills, L. N., Knight, H., Pelloux, J., Hetherington, A. M., & Sanders, D. (2005). The vacuolar Ca^{2+}-activated channel TPC1 regulates germination and stomatal movement. *Nature*, *434*(7031), 404-408.

Penninckx, I. A., Eggermont, K., Terras, F. R., Thomma, B. P., De Samblanx, G. W., Buchala, A., Métraux, J. P., Manners, J. M., & Broekaert, W. F. (1996). Pathogen-induced systemic activation of a plant defensin gene in *Arabidopsis* follows a salicylic acid-independent pathway. *Plant Cell*, *8*(12), 2309-2323.

Perochon, A., Dieterle, S., Pouzet, C., Aldon, D., Galaud, J. P., & Ranty, B. (2010). Interaction of a plant pseudo-response regulator with a calmodulin-like protein. *Biochemical and Biophysical Research Communications*, *398*(4), 747-751.

Pittman, J. K., & Hirschi, K. D. (2003). Don't shoot the (second) messenger: endomembrane transporters and binding proteins modulate cytosolic Ca^{2+} levels. *Current Opinion in Plant Biology*, *6*(3), 257-262.

Pittman, J. K., Shigaki, T., Cheng, N. H., & Hirschi, K. D. (2002a). Mechanism of N-terminal autoinhibition in the *Arabidopsis* Ca^{2+}/H^+ Antiporter CAX1. *Journal of Biological Chemistry*, *277*(29), 26452-26459.

Pittman, J. K., Shigaki, T., & Hirschi, K. D. (2005). Evidence of differential pH regulation of the *Arabidopsis* vacuolar Ca^{2+}/H^+ antiporters CAX1 and CAX2. *FEBS Letters*, *579*(12), 2648-2656.

Pittman, J. K., Shigaki, T., Marshall, J. L., Morris, J. L., Cheng, N. H., & Hirschi, K. D. (2004). Functional and regulatory analysis of the *Arabidopsis thaliana* CAX2 cation transporter. *Plant Molecular Biology*, *56*(6), 959-971.

Pittman, J. K., Sreevidya, C. S., Shigaki, T., Ueoka-Nakanishi, H., & Hirschi, K. D. (2002b). Distinct N-terminal regulatory domains of Ca^{2+}/H^+ antiporters. *Plant Physiology*, *130*(2), 1054-1062.

Popescu, S. C., Popescu, G. V., Bachan, S., Zhang, Z., Seay, M., Gerstein, M., Snyder, M., & Dinesh-Kumar, S. P. (2007). Differential binding of calmodulin-related proteins to their targets revealed through high-density *Arabidopsis* protein microarrays. *Proceedings of the National Academy of Sciences*, *104*(11), 4730-4735.

Pottosin, I. I., & Schönknecht, G. (2007). Vacuolar calcium channels. *Journal of Experimental Botany*, *58*(7), 1559-1569.

Punshon, T., Hirschi, K., Yang, J., Lanzirotti, A., Lai, B., & Guerinot, M. L. (2012). The role of CAX1 and CAX3 in elemental distribution and abundance in *Arabidopsis* seed. *Plant Physiology*, *158*(1), 352-362.

Qi, Z., Stephens, N. R., & Spalding, E. P. (2006). Calcium entry mediated by GLR3. 3, an *Arabidopsis* glutamate receptor with a broad agonist profile. *Plant Physiology*, *142*(3), 963-971.

Quan, R., Lin, H., Mendoza, I., Zhang, Y., Cao, W., Yang, Y., Shang, M., Chen, S., Pardo, J. M., & Guo, Y. (2007). SCABP8/CBL10, a putative calcium sensor, interacts with the protein kinase SOS2 to protect *Arabidopsis* shoots from salt stress. *Plant Cell*, *19*(4), 1415-1431.

Radford, J. E., Vesk, M., & Overall, R. L. (1998). Callose deposition at plasmodesmata. *Protoplasma*, *201*(1-2), 30-37.

Ranf, S., Wünnenberg, P., Lee, J., Becker, D., Dunkel, M., Hedrich, R., Scheel, D., & Dietrich, P. (2008). Loss of the vacuolar cation channel, *AtTPC1*, does not impair Ca^{2+} signals induced by abiotic and biotic stresses. *Plant Journal*, *53*(2), 287-299.

Reddy, A. S. (2007). Alternative splicing of pre-messenger RNAs in plants in the genomic era. *Annual Review of Plant Biology*, *58*, 267-294.

Reddy, A. S., Ali, G. S., Celesnik, H., & Day, I. S. (2011). Coping with stresses: roles of calcium- and calcium/calmodulin-regulated gene expression. *Plant Cell*, *23*(6), 2010-2032.

Rienmüller, F., Beyhl, D., Lautner, S., Fromm, J., Al-Rasheid, K. A., Ache, P., Farmer, E. E., Marten, I., & Hedrich, R. (2010). Guard cell-specific calcium sensitivity of high density and activity SV/TPC1 channels. *Plant and Cell Physiology*, *51*(9), 1548-1554.

Ritchie, R. J. (2006). Consistent sets of spectrophotometric chlorophyll equations for acetone, methanol and ethanol solvents. *Photosynthesis Research*, *89*(1), 27-41.

Roberts, A. G., & Oparka, K. J. (2003). Plasmodesmata and the control of symplastic transport. *Plant, Cell & Environment*, *26*(1), 103-124.

Routzahn, K. M., & Waugh, D. S. (2002). Differential effects of supplementary affinity tags on the solubility of MBP fusion proteins. *Journal of Structural and Functional Genomics*, *2*(2), 83-92.

Roux, M., Schwessinger, B., Albrecht, C., Chinchilla, D., Jones, A., Holton, N., Malinovsky, F. G., Tör, M., de Vries, S., & Zipfel, C. (2011). The *Arabidopsis* leucine-rich repeat receptor–like kinases BAK1/SERK3 and BKK1/SERK4 are required for innate immunity to hemibiotrophic and biotrophic pathogens. *Plant Cell*, *23*(6), 2440-2455.

Rueda-Romero, P., Barrero-Sicilia, C., Gómez-Cadenas, A., Carbonero, P., & Oñate-Sánchez, L. (2012). *Arabidopsis* thaliana DOF6 negatively affects germination in non-after-ripened seeds and interacts with TCP14. *Journal of Experimental Botany*, *63*(5), 1937-1949.

Sachdev, D., & Chirgwin, J. M. (1999). Properties of soluble fusions between mammalian aspartic proteinases and bacterial maltose-binding protein. *Journal of Protein Chemistry*, *18*(1), 127-136.

Saleh, L., & Plieth, C. (2013). A9C sensitive Cl^--accumulation in *A. thaliana* root cells during salt stress is controlled by internal and external calcium. *Plant Signaling & Behavior*, *8*(6), e24259.

Salnikov, V. V., Grimson, M. J., Seagull, R. W., & Haigler, C. H. (2003). Localization of sucrose synthase and callose in freeze-substituted secondary-wall-stage cotton fibers. *Protoplasma*, *221*(3-4), 175-184.

Sanders, D., Pelloux, J., Brownlee, C., & Harper, J. F. (2002). Calcium at the crossroads of signaling. *Plant Cell*, *14*(suppl 1), S401-S417.

Sarhan, M. F., Tung, C. C., Van Petegem, F., & Ahern, C. A. (2012). Crystallographic basis for calcium regulation of sodium channels. *Proceedings of the National Academy of Sciences*, *109*(9), 3558-3563.

Schaaf, G., Catoni, E., Fitz, M., Schwacke, R., Schneider, A., Wirén, N. V., & Frommer, W. B. (2002). A putative role for the vacuolar calcium/manganese proton antiporter AtCAX2 in heavy metal detoxification. *Plant Biology*, *4*(5), 612-618.

Schiøtt, M., Romanowsky, S. M., Bækgaard, L., Jakobsen, M. K., Palmgren, M. G., & Harper, J. F. (2004). A plant plasma membrane Ca^{2+} pump is required for normal pollen tube growth and fertilization. *Proceedings of the National Academy of Sciences*, *101*(25), 9502-9507.

Schmittgen, T. D., & Livak, K. J. (2008). Analyzing real-time PCR data by the comparative CT method. *Nature Protocols*, *3*(6), 1101-1108.

Schulze, C., Sticht, H., Meyerhoff, P., & Dietrich, P. (2011). Differential contribution of EF-hands to the Ca^{2+}-dependent activation in the plant two-pore channel TPC1. *Plant Journal*, *68*(3), 424-432.

Schwab, R., Ossowski, S., Riester, M., Warthmann, N., & Weigel, D. (2006). Highly specific gene silencing by artificial microRNAs in *Arabidopsis*. *Plant Cell*, *18*(5), 1121-1133.

Shear, C. B. (1975). Calcium-related disorders of fruits and vegetables. *HortScience*, *10*(4), 364-365.

Sheen, J. (2001). Signal transduction in maize and *Arabidopsis* mesophyll protoplasts. *Plant Physiology*, *127*(4), 1466-1475.

Sheen, J., Hwang, S., Niwa, Y., Kobayashi, H., & Galbraith, D. W. (1995). Green-fluorescent protein as a new vital marker in plant cells. *Plant Journal*, *8*(5), 777-784.

Shigaki, T., Cheng, N. H., Pittman, J. K., & Hirschi, K. (2001). Structural determinants of Ca^{2+} transport in the *Arabidopsis* H^+/Ca^{2+} antiporter CAX1. *Journal of Biological Chemistry*, *276*(46), 43152-43159.

Shigaki, T., & Hirschi, K. D. (2006). Diverse functions and molecular properties emerging for CAX cation/H^+ exchangers in plants. *Plant Biology*, *8*(4), 419-429.

Shimada, Y., Goda, H., Nakamura, A., Takatsuto, S., Fujioka, S., & Yoshida, S. (2003). Organ-specific expression of brassinosteroid-biosynthetic genes and distribution of endogenous brassinosteroids in *Arabidopsis*. *Plant Physiology*, *131*(1), 287-297.

Sivaguru, M., Fujiwara, T., Šamaj, J., Baluška, F., Yang, Z., Osawa, H., Maeda, T., Mori, T., Volkmann, D., & Matsumoto, H. (2000). Aluminum-induced 1-3-β-d-glucan inhibits cell-to-cell trafficking of molecules through plasmodesmata. a new mechanism of aluminum toxicity in plants. *Plant Physiology*, *124*(3), 991-1006.

Small, I., Wintz, H., Akashi, K., & Mireau, H. (1998). Two birds with one stone: genes that encode products targeted to two or more compartments. *Plant Molecular Biology*, *38*(1-2), 265-277.

Simon, E. W. (1978). The symptoms of calcium deficiency in plants. *New phytologist*, *80*(1), 1-15.

Simpson, G. G., & Dean, C. (2002). *Arabidopsis*, the rosetta stone of flowering time?. *Science*, *296*(5566), 285-289.

Simpson, C., Thomas, C., Findlay, K., Bayer, E., & Maule, A. J. (2009). An *Arabidopsis* GPI-anchor plasmodesmal neck protein with callose binding activity and potential to regulate cell-to-cell trafficking. *Plant Cell*, *21*(2), 581-594.

Smart, M. G., Aist, J. R., & Israel, H. W. (1986). Structure and function of wall appositions. 1. General histochemistry of papillae in barley coleoptiles attacked by *Erysiphe graminis* f. sp. *hordei*. *Canadian Journal of Botany*, *64*(4), 793-801.

Smith, J. A. C. (1991). Ion transport and the transpiration stream. *Botanica Acta*, *104*(6), 416-421.

Silva-Filho, M. C. (2003). One ticket for multiple destinations: dual targeting of proteins to distinct subcellular locations. *Current Opinion in Plant Biology*, *6*(6), 589-595.

Sistrunk, M. L., Antosiewicz, D. M., Purugganan, M. M., & Braam, J. (1994). *Arabidopsis TCH3* encodes a novel Ca^{2+} binding protein and shows environmentally induced and tissue-specific regulation. *Plant Cell*, *6*(11), 1553-1565.

Snedden, W. A., & Fromm, H. (1998). Calmodulin, calmodulin-related proteins and plant responses to the environment. *Trends in Plant Science*, *3*(8), 299-304.

Stephens, N. R., Qi, Z., & Spalding, E. P. (2008). Glutamate receptor subtypes evidenced by differences in desensitization and dependence on the *GLR3.3* and *GLR3.4* genes. *Plant Physiology*, *146*(2), 529-538.

Storey, R., & Leigh, R. A. (2004). Processes modulating calcium distribution in citrus leaves. an investigation using X-ray microanalysis with strontium as a tracer. *Plant Physiology*, *136*(3), 3838-3848.

Stone, B. A., Evans, N. A., Bonig, I., & Clarke, A. E. (1984). The application of Sirofluor, a chemically defined fluorochrome from aniline blue for the histochemical detection of callose. *Protoplasma*, *122*(3), 191-195.

Strynadka, N. C., & James, M. N. (1989). Crystal structures of the helix-loop-helix calcium-binding proteins. *Annual Review of Biochemistry*, *58*(1), 951-999.

Sturn, A., Quackenbush, J., & Trajanoski, Z. (2002). Genesis: cluster analysis of microarray data. *Bioinformatics*, *18*(1), 207-208.

Swartzberg, D., Dai, N., Gan, S., Amasino, R., & Granot, D. (2006). Effects of cytokinin production under two SAG promoters on senescence and development of tomato plants. *Plant Biology*, *8*(5), 579-586.

Swartzberg, D., Hanael, R., & Granot, D. (2011). Relationship between hexokinase and cytokinin in the regulation of leaf senescence and seed germination. *Plant Biology*, *13*(3), 439-444.

Sze, H., Liang, F., Hwang, I., Curran, A. C., & Harper, J. F. (2000). Diversity and regulation of plant Ca^{2+} pumps: insights from expression in yeast. *Annual Review of Plant Biology*, *51*(1), 433-462.

Taniguchi, M., Kiba, T., Sakakibara, H., Ueguchi, C., Mizuno, T., & Sugiyama, T. (1998). Expression of *Arabidopsis* response regulator homologs is induced by cytokinins and nitrate. *FEBS Letters*, *429*(3), 259-262.

Tapken, D., Anschutz, U., Liu, L. H., Huelsken, T., Seebohm, G., Becker, D., & Hollmann, M. (2013). A plant homolog of animal Glutamate Receptors is an ion channel gated by multiple hydrophobic amino acids. *Science Signaling*, *6*(279), ra47.

Tapken, D., & Hollmann, M. (2008). *Arabidopsis thaliana* glutamate receptor ion channel function demonstrated by ion pore transplantation. *Journal of Molecular Biology*, *383*(1), 36-48.

Teakle, N. L., & Tyerman, S. D. (2010). Mechanisms of Cl⁻ transport contributing to salt tolerance. *Plant, cell & environment*, *33*(4), 566-589.

Teardo, E., Formentin, E., Segalla, A., Giacometti, G. M., Marin, O., Zanetti, M., Schiavo, F. L., Zoratti, M., & Szabò, I. (2011). Dual localization of plant glutamate receptor AtGLR3.4 to plastids and plasmamembrane. *Biochimica et Biophysica Acta (BBA)-Bioenergetics*, *1807*(3), 359-367.

Terpe, K. (2003). Overview of tag protein fusions: from molecular and biochemical fundamentals to commercial systems. *Applied Microbiology and Biotechnology*, *60*(5), 523-533.

Thomas, C. L., Bayer, E. M., Ritzenthaler, C., Fernandez-Calvino, L., & Maule, A. J. (2008). Specific targeting of a plasmodesmal protein affecting cell-to-cell communication. *PLoS Biology*, *6*(1), e7.

Tolia, N. H., & Joshua-Tor, L. (2006). Strategies for protein coexpression in *Escherichia coli*. *Nature Methods*, *3*(1), 55-64.

Tunc-Ozdemir, M., Rato, C., Brown, E., Rogers, S., Mooneyham, A., Frietsch, S., Myers, C. T., Poulsen, L. R., & Harper, J. F. (2013a). Cyclic nucleotide gated channels 7 and 8 are essential for male reproductive fertility. *PloS One*, *8*(2), e55277.

Tunc-Ozdemir, M., Tang, C., Ishka, M. R., Brown, E., Groves, N. R., Myers, C. T., Rato, C., Poulsen, L. R., McDowell, S., Mittler, R., & Harper, J. F. (2013b). A cyclic nucleotide-gated channel (CNGC16) in pollen is critical for stress tolerance in pollen reproductive development. *Plant Physiology*, *161*(2), 1010-1020.

Turano, F. J., Muhitch, M. J., Felker, F. C., & McMahon, M. B. (2002). The putative glutamate receptor 3.2 from *Arabidopsis thaliana* (AtGLR3.2) is an integral membrane peptide that accumulates in rapidly growing tissues and persists in vascular-associated tissues. *Plant Science*, *163*(1), 43-51.

Turgeon, R., & Wolf, S. (2009). Phloem transport: cellular pathways and molecular trafficking. *Annual Review of Plant Biology*, *60*, 207-221.

Uetz, P., Giot, L., Cagney, G., Mansfield, T. A., Judson, R. S., Knight, J. R., Lockshon, D., Narayan, V., Srinivasan, M., Pochart, P., Qureshi-Emili, A., Li, Y., Godwin, B., Conover, D., Kalbfleisch, T., Vijayadamodar, G., Yang, M., Johnston, M., Fields, S., & Rothberg, J. M. (2000). A comprehensive analysis of protein–protein interactions in *Saccharomyces cerevisiae*. *Nature*, *403*(6770), 623-627.

Urquhart, W., Gunawardena, A. H., Moeder, W., Ali, R., Berkowitz, G. A., & Yoshioka, K. (2007). The chimeric cyclic nucleotide-gated ion channel ATCNGC11/12 constitutively induces programmed cell death in a Ca^{2+} dependent manner. *Plant Molecular Biology*, *65*(6), 747-761.

Urquhart, W., Chin, K., Ung, H., Moeder, W., & Yoshioka, K. (2011). The cyclic nucleotide-gated channels AtCNGC11 and 12 are involved in multiple Ca^{2+}-dependent physiological responses and act in a synergistic manner. *Journal of Experimental Botany*, *62*(10), 3671-3682.

Vadassery, J., Reichelt, M., Hause, B., Gershenzon, J., Boland, W., & Mithöfer, A. (2012). CML42-mediated calcium signaling coordinates responses to *Spodoptera herbivory* and abiotic stresses in *Arabidopsis*. *Plant Physiology*,*159*(3), 1159-1175.

Valentim, F. L., Neven, F., Boyen, P., & van Dijk, A. D. (2012). Interactome-wide prediction of protein-protein binding sites reveals effects of protein sequence variation in *Arabidopsis thaliana*. *PloS One*, *7*(10), e47022.

Vandenbroucke, I. I., Vandesompele, J., De Paepe, A., & Messiaen, L. (2001). Quantification of splice variants using real-time PCR. *Nucleic Acids Research*, *29*(13), e68-e68.

Vanderbeld, B., & Snedden, W. A. (2007). Developmental and stimulus-induced expression patterns of *Arabidopsis* calmodulin-like genes *CML37*, *CML38* and *CML39*. *Plant Molecular Biology*, *64*(6), 683-697.

Vincill, E. D., Bieck, A. M., & Spalding, E. P. (2012). Ca^{2+} conduction by an amino acid-gated ion channel related to glutamate receptors. *Plant Physiology*, *159*(1), 40-46.

Vincill, E. D., Clarin, A. E., Molenda, J. N., & Spalding, E. P. (2013). Interacting glutamate receptor-like proteins in phloem regulate lateral root initiation in *Arabidopsis*. *Plant Cell*, *25*(4), 1304-1313.

Vongsamphanh, R., Fortier, P. K., & Ramotar, D. (2001). Pir1p mediates translocation of the yeast Apn1p endonuclease into the mitochondria to maintain genomic stability. *Molecular and Cellular Biology*, *21*(5), 1647-1655.

Waadt, R., Schmidt, L. K., Lohse, M., Hashimoto, K., Bock, R., & Kudla, J. (2008). Multicolor bimolecular fluorescence complementation reveals simultaneous formation of alternative CBL/CIPK complexes in planta. *Plant Journal*, *56*(3), 505-516.

Walker, A. R. (1972). The human requirement of calcium: should low intakes be supplemented?. *The American Journal of Clinical Nutrition*, *25*(5), 518-530.

Walter, M., Chaban, C., Schütze, K., Batistic, O., Weckermann, K., Näke, C., Blazevic, D., Grefen, C., Schumacher, K., Oecking C., Harter, K., & Kudla, J. (2004). Visualization of protein interactions in living plant cells using bimolecular fluorescence complementation. *The Plant Journal*, *40*(3), 428-438.

Wang, L., Tsuda, K., Sato, M., Cohen, J. D., Katagiri, F., & Glazebrook, J. (2009). *Arabidopsis* CaM binding protein CBP60g contributes to MAMP-induced SA accumulation and is involved in disease resistance against *Pseudomonas syringae*. *PLoS Pathogens*, *5*(2), e1000301.

Wang, X., Sager, R., Cui, W., Zhang, C., Lu, H., & Lee, J. Y. (2013). Salicylic acid regulates plasmodesmata closure during innate immune responses in *Arabidopsis*. *Plant Cell*, doi/10.1105/tpc.113.110676

Warren, C. R. (2008). Rapid measurement of chlorophylls with a microplate reader. *Journal of Plant Nutrition*, *31*(7), 1321-1332.

Waugh, D. S. (2005). Making the most of affinity tags. *Trends in Biotechnology*, *23*(6), 316-320.

Weaver, C. M., & Heaney, R. P. (2006). *Calcium in human health*. Humana Press, USA.

Weaver, C. M., Proulx, W. R., & Heaney, R. P. (1999). Choices for achieving adequate dietary calcium with a vegetarian diet. *American Journal of Clinical Nutrition*, *70*(3), 543s-548s.

Weaver, L. M., & Amasino, R. M. (2001). Senescence is induced in individually darkened *Arabidopsis* leaves, but inhibited in whole darkened plants. *Plant Physiology*, *127*(3), 876-886.

White, P. J. (1998). Calcium channels in the plasma membrane of root cells. *Annals of Botany*, *81*(2), 173-183.

White, P. J. (2001). The pathways of calcium movement to the xylem. *Journal of Experimental Botany*, *52*(358), 891-899.

White, P. J., & Broadley, M. R. (2003). Calcium in plants. *Annals of botany*, *92*(4), 487-511.

White, P. J., & Broadley, M. R. (2005). Biofortifying crops with essential mineral elements. *Trends in Plant Science*, *10*(12), 586-593.

White, P. J., & Broadley, M. R. (2009). Biofortification of crops with seven mineral elements often lacking in human diets–iron, zinc, copper, calcium, magnesium, selenium and iodine. *New Phytologist*, *182*(1), 49-84.

Willett, W. C. (1994). Diet and health: what should we eat?. *Science*, *264*(5158), 532-537.

Winter, D., Vinegar, B., Nahal, H., Ammar, R., Wilson, G.V., & Provart, N. J. (2007) An "Electronic Fluorescent Pictograph" browser for exploring and analyzing large-scale biological data sets. *PLoS One*, *2*(8), e718. doi:10.1371/journal.pone.0000718.

Wolf, S., Lucas, W. J., Deom, C. M., & Beachy, R. N. (1989). Movement protein of tobacco mosaic virus modifies plasmodesmatal size exclusion limit. *Science*, *246*(4928), 377-379.

Wu, Q., Shigaki, T., Han, J. S., Kim, C. K., Hirschi, K. D., & Park, S. (2012). Ectopic expression of a maize calreticulin mitigates calcium deficiency-like disorders in *sCAX1*-expressing tobacco and tomato. *Plant Molecular Biology*, *80*(6), 609-619.

Xu, G. Y., Rocha, P. S., Wang, M. L., Xu, M. L., Cui, Y. C., Li, L. Y., Zhu, Y. X., & Xia, X. (2011). A novel rice calmodulin-like gene, *OsMSR2*, enhances drought and salt tolerance and increases ABA sensitivity in *Arabidopsis*. *Planta*, *234*(1), 47-59.

Yamanaka, T., Nakagawa, Y., Mori, K., Nakano, M., Imamura, T., Kataoka, H., Terashima, A., Lida, K., Kojima, I., Katagiri, T., Shinozaki, K., & Iida, H. (2010). MCA1 and MCA2 that mediate Ca^{2+} uptake have distinct and overlapping roles in *Arabidopsis*. *Plant Physiology*, *152*(3), 1284-1296.

Yoo, S. D., Cho, Y. H., & Sheen, J. (2007). *Arabidopsis* mesophyll protoplasts: a versatile cell system for transient gene expression analysis. *Nature Protocols*, *2*(7), 1565-1572.

Yoshioka, K., Moeder, W., Kang, H. G., Kachroo, P., Masmoudi, K., Berkowitz, G., & Klessig, D. F. (2006). The chimeric *Arabidopsis* CYCLIC NUCLEOTIDE-GATED ION CHANNEL11/12 activates multiple pathogen resistance responses. *Plant Cell*, *18*(3), 747-763.

Yuen, C. C., & Christopher, D. A. (2013). The group IV-a cyclic nucleotide-gated channels, CNGC19 and CNGC20, localize to the vacuole membrane in *Arabidopsis thaliana*. *AoB Plants*, doi: 10.1093/aobpla/plt012.

Zambryski, P. (2004). Cell-to-cell transport of proteins and fluorescent tracers via plasmodesmata during plant development. *The Journal of Cell Biology*, *164*(2), 165-168.

Zambryski, P., & Crawford, K. (2000). Plasmodesmata: gatekeepers for cell-to-cell transport of developmental signals in plants. *Annual Review of Cell and Developmental Biology*, *16*(1), 393-421.

Zhang, J., Shao, F., Li, Y., Cui, H., Chen, L., Li, H., Zou, Y., Long, C., Lan, L., Chai, J., Chen, S., Tang, X., & Zhou, J. M. (2007). A *Pseudomonas syringae* effector inactivates MAPKs to suppress PAMP-induced immunity in plants. *Cell Host & Microbe*, *1*(3), 175-185.

Zhang, X., Henriques, R., Lin, S. S., Niu, Q. W., & Chua, N. H. (2006). *Agrobacterium*-mediated transformation of *Arabidopsis thaliana* using the floral dip method. *Nature Protocols*, *1*(2), 641-646.

Zhang, Y., Xu, S., Ding, P., Wang, D., Cheng, Y. T., He, J., Gao, M., Xu, F., Zhu, Z., Li, X., & Zhang, Y. (2010). Control of salicylic acid synthesis and systemic acquired resistance by two members of a plant-specific family of transcription factors. *Proceedings of the National Academy of Sciences*, *107*(42), 18220-18225.

Zhao, J., Barkla, B. J., Marshall, J., Pittman, J. K., & Hirschi, K. D. (2008). The *Arabidopsis cax3* mutants display altered salt tolerance, pH sensitivity and reduced plasma membrane H^+-ATPase activity. *Planta*, *227*(3), 659-669.

Zhao, J., Shigaki, T., Mei, H., Guo, Y. Q., Cheng, N. H., & Hirschi, K. D. (2009). Interaction between *Arabidopsis* Ca^{2+}/H^+ exchangers CAX1 and CAX3. *Journal of Biological Chemistry*, *284*(7), 4605-4615.

Zipfel, C. (2008). Pattern-recognition receptors in plant innate immunity. *Current Opinion in Immunology*, *20*(1), 10-16.

Zipfel, C., Kunze, G., Chinchilla, D., Caniard, A., Jones, J. D., Boller, T., & Felix, G. (2006). Perception of the bacterial PAMP EF-Tu by the receptor EFR restricts *Agrobacterium*-mediated transformation. *Cell*, *125*(4), 749-760.

Zipfel, C., & Robatzek, S. (2010). Pathogen-associated molecular pattern-triggered immunity: Veni, vidi…?. *Plant physiology*, *154*(2), 551-554.

Zipfel, C., Robatzek, S., Navarro, L., Oakeley, E. J., Jones, J. D., Felix, G., & Boller, T. (2004). Bacterial disease resistance in *Arabidopsis* through flagellin perception. *Nature*, *428*(6984), 764-767.